Author/s:
Ntouma, Viktoria

Title:
Mitochondrial Stress and Metabolic Dysfunction in the Liver: A Role for The Unfolded Protein Response

Date:
2019

Persistent Link:
https://hdl.handle.net/11343/237488

MITOCHONDRIAL STRESS AND METABOLIC DYSFUNCTION IN THE LIVER: A ROLE FOR THE UNFOLDED PROTEIN RESPONSE

Viktoria Ntouma

BSc (Honours), MSc

Submitted in total fulfilment of the requirements of the degree of

Doctor of Philosophy

August 2019

Department of Medicine (Austin Health)

Faculty of Medicine, Dentistry and Health Science

ABSTRACT

Liver dysfunction and fat accumulation in liver correlates with metabolic syndrome, also increases the risk of development of type 2 diabetes, advanced liver disease and several other complications. There are no simple or widely effective medical solutions to these conditions and further studies are required for clarification of mechanisms involved. Mitochondria are the powerhouses of the cell, responsible for cellular energy production and help maintain the cellular environment through complex procedures. Thus, it is fundamental for the mitochondria to function properly. Mitochondrial dysfunction is known to be associated with metabolic diseases including NASH and Type 2 diabetes where it has been implicated in hepatic fat accumulation and hepatic insulin resistance. Various enzymes and proteins are required to make mitochondria function properly. Mitochondrial dysfunction can be caused by build-up of reactive-oxygen-species which leads to the activation of a stress response known as the mitochondrial-unfolded-protein-response (UPRmt). Failure of these responses to adapt to or repair damage from stress results in mitochondrial dysfunction and may lead to apoptosis and eventually death. Ubiquitin-like-5 (UBL5) is a protein that was first discovered in the obese Israeli sand rat, associated with weight gain. Studies in *C. elegans* have shown that UBL5 is involved in the activation of the mitochondrial unfolded protein response (UPRmt) to ensure that chaperone proteins are transcribed to relieve the ensuing stress. This pathway upregulates mitochondrial proteases and chaperone proteins to alleviate proteostatic stress. To further explore how mitochondrial stress through the mitochondrial unfolded protein response lead to liver dysfunction, we generated a tamoxifen-inducible, liver-specific UBL5 knockout mouse. In earlier studies, we performed systematic assessments of the role of UBL5 in mitochondrial function and energy metabolism. We found that mice with complete deletion of UBL5 in liver are glucose intolerant and present with features of liver

failure (gross steatosis, apoptosis and significantly increased hepatic enzymes). Furthermore, these mice present with oxidative stress reduced mitochondrial respiration, increased ROS levels and decreased UPRmt gene expression (CHOP, ClpP, ClpX, Lonp1, HSP10, HSP70, ATF-5) while mtHSP70 was upregulated. PGC1a mitochondrial biogenesis gene was also downregulated. Our heterozygous mice (50% UBL5 reduction), however, did not present with any defects when on a chow diet. Therefore, our aim was to determine whether exposing the heterozygous mice to high-fat diet rich in cholesterol (HFD) would make them more susceptible to liver stress. We found that following 2 months of HFD feeding, the heterozygous mice were healthier than the wildtype controls. They displayed better glucose tolerance, liver enzyme levels and histology. Furthermore, gene expression of UPRmt were significantly higher in the HFD heterozygous mice compared to the HFD fed wildtype controls. The UBL5 KO mice were then treated with pioglitazone, or an ACE2-containing virus to determine if such treatments provide benefit. Liver enzymes and fat accumulation showed significant improvement after treatment with both pioglitazone & ACE2. Which had UPRmt upregulated in pioglitazone treated group and normalized in ACE2 treated UBL5 KO mice. The current dissertation demonstrated that a liver-specific deletion of the mitochondrial stress response gene UBL5 in adult mice leads to reduced UPRmt, mitochondrial dysfunction / hepatic failure and early death. We have generated a model that develops severe fatty liver disease and have shown that both genetic & pharmacological therapies may diminish this disease process. This study provides the first evidence for a critical role for UBL5 and UPRmt in hepatic function. However, the main reason of liver failure remains unknown and further study is required. In lower species the homeostatic nature of the UPRmt it is well-known. If this pathway is sustained in mammals, controlling this stress response might help to establish a therapeutic strategy to cure disease characterized by mitochondrial disruption.

DECLARATION

This is to certify that:

i. The dissertation comprises only my original work towards the PhD, except where indicated in the Preface,

ii. Acknowledgement has been made in the text to all other material used,

iii. The thesis is less than 100,000 words in length, exclusive of tables, maps, bibliographies and appendices.

……

Viktoria Ntouma

August 2019

PREFACE

Ozgene (Bentley DC, WA, Australia) designed and produced the targeting construct for the generation of UBL5 knockout mice.

Plasma concentrations of cholesterol and triglycerides were measured by Jennifer Horvath, Clinical Trials Department, Austin Pathology, Austin Health.

We obtained the virus recombinant adeno-associated viral vector serotype 2/8 with *ACE2* (rAAV2/8-ACE2) and the vehicle vector (rAAV2/8+ Human serum albumin (HAS)) from our collaborator Dr. Chandana Herath (Angus group) (The University of Melbourne, Austin Health) (Mak et al., 2015a).

The human liver samples were received by the Victorian Cancer Biobank (Austin Health) with the help from A/Prof. Elif I Einchi.

In addition, all the training I received at the start of the current PhD project were carried out by Dr. Benjamin Lamont, Dr. Barbara Fam, Dr. Salvatore Mangiafico and A/Prof Sofianos Andrikopoulos.

I, Viktoria Ntouma, contributed in a major fashion to all the design, organization, conduction of the experiments, analyses of the datasets and writing of the scientific papers that are currently in writing progress. Mr. Christian Haralambous assisted in experiments such as oral glucose tolerance and mitochondrial respirometer (oroboros).

PUBLICATIONS

Published Abstracts and Conference Presentations:

Ntouma V. Haralambous C, Fam BC. Andrikopoulos S. Mitochondrial Stress and Metabolic Dysfunction in the Liver – A Role For The Unfolded Protein Response. 2019 August. Australian Diabetes Congress. (Poster presentation)

Ntouma V. Haralambous C, Andrikopoulos S. Liver-Specific Deletion of the Mitochondrial Stress UBL-5 Gene Leads to Fatty Liver That Is Rescued by Pioglitazone Administration or ACE2 Overexpression. American Diabetes Association, July 2018

Ntouma V. Haralambous C. Lamont B. Ekinci E. Liver-Specific deletion of UBL-5 associated mitochondrial stress is associated with liver failure that is improved by ACE2 expression or pioglitazone administration. August 2017- Australian Diabetes Society Oral presentation, elected for Pincus Taft young Investigator, Finalist

Ntouma V. Lamont B. Haralambous C. Mangiafico S. Andrikopoulos S. Liver-Specific Deletion of The Mitochondrial Stress Gene UBL-5 Leads To Liver Failure. August 2016 – Australian Diabetes Society. Oral presentation, elected for Pincus Taft young Investigator, Finalist

Manuscripts in progress:

Impaired liver function and morphology in liver-specific deletion of the mitochondrial gene UBL5

Viktoria Ntouma, Christian Haralambous, Barbara Fam, Sofianos Andrikopoulos

Rescue of UBL5 KO mice by ACE2 and/or pioglitazone therapies (survival and outcome)

Viktoria Ntouma, Christian Haralambous, Barbara Fam, Chandana Herath, Sofianos Andrikopoulos

Induced fatty liver in heterozygous UBL5 mice versus controls using 21% fat, 2% cholesterol diet

Viktoria Ntouma, Christian Haralambous, Barbara fam, Sofianos Andrikopoulos

ACKNOWLEDGMENTS

I would like to acknowledge my primary supervisor Associate Professor Sofianos Andrikopoulos, to whom I am incredibly thankful for giving to me this great opportunity to work on this fabulous project. I was looking for a project for a long time, it almost felt like impossible and that I would never do a PhD. Then it was when my dearest friend Chrisa introduced me to Sof and he suggested me to “give it a shot” one more time. I immediately felt like home in his laboratory and decided to apply for PhD again with the University of Melbourne. Sof I will always be grateful for your mentorship and guidance toward my PhD journey. You have given to me multiple chances to attend scientific meetings in Australia and overseas, which greatly benefits me in my career. I will never forget the knowledge and mentorship you have shared with me. I also would like to thank my secondary supervisor Associate Professor Elif I Ekinchi for her advice and encouragement to broaden my horizons in research. Thank you Elif for your optimism, enthusiasm about research and the positive energy you always have and project to others. Also, I would like to thank Professor Joseph Proietto that always provided me with inspiration and motivation. Jo your passion for research and your innovative ideas will always guide me in the future.

I would also like to sincerely thank Dr. Barbara Fam who helped me through my entire PhD and assisted me greatly with my thesis writing and with all my presentations and posters. Barbara, thank you for your constant guidance, mentorship and support, you were always there in my best and my worst, you always managed to handle all my stress and all my meltdowns in the best way you could. You treated me and Christian like your family members and was looking after us all these years. I am very glad we had the chance to work together and I hope we will continue in the future.

I owe a particular thanks to Dr. Benjamin Lamont for starting this project and providing me with all his knowledge and wisdom. Ben, you are a great scientist and you will be

always my role model even if you decided to step away from research. Your deep understanding of science and your calm passiveness of knowledge guided me at the beginning of my PhD and taught me how a good teacher/supervisor should be.

Most importantly I would like to thank all the past and present Andrikopoulos lab members. I could never have succeeded without your help and support. To Christian Haralambous, thank you for being there for me through my entire PhD. You supported and helped me more than anyone through this journey, I don't know how I would manage to do it if you were not there. I will never forget all these long days and nights we spent in the lab together. Thank you for cheering me up when I was sad, standing all my craziness, criticizing my thoughts, improving my writing, explaining difficult theories and helping me with my experiments. You are the best Christian; I will never forget the fun we had together and you will be always my friend. To Dr. Chrisa Xiruchaki, thank you for introducing me to this lab and for making the PhD experience more pleasant, I will never forget the great time we had together, our long chats, coffees and all the fun we had together. Chrisa, you will be always my friend and sister. To Dr. Salvatore Mangiafico thank you for challenging me in my PhD, we may have had some arguments but we also had fun. I know that you always cared about all the students and about the lab. To Miss. Amy Huang, Dr. Jessie Yung, Dr. Christo Joannides, Dr. Evelyn Martin and Mr. Yanni Arsenakis, all of whom were next to me during this years, your help and advice undoubtedly helped me get through this PhD.

Moreover, I would like to thank Dr. Chandana Herath who played a very important advisory role in the completion of my PhD. As my advisory committee, I thank you for your help and guidance through my whole journey.

Generally, I would like to thank to everybody from the Department of Medicine (Austin Health) with a special thanks to Mrs. Joanne Mayall, Mrs. Minh Nguyen, Mrs. Gina Barri-Rewell, Mr. Joey Santos and Mrs. Meri Kalajdziovski for their IT support and their help inside and outside the lab.

Last but not least, to my family. To my husband George Zisis, I am appreciative for your acceptance and kindness during this tough stage of my life and for being my biggest

supporter. Also to my big sister Lily Ntouma thank you for being my first best friend and my first role model, I look up to you in every sense of the word. Finally, to my parents Yanni (Ioanni) Ntouma and Xenia Ntouma thank you for all the opportunities you have given me in order to reach the utmost success. I would not have completed this PhD without your understanding, tremendous support and endless belief in me. Thank you for constantly putting my happiness before your own and for loving me unconditionally.

TABLE OF CONTENTS

LIST OF TABLES

LIST OF FIGURES

ABBREVIATIONS

4-HNE	4-hydroxynonenal
4-OHT	4-hydroxytamoxifen
A260	Absorbance at 260 nm
A280	Absorbance at 280 nm
AAA	ATPase associated with diverse cellular activities
ACACA	Acetyl-CoA carboxylase 1
ACE2	Angiotensin-Converting Enzyme 2
ADP	Adenosine disphosphate
ALP or AP	alkaline phosphatase
ALT	alanine aminotransferase
AMA	Antimycin-A
AMV	Avian Myeloblastosis Virus
Ang-(1-7)	Angiotensin 1 to 7
APN	Australian Phenomics Network
AST	aspartate aminotransferase
ATF4	Activating transcription factor 4
ATF5	Activating transcription factor 5
ATF6	Activating transcription factor 6
ATP	Adenosine trisphosphate
AUC	Area under curve
BHYB	Beta-hydroxybutyrate
Bili	Bilirubin
BMI	Body-mas index
bp	Base pairs

BRF	Bioresources Facility
BSA	Bovine serum albumin
Ca^{2+}	Calsium
CAC	Citric acid cycle
cDNA	Complementary DNA
CHOP	CCAAT/enhancer-binding protein homologous protein
CI	Complex I
CII	Complex II
CIII	Complex III
Clpp	Caseinolytic Mitochondrial Matrix Peptidase Proteolytic Subunit
ClpP-1	Clp protease proteolytic subunit
Clpx	Caseinolytic Mitochondrial Matrix Peptidase Chaperone Subunit
ClpXP	ATP-dependent Clp protease ATP-binding subunit clpX-like
CO_2	Carbon dioxide
CoA	Coenzyme A
COL13A1	Collagen alpha-1
Con	Controls
CPT1-α	Carnitine palmitoyltransferase 1A
Cre/lox	Site-specific recombinase
Ct	Cycle threshold
Ctc-c	Cytochrome-C
DEPC	Diethyl pyrocarbonate
DMSO	Dimethyl Sulfoxide
DNA	Deoxyribonucleic acid
dNTP	Deoxyribose nucleotide triphosphates
DTT	Dithiothreitol
DVE-1	Defective proventriculus in Drosophila homolog
DZ	Dizygotic
e.g	exempli gratia, for example

ECL	Enhanced chemiluminescence
EDTA	Ethylenediaminetetraacetic acid
eIF2α	Eukaryotic translation-initiation factor 2 alpha
ER	Endoplasmic reticulum
et al.	et alii; and others
ETC	Electron transport chain
$FADH_2$	Flavin adenine dinucleotide
FASN	Ethylenediaminetetraacetic acid
FBS	Fetal bovine serum
FCCP	Carbonyl cyanide 4-(trifluoromethoxy) phenylhydrazone
FDFT1	Farnesyl diphosphatase farnesty transferase 1
Flp/Frt	Site-directed recombination technology
GAPDH	Glyceraldehyde-3-phosphate dehydrogenase
GWAS	Genome wide association studies
GTT	Glucose tolerance test
H&E	Hematoxylin and eosin
H_2O	Water
HAF-1	HAIF transporter (PGP related)
HAS	Human serum albumin
HBSS	Hanks' balanced salt solution
HDL	High-density lipoprotein
HEPES	4-(2-hydroxyethyl)-1-piperazineethanesulfonic acid
HFD	High fat diet
HF-fed	High fat fed
HSP	Heat shock protein
HSP10	Heat shock protein 10
HSP60	Heat shock protein 60
HSP70	Heat shock protein 70
i.e	id est; that is
i.p	Intraperitoneal
ID	Internal diameter

IR	Insulin receptor
IRE	Inositol requiring
IRS	Insulin receptor substrate
IU	International unit
Kb	Kilo base pair
KCL	Potassium Chloride
KD	Knock down
kg	Kilograms
KH2PO4	Monopotassium phosphate
KO	Knock out
LDL	Low density lipoprotein
Lonp-1	Lon Peptidase 1
LoxP	“floxed” allele
Mag	Magnesium chloride
Mal	Malate
Mas	MAS proto-oncogene or MAS1 proto-oncogene G protein-coupled receptor
MCM	Mer cre mer
MC	monozygotic
ml	Mililitre
mmol	Milimoles
MNDA	Malondialdehyde
mRNA	Messenger RNA
NaCl	Sodium chloride
NAD+	Nicotinamide adenine dinucleotide
NADH	reduced nicotinamide adenine dinucleotide
NAFLD	Non-alcoholic fatty liver disease
NaOH	Sodium hydroxide
NASH	Non-alcoholic steatohepatitis
NDUFB3	NADH dehydrogenase (ubiquinone) 1 beta subcomplex 3
NDUFB5	NADH dehydrogenase (ubiquinone) 1 beta subcomplex 5

NDUFS1	NADH ubiquinone oxidoreductase 75kDa subunit
NDUFV1	NADH ubiquinone oxidoreductase core subunit V1
ng	Nanogram
nM	Nanomolar
NPY	Neuropeptide Y
OGTT	Oral glucose tolerance test
OXPHOS	Oxidative phosphorylation
PBS	Phosphate buffered saline
PCR	Polymerase chain reaction
PERK	protein kinase RNA-like ER kinase
PGC-1α	Peroxisome proliferator-activated receptor gamma coactivator-1 alpha
pH	acidity or alkalinity of a solution on a logarithmic scale
Pl-3K	phosphatidylinositol-3 kinase
PNPLA3	Patatin-like phospholipase domain-containing 3
PPARs	Peroxisome proliferator-activated receptors
PPARα	Peroxisome proliferator-activated receptor alpha
PPARγ	Peroxisome proliferator-activated receptor gamma
PVDF	Polyvinylidene fluoride
Pyr	Pyruvate
rAAV2/8	recombinant adeno-associated viral vector serotype 2/8
RG	Right gastrocnemius
RNA	Ribonuclei acid
RNA	Ribonucleic acid
RNAse	Ribonuclease
ROS	Reactive oxygen species
Rot	Rotonone
rRNA	ribosomal RNA
SDHB	Succinate dehydrogenase (ubiquinone) iron-sulfur subunit
SEM	Standard error of the mean
SNP	Single nucleotide polymorphism

SPG7	Spastic paraplegia 7
T2D	Type 2 diabetes
TAE	Tris-acetic acid EDTA
Taq	Themus aquaticus
TBE	Tris-borate EDTA
TCA	tricarboxylic acid
TE	Tris-EDTA
TEMED	Tetramethylethylenediamine
TTR	Transthyretin
U	Units
UBL5	Ubiquitin-like protein-5
$UBL5^{Liver-/-}$	UBL5 homozygous mice
$UBL5^{Liver-/+}$	UBL5 heterozygous mice
UPR	Unfolded protein response
UPR^{ER}	Endoplasmic reticulum unfolded protein response
UPRmt	Mitochondrial unfolded protein response
UV	Ultraviolet light
VLDL	Very low density lipoprotein
WAT	White adipose
XBP-1	X binding protein 1
ΔΔCt	Comparative Ct

CHAPTER 1: LITERATURE REVIEW

1.1 Introduction

Mitochondria are the powerhouses centres of the cell whose actions are critical for normal cell functioning. The most important role of mitochondria is to generate the energy the cell needs but they are also known to play a crucial role in metabolism and cell death (Manoli et al., 2007). Mitochondrial dysfunction is known to be associated with several diseases including non-alcoholic steatohepatitis (NASH) and Type 2 diabetes where it has been implicated in hepatic fat accumulation and hepatic insulin resistance (Ekström & Ingelman-Sundberg, 1989; García-Ruiz et al., 2006; Hagihara, Sato, Fukuhara, Tsutsumi, & Ōyanagui, 1973; D. E. Kelley, J. He, E. V. Menshikova, & V. B. Ritov, 2002; G. Marchesini et al., 2001; Marchesini et al., 1999; G. Marchesini et al., 2003; Moriya et al., 2001; Nobuhir et al., 1977; D. Pessayre & B. Fromenty, 2005). Mitochondrial dysfunction can be caused by build-up of reactive oxygen species (ROS) which leads to the activation of a stress response known as the mitochondrial unfolded protein response (UPRmt). Studies in *C. Elegans* and mammalian cells have shown that a gene called ubiquitin-like protein-5 (UBL5) is involved in the UPRmt, to ensure chaperone proteins (proteins that lead proteins toward the correct pathway for folding) are transcribed and available to relieve stress. Failure of these responses to adapt to or repair damage from stress results in mitochondrial dysfunction and may lead to apoptosis and eventually cell death (Benedetti, Haynes, Yang, Harding, & Ron, 2006). Also, up-regulated levels of *UBL5* may be associated with metabolic disorders such as dyslipidaemia and hyperinsulinemia. However, the actual mechanism(s) underlying the action of *UBL5* in metabolic disorders as well as liver dysfunction has not been fully clarified. (Bozaoglu et al., 2006a; Jowett et al., 2004). The work in this thesis will document the systematic assessment of the role of the UPRmt and in particular, the role of UBL5 using a liver-

specific loss of function mouse model. This chapter will further describe in detail the importance of normal mitochondrial function, the role of mitochondrial dysfunction in the pathogenesis of metabolic disorders and the importance of the stress gene UBL5 in mitochondrial function.

1.2 Mitochondria

Most eukaryotic cells contain a double bound membrane organelle called mitochondrion. It consists of an outer membrane, inner membrane, the interstitial space of membranes and the matrix. The matrix is responsible for many metabolic reactions, including the citric acid cycle, whilst the inner membrane is involved in aerobic respiration and is also the site of the electron transport chain (B. Alberts et al., 2002). The most important role of mitochondria is to generate energy that the cell needs (Manoli et al., 2007). This is dependent on cytosolic respiration, where products such as NADH, glucose and pyruvate are oxidized (Voet, Judith, & Pratt, 2006; Voet, Voet, & Pratt, 1999). Mitochondria are responsible for the cycle of citric acid and pyruvate transfer, where products of glycolysis (pyruvate molecules) are transferred through the inner mitochondrial membrane into the matrix and conjugate with coenzyme A (CoA) by oxidation to form CO_2, NADH and Acetyl-CoA. Moreover, pyruvate molecules can form oxaloacetate through carboxylation. This reaction occurs when the energy needs of the tissue are increased (Berg, Tymoczko, & Stryer, 2008; Williamson & Corkey, 1969). In the matrix, the citric acid cycle releases two carbon dioxide molecules and produces NADH and Flavin adenine dinucleotide ($FADH_2$), and through the electron transport chain the redox energy from NADH and $FADH_2$ is converted to oxygen. Energy rich molecules can also be generated through glycolysis in the cytoplasm (Berg et al., 2008; Nishikawa et al., 2000; Williamson & Corkey, 1969). Also, mitochondria have the ability to store calcium (Ca^{2+}) temporarily and contribute to cellular Ca^{2+} homeostasis, Ca^{2+} signalling and induce apoptosis (Hajnóczky et al., 2006; Siegel, Agranoff, Albers, Fisher, & Uhler, 1999).

In addition, mitochondria are also involved in a number of different processes including; signalling via mitochondrial ROS (X. Li et al., 2013) and hormones (Klinge, 2008), synthesis of steroids (Rossier, 2006), metabolic regulation (McBride, Neuspiel,

& Wasiak, 2006) and apoptosis (death of the cell) (Green, 2005; Koopman, Willems, & Smeitink, 2012).

1.2.1 Mitochondrial metabolic Pathways:

The breakdown of nutritional molecules (from food) to energy is a process called cellular respiration. Mitochondria perform several metabolic processes (including glycolysis, fatty acid β-oxidation, amino acid catabolism, citric acid cycle and electron transport chain) to provide the cell with the required energy (Figure 1.1).

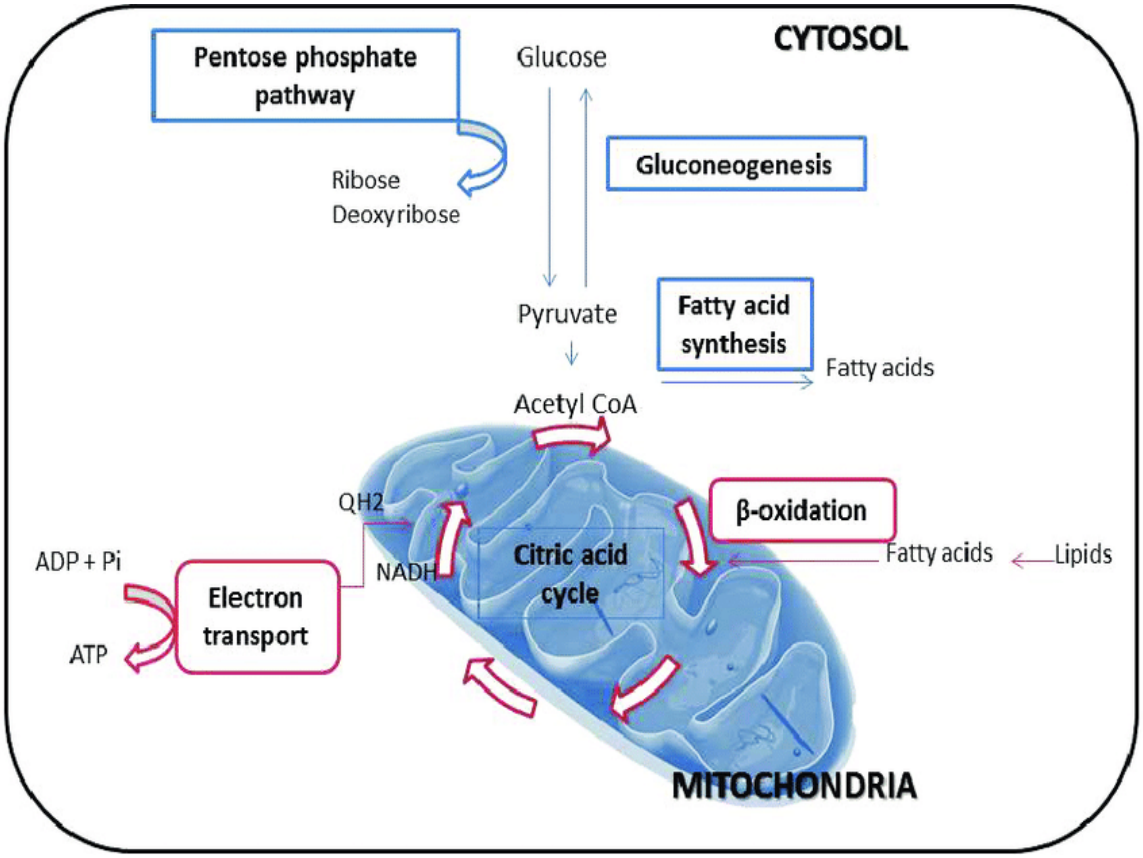

Figure 1.1: Mitochondrial metabolic pathways: Mitochondria is important in energy metabolism (citric acid cycle, oxidative phosphorylation, and fatty acid breakdown pathways), biosynthesis, and catabolism (Ortiz et al., 2016).

Glycolysis involves a group of reactions that breakdown glucose to two molecules of pyruvic acid (pyruvate) and adenosine triphosphate (ATP) under aerobic conditions and lactate under anaerobic conditions with small amounts of energy. First, glucose is phosphorylated to glucose -6- phosphate via the intermediates glucose1,

6-diphosphate, glyceraldehyde-3-phosphate and phosphoenolpyruvate leading to the production of pyruvate. Pyruvate can be used in anaerobic respiration or aerobic respiration. In the presence of oxygen, pyruvate converts to acetyl coenzyme A (CoA) and enters the tricarboxylic acid cycle. The net energy gain of this route is two ATP molecules for each molecule of degraded glucose. It includes a single redox reaction, in which nicotinamide adenine dinucleotide (NADH) cytoplasmic molecules are generated. In aerobic organisms, the NADH formed during glycolysis transports its electrons to O_2 through the electron transport chain for oxidative phosphorylation and thus regenerates NAD^+. Under anaerobic conditions, NAD^+ is regenerated during the synthesis of lactic acid or ethanol from pyruvate (B. Alberts et al., 2002; P. Alberts et al., 2002; Reece et al., 2011) .

Another metabolic reaction is gluconeogenesis; the synthesis of glucose from non-carbohydrate sources, such as lactic acid, certain amino acids and glycerol. The main organ for gluconeogenesis is the liver and through this metabolic pathway the body maintains blood glucose at normal levels. Although many of the gluconeogenic reactions are common to the glycolytic reactions, gluconeogenesis and glycolysis are regulated inversely, so that when one pathway is active the other is inactive (B. Alberts et al., 2002).

Fatty acid β-oxidation is the major metabolic pathway that is responsible for the mitochondrial breakdown of long-chain acyl-CoA molecules to acetyl -CoA molecules. The four main enzymes that are involved in this process are, acetyl -CoA dehydrogenase, enoyl -CoA hydrates, hydroxyacyl -CoA dehydrogenase and ketoacyl CoA thiolase. At the end of each β-oxidation cycle, two new molecules are formed; an acetyl-CoA and an acyl-CoA that is two carbons shorter and enters the citric acid cycle. Additionally, during β-oxidation NADH and Flavin adenine dinucleotide ($FADH_2$) are formed. The $FADH_2$ and NADH produced during the process of fatty acid β-oxidation are used by the electron transport chain to produce ATP (B. Alberts et al., 2002) (Reece et al., 2011). Transcriptional and post-transcriptional mechanisms regulate the proteins involved in fatty acid β-oxidation. The most well-known transcriptional regulators of fatty acid β-oxidation are the peroxisome proliferator-activated receptors (PPARs) and a transcriptional factor coactivator peroxisome proliferator-activated

receptor gamma coactivator-1 alpha (PGC-1α) (Huss Janice & Kelly Daniel, 2004). PGC-1α is responsible for mitochondrial biogenesis, and cellular energy metabolism in several organs such as liver. In liver PGC-1a also regulates gluconeogenesis, fatty acid β-oxidation, heme biosynthesis and ketogenesis (Handschin et al., 2005; Rhee et al., 2003).

Amino acid catabolism is a digestion process of proteins which involves a breakdown of micro-molecules into amino acids. Amino acids are mainly used for peptide and protein synthesis and for the synthesis of additional amino acids and other nitrogen compounds. When the amino acids exceed what was needed for biosynthesis, they are degraded and used as metabolic fuel. Carbon skeleton is converted to Acetyl-CoA, Acetoacetyl -CoA, pyruvate or citric acid cycle intermediates. The amino group nitrogen is converted to urea and excreted in the urine. Also, glucose, fatty acids, ketone bodies can be formed from amino acids (Felig, 1975; G. Wu, 1998).

The citric acid cycle (CAC) is also known as the tricarboxylic acid cycle or the Krebs cycle. It takes place in mitochondria and it is a metabolic pathway by which all aerobic organisms generate energy through a breakdown of fuel molecules in the cell. It is a series of eight chemical reactions that generate energy through the oxidation of acetate (in the form of acetyl-CoA) resulting from carbohydrates, fats, and proteins into carbon dioxide (CO_2) and high-energy molecules such as GTP/ATP and $FADH_2$. Through oxidative phosphorylation NAD^+ reduces to NADH that is used for ATP production (B. Alberts et al., 2002; Holloszy, Oscai, Don, & Molé, 1970).

1.2.1.1 Electron Transport Chain and Oxidative Phosphorylation

The electron transport chain (ETC) consists of protein complexes such as electron acceptors and organic molecules (Complexes I to IV, ubiquinone and cytochrome c) that are located in the inner membrane of the mitochondria. All the electrons that enter the ETC are derived from NADH and $FADH_2$ molecules (obtained from glycolysis, the citric acid cycle or fatty acid oxidation). Oxidative phosphorylation (OXPHOS) is the metabolic pathway in which electrons are passed from one member of the transport chain to another in a series of redox reactions. These redox reactions release energy which is captured as a proton gradient and is used to form ATP (ATP

synthase also known as Complex V), this process is called chemiosmosis (B. Alberts et al., 2002; Starkenburg et al., 2006). Even though oxidative phosphorylation is essential for metabolism, it produces ROS products such as superoxide and hydrogen peroxide. ROS may lead to the spread of free radicals that can damage cells leading to disease and possibly aging (Schieber & Chandel, 2014). Mitochondria play an important role in maintaining metabolic homeostasis. An imbalance in any of the steps of these critical pathways, could lead to reduced ATP synthesis and possible cell death (Eguchi, Shimizu, & Tsujimoto, 1997; Ha & Snyder, 1999; Tiwari, Belenghi, & Levine, 2002).

1.2.2 Mitochondrial Dysfunction

Mitochondrial dysfunction has been linked to several disorders that affect energy metabolism. Insulin resistance, a state that is commonly observed in patients with obesity and/or type 2 diabetes, is linked to mitochondrial dysfunction (Lowell & Shulman, 2005) (Abdul-Ghani & DeFronzo, 2008). In addition, it is implicated in most liver diseases and in early graft dysfunction after liver transplantation (Chan, 2006; Fernández-Silva, Enriquez, & Montoya, 2003; Kikis, Gidalevitz, & Morimoto, 2010; Rector et al., 2010; Shutt & Shadel, 2010).

Mitochondria are capable of their own replication, transcription, and translation of DNA. Most of the mitochondrial proteins are encoded by nuclear DNA, translated in the cytoplasm and conveyed into the mitochondria. Mutations in mitochondrial DNA and nuclear DNA genes are linked to mitochondrial disorders. However, only few of these mutations have been characterized. (Anderson et al., 1981; Shoffner, 1995; Douglas C Wallace, 1992). Genetic mutations in genes that regulate important metabolic pathways (such as protein homeostasis (proteostasis) and proper protein folding, can lead to mitochondrial dysfunction). (Bukau, Weissman, & Horwich, 2006; T. Tatsuta & T. Langer, 2008; Young, Agashe, Siegers, & Hartl, 2004). This could lead to an increased accumulation of unfolded proteins in the mitochondrion. When the proper protein-folding exceeds the capacity of chaperones (proteins that lead proteins toward the correct pathway for folding), protein miss -folding and aggregation may occur. In case of an increased accumulation of unfolded proteins in the mitochondria

the cells trigger an adaptive protective mechanism against misfolded or unfolded proteins (T. Tatsuta & T. Langer, 2009).

Several aspects and complications can stress the mitochondrial protein folding environment, one of the most common is increased ROS production (oxidative stress), also environmental factors such as toxins and temperature may impair the protein folding pathway (B. M. Baker & Haynes, 2011).

1.2.2.1 Mechanisms of mitochondrial dysfunction

Physiologically there is a modest amount of ROS that is generated within mitochondria during cellular respiration, which is then degraded by the protective mechanism inherent to the cell. Under normal circumstances, generation of ATP and ROS rise when there is increased demand for the respiratory chain to metabolise more substrates or reoxidize NADH and $FADH_2$. In small amounts, ROS can be beneficial to the cell, though increased ROS levels are extremely harmful and can cause impairment of oxidative phosphorylation leading to oxidative stress (X. Wang & Michaelis, 2010).

Oxidative stress is one of the primary defects responsible for mitochondrial dysfunction. Mitochondrial permeability transport pores are triggered to open when oxidative stress occurs and this allows the protons out of the intermembrane space. Cytochrome-C is released into the cytosol and activates caspases leading the cell to death (apoptosis). Also apoptosis can be induced through upregulation of Fas-ligand transcription that binds to death receptors on hepatocytes (D. Pessayre, Berson, Fromenty, & Mansouri, 2001).

Due to mitochondrial damage and increased ROS levels impairment in fatty acid β-oxidation may occur. This can lead to fatty acids forming into triglycerides that usually are exported from the cell as lipoproteins (VLDLs) or are stored within the cell as lipid vesicles. However, the reason for triglyceride accumulation remains unclear. Increased levels of the remaining unused fatty acids may form micelles with the neutral triglycerides, preventing their export from the cell and leading to toxicity (Fromenty &

Pessayre, 1995; Rosca et al., 2012).This can lead to formation of micro-vesicular steatosis (small lipid-consecrating vesicles) in the cell (Fromenty & Pessayre, 1995).

1.2.2.2 Defects associated with mitochondrial dysfunction

Several disorders have linked in the past with mitochondrial dysfunction. Including, but not limited to type 2 diabetes, metabolic syndrome, non-alcoholic liver disease, cancer, heart disease (Henze & Martin, 2003; Kim, Wei, & Sowers James, 2008; Lesnefsky, Moghaddas, Tandler, Kerner, & Hoppel, 2001; McBride et al., 2006; Douglas C. Wallace, 2005).

1.2.2.2.1 Metabolic Syndrome

Metabolic syndrome is a global public health problem. It correlates with several disorders such as central obesity, hypertension, glucose intolerance and dyslipidaemia, and eventually may lead to the development of type 2 diabetes, Non-alcoholic fatty liver disease (NAFLD) and cardiovascular disease (Eckel, Grundy, & Zimmet, 2005). Sedentary lifestyle and consumption of high energy diets are the major causes of metabolic syndrome, although genetic factors may also play a role (Isomaa, 2003).

Type 2 Diabetes is the result of a multi-interaction mechanism of a variety of metabolic disorders and each one of these may have a different cause. Over recent years, efforts have focused in studying environmental and genetic factors that are linked to T2D, whilst understanding the contribution of each of these factors has been difficult. It is estimated that if one parent has diabetes there is 40% chance for children to develop the condition during their lifetime and 70% chance if both parents are affected (Meigs, Cupples, & Wilson, 2000). Furthermore a study from Finland showed that monozygotic (MC) twins have higher chances of developing T2D (20% pairwise) compared with dizygotic (DZ) twins (8% pairwise) and showed that heritability was the lead cause (46%) followed by shared and unshared environmental effects (15% and 38% respectively) (Murea, Ma, & Freedman, 2012)

(Kaprio et al., 1992). In addition, a systematic review summarised environmental factors that could affect genetic factors and potentially lead to obesity, hypertension, increased blood lipid levels, prediabetes and eventually T2D. Among these factors are air pollution, stress, unhealthy diet and physical inactivity (Dendup, Feng, Clingan, Astell-Burt, & health, 2018). Genome wide association studies (GWAS) that are currently the gold standard methodology to identify genes associated with T2D have indicated several gene candidates that contribute toward development of T2D. Some of the key genes involved in the process of insulin secretion include KCNJ11, HNF1A/1B, WFS1, GCK, TCF2 (Gloyn et al., 2003) (Murea et al., 2012) and the PPARG that is implicated in insulin resistance (Altshuler et al., 2000) (Murea et al., 2012). Genetic research has evolved over the past few years, with research focussing on understanding the roles and involvement of genes towards the development of T2D.

Mitochondria are essential for the maintenance of metabolic homeostasis and normal cell function. As a powerhouse of the cell it is important for metabolism of nutrients and energy production (ATP) (Douglas C. Wallace, 2005). Several factors (genetic and external) could affect mitochondrial activity, among them are hormones, nutrients, hypoxia, aging and temperature. This may impact cells proliferation, growth and survival (Frisard & Ravussin, 2006; Kim et al., 2008; Douglas C. Wallace, 2005). Many chronic diseases such as obesity, type 2 diabetes, insulin resistance, cancer and cardiovascular disease may associate with mitochondrial dysfunction (Henze & Martin, 2003; Kim et al., 2008; Lesnefsky et al., 2001; McBride et al., 2006; Douglas C. Wallace, 2005). Yet, it is not clear if mitochondrial dysfunction is the prime cause of these dysfunctions.

Liver is essential in metabolism, it plays a key role in energy balance (carbohydrate metabolism, fat metabolism and protein metabolism and plays a vital role in the development of type 2 diabetes and metabolic syndrome (L. J. C. p. Rui, 2011). Studies have shown that NAFLD is a risk factor that implicates type 2 diabetes and insulin resistance (Lonardo & Trande, 2000; Giulio Marchesini et al., 2001; Giulio Marchesini et al., 2003). A study on patients with biopsy proven NAFLD (with normoglycemia and normal body weight) versus patients with type 2 diabetes showed that both groups share similar clinical and laboratory data. These data included a 50% reduction of glucose disposal during euglycemic clamp, increased basal free fatty

acids and similarly reduced insulin-mediated suppression of post-absorptive hepatic glucose production (Lonardo & Trande, 2000). Therefore, NAFLD with specific hepatic insulin resistance could be considered as an extra feature of metabolic syndrome. Additionally, data reports presented NAFLD as a risk factor of some individual components (arterial hypertension) (Donati et al., 2004; Ikai et al., 1993) and dyslipidaemia (Lonardo, Bellini, Tartoni, Tondelli, & hepatology, 1997) of metabolic syndrome.

1.2.2.2.2 Diabetes Mellitus

Diabetes Mellitus is characterized by hyperglycaemia that is caused because of defects in insulin secretion, insulin action or the combination of these two aspects (American Diabetes, 2009; care, 2013). Chronic hyperglycaemia can cause dysfunction of multiple organs such as kidneys, eyes, feet, blood vessels and heart (American Diabetes, 2009; care, 2013).

Diabetes can be divided in two broad etiopathogenetic categories: Type 1 diabetes with complete deficiency of insulin and Type 2 diabetes that combines resistance to insulin action and an insufficient compensatory insulin secretory response (American Diabetes, 2009; Diabetes, 1979; Gale, 2006). Recent evidence suggests that mitochondrial dysfunction plays a significant role in impaired insulin action and impaired insulin release. Given the important role of mitochondria in aerobic metabolism, they may be implicated in diabetes through different metabolic tissues such as pancreas, liver and muscle (Sivitz & Yorek, 2010). Studies have shown that patients with diabetes present with abnormally shaped and less dense mitochondria (D. E. Kelley, J. He, E. V. Menshikova, & V. B. J. D. Ritov, 2002; Morino et al., 2005; Ritov et al., 2005). Studies in insulin deficient rodents have shown reduced mitochondrial cristae and growth of electron-dense granules with the presence of lipid droplets around the mitochondria (Chao et al., 1976). Furthermore, rats with induced diabetes (either with alloxan or streptozotocin) showed swelling and damaged mitochondria, that were decreased in number in liver and heart (Herlein, Fink, O'Malley, & Sivitz, 2008; Marinari, Monacelli, Cottalasso, & Novelli, 1974).

1.2.2.2.2.1 Type 1 Diabetes

Type 1 diabetes is an immune-mediated disorder affecting 5-10% of all the diabetic patients and results from an autoimmune destruction of the pancreatic β-cells. It is characterized by hyperglycaemia and the causes are still not clearly understood (American Diabetes, 2009; care, 2013; Daneman, 2006; Roep, 2003).

1.2.2.2.2.2 Type 2 Diabetes

Type 2 diabetes accounts for approximately 90-95% of those suffering from diabetes (American Diabetes, 2009). Type 2 diabetes is a progressive syndrome; it involves disorders in insulin release and insulin action. It presents with both β-cell dysfunction of pancreas and insulin resistance in insulin sensitive organs such as liver, muscle and adipose tissue (Kahn, Hull, & Utzschneider, 2006; lancet, 1998).

1.2.2.2.3 Liver Function and Dysfunction

The liver is a large secretory organ, responsible for the production of very low-density lipoprotein (VLDL), high-density lipoprotein (HDL) particles, also lipoproteins particles (such as cholesterol and triglycerides), hormones, albumin and blood clotting factors. The liver is a major regulator of triglycerides and glucose in the blood with hepatocytes as the primary cells performing these functions. The liver regulates carbohydrate and whole-body lipid and urea metabolism and is highly responsive to nutritional flux (Rolfe & Brown, 1997; L. Rui, 2014). It produces most of the plasma proteins and controls the detoxification of exogenous chemicals. In liver mitochondria, ammonia becomes detoxified through specific enzymes (Häussinger, Sies, & Gerok, 1985). The liver along with muscle and white adipose tissue are major targets of insulin and glucagon. Insulin upregulates glycogen synthesis, the additional glucose is polymerized and stored for subsequent glycogenolysis. During times of lowered blood glucose levels, it is released to distribute to glucose dependent tissues (Knauf et al., 2005; L. Rui, 2014).

The liver also acts as a reserve for energy storage. Mechanisms including glycogenesis and lipogenesis regulate the storage of carbohydrates and fats in the liver. They are stored as glycogen and triglycerides in the form of lipid droplets that

can be used for VLDL production. This can then be utilised for further energy supply to other organs. Furthermore, fasting and increased glucagon secretion lead to stimulation of glycogenolysis, ketone body production, fatty acid oxidation and gluconeogenesis (Markan & Potthoff, 2016). The liver is also responsible for the clearance of dietary fats or fats that are products of lipolysis from adipose tissue (Knauf et al., 2005; L. Rui, 2014). The liver's proper function is essential to maintain all these metabolic pathways. Impaired hepatic function may lead to acute and chronic liver failure and in more severe conditions it could be fatal. Because of the complexity of liver's function, liver dysfunction can affect other organs/systems. (Younossi et al., 2011).

1.2.2.2.3.1 Non-alcoholic fatty liver disease

NAFLD presents with excess fat accumulation in the liver that is independent of alcohol induced damage. Its progressive nature leads to serious complications such as liver fibrosis and cirrhosis. NAFLD is one of the most common liver diseases worldwide, as it affects up to one third of the adult population and has become one of the major health problems along with obesity. The major risk factors for NAFLD development are metabolic syndrome, obesity, insulin resistance, diabetes and increased age. may play an important role in the development of NAFLD. Recent studies suggest that genetic factors may play an important role in the development of NAFLD. Evidence emerging from several studies such as twin, epidemiological and familial suggest that NAFLD and metabolic cirrhosis may be heritable (Schwimmer et al., 2009). Genome wide association studies (GWAS) have identified Patatin-like phospholipase domain-containing 3 (PNPLA3) gene variants to be important in identification of increased hepatic lipid content in people coming from different backgrounds (inter-individual and ethnicity-related)(Sookoian & Pirola, 2011). Furthermore, a GWAS study reported a SNP in the gene encoding farnesyl diphosphatase farnesty transferase 1 (FDFT1) to be associated with NAFLD by playing a role in cholesterol biosynthesis (Ballestri, Day, & Daly, 2011). Also in the same study a variant of the collagen gene (COL13A1) was found to be associated with inflammation and fibrosis (Ballestri et al., 2011). Additionally, some multicentre case-control studies showed the important role of genetic variants in the development of

oxidative stress (beta-globin mutations) (Paola Dongiovanni, M Anstee, & Valenti, 2013), fibrogenesis (kruppel-like factor 6) (Miele et al., 2008) in insulin signalling (P Dongiovanni et al., 2010) that contribute toward progression of NAFLD to NASH (Anstee, Day, & hepatology, 2013; Dixon, Bhathal, & O'Brien, 2001; Farrell & Larter, 2006)

1.2.2.2.3.2 Steatohepatitis

NASH is a progressive form of NAFLD. In contrast, 2-3% of patients present with NASH. NASH is characterised by fat accumulation plus lobular inflammation, degenerating or ballooned hepatocytes, mallory bodies and fibrosis, that can lead to cirrhosis. Increased fatty acids, oxidative stress and inflammation aid in the development of steatohepatitis and insulin resistance (Xu et al., 2003). Pathogenesis of NASH involves several factors, oxidative stress and insulin resistance are the most important aspects. Initially insulin signalling in the liver is mediated by the IR receptor, that signals via a kinase downstream (tyrosine kinase), protein B/Akt (M. Lu et al., 2012). The Akt signals through transcription factors such as mammalian target of rapamycin complex 1 (mTorc1) (controls protein synthesis) and Foxo (suppressing glucose production) to coordinate hepatic metabolism. When the tyrosine kinase is activated in the IR it triggers the activation of proteins such as (IRS1 - IRS4) that are essential in signalling pathways including activation of phosphatidylinositol-3 kinase (Pl-3K) (Taniguchi, Emanuelli, & Kahn, 2006). Pl-3K is responsible for the metabolic action of insulin such as lipid, glycogen and protein synthesis and distribution of glucose for important cellular functions (Taniguchi et al., 2006) (Boucher, Kleinridders, & Kahn, 2014; De Meyts, 2016; Dufour, Clavien, Graf, & Trautwein, 2010). This signal may be disturbed under oxidative stress because of the stimulation of NF-kB and JNK pathways that cause phosphorylation of insulin-receptor substrates (Hotamisligil, 2006). Under normal conditions the transcription factor PPAR-γ is activated by insulin that stimulates adipogenesis and lipid storage. PPAR-γ is not stimulated when insulin resistance takes place (Dufour et al., 2010). The hepatocyte cannot cope with the excessive amount of fatty acids and cytokines, thus resulting in the activation of several mechanisms that will stress the cell and lead to mitochondrial dysfunction and fat accumulation. For example, fat starts to accumulate in the cell due to the mitochondrial incapability of increasing β-oxidation,

it is unable to cope with the increasing demands and stores in the cell. A major cause of mitochondrial dysfunction is the increased amount of ROS that triggers production of lipid peroxidation (Neuschwander-Tetri & Caldwell, 2003; Dominique Pessayre, Mansouri, & Fromenty, 2002). Lipids are the main cellular components vulnerable to damage by ROS leading to lipid peroxidation. The toxic by-products that are usually produced from this metabolic pathway are malondialdehyde (MNDA) and 4-hydroxynonenal (4-HNE). This may result in an increase in the immune reaction (pre-inflammatory cytokines TNF-α and IL-8) and impairment of the electron transport chain, cell toxicity and death (through Fas ligand expression in hepatocytes). There may be increased collagen production and fibrogenesis through increased levels of growth factor-β and stellate cell stimulation (D. Pessayre et al., 2001). These may lead to histological abnormalities that are shown in patients with NASH. Studies show that about 20% of patients that suffer from NASH may develop cirrhosis and hepatocellular carcinoma (Ratziu et al., 2002).

Further some studies support that mitochondrial dysfunction is implicated in patients with NASH. Electron microscopy images taken from patients with NASH have shown patterns of mitochondrial injury, loss of cristae and crystalline inclusion (Sanyal et al., 2001a). Moreover, there is an approximate 50-70% reduction in the activity of mitochondrial respiratory chain complexes (Pérez-Carreras et al., 2003).

1.2.2.2.3.3 Mitochondria and liver disease

Acute and chronic liver disease is associated with inherited or acquired mitochondrial dysfunction (Mansouri, Gattolliat, & Asselah, 2018). Since liver is a highly metabolic organ, twenty percent of the cytoplasmic volume of hepatocytes contain mitochondria (Ceni, Mello, & Galli, 2014; Miller, Suzuki, Ciftci-Yilmaz, & Mittler, 2010; Waris & Ahsan, 2006). Thus, patients with mitochondrial defects have the propensity to develop mild liver abnormalities or acute liver failure. Defects in the metabolic functions of the liver mitochondria can lead to reduction of cellular energy stores, increased production of ROS, oxidative stress that eventually leads to apoptosis (Kokoszka, Coskun, Esposito, & Wallace, 2001; Rolo, Teodoro, Palmeira, & medicine, 2012).

Autosomal mutations in nuclear genes that can cause rearrangement or deletion of mitochondrial DNA can lead to mitochondrial hepatopathy, a condition that is associated with liver damage/failure. (W. S. Lee & Sokol, 2007) On the other hand, secondary hepatopathies may develop because of defects in mitochondrial function. The most well-known secondary hepatopathies include alcohol-induced liver disease, acute fatty liver of pregnancy, non-alcoholic fatty liver disease and steatohepatitis (NAFLD, NASH respectively), drug-induced liver diseases and chronic hepatitis C (Alberio, Mineri, Tiranti, & Zeviani, 2007; Fellman & Kotarsky, 2011; Koopman et al., 2012; Suomalainen & Isohanni, 2010).

Studies have shown that patients with subtle inherited or acquired defects in mitochondrial function are at higher risk of developing certain types of liver disease. These deficiencies appear when hepatocytes are under an additional physiological stress that exceeds their metabolic capacity (such as in response to various drugs) (Fromenty & Pessayre, 1995; Neuschwander-Tetri & Caldwell, 2003; D. Pessayre et al., 2001; Dominique Pessayre et al., 2002).

1.3 Unfolded Protein Response

Proper protein folding is essential for the cell's normal function and survival (S. Lindquist & E. A. Craig, 1988). The unfolded protein response (UPR) was first identified in bacteria exposed to high temperatures (Tissiéres, Mitchell, & Tracy, 1974). The proteins involved in this protective response became known as heat-shock proteins (S. Lindquist & E. A. Craig, 1988). In mammalian cells, the most well-defined unfolded protein response is mediated by proteins that span the endoplasmic reticulum (ER) membrane (the UPR^{ER}). While the UPR^{ER} is well described in the literature, there is another form of protective response. This occurs in the mitochondria and is called the mitochondrial unfolded protein response (UPRmt). Both responses are triggered to ensure correct protein handling. These pathways will be described in more detail below.

1.3.1 The endoplasmic reticulum unfolded protein response (UPR^{ER})

Protein folding in the ER is sensitive to several conditions such as the environmental redox state, ATP levels and calcium concentration (Schröder & Kaufman, 2005). The UPR^{ER} is a cellular response that is activated upon the accumulation of misfolded proteins in the ER that can disturb homeostasis. The intra-luminal sections of the ER sense the unfolded proteins while the cytosolic segments transmit the signals to the nucleus (Patil & Walter, 2001). This UPR^{ER} prevents the accumulation of deleterious unfolded protein aggregates and resolves the protein folding defect (Figure 1.2).

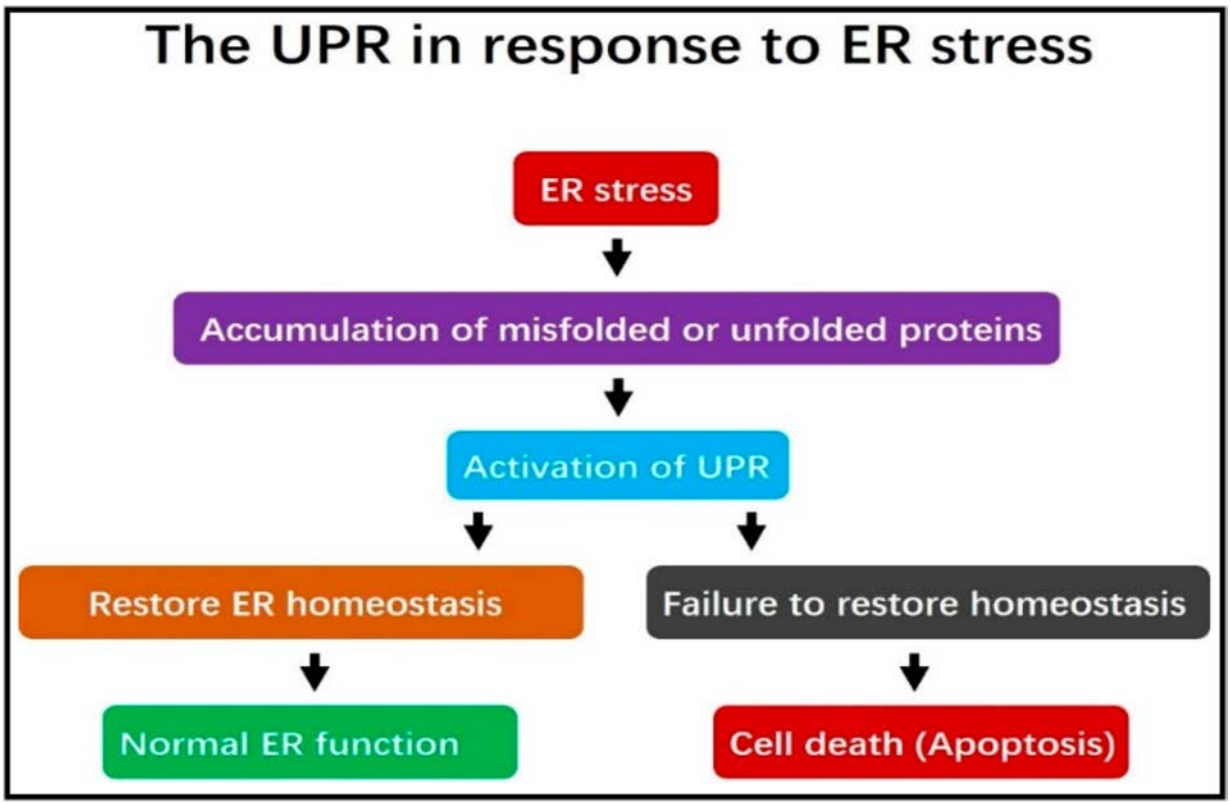

Figure 1.2: Endoplasmic reticulum unfolded protein response.

The UPR^{ER} is characterized by the activation of three separate signal transcription pathways. The transcription factor (ATF) 6α, inositol requiring (IRE) 1α and protein kinase RNA-like ER kinase (PERK) (K. Zhang & Kaufman, 2006).

Normally, the ER stress sensors are bound by the ER chaperone BiP. When stress occurs, BiP binds to unfolded proteins leading to the activation of IRE1α, PERK and ATF6α transcription factors (Naidoo & Brown, 2012; Shen, Zhang, & Kaufman, 2004; K. Zhang & Kaufman, 2006). PERK phosphorylates the eukaryotic initiation transcription factor 2 (eIF2a) and inhibits the protein translation. ATF6 transcription factor leads to stimulation of molecular chaperones and regulates the ER folding capacity (Naidoo & Brown, 2012). IRE1a activates the splicing of X binding protein 1 (XBP-1) that induces degradation of proteins that cannot be refold (due to excessive damage). In case of failure to restore the homeostasis in the ER the NRF-2 transcription factor and ATF4 (transcription factor) leads to apoptotic signalling to resolve the stress (Naidoo & Brown, 2012). Thus, the UPR^{ER} is essential for the proper protein folding and homeostasis in ER.

There are several studies that suggest that the UPR^{ER} becomes activated in numerous liver diseases such as obesity associated fatty liver disease, alcohol induced hepatic injury and viral hepatitis (Liberman et al., 1999; Tardif, Mori, & Siddiqui, 2002; Xu, Jensen, & Yen, 1997). Hepatocyte apoptosis occurs in most cases of liver dysfunction, an event that could lead to an increase in ER stress. Most of the hepatopathies are accompanied by steatosis, given that ER plays a key role in regulation of lipid metabolism in hepatocytes. Current studies using animal models of insulin resistance demonstrate a correlation between UPR and ER stress in liver disease and hepatic steatosis. (Liberman et al., 1999; Tardif et al., 2002; Xu et al., 1997). Ji et al studied a mouse model of alcoholism and found that mice treated with alcohol for a prolonged period of time increased homocysteine levels in their plasma and stimulated upregulation of ER stress markers in the liver (Ji & Kaplowitz, 2003). Overexpression of BiP chaperones in *ob/ob* mice improved the ER stress in the liver (Kammoun et al., 2009; Rutkowski et al., 2008). Heterozygous mice with whole-body deletion of XBP1 developed insulin resistance and deprived glucose homeostasis on a high fat diet (HFD), suggesting that a proper function of ER stress could assist to the pathology of the Metabolic Syndrome (Özcan et al., 2006). Also mice with liver specific

deletion of XBP1 showed reduced levels of serum lipids and reduced lipogenesis in the liver (A.-H. Lee, Scapa, Cohen, & Glimcher, 2008). However, another model with an inducible deletion of XBP1 in the liver increased JNK activity and hepatic ER stress, but had increased insulin sensitivity, suggesting that ER stress alone is not enough to cause insulin resistance (Jurczak et al., 2012).

Similarly, the mitochondria have its own distinct UPR, which involves an upregulation of chaperones and proteases to deal with misfolded proteins. The UPRmt likely performs a very important protective role when metabolic demands are elevated, such as exposure to excess nutrients where it may prevent excessive increases in mitochondrial metabolism that limit ROS generation and mitochondrial damage and downstream apoptosis (Benedetti et al., 2006; C. M. Haynes & Ron, 2010; Cole M. Haynes, Yang, Blais, Neubert, & Ron, 2010; Marker et al., 2012; Q. Zhao et al., 2002).

1.3.2 The mitochondrial unfolded protein response (UPRmt)

Most mitochondrial proteins are synthesised in the cytosol and are transported in an unfolded state into the mitochondria, however, a small number of abundant proteins are also synthesised in the mitochondrial matrix (Neupert, 1997). Mitochondria contain approximately 1000 proteins. The endogenous genome encodes 13 of these proteins and they are expressed and folded by mitochondrial machinery and function as subunits of the electron transport chain. The remaining mitochondrial proteins are encoded in the nucleus (Milenkovic, Müller, Stojanovski, Pfanner, & Chacinska, 2007). When proteins translocate to the mitochondrion they need to be partially or fully unfolded prior to import (Eilers, Hwang, & Schatz, 1988; Lithgow, 2000). The proteins that are being imported in the mitochondrion are refolded by mitochondrial chaperones (heat shock proteins such as HSP60 and HSP70) (Deocaris, Kaul, Wadhwa, & chaperones, 2006; F.-U. Hartl, Martin, Neupert, & structure, 1992; Manning-Krieg, Scherer, & Schatz, 1991).

Accurate communication between nuclear and the mitochondrion is required because mitochondrial proteins are encoded by these organelles. The amount of misfolded or unfolded proteins can be increased in the mitochondria due to cell stress, including those induced by excessive heat, increased ROS levels, increased demand

for mitochondrial biogenesis, mutations in mitochondrial proteins, ingestion of heavy metals and starvation. In response, the mitochondrion with the nucleus attempts to cope with the stress and restore protein homeostasis through transcriptional activation of genes that encode for chaperones and proteases. This route is known as the UPRmt (Takunari Yoneda et al., 2004). Proteostasis (protein homeostasis) in the cell is safeguarded by the chaperones that promote protein folding and congregation (F. U. Hartl, Bracher, & Hayer-Hartl, 2011). Initially, UPRmt was identified in bacteria, that where exposure to stressful conditions such as elevated temperature. This led to activation of heat shock proteins, that are responsible for protein folding. (S. Lindquist & E. Craig, 1988). The UPRmt is responsible for maintaining the integrity of the mitochondrial organelle and up-regulates the expression of mitochondria-specific chaperones or otherwise heat shock proteins (e.g. MtHsp70, MtHsp60/Hsp10), proteases such as spastic paraplegia 7 (SPG7) and ATP-dependent ClpXP protease proteolytic subunit (ClpP) and catalytic (ClpX) and transcription factors such as ATF5 (mammalian analogue) or ATSF-1 (worm analogue) and CHOP (the signalling proteins) (Fiorese et al., 2016; T. Yoneda et al., 2004; Q. Zhao et al., 2002; Quan Zhao, Jianghui Wang, Ilya V Levichkin, Stan Stasinopoulos, Michael T Ryan, & Nicholas J Hoogenraad, 2002). Increased UPRmt was shown to promote longevity in worms and lack of it led to lifespan suppression (Tian et al., 2016).

The UPRmt has been described in worms (*C. elegans*) and in mammals respectively. Although the procedure is the same the difference is in the chaperones involved.

1.3.2.1 Heat shock proteins involved in UPRmt

Heat shock proteins as the name suggests, were first discovered by exposing the fruit fly *Drosophila* to heat (Tissiéres et al., 1974). These proteins are produced by cells in response to stressful conditions (for instance heat, increased ROS levels, cold, UV light, toxicity etc.) (Richter, Haslbeck, & Buchner, 2010). Most of these act as chaperones. Through transcriptional regulation they stabilize and fold new incoming proteins and helping to refold unfolded proteins that were damaged by the stress (De,

1999). Heat shock proteins are named per their molecular weight (e.g, HSP10, HSP60, HSP70 and HSP90 etc.) (Z. Li & Srivastava, 2004). There are several kinds of heat shock proteins but we mostly focussed on the mitochondrial ones (HSP10, HSP60 and HSP70) (Chakraborty et al., 2010; Cheng et al., 1989; Yamano, Kuroyanagi-Hasegawa, Esaki, Yokota, & Endo, 2008). Disruption of proteostasis by any stress within the mitochondria can trigger the release of the heat shock proteins (Quan Zhao, Jianghui Wang, Ilya V Levichkin, Stan Stasinopoulos, Michael T Ryan, & Nicholas J Hoogenraad, 2002). Mitochondria have multiple molecular chaperones located in the matrix and intermembrane space to be able to promote efficient mitochondrial protein folding (Bukau et al., 2006; C. M. Haynes & Ron, 2010; Young et al., 2004). The most well described heat shock proteins in the mitochondria are HSP60 and HSP70mt.

HSP60 is localized in the matrix and consists of two subunits; HSP10 and HSP60 that together they form a complex where they act to fold small and soluble monomeric proteins (Chakraborty et al., 2010; Cheng et al., 1989; Yamano et al., 2008).

HSP70mt acts to translocate polypeptides through the mitochondrial protein import channel to the matrix (Chacinska, Koehler, Milenkovic, Lithgow, & Pfanner, 2009; Kang et al., 1990). It also prevents aggregation and is responsible for the protein folding and complex assembly of the imported polypeptides (Q. Liu, Krzewska, Liberek, & Craig, 2001; Ostermann et al., 1990; Scherer, Krieg, Hwang, Vestweber, & Schatz, 1990). Though the molecular mechanism and role of Hsp70 in protein folding process or in dissolving aggregates remain unclear.

Whereas mutually HSP60 and HSP70 are responsible for the proper folding of the newly imported proteins, they have also roles in the mitochondrial quality control (Haider, Robin, Fang, & Avadhani, 2002; Takunari Yoneda et al., 2004; Q. Zhao et al., 2002).

1.3.2.2 Proteases involved in UPRmt

The proteases are another important factor in the UPRmt pathway. When the unfolded proteins fail to fold, or assemble properly, the proteases recognise the damaged proteins and degrade them. The best known mitochondrial proteases are ClpXP and LON. Both are located in the mitochondrial matrix and belong to “ATPase associated with diverse cellular activities” (AAA) family of proteases. They are primarily responsible for the degradation of unfolded/misfolded soluble proteins (T. Tatsuta & T. J. T. E. j. Langer, 2008); (T. Tatsuta & T. J. R. i. m. Langer, 2009), with the LON protease found to degrade oxidative-damaged proteins and the ClpXP that requires ATP energy for protein degradation (Bota & Davies, 2002). ClpXP separates in two distinct proteins the catalytic subunit hexamers of a AAA+ ATPase (ClpX) that tags and binds to proteins and the proteolytic tetradecameric peptidase (ClpP) (Figure 1.3) (R. Sauer & Baker, 2011). Knockdown of ClpP during mitochondrial stress has been shown to prevent the production of the mitochondrial chaperones that are involved in the unfolded protein response (C. M. Haynes, K. Petrova, C. Benedetti, Y. Yang, & D. J. D. c. Ron, 2007). A similar effect was observed in mammalian cells that supported these findings (Rath et al., 2012). Worms with ClpP knockout developed slower under mitochondrial stress (Cole M Haynes et al., 2007). Furthermore, overexpression of ClpX *in vitro* in mouse myoblast cell lines resulted in the upregulation of genes involved in UPRmt such as CHOP and HSP60 (Al-Furoukh et al., 2015).

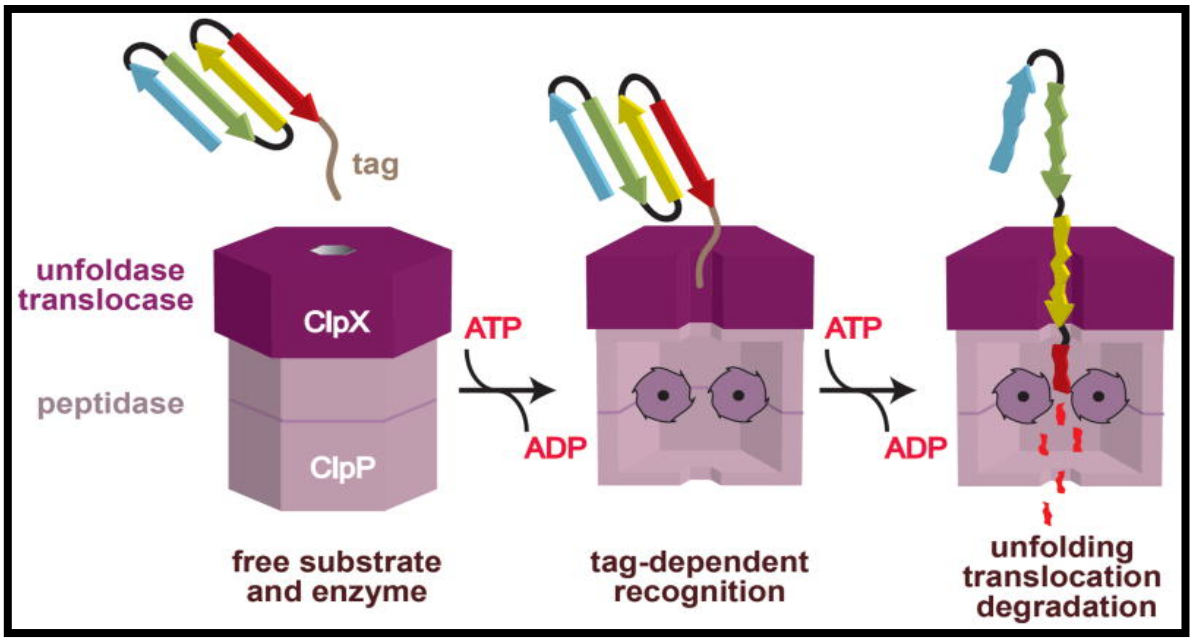

Figure 1.3 The schematic of ClpXP protease action. The ClpX hexamer recognize and tags the unfolded proteins then translocate the unfolded protein into the degradation chamber of ClpP to achieve proteolysis. (ATP dependent steps) (T. A. Baker & Sauer, 2012).

1.3.2.3 Transcription factors involved in UPRmt

Transcription factors are proteins that control and trigger the transcription of genetic information by binding to the DNA sequence. Transcription factors are also responsible for the signaling and the production of other proteins. For the UPRmt the most important transcription factors are CHOP, ATF5 and UBL5 in mammals, and in worms are ATSF-1 (where ATF5 is the mammalian analogue), UBL5 and DVE-1 (Fiorese et al., 2016; Cole M Haynes et al., 2007; C. M. Haynes & Ron, 2010).

The transcription factor CHOP, was found to promote the production of HSP60 and ClpP *in vitro* (Quan Zhao, Jianghui Wang, Ilya V Levichkin, Stan Stasinopoulos, Michael T Ryan, & Nicholas J %J The EMBO journal Hoogenraad, 2002). Moreover, CHOP was found to be upregulated in situations of mitochondrial stress (J. E. Aldridge, T. Horibe, & N. J. J. P. o. Hoogenraad, 2007b; T. Horibe & N. J. J. P. o. Hoogenraad, 2007; Weiss et al., 2003; Quan Zhao, Jianghui Wang, Ilya V Levichkin, Stan Stasinopoulos, Michael T Ryan, & Nicholas J %J The EMBO journal Hoogenraad, 2002).

In worms the transcription factor ATFS-1 was found essential for UPRmt signaling and vital for survival under stressful conditions that initiate protein misfolding (Lies & Maurizi, 2008). In worms when there is no stress, ATFS-1 is imported normally in the mitochondrion and becomes degraded by proteases such as LON. When stress occurs and there is accumulation of unfolded proteins, ATFS-1 translocate to the nucleus to activate the protective response (upregulates the heat shock proteins and proteases) (C. M. Haynes & Ron, 2010; Melber & Haynes, 2018). That promotes survival and recovery of the mitochondrial network.

ATF5 is a transcription factor (mammalian analogue of ATSF-1) regulated by mitochondrial import efficiency similarly to ATFS1 (Fiorese et al., 2016). ATF5 expression was shown to restore UPRmt activation when expressed in worms lacking ATFS-1 (Fiorese et al., 2016). The same study showed that in mammalian HeLa cells, the analogue of ATFS-1 was the ATF5 transcription factor that was demonstrated to act in similar ways. ATF5 was essential for the UPRmt and for the recovery of the cell through OXPHOS and cell growth during mitochondrial dysfunction (via upregulation of mitochondrial chaperones and proteases) (Fiorese et al., 2016). ATSF-1 is important in OXFHOS complex assembly, it was found to bind to NADH ubiquitinone oxidoreductase assembly factors (Ghezzi & Zeviani, 2012; A. M. Nargund, C. J. Fiorese, M. W. Pellegrino, P. Deng, & C. M. J. M. c. Haynes, 2015) also worms with deletion of ATSF-1 presented with defects in OXPHOS and had reduced oxygen consumption (A. M. Nargund et al., 2015). The same study showed that during mitochondrial stress the ATSF-1 was shown to be a negative regulator of OXPHOS and TCA-cycle (A. M. Nargund et al., 2015).

The transcription factor DVE-1 (in worms) and the co-factor UBL5 (in both worms and mammals) are also linked to the UPRmt (Cole M Haynes et al., 2007). Both are essential for the activation of the mitochondrial molecular chaperones. The UBL5 was found to form complex with DVE-1 and HAF-1 and was upregulated during mitochondrial stress. Also, the mammalian analogues of DVE-1 and UBL-5 (SatB2 and UBL5) was found to form a complex. That shows potential similar action in mammals (Cole M Haynes et al., 2007). The UBL5 is described in greater detail in (Section 1.3.2.6).

1.3.2.4 UPRmt in *C. elegans*

Most of what is known about the UPRmt signalling is derived from studies in worms *C. elegans*, though many of the genes involved are highly conserved and probably perform similar roles in mammalian cells. Investigations revealed potential genes that are involved in this process (Figure 1.4) (Broadley & Hartl, 2008) (Takunari Yoneda et al., 2004). The findings suggest that when stress occurs in the mitochondrial matrix, Clpp-1, a mitochondrial function protease, appears to be essential in the activation of the UPRmt response. In the presence of misfolded proteins, Clpp-1 degrades the misfolded proteins to peptides and release ligands through transporter HAF-1 to the cytosol. Following the transcription factor ATFS-1 is activated by detection of the peptidases and ligands via specific receptor or the efflux rate (in the cytosol) and complex formation with UBL5/DVE-1. This complex formation translocates from the cytosol to the nucleus where (ATSF-1/DVE-1/UBL5 complex) binds to HSP60 promoter and transcriptionally activates the expression of the protective UPRmt target genes/chaperones (HSP60, HSP10 and HSP6). These mitochondrial chaperones subsequently translocate to the mitochondria to rebalance the mitochondrial proteostasis and restore protein homeostasis by refolding unfolded proteins (Broadley & Hartl, 2008; Takunari Yoneda et al., 2004). Also, the stressed mitochondria produce ROS and this leads to activation of the kinase GCN-2 which decreases the global translation by phosphorylation of eIF2a, and blocks the protein translation (Nargund, Pellegrino, Fiorese, Baker, & Haynes, 2012).

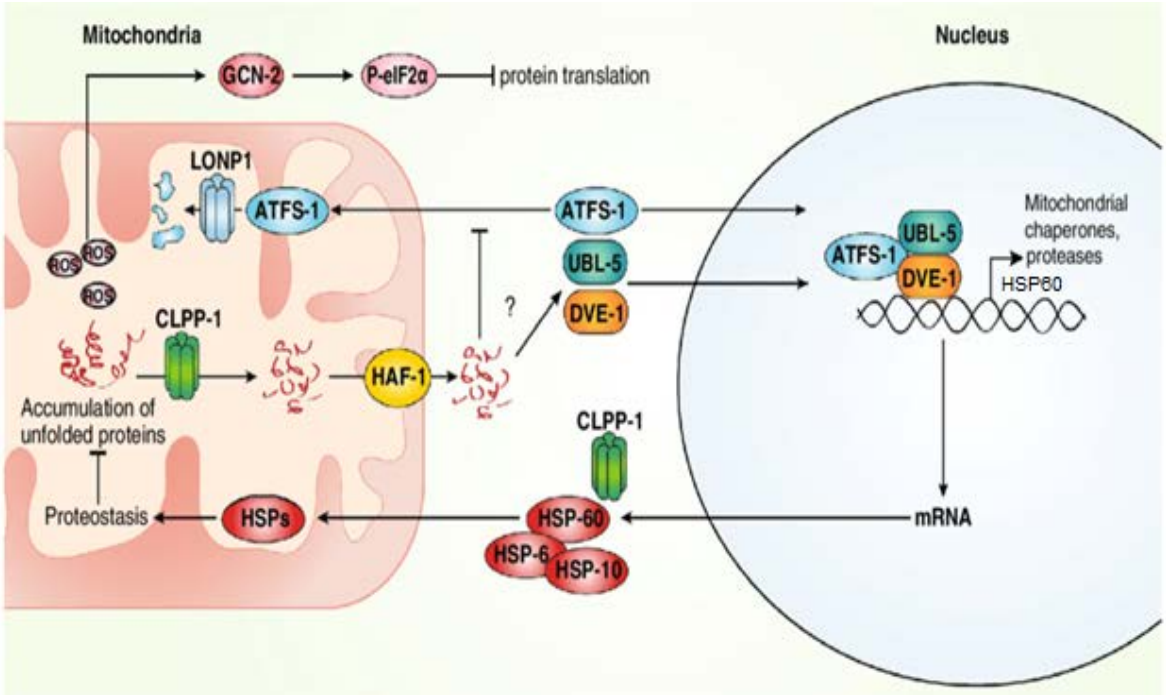

Figure 1.4: Mitochondrial unfolded protein response pathway in *C. elegans*. Accumulation of unfolded proteins activate response. The unfolded proteins are processed into short peptides by CLPP-1 and after exported through HAF-1 transporter into the cytoplasm. AFS-1 transcription factor together with DVE-1/UBL5 complex activate the UPRmt genes that alter proteostasis. (HSPs = heat shock proteins) (Mottis, Jovaisaite, & Auwerx, 2014).

1.3.2.5 Mammalian UPRmt

Similar to the worms, mammalian cells also have the UPRmt as shown in (Figure 1.5). Studies in mammals have revealed some important genes and proteins that are involved in the UPRmt signalling.

Not unlike the UPRmt in *C. elegans*, the UPRmt in mammals also becomes activated in response to changes in cellular homeostasis and increased unfolded and misfolded proteins (Figure 1.4 and Figure 1.5). Although it is more complex and requires further studies to be done to elucidate the actual mechanism. The limited mammalian studies available have shown that that shock proteins are involved in the UPRmt as well.

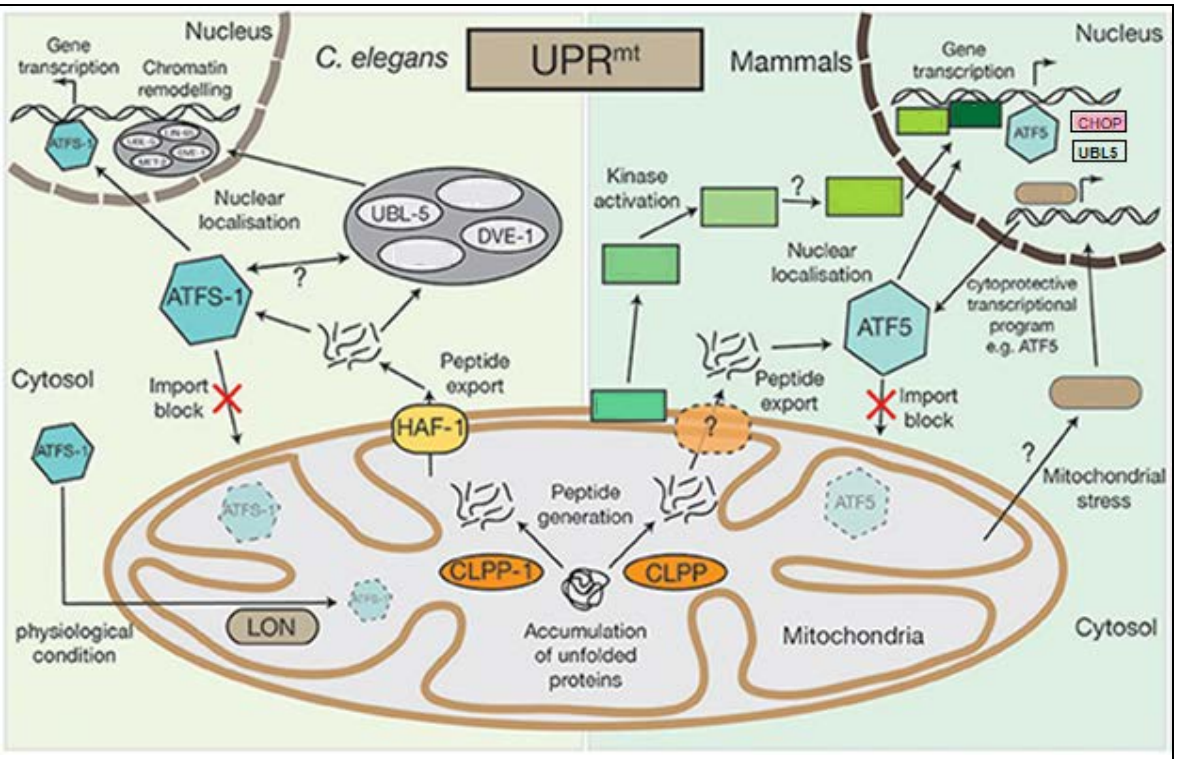

Figure 1.5: A comparison of UPRmt in *C. elegans* and mammals: An increased build - up of unfolded/ misfolded proteins in the mitochondrion activates the UPRmt mutually in worms and mammals . (Callegari, Dennerlein, & biology, 2018).

In mammalian cells the mammalian analogue of ATSFS-1 transcription factor (transcription factor in worms) is ATF5 that acts in similar ways. Typically, ATF5 gathers within mitochondria, but upon dysfunction in respiratory chain, increased levels of ROS or mitochondrial protein folding stress, ATF5 translocates in the nucleus and triggers the activation of the UPRmt (Fiorese et al., 2016). Also, apart from the well-known role of CHOP in endoplasmic reticulum stress signalling and unfolded protein response (Schröder, 2006), CHOP also seems to be implicated in UPRmt, and thought to play the role as a transcription factor (J. E. Aldridge, T. Horibe, & N. J. Hoogenraad, 2007a; T. Horibe & N. J. Hoogenraad, 2007). Upon overexpression of ornithine transcarbamylase which initiates the congregation of unfolded proteins in the mitochondria (Quan Zhao, Jianghui Wang, Ilya V Levichkin, Stan Stasinopoulos, Michael T Ryan, & Nicholas J Hoogenraad, 2002). A study in mice with induced cancer (via doxycycline supplement in the water) showed that increased ROS levels upregulated UPRmt and induces CHOP/ATF5 formation (Kenny, Craig, Villanueva, & Germain, 2019). Al-Furukh showed in mammalian myoblasts that Clpx overexpression

induced the activation of UPRmt (CHOP, HSP60, HSP10 and HSP70). Also in the same study, they suppressed the expression of Clpp in C2C12 mammalian cells and transfected them with Clpx (confirmed upregulation) and saw a selective stimulation of mitochondrial chaperones such as HSP60, HSP70, CHOP, ATF5 and UBL5 (Al-Furoukh et al., 2015). Similarly, in mammalian systems the newly synthesized mitochondrial proteins were shown to be fold by mitochondrial HSP70 (L. Mizzen, Kabiling, & Welch, 1991; L. A. Mizzen, Chang, Garrels, & Welch, 1989; Wadhwa, Taira, & Kaul, 2002). A study in mice showed that knockout of Clpp protease led to retardation of mice and increased inflammation, mitochondrial damage and high Clpx levels (Gispert et al., 2013).

These chaperone proteins are expected to bind and assist in the reassembly of misfolded mitochondrial proteins and limit their potential harmful effects on cell function and viability. Although the UPRmt pathway has been well studied in worms, in mammals it is not completely inferred. More studies are required to understand and establish if this biological pathway presents similarities among species.

1.3.2.6 Ubiquitin-like protein 5 (UBL5)

UBL5 was initially described as a gene that was up-regulated in the brain in association with obesity (Collier et al., 2000). Subsequent studies have also shown that variations in this gene may be linked to other aspects of the metabolic syndrome such as hyperinsulinemia, hypertriglyceridemia and increased cholesterol levels (Bozaoglu et al., 2006b; Jowett et al., 2004). While the pathways linking UBL5 to the metabolic syndrome have not yet been clearly elucidated we believe that studies in *C. elegans* and mammalian cells suggesting a role for UBL5 in the mitochondrial stress response (Benedetti et al., 2006; C. M. Haynes, K. Petrova, C. Benedetti, Y. Yang, & D. Ron, 2007). Where UBL5 was found to act as a co-factor that is important for the signalling of the UPRmt may provide an important clue (C. M. Haynes et al., 2007). We discuss below in more detail how we believe UBL5 through its putative role in preserving mitochondrial function may be important for maintenance of normal energy homeostasis and cellular function.

1.3.2.6.1 Discovery of UBL5

The UBL5 gene also known as BEACON and Hub1 (in yeast), is located on chromosome 19p13.2. The 19p13 region has been linked with obesity-related traits (Boright, Connelly, Brunt, Morgan, & Hegele, 1998; Imperatore et al., 2000; Nishina, Johnson, Naggert, & Krauss, 1992; Rotter et al., 1996). The UBL5 gene encodes a 73 amino acid protein called ubiquitin-like protein 5 and has a molecular weight of 8.5 kD and a pI of 8.6 (Friedman, Koop, Raymond, & Walter, 2001; McNally et al., 2003). Between species the 73-amino acid sequence shows great conservation. In fact, the alignment shows 100% homology between mouse, human and rat, 80% with *C. elegans*, and 65% with S. cerevisiae (Collier et al., 2000; Jowett et al., 2004). In humans, the gene contains five exons and four introns, with length 2,194 nucleotides (Figure 1.6) (Collier et al., 2000), human UBL5 gene has the same number of exons as mice and rats.

The size of the gene is between 340 bp to 1939 bp depending on the kind of species or tissue (Table 1.1). The only major difference in UBL5 structure, comparing different species is that in *C. elegans* has only two exons and one intron and the PCR product of *P. Obesus* showed a 413 mRNA with four exons instead of five (Collier et al., 2000). The coding region of the gene is from exon 2 to exon 5 and the non-coding is the exon one (Figure 1.6) (Walder, Segal, Jowett, Blangero, & Collier, 2003).

Table 1.1: Resemblance of the UBL5 genes in different species. (Collier et al., 2000)

Species	Accession Number	Chromosome	Size (bp)	Number of exons
Homo Sapiens (Human) Transcript 1	NM_024292	19	537	5
Homo Sapiens (Human) Transcript 2	NM_001048241	19	457	5
Mus Musculus (Mouse)	NM_025401	9	1939	5
Rattus Novegicus (Rat)	NM_001048243	8	495	5
Psammomys obesus (Gebril)	AF318186	Not known	413	4
Caenorhabdities elegans (Worm)	NM_059239	1	340	2

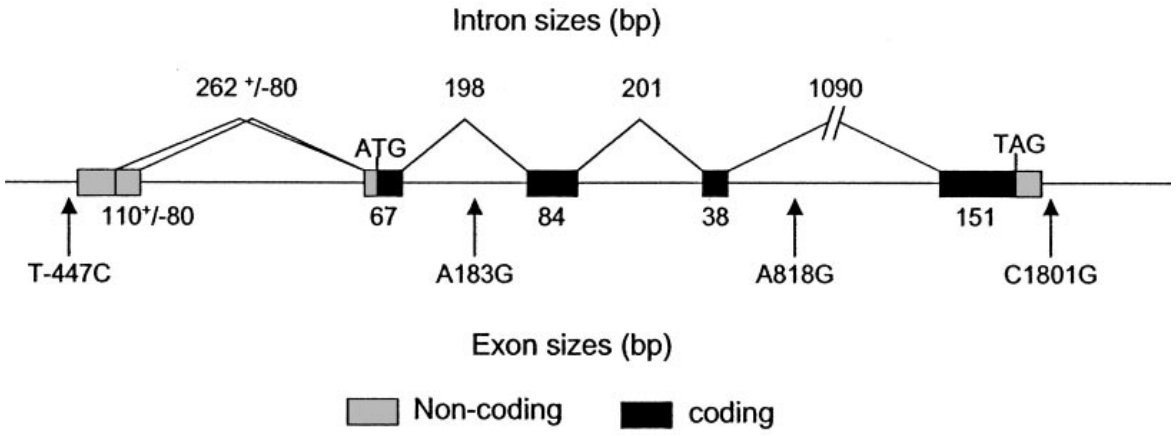

Figure 1.6: Structure of the human *UBL5* gene (Collier et al., 2000; Jowett et al., 2004; Walder et al., 2003).

The UBL5 protein resembles the structure of a small protein in eukaryotes called ubiquitin which is mostly involved in protein degradation. For that reason it was named “ubiquitin-like” (Friedman et al., 2001). Although, UBL5 and ubiquitin lack sequence similarity (~25%). At the C-terminus UBL5 contains a di-tyrosine motif instead of di-glycine that helps ubiquitin-like proteins to match with target proteins, therefore UBL5 has different functions from ubiquitin, and it belongs to a separate class from ubiquitin-like genes (Figure 1.7) (Friedman et al., 2001; McNally et al., 2003; Ramelot et al., 2003).

Figure 1.7: Alignment of UBL5 and Ubiquitin. The amino acid sequence alignment that illustrates the mutual secondary structure of UBL5 and ubiquitin, the di-glycine residues at the C-terminus that is required for conjugation is misplaced in UBL5 by di-thyrosine. Also, the UBL5’s sequence appears to be 4 amino acids smaller than ubiquitin’s. (McNally et al., 2003)

In the mammalian system, *UBL5* was first identified as upregulated in the hypothalamus of overweight Israeli sand rats (Psammomys Obesus) (Collier et al.,

2000) a polygenic rodent model of obesity. Also UBL5 was detached from a screen of human iris cDNA library by Friedman and his team (Friedman et al., 2001). Expression of the gene has been observed in several tissues such as heart, skeletal muscle, kidney, liver, adipose tissue, and pancreatic islets (Brailoiu et al., 2003; Brailoiu et al., 2002; Friedman et al., 2001; Ng et al., 2006; Rucinski, Andreis, Ziolkowska, Nussdorfer, & Malendowicz, 2005; F. Wang et al., 2006; Ziolkowska, Rucinski, Di Liddo, Nussdorfer, & Malendowicz, 2004).

1.3.2.6.2 UBL5 and the Metabolic Syndrome

As we mentioned above UBL5 was found elevated along with other genes in the hypothalamus of obese (*P. obesus*) animals matched up to lean controls (Collier et al., 2000; Walder et al., 2002). It was reported to be responsible for the higher expression levels of a strong appetite-simulating orexigenic Neuropeptide Y (NPY) (Billington, Briggs, Grace, & Levine, 1991; Collier et al., 2000; Hanson & Dallman, 1995; Tatemoto, Carlquist, & Mutt, 1982). Thin *P. obesus* showed increased food intake and elevated body weight after infusion of UBL5 and NPY jointly, with more dramatic results than that of the NPY infusion itself (Collier et al., 2000). Human studies have further supported an association between UBL5 and the metabolic syndrome. a human study sequenced UBL5 in 40 unrelated individuals and found four variant single nucleotide polymorphisms (SNPs). In two cohorts of nonrelated individuals from Mauritius and Nauru two SNPs were observed that were primarily associated with obesity, total body fat, increased waist/hip ratio and other metabolic syndrome related characteristics (Jowett et al., 2004). An additional study was done to support these findings in a cohort of fasted Mexican/American population, and the findings showed association connecting five SNPs within UBL5 with waist to hip ratio and circulating insulin and total cholesterol levels (Bozaoglu et al., 2006a). In both studies among these populations three SNPs (A800T, A818G and C1801G) appeared identical. Similarly, a Caucasian population showed an association with obesity and a G860T SNP (Sentinelli et al., 2008). While the pathways linking UBL5 to the metabolic syndrome have not yet been clearly elucidated, studies in *C. elegans* and mammalian

cell lines suggesting a role for UBL5 in the mitochondrial stress response (Benedetti et al., 2006; C. M. Haynes et al., 2007).

1.3.2.6.3 UPRmt and UBL5

To date, some studies have linked UBL5 with the UPRmt pathway in worms (*C.elegans*) (Broadley & Hartl, 2008; Takunari Yoneda et al., 2004). Although the role of UBL5 in mammalian UPRmt pathway was shown *in vitro* but still remains unclear *in vivo* (Mishra et al., 2011; Oka et al., 2014; Švéda, Častorálová, Lipov, Ruml, & Knejzlík, 2013; Wilkinson et al., 2004; Yashiroda & Tanaka, 2004; Zhao et al., 2011). In *C. elegans* the UPRmt is dependent on *UBL5* forming a complex with the homeobox transcription factor DVE-1. A knockout of *UBL5* prevented the UPRmt signal and there was no production of the protective heat shock proteins and proteases (C. M. Haynes et al., 2007). Following mitochondrial stress DVE-1 undergoes nuclear re-distribution and binds to the promoters of molecular chaperone genes (including *HSP60*). SATB2 is the mammalian ortholog of DVE-1 and can also form a complex with mammalian UBL5, suggesting a similar role for these two proteins in the UPRmt in mammalian cells (C. M. Haynes et al., 2007; Pellegrino, Nargund, & Haynes, 2013). In mammalian cells overexpression of the ClpX protease was shown to upregulate *UBL5* levels along with CHOP transcription factor and HSP60 and HSP70mt heat shock proteins, that study links *UBL5* to the mammalian UPRmt (Al-Furoukh et al., 2015). Although these studies prove involvement of UBL5 *in vitro*, further studies required to elucidate the function of UBL5 in mammalian system.

1.4 Rationale of the study

The role of liver mitochondrial function in metabolism in a mammalian system remains unclear. The UPRmt acts as a protector in mitochondrial stress and impaired UPRmt results in poor mitochondrial metabolism. Studies in *C. Elegans* have demonstrated that UBL5 is essential for the activation of the UPRmt. Mitochondrial dysfunction within the liver is known to contribute to various metabolic disorders. Furthermore, there is evidence in humans of an association of genetic variations in the UBL5 gene and the metabolic syndrome. Therefore, we hypothesise that the absence of UBL5 in the liver will lead to mitochondrial dysfunction. This dysfunction will result in poor mitochondrial respiration which will lead to poor liver function. The decrease in function should manifest as decreased glucose tolerance and potentially liver failure through apoptosis.

1.5 Overall Aim

The overall aim of this study was to investigate the UPRmt in liver function and metabolism in mammalian systems and how a novel stress gene UBL5 is involved in this pathway. We have designed a mouse model that has specific conditional deletion of UBL5 within the liver. Using this mouse model, we aim to test the above hypothesis with the following specific aims:

1.5.1 Specific aims

The specific aims of this study are:

1. Generation of a novel liver specific UBL5 knockout mouse (UBL5 KO).
   (UBL5 liver specific knockout mouse was generated using the Cre/loxP system).
2. Determine:
   - If mitochondrial function is impaired in UBL5 KO liver specific mice.
   - How UBL5 is involved in the mitochondrial unfolded protein response pathway in mammals
   - The role of UBL5 and the UPRmt in liver function

CHAPTER 2: METHODOLOGY AND MATERIALS

This Chapter contains the general materials and methods used for this thesis. Details of experimental protocols will be documented in separate results chapters.

2.1 Materials

2.1.1 Reagents

All chemicals and reagents were purchased from Sigma Aldrich (St. Luis, MO, USA) unless otherwise stated.

Taq polymerase, 10X PCR buffer, dNTPs, 100bp marker and 6X loading dye were purchased from New England Biolabs (Ipswich, MA, USA). Proteinase K and molecular grade agarose were from Amresco (Solon, OH, USA). RNAse from Roche (Indianapolis, IN, USA). GelRed was purchased from Fisher Biotec /Biotium (Hayward, CA, USA). Sodium chloride, tris-hydrochloride, EDTA, phenol, 8-hydroxyquinolone, glycerol, Trizma base, HEPES, DTT, tamoxifen, DMSO, rotenone, oligomycin, antimycin, were purchased from Sigma-Aldrich (St. Louis, MO, USA). Potassium chloride, magnesium chloride, sodium dodecyl sulphate, sodium acetate, sodium hydroxide, glacial acetic acid and bromophenol blue were from BDH (Kilsyth, VIC, Australia). Protein assay dye reagent, BSA standard, tris-tricine gels, acrylamide, Precision Plus Protein All Blue Standards and Kaleidoscope Polypeptide Standard were purchased from Bio-Rad Laboratories (Hercules, CA, USA). Ethanol, methanol and chloroform was from ChemSupply (Gillman, SA, Australia). K-lactobionate was purchased from (Aldrich, Australia). TEMED and BSA were purchased from MP Biomedicals (Aurora, OH, USA). Isopropanol was from Merck (Kilsyth, VIC, Australia). Ammonium persulfate was from Ajax Finechem (Seven Hills, NSW, Australia). Tricine was from Acros Organics (Morris Plains, NJ, USA). The ECL Reagent was purchased

from Pierce (Rockford, IL, USA). The developer and fixer solutions were purchased from AGFA (Mortsel, Belgium). The Trizol® Reagent and PBS tablets purchased from Invitrogen (Carlsbad, CA, USA). DNA-freeTM DNA removal kit and Superase-InTM was from Ambion (Austin, TX, USA). The AMV Reverse Transcriptase System, RNasin® Plus RNase Inhibitor were purchased from Promega (Madison, WI, USA). SYBR® Green PCR Master Mix, Taqman® Master Mix and Taqman® Gene Expression Assays were purchased from Applied Biosystems (Foster City, CA, USA). All primers were purchased from Geneworks (Hindmarsh, SA, Australia). The PVDF membrane was purchased from Millipore (Billerica, MA, USA). M199 washing Medium with Glutamax™ (DMEM) and penicillin/streptomycin mix were purchased from Gibco (Sigma Aldrich, Castle Hill NSW). Sodium pentobarbitone was purchased from Therapon (Burwood, VIC, Australia). Heparin was from David Bull Laboratories (Mulgrave, VIC, Australia). 0.9% saline solution and glucose intravenous infusion BP 50% were purchased from Astra Pharmaceuticals (North Ryde, NSW, Australia).

2.1.2 Equipment

Scissors and forceps were from Livingstone International (Leichart, NSW, Australia), All syringes and needles were from Terumo Medical Corporation (Elkton, MD, USA). The gavage needle (20-gauge, 38mm long, with a 2¼ mm ball end) was purchased from Able Scientific (Canning Vale, WA, and Australia).

The GeneAmp PCR System 2700 machine, ABI PRISM® 7700 Sequence Detection System and Primer Express® Software were manufactured by Applied Biosystems (Foster City, CA, USA).

2.1.3 Animals

C57BL/6J mice were purchased from Walter and Eliza Hall Institute (Kew, VIC, Australia). The heterozygous UBL5 mice are generated by OZgene. The MerCreMer mice were obtained from Mounia Tannour-Louet (Baylor College of Medicine, Houston, USA).

2.1.4 Diet

The standard non-purified rodent chow diet in pelleted form (7% simple sugars, 3% fat, 50% polysaccharide, 15% protein (w/w), energy 3.5 kcal/g), was purchased from Barastoc Stockfeed (Pakenham, VIC, Australia) (Appendix I).
The SF11-109, high-fat rodent food (21% fat, 2% cholesterol semi-pure rodent diet) was purchased from Specialty Feeds (Glen Forest, WA, Australia). Refer to (Appendix II, page 221 - 222) for full composition of the and 21% (w/w) high-fat rodent food.

2.1.5 Therapies

Pioglitazone drug powder was purchased from (Sigma Aldrich, Castle Hill NSW).
ACE2 gene we obtained the virus recombinant adeno-associated viral vector serotype 2/8 with *ACE2* (rAAV2/8-ACE2) and the vehicle vector (rAAV2/8+ Human serum albumin (HAS)) from our collaborator Dr Chandana Herath (Mak et al., 2015b).

2.2 Methods

2.2.1 Animal Housing, Care and Maintenance

All mice were housed and inbreed in the Austin Hospital BioResources Animal Facility of the Department of Medicine (AH/NH), at the Heidelberg Repatriation Hospital (Heidelberg Heights, VIC, Australia).

Room temperature was kept persistent at 21 - 23 ^{o}C. A 12-hour dark/light artificial lightening cycle was maintained. All mice were feed standard non-purified rodent chow diet in pelleted form (74% carbohydrates, 20% protein and 6% fat) was purchased from Barastoc Stockfeed (Pakenham, VIC, Australia). All food and water were provided *ad libitum*. All animal procedures were approved by the Animal Ethics Committee, Austin and Repatriation Medical Centre. (AEC#: A2014/05194 and A2017/05431).

2.2.2 Breeding

All mice were housed and inbreed in the Austin Hospital Bio Resources Animal Facility of the Department of Medicine (AH/NH), at the Heidelberg Repatriation Hospital (Heidelberg Heights, VIC, Australia).

2.2.3 Tamoxifen Administration

Tamoxifen (30 mg/ml suspension of tamoxifen in a 1.5% solution of Methylcellulose) gavages were performed on mice by Dr. Ben Lamont. All the animals received 3 doses of tamoxifen (200 µl per gavage = 6 mg tamoxifen) by using 1ml syringe and mouse gavage metal needles with soft ball end point.

2.2.4 Mouse Tail Genomic DNA Preparation for Genotyping:

Genotyping was performed by using RedTAQ kit. At weaning mouse tail (0,5 cm - 1 cm) was snipped off the mouse and placed in PCR snips, 100 µl of 50 mM NaOH was added per tail/tube, after incubated at 96oC for ten minutes in the PCR machine, after cooling down for couple minutes 10 µl of 1M Tris (pH 8,0) added in the mix.

2.2.5 Polymerase Chain Reaction (PCR)

A 20 µL genotyping PCR reaction mixture be made up of 10µl RedTAQ, 1.6 µl of Primer Mix (P295 + P296 for UBL5 gene and 555 + 556 for Cre), 6.4 µl of Nuclease free water and 2µl of tail digest. The genotyping PCR cycling program was for UBL5 detection 95 ^{o}C for 2 minutes; 40 cycles (94 ^{o}C for 30 seconds, 68 ^{o}C for 1 minute, 72 ^{o}C for 30 seconds); hold on 4 ^{o}C. Similar procedure was followed for Cre with slightly different temperatures, 92 ^{o}C for 2minutes; 35 cycles (94 ^{o}C for 30 seconds, 51 ^{o}C for 1 minute and 72 ^{o}C for 30 seconds); hold on 4 ^{o}C. All primers were designed using the Primer Express® Software.

2.2.6 Agarose Gel Electrophoresis

The samples were loaded onto 2% analytical agarose gel with 3µl GelRed. 1x TBE (89 mM Tris borate, 2mM EDTA pH 8.2 - 8.4) buffer was used as running buffer. Gels were run at 95V for 25 minutes and viewed under UV light with the Quantity One® Software.

2.2.7 Tissue and blood collection

After animals were euthanized via CO_2 chamber or alternatively with Nembutal (sodium pentobarbitone 12 mg/kg body weight) using 0.5 ml insulin syringes, blood plasma was collected via cardiac puncture, using a 1 ml syringe and a 25G ⅝" needle, and placed in 1.5 ml Eppendorf tubes treated with 1000 IU/ml heparin to prevent clotting, and centrifuged immediately, plasma collected and stored at -80 ^{o}C until examined for liver function tests. Immediately after cardiac puncture, mice were sacrificed and tissues were excised, preserved in liquid nitrogen and stored at -80 ^{o}C for the next analyses. Tissues collected included liver, RG muscle, white adipose tissue (WAT), Brain (hypothalamus, cortex, and cerebellum), heart and tail. Also, part of liver was collected in histological cassettes and fixed in formaldehyde for 48 hours and after stored in 70% ethanol for further histological analysis. Body weight and liver weight were measured after the subjects were culled.

2.2.8 Blood glucose

Blood glucose throughout the experiments was monitored using a glucometer. (Optium-Point of Care, Medicine, MA, USA.).

2.2.9 Plasma liver function tests

Plasma liver function tests were performed by Department of Pathology, Austin Health (Level 6, Harold Stokes Building, Studley Road, Heidelberg, 3084).

2.2.10 Hepatocytes isolation

To isolate hepatocytes: Warm to 37 ^{o}C the 155 ml HBSS buffer and 40 ml Collagenase A buffer (in water bath). Calibrate the circulating pump with 50 ml HBSS. Anesthetize mice as stated in (section 2.2.10). Connect the circulating pump with the hepatic portal vein, cut the inferior vena cava. First perfuse with HBSS, 100 ml per 20 minutes and after with Collagenase A. Remove the whole liver in 5 ml HBSS. Under the fume hood: using the bacterial spreader massage the liver in petri-dish. Using 40 µm cell strainer filter the cells, top up with 45 ml HBSS and spin (Eppendorf, Centrifuge 5810R) on 340 rpm x 4 ^{o}C for five minutes, resuspend and add 25ml HBSS and spin again for five minutes, resuspend and add 25 ml ice cold washing medium M199 and spin for five minutes, repeat two more times. Resuspend the cell pallet in up to 15 ml of warm culture medium M199 (45 ml washing M199 medium plus 5 ml FBS, plus 5 µl EGF, plus 7 µl Insulin. Using six well-plate we seeded 0.40 x 10^{6} cells/ml. Incubated in 37 ^{o}C incubator, 5% CO_2 for six hours.

2.2.10.1 HBSS buffer for perfusion

To make up four stock solutions, we brought each solution to 1 L (w/ddH_2O): (A) Dextrose 10.0 g, (B) $MgCl_2.6H_2O$ 1.0 g plus $MgSO_4.7H_2O$ 1.0 g. (C) KCl 4.0 g plus KH_2PO 4 0.6 g plus NaCl 80.0 g plus Na^2HPO_4 0.49 g (D) HEPES 48.0 g 7.5 pH. To make 1x working solution of HBSS we combined 100 ml of each stock and added 600ml ddH_2O, after adjusting the pH to 7.4 using pH meter (HI22II pH/ORP Meter. HANNA Instruments) and filter sterilized under the hood using (Millipore pump 0.22 µM filter).

2.2.10.2 Collagenase A Buffer

To make the buffer, under the fume hood we combined NaCl 3.9 g plus KCL 0.5 g plus $CaCl_2.2H_2O$ 0.7 g plus HEPES 24.0 g plus NaOH (8N/ddH_2O) 8.25 ml, we topped up to 900 ml with ddH_2O. Filter sterilized in the T.C hood using the (Millipore pump with 0.2222 µM filter). The solution was stored in 4 ^{o}C. We added 1 ml of collagenase A (20 mg/ml ddH_2O) to 39 ml of Buffer.

2.2.10.3 M119 Medium

Washing medium M199: we added 500 ml M199 plus 5 ml glutamine plus 5 ml penicillin /streptomycin under the fume-hood.

Culture medium M199: we added 45 ml washing M199 medium plus 5 ml FBS, plus 5 µl EGF, plus 7 µl Insulin (2 mg/ml pure H_2O) pH 7, plus 20 µl dexamethasone (10 mg/ml 100% Ethanol) under the fume-hood.

2.2.11 Histology

All the histological procedures such as embedding, cutting in microtome and Hematoxylin & Eosin stains were performed by the Department of Pathology, Austin Health (Level 6, Harold Stokes Building, Studley Road, Heidelberg, 3084).

2.2.12 Scoring

The slides were scored by the Melbourne university and histology report was given by APN staff using a grading scale ranging from 0 to 5 was used to illustrate degrees of change (Grade 0: Unremarkable tissue, Grade 1: Mild [1-2 foci], Grade 2: Mild to moderate [3-6 foci], Grade 3: Moderate [7-12 foci], Grade 4: Moderate to severe [multifocal], Grade 5: Severe [Diffuse]).

2.2.13 RNA Extraction

To extract RNA from all the tissues, approximately 50 -100 mg of tissue were homogenized in 1ml of Trizol, using the Polytron Homogeniser. In samples with high content of protein, fat polysaccharides or extracellular material such us muscle, white adipose tissue or brain, an additional isolation step was performed, following homogenization insoluble material from the homogenate was removed by centrifugation at 12.000 X g for 10 minutes at 2 to 8 ^{o}C, and the clear homogenate solution was transferred into a new tube. All the samples were incubated for 5 minutes at 15 to 30 ^{o}C and 0.2 ml of chloroform was added in each tube. Samples were vigorously shaken by hand for 15 seconds and incubated at 15 to 30 ^{o}C for 2 to 3 minutes. Samples were centrifuged at 12,000 X g for 15 minutes at 2 to 8 °C. The

upper aqueous phase was collected and RNA was precipitated using the same amount of isopropyl alcohol of the amount of the aqueous phase, incubated at 15 to 30 ^{o}C for 10 minutes and centrifuged at 12,000 X g for 10 minutes at 2 to 8 °C. The RNA pellet was washed with 75% ethanol, air-dried for 10 minutes, resuspended in DEPC water (0.2% v/v) and stored at -80 ^{o}C.

The concentration of RNA was calculated using the absorbance at 260nm (A260) (Concentration of RNA in µg/µL = A260 X 40 X dilution factor/1000). RNA purity was estimated by the A260/A280 ratio, where good RNA purity was indicated by a ratio of 1.8 - 2.0.

2.2.14 DNAse Treatment

The RNA was DNAse treated to eliminate any DNA that co-extracted during the RNA extraction, using the Ambition's DNA-free TM kit. Per the concentration of the RNA in the sample, briefly a 2 µg sample of RNA was combined with approximately 20µl of nuclease-free water, to bring the final solution to 0.1µg/µl, and 0.5 µl TURBO DNase (Ambius). The solution was incubated at 37 ^{o}C for 30 minutes using the heat block. To inactivate the DNase, 2 µl of inactivation reagent was added, the mixture was mixed and incubated for 5 minutes. The tubes were centrifuged at 10,000g for 1.5 minutes. Approximately 20 µl of supernatant that contains the RNA was transferred to a new PCR (0.2 µl) tubes and either used for cDNA synthesis or stored at -80 ^{o}C for future use.

2.2.15 cDNA synthesis

Reverse transcription of a DNAse treated RNA was performed using random primers with a Super Script TM III reverse transcriptase system per the manufacturer's instructions. A 20 µl reaction containing of 1µl random primers (0.1mg/ml), 1 µl dNTPs (10mM), 9µl RNAase free water and 2 µl of RNA (from 20 µl solution), the solution was heated at 65 ^{o}C for five minutes and then rest for one minute at 4 ^{o}C in PCR machine. After 4µl of 5 X First-Strand Buffer (240mM Tris-HCL [pH 8.3], 375 mMKCL, 15 mM MgCl2), 1 µl DTT (0.1 M), 1 µl RNase out water and 1µl of Superscript III (200 units/ul) were added in to each tube and the final mixture was subjected to thermal cycling at the following temperatures: 25 ^{o}C for 5 minutes, 50 ^{o}C for 60 minutes, 70 ^{o}C for 15

minutes and 4 ^{o}C for 5 minutes. After the reverse transcription, each cDNA sample was diluted by adding 40 µl of RNase free water, all the samples were stored at -80 ^{o}C or used immediately for Real Time PCR.

2.2.16 Real Time PCR

Real Time PCR (RT-PCR) was performed in 384 - wells plates using Taqman® reaction chemistries. A 10 µl reaction was added per well that contained TaqMan® Universal PCR Master Mix (5µl), gene of interest (0.5 µl), RNase free water (1.5 µl) and 3 µl of cDNA sample. Each sample was run in duplicate. The Real - Time PCR reaction was performed by using the ABI 7500 Real Time PCR machine (Applied Biosystems, Forest City, CA, USA), ViiA 7 Software (v1,2). The samples were exposed to the following conditions: 50 ^{o}C for 2 minutes, 95 ^{o}C for 10 minutes, then 40 incessant cycles of heating to 95 ^{o}C for 10 seconds and cooling 60 ^{o}C for 1 minute.RT-PCR gene expression was calculated relative to *GAPDH*. We tested different control gene in our lab including *β-actin*, *18s* and *GAPDH* and we found *GAPDH* to be more stable (data not shown), Therefore, we decided to use *GAPDH* as the housekeeper for this study. Also, these house keeper genes have been used in research for C57BL/6 mice (Day et al., 2018).

2.2.17 Oroboros (Mitochondrial respiration and ROS measurement):

Oroboros experiments were performed at Victoria University (Footscray VIC, Australia). After preparation of the respirometer (washing stoppers and chambers with ethanol and milli-Q H2O, calibration of respirometer and ROS). Liver tissue was prepared in 2 ml MIRO and 2 mg of fibre was dried in the filter paper before weighing them on weighting paper. Oxygen was injected to the chamber until the reading reaches 420, and when was stabilised the tissue was added. For complex ROS, 5 µl of superoxide dismutase 10 U, 5µl of amplex ultra red 50umol and 10 µl horseradish peroxidase 25 U were added to the chamber. To measure the lacking of Complex I we added 5 µl malate 5 mM^{-1} and 10 µl pyruvate 5 mM^{-1} to chamber. Following we waited for flux to be stable and to measure the Complex I by adding to chamber 24 µl of magnesium chloride 250 mM and 20 µl of ADP 5 mM^{-1} and waited for the flux to be

stable. For the Complex I and Complex II together (OXPHOS) we added 20 µl succinate 10 mM^{-1}. For damage test 5 µl of cytochrome-C 10 mM^{-1} was added. Following maximum respiration was measured by adding 0.5 mM^{-1} FCCP 1µl. Then we inhibited Complex I with 1 mM^{-1} rotenone 2 µl. Finally, we inhibited Complex III by adding 5 μM^{-1} antimycin - A 2 µl (non-mitochondrial respiration).

2.2.18 Anaesthesia

Mice were anesthetized with Nembutal (sodium pentobarbitone 12 mg/kg body weight) using 0.5 ml insulin syringes.

To reduce stress in animals, tests usually are performed on anesthetized mice. Although recent studies have shown that anaesthesia may have an effect on heart rate and the flow of the blood, and also may provoke hyperglycaemia in rodents (Brown et al., 2004) (Pomplun, Möhlig, Spranger, Pfeiffer, & Ristow, 2004) (Brown, Umino, Loi, Solessio, & Barlow, 2005). Aynsley - Green et,al suggest that pentobarbitone anaesthesia may result in hyperglycaemia and glucose intolerance, perhaps because of the defect in peripheral glucose absorption (Aynsley-Green, Biebuyck, & Alberti, 1973).

Thus, tests that involve glucose metabolism in anesthetized mice may show abnormal and unrealistic. To avoid unwanted effects all these tests should be performed in conscious rodents.

2.2.19 Oral Glucose Tolerance Tests (OGTT)

This method was performed according to Andrikopoulos et.al (Andrikopoulos, Blair, Deluca, Fam, & Proietto, 2008). All mice were fasted from 8 am till 2 pm (6 hours) with ad libitum access to water. On conscious mice, a bolus of glucose was delivered into the stomach by a gavage needle (20-gauge, 38 mm long curved, with a 21/4 mm ball end; Able Scientific, Canning Vale, Western Australia, Australia) and 200µl of blood was tested at 0, 15, 30, 60, and 120 min for plasma glucose and insulin analyses. Immediate centrifugation was performed and the plasma was separated from red blood cells and stored at -20 ^{o}C until analysed.

2.2.20 Pyruvate Tolerance Test

Pyruvate tolerance tests were performed by intraperitoneal injection of pyruvate (2 g/kg) after fasting overnight. Blood glucose levels were measured before injection (0 min) and at 15, 30, 60, and 120 min after injection.

2.2.21 Statistical Analysis:

Statistical tests and graphs design were performed by using Graph Pad® Prism 6 software. Results were stated as mean ± standard error of the mean (SEM). To determine the area under curve (AUC) the trapezoidal rule was used. Non-parametric test was performed to calculate the statistical significance. Dissimilarities were considered to be important where the p-value of the data sets was equal to or less than 0.05.

CHAPTER 3: GENERATION OF A LIVER SPECIFIC INDUCIBLE UBL5 KNOCKOUT MOUSE MODEL

3.1 Introduction

The liver is responsible for several functions, such as bile acid secretion, reallocating nutrients, producing digestive enzymes, removing toxins, and performing ureagenesis from harmful substances. When the liver becomes damaged (either through genetic or environmental factors such as alcohol abuse, viruses, increased ROS levels etc.), liver dysfunction occurs which can affect overall whole body health (Peterson, 1960).

Mitochondria are essential for energy homeostasis, metabolism, and cell death. Mitochondria generate ATP energy via the electron transport chain. Leakage of electrons can occur In the mitochondrial respiratory pathway that triggers the production of reactive oxygen species (ROS). Increased levels of ROS are damaging for the DNA and can induce cellular aging. Literature suggests that increased ROS levels can cause mitochondrial dysfunction that eventually may lead to several liver diseases such as cancer, non-alcoholic fatty liver disease and alcoholic liver disease (Yamashina, Sato, Kon, Ikejima, & Watanabe, 2009). Thus, protecting mitochondria from harmful environmental effects can be a potential approach to halt or even prevent liver disease.

The role of UBL5 has not been clearly defined in mammals. Although it is known for its splicing role in yeast and worms (Boright et al., 1998; Broadley & Hartl, 2008; Imperatore et al., 2000; Nishina et al., 1992; Rotter et al., 1996; Takunari Yoneda et al., 2004), recent studies have demonstrated that it may have a protective role in

mitochondrial stress, triggering the UPR^{mt} to help the cell maintain health (as described in Chapter 1).

Given that the liver is an important metabolic organ a disturbance in mitochondrial function through UPRmt could possibly lead to metabolic dysfunction. A knockout model in which *UBL5* (ubiquitously expressed) had been inducibly deleted specifically in the liver would be a reasonable starting point in studying the functions of UPRmt and *UBL5* in mammals and trying to identify any possible correlation with metabolic syndrome and liver dysfunction. The role of UBL5 in metabolism and mitochondrial function specifically in the liver of rodents is the primary theme of this PhD thesis study.

Genetically modified rodents are used widely in all areas of research as it facilitates the study of genes and their functions and allows for an in-depth analysis of the underpinning molecular and cellular mechanisms involved in an *in vivo* system Therefore, in order to gain a greater understanding of the role of UPRmt (via *UBL5* targeting) in the liver, we generated a conditional inducible liver specific mouse.

Our laboratory has previously studied the role of UBL5, in two genetically modified systems; muscle specific and whole body knockout mice. The resulting phenotype of the whole-body deletion of *UBL5* led to embryonic lethality, also the homozygous muscle specific *UBL5* knockouts were embryonically lethal while heterozygous were normal and did not present any phenotype. This suggests that *UBL5* is a vital gene and plays an important role in development.

3.1.1 Conditional / Inducible Gene deletion

In vivo genomic manipulation to generate tissue-specific knockout conditional gene deletion involves the use of site-specific recombinases. The two major site-specific recombination systems are the Cre/Lox system from the bacteriophage P1 (Gopaul & Van Duyne, 1999; Brian Sauer, 1994) and the Flp/Frt from Saccharomyces cerevisiae (Brian Sauer, 1994). Those site-specific DNA recombinases Cre and Flp catalyze recombination of DNA flanked by their corresponding recognition sequence loxP for Cre and Frt for Flp. To generate a knockout model using these site-specific recombination systems two different mouse lines are required. Firstly, a transgenic

mouse line is needed that expresses the recombinase in a specified tissue (such as the liver) by its upstream promoter, and secondly a mouse model that has the targeted gene (gene of interest) flanked by recognition sequences. After breeding these two lines, the offspring will have the target DNA segment (for example: gene of our interest, (*UBL5*)) deleted in the specific tissue (for example: tissue of our interest (liver)) directed by the promoter (Brian Sauer, 1994; B Sauer & Henderson, 1988). There are numerous well characterized promoters that have been used in research to manipulate genes in specific tissues along with the TTR promoter for the liver (Lamont et al., 2006; Tannour-Louet, Porteu, Vaulont, Kahn, & Vasseur-Cognet, 2002; Y. Wang, Xu, Pierson, O'Malley, & Tsai, 1997), the rat insulin 2 promoter (RIP) to drive gene expression in pancreatic β-cells and the Mip-Cre promoter for the pancreatic β-cells in mice (Kebede et al., 2008; Kulkarni et al., 1999; Wicksteed et al., 2010) and also the muscle creatinine kinase (MCK) promoter for the muscle (Bruning et al., 1998; Jaynes, Johnson, Buskin, Gartside, & Hauschka, 1988; Johnson, Wold, & Hauschka, 1989).

An inducible system is used to activate Cre at specific times, so the consequences of gene deletion can be studied at different life stages of the animal. By fusing Cre with the ligand binding domain of the steroid receptor, Cre activity can be induced (Kaczmarczyk & Green, 2003; Metzger, Clifford, Chiba, & Chambon, 1995). When this ligand is not present the steroid receptors reside in the cytoplasm bound by heat shock proteins. Upon activation with specific substrates, heat shock proteins dissociate and translocate the ligand-bound receptor into the nucleus where it binds to receptive DNA elements to alter the gene expression (Metzger et al., 1995). For example, MerCreMer (MCM) is an inducible Cre recombinase which has been fused at either Cre end by modified estrogen receptor ligand binding domains (LBDs). Tamoxifen and 4-hydroxytamoxifen (4-OHT) are the substrates that can activate MCM (Y. Zhang et al., 1996) (Figure 3.1 and Figure 3.4). Gene deletion is under the strict control of MCM because in the absence of the ligand, the gene of interest remains intact. This system has been used successfully to control gene deletion in many tissues such as liver (Tannour-Louet et al., 2002), heart (Sohal et al., 2001; Xiong et al., 2007), prostate (Birbach, Casanova, & Schmid, 2009) and renal epithelial cells (Ouvrard-Pascaud et al., 2004). Moreover, MCM can be induced with tamoxifen or 4-

OHT so the timing of gene deletion can be controlled (Rosenthal *et al.*, 1989; Jiang *et al.*, 2002).

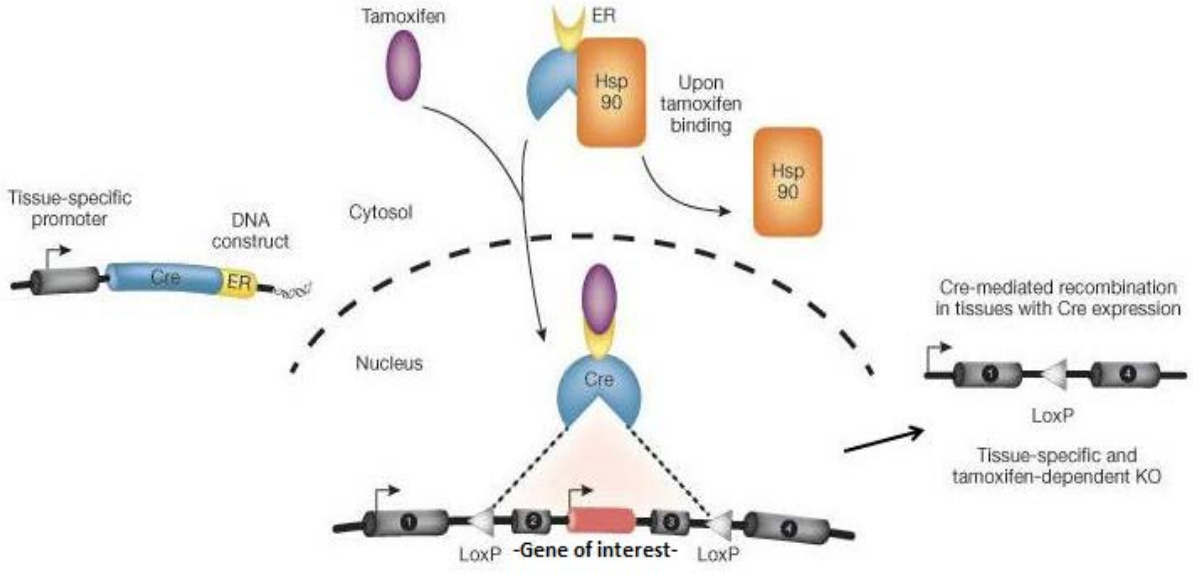

Figure 3.1: Tamoxifen-Inducible Cre/loxP system. Cre recombinase enzyme recognizes specific gene sequences that have LoxP sites. Upon the tamoxifen induction Cre is activated and excises the DNA sequence that is between these loxP sites. (Picture taken from Journal of Investigative Dermatology: Research Techniques Made Simple. Gene Knockout in Mice. Authors: Christian Günschmann, Elena Chiticariu, Bhavuk Garg, Merve Meliha Hiz, Yora Mostmans, Maria Wehner, Lukas Scharfenberger).

3.2 Chapter aims

This main aim of this chapter is to generate the experimental liver specific *UBL5* knockout (KO) mouse (UBL5 KO) model using the TTR-MCM system to investigate the *in vivo* role of UBL5 in mitochondrial function and metabolism.

3.3 Experimental Methods

The procedures used in this Chapter are detailed in the following sections. A general overview of laboratory materials and methods are described in Chapter 2.

3.3.1 UBL5lox$^{+/-}$ mouse construct

Ozgene Pty (Bentley DC, WA, Australia) was commissioned to generate floxed UBL5 mice (UBL5lox$^{+/-}$) allowing us to delete the *UBL5* gene in the specific tissue (liver) with an appropriate Cre transgenic mouse line. The coding regions of UBL5 are the DNA encompassing Exon 2 to Exon 5 (about 2kb) and were selected as target for deletion because this region encodes for the UBL5 protein. By deleting the coding region, we would expect the UBL5 protein to be absent (Figure 3.2).

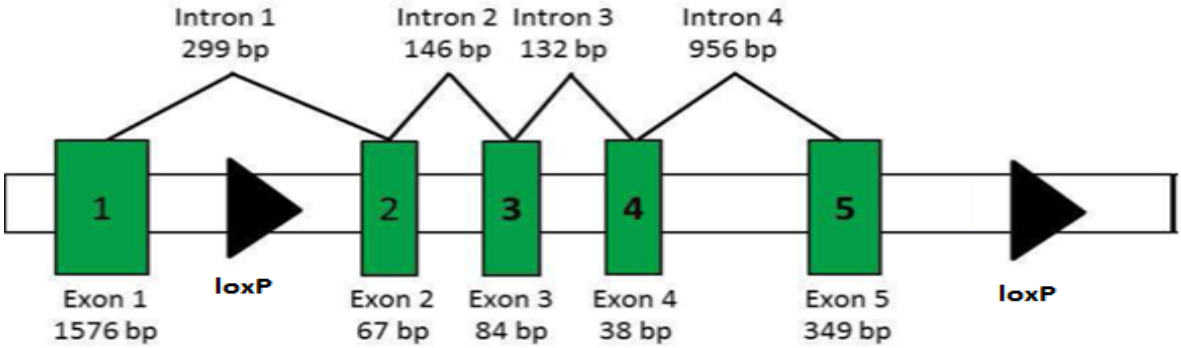

Figure 3.2: U*BL5* gene flanked with loxP sites: The targeting construct used to generate UBL5lox$^{+/-}$ mice: The UBL5 coding region that includes exon 1, exon 2, exon 3 and exon 5 is flanked by loxP sites. The exon 1 is non-coding so it was not included.

Once generated, animals were housed at the Bioresources Facility (BRF) at the Austin Hospital, Heidelberg, Victoria. The UBL5lox$^{+/-}$ mice were bred with wild type C57BL/6J mice in order to obtain offspring and maintain the homogenous background. Both male and female mice were used for the breeding purposes.

3.3.2 Transthyretin (TTR) promoter - MerCreMer (TTR-MCM) mouse construct

To avoid the potential for embryonic lethality (as we had in the past with whole body and liver specific UBL5 KO mice) we obtained a tamoxifen inducible liver specific MerCreMer mouse (TTR-MCM) by Dr Mounia Tannour Louet (Hepatology 2002, 35:10072-1081). These mice utilise the mouse transthyretin (TTR) gene promoter to drive Cre expression specifically in the liver, with virtually undetectable Cre activity in

other tissues including the brain (Tannour-Louet et al., 2002; Wicksteed et al., 2010). This unique mouse has a-3kb TTR promoter which directly targets transgene expression to the liver because this transcriptional regulatory sequence from the TTR gene encodes a serum steroid hormone carrier produced in hepatocytes (Figure 3.3) (Rausa et al., 2000; Tannour-Louet et al., 2002; H. Wu et al., 1996). We will refer to these mice as liver specific Cre mice (LS.MCM).

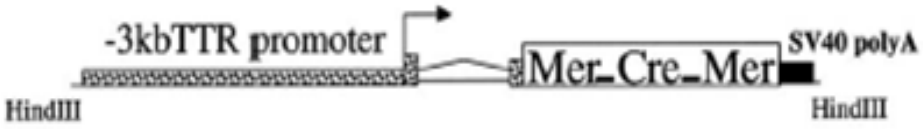

Figure 3.3: TTR promoter. Transcriptional regulatory sequence from the TTR gene, which encodes a serum thyroid hormone carrier produced in hepatocytes (targets transgene expression specifically to the liver) (Tannour-Louet et al., 2002).

As previously published (Tannour-Louet et al., 2002), MCM sequesters to the cytoplasm by the HSP90 complex. Upon induction with tamoxifen or its active metabolite 4-OHT, the HSP90 dissociates from the MCM and Cre activity become activated. The MCM/HSP90 complex dissociates and the induced MCM then translocates directly to the nucleus, where the DNA flanked by specific loxP sites becomes excised (Figure 3.4) (Tannour-Louet et al., 2002).

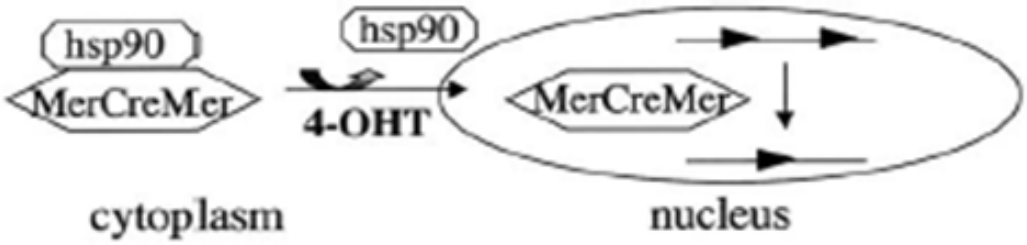

Figure 3.4: MerCreMer induction by Tamoxifen. Cre activation by tamoxifen (4-OHT) follows the heat shock protein dissociation and translocation of the ligand-bound receptor into the nucleus and excision of the DNA sequence that is flanked by loxP sites (Tannour-Louet et al., 2002).

3.3.3 Generation of inducible *UBL5* liver-specific KO mouse

UBL5lox$^{+/-}$ mice were bred with Cre$^{+/-}$ mice in order to generate UBL5lox$^{+/-}$ Cre$^{+/-}$ (heterozygous Cre positive) mice for tissue specific knockout mouse generation via the conditional Cre/lox system. Both male and female mice were used for the breeding. The UBL5lox$^{+/-}$ mouse when combined with an inducible tissue specific MCM receptor facilitates the conditional control of the tissue-specific gene *UBL5* deletion. Tamoxifen administration activates MCM and provides total control of the gene deletion. This breeding strategy provided us with UBL5 heterozygous Cre positive mice (UBL5$^{+/-}$ Cre$^{+/-}$), UBL5 heterozygous Cre negative (UBL5$^{+/-}$Cre$^{-/-}$), wild type Cre positive (UBL5$^{+/+}$Cre$^{+/-}$) and wild type Cre negative (UBL5$^{+/+}$Cre$^{-/-}$).

The second line was for the obtainment of a homozygous floxed mouse (UBL5$^{-/-}$) Cre positive that would be our UBL5 KO mouse used for the experiments. This was achieved by intercrossing two heterozygous mice; one Cre positive and one Cre negative which provided us with 1:2:1 ratio (25% wild-type mice, 50% heterozygous mice and 25% homozygous mice) (Figure 3.5). We did not observe a deviation from this expected ratio. The offspring were kept and tailed for genotyping to identify knockout mice.

Maintenance of the colony was continued with the same breeding strategy and new breeding pairs were determined once the previous breeding pair reaches 6 months old.

For the purposes of this thesis and for simplicity, the experimental genotypes will be referred to as the following:

- UBL5 liver specific homozygous Cre positive mice (UBL5$^{-/-}$Cre$^{+/-}$) will be referred to as **UBL5 KO** (UBL5$^{Liver-/-}$).
- heterozygous Cre positive (UBL5$^{+/-}$Cre$^{+/-}$) mice as **heterozygous** (UBL5$^{Liver+/-}$).
- The (UBL5$^{+/+}$Cre$^{+/-}$) which is wild type Cre positive will be referred as to **control** mice.

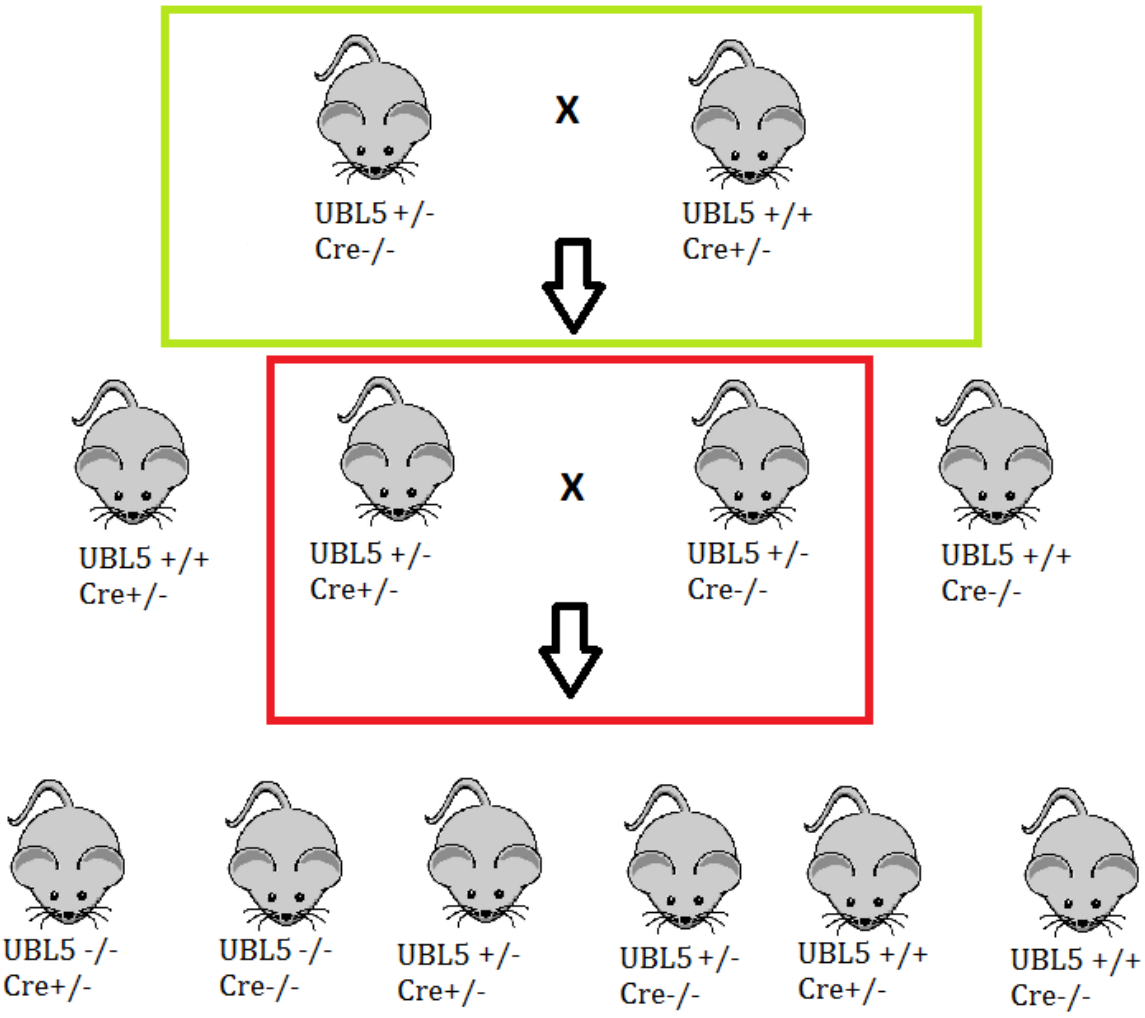

Figure 3.5: Breeding of the progeny. In **green box** we show the heterozygous Cre negative ($UBL5^{+/-}Cre^{-/-}$) crossed with wild type Cre positive ($UBL5^{+/+}Cre^{+/-}$). In the **red box** are the Heterozygous Cre positive ($UBL5^{+/-}Cre^{+/-}$) and Heterozygous Cre negative ($UBL5^{+/-}Cre^{-/-}$), on the left of the red box is the wild type Cre positive and on the right of the red box is the wild type Cre negative. The homozygous Cre positive mouse is ($UBL5^{-/-}Cre^{+/-}$) and the homozygous Cre negative is ($UBL5^{-/-}Cre^{-/-}$). The expected ratio of this method of breeding was: 25% wild-type mice, 50% of heterozygous mice and 25 % of homozygous mice.

3.3.4 Tamoxifen Administration (Optimization)

As mentioned above, tamoxifen was used to activate Cre in the UBL5 KO mice and littermates. We chose tamoxifen over 4-OHT because that was the most accurate method our laboratory group had established at the commencement of the study and based on the literature (dos Santos et al., 2008) (Whitfield, Littlewood, & Soucek, 2015). In previous years, we tested tamoxifen treatment via food intake and water

intake and we established (also based on the literature) that delivering tamoxifen gavages provided us with the fastest and most accurate way to achieve gene knockout in mice (dos Santos et al., 2008) (Whitfield et al., 2015) (Xirouchaki et al., 2016). The dose of tamoxifen for each mouse was previously determined by our laboratory to be optimal at 6 mg/mouse and administered once a day. A dose of 6 mg/mouse was made by diluting 120 milligrams of tamoxifen in 4 ml of 1.5% methylcellulose as a carrier. The suspension was mixed using a sonicator (MISONIX, Ultrasonic Liquid Processor, XL-2000 series) and stored at 4 °C until use. The 1.5% w/v methylcellulose solution was used as the vehicle control for the tamoxifen treated animals. The tamoxifen suspension was mixed by inversion prior to drawing into a 1 ml syringe fitted with a gavage needle (20-gauge, 38mm long curved, with a 2¼ mm ball end). Adult mice (UBL5 KO, heterozygous and control mice) were gavaged with either 200 µL of vehicle or tamoxifen suspension for 3 consecutive days and were left to rest for 1 week prior to experiments. Body weight and food intake were monitored throughout the course of treatment. Vehicle-treated mice were housed separately from tamoxifen-treated mice to avoid cross contamination of tamoxifen. The timeline of tamoxifen induction is illustrated in (Figure 3.6). Because we were not certain when the deletion of UBL5 would occur, we chose to cull our animals at two timepoints; on the 10th and 15th day after the 1st tamoxifen administration. On the 10th day mice were culled and plasma and tissues (liver, heart, muscle, brain, white adipose, kidney) were collected for further investigation.

We found that some UBL5 KO mice became sick and died before they reach the 15th day (time point). Therefore, we did not proceed further with this time point and performed all the experiments on the 10th day following tamoxifen administration.

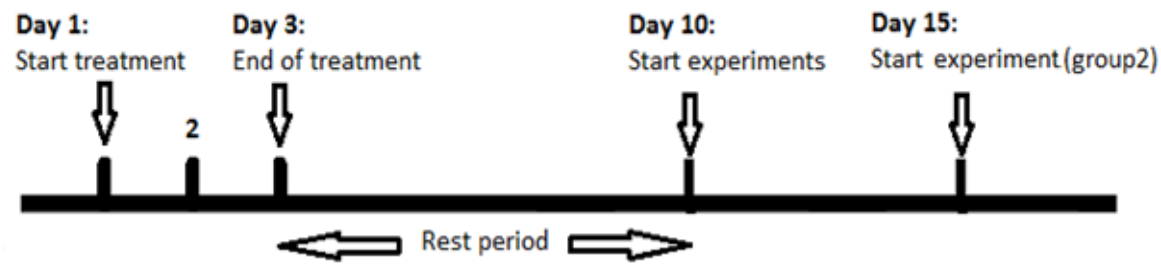

Figure 3.6: Timeline of tamoxifen induction of UBL5 KO mice and littermates.

3.3.5 Tissue Collection

Plasma, liver, brain (hypothalamus, cortex and cerebellum), heart, kidneys, skeletal muscles and white adipose tissues were collected as described in (Chapter 2) on the 10th day after the first tamoxifen gavage.

3.3.6 Genotyping

For the genotyping: ligating homologous fragments of UBL5 were generated by PCR, genomic DNA that include the 5' homology arm, 3' homology arm and the loxP arm. Both homology arms were approximately 5-6 kb in length and the loxP arm was approximately 2 kb. After genomic DNA, the sequence of the fragments was confirmed by DNA sequencing.

Genotyping was performed by using RedTAQ kits. Mouse tail (0.5 cm-1 cm) was collected and placed in PCR tubes and 100 µl of 50 mM NaOH was added per tail/tube. Each sample was incubated at 96 ^{o}C for ten minutes in the PCR machine and left to cool for 1-2 minutes. At the final stage, 10 µl of 1 M Tris (pH 8,0) added in the mix (Chapter 2). Primers P295 and P296 were designed and used to amplify the remaining lox site in our mouse model (Figure 3.7). To identify if the mice are Cre positive or not, P555 and P556 primers were used (Table 3.1).

Following agarose gel electrophoresis was done of PCR product (Chapter 2). The primer sequences used are detailed in (Table 3.1).

Table 3.1: Primer sequences used for genotyping.

Template	Primer	Sequence (5’ to 3’)
UBL5	P295 (Forward)	GCC CGC ACT GCC GCA GTT AAG
	P296 (Reverse)	TGG AGC TAC ACC AGG TGG AGG
Cre	P555 (Forward)	GCG GTC TGG CAG TAA AAA CTA TC
	P556 (Reverse)	GTG AAA CAG CAT TGC TGT CAC TT

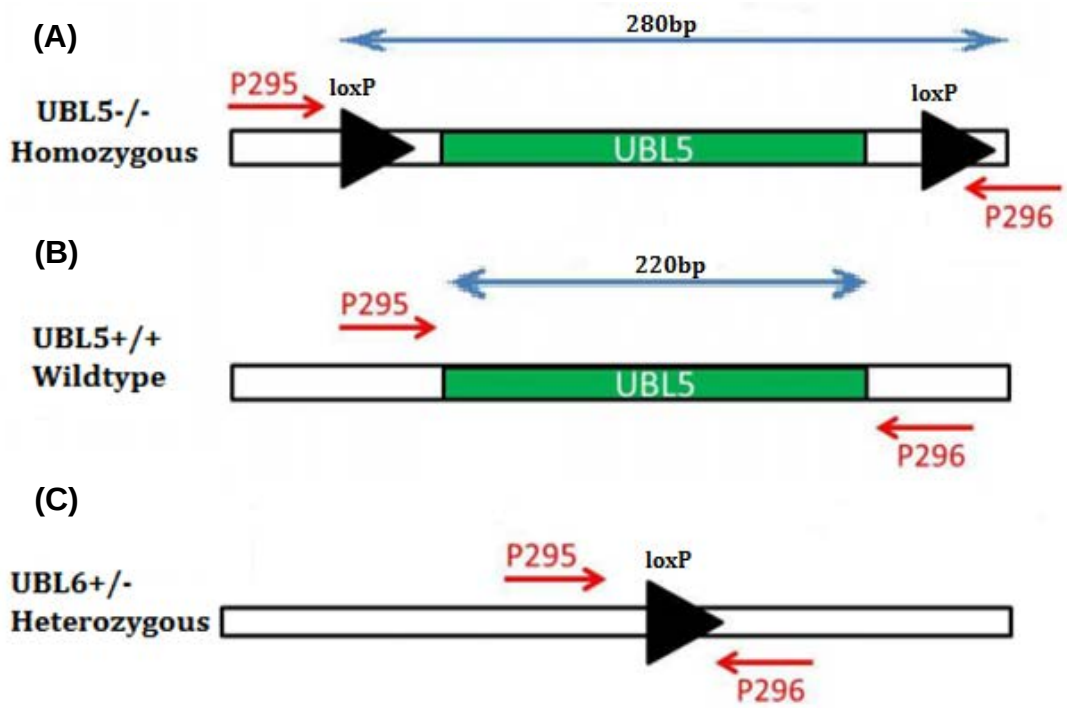

Figure 3.7: Position of primers and loxP sites in our UBL5 knockout mice and littermates. A diagram showing the position of primers P295 and P296 where the **(A)** homozygous knockout has two loxP sites, **(C)** heterozygous one loxP site and **(B)** wild type none sites.

3.3.7 Gene Expression Studies and genotyping.

For real time PCR: As detailed in Chapter 2, RNA was extracted from the various tissues treated with DNAse and reversed-transcribed to produce cDNA. The gene expression of *UBL5* was measured and the housekeeper gene *GAPDH* rRNA was measured by Real Time PCR utilising SYBR Green chemistry. The primer sequences are detailed in (Table 3.2).

Table 3.2. Primer sequences used for gene expression studies on liver specific inducible *UBL5* knockout mice.

Template	Primer	Sequence (5' to 3')
GAPDH	(Forward)	CATCACTGCCACCCAGAAGACTG
	(Reverse)	ATGCCAGTGAGCTTCCCGTTCAG
UBL5	P295 (Forward)	GCC CGC ACT GCC GCA GTT AAG
	P296 (Reverse)	TGG AGC TAC ACC AGG TGG AGG

3.4 Results

3.4.1 Genotyping of progeny

For UBL5 KO (UBL5$^{-/-}$ homozygous) mice, a PCR product band of 280 bp is expected to be observed. For wild-type (UBL5$^{+/+}$) mice a band product of 220 bp is expected and for the heterozygous (UBL5$^{+/-}$) both bands are expected to be observed. The (Figure 3.8, A) shows a representation of the genotyping outcomes expected for all groups. As can be seen in (Figure 3.8, B) for the Cre positive we expected to see a band of 400 bp and for Cre negative no band.

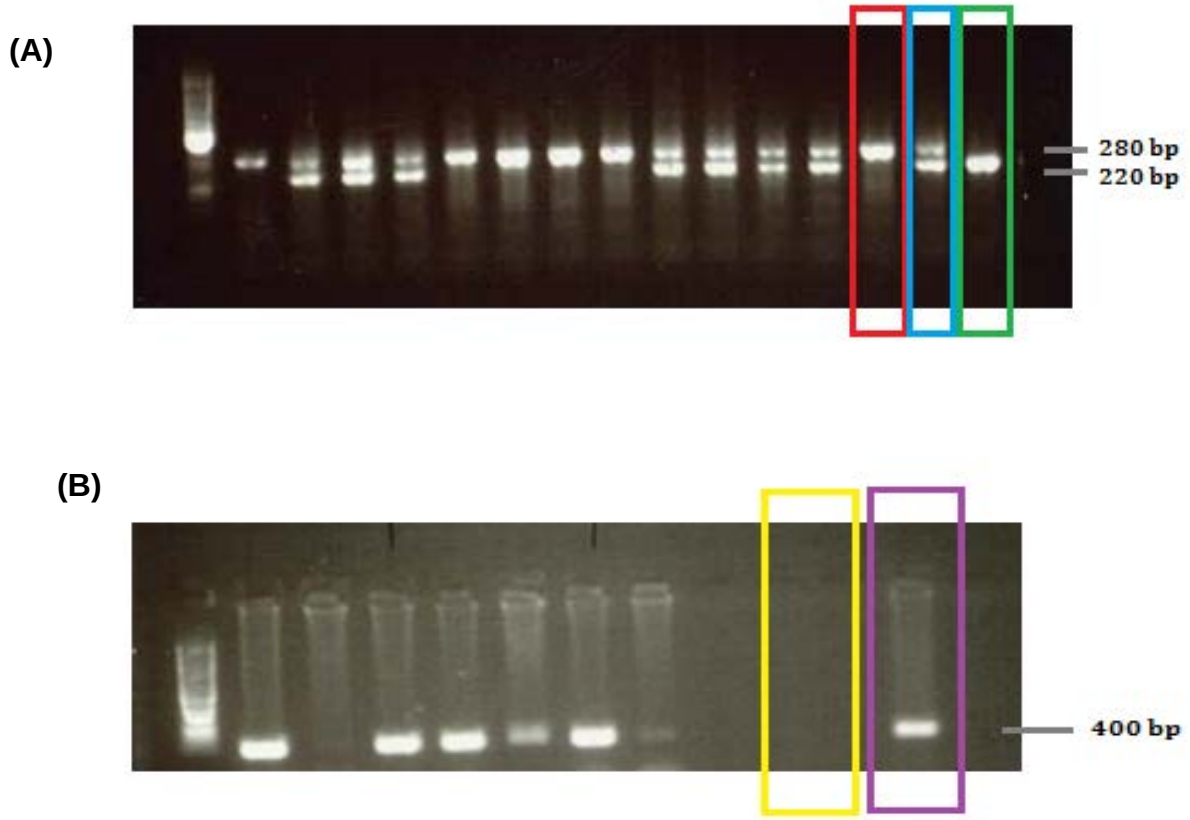

Figure 3.8: Genotyping of UBL5 KO mice and littermates. (A) Shows the positions of primers P295 and P296 in the **red** box is the 280 bp band of UBL5$^{-/-}$ homozygous mice, when both loxP sites are presented. In the **blue** box is the double band expressed in both 220 bp and 280 bp for UBL5$^{+/-}$ heterozygous mice with one loxP site and in the **green** box is the 220 bp band that represents the wildtype mice that have no loxP sites. **(B)** Shows the positions of primers P555 and P556. In the **purple** box is the Cre positive band that expresses and the **yellow** one represents the Cre negative that there is no band.

3.4.2 Body weight and food intake

The body weight and food intake was measured daily to see if the wellbeing of mice was affected by tamoxifen administration.

As it can be seen in (Figure 3.9) there were no changes in body weight between the groups (UBL5 KO, heterozygous and control mice). Also, the food intake did not show differences between groups (Figure 3.10).

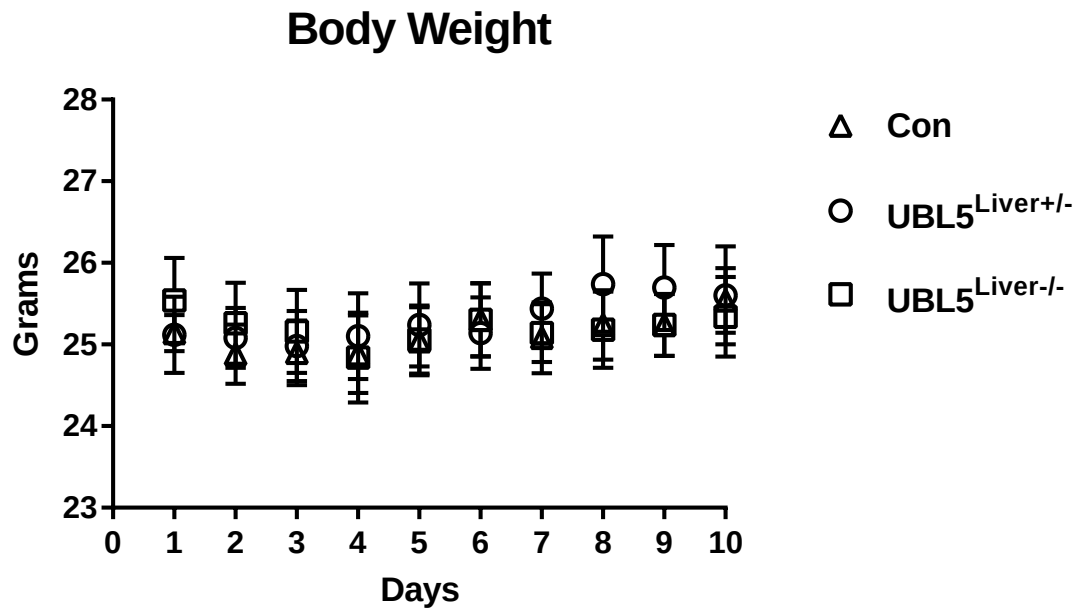

Figure 3.9: Body weight. A daily body weight measure for control mice (Con) shown in green circle, heterozygous mice ($UBL5^{Liver+/-}$) shown in blue square and homozygous mice / UBL5 KO ($UBL5^{Liver-/-}$) shown in red triangle. Values presented as mean ± SEM. N=10.

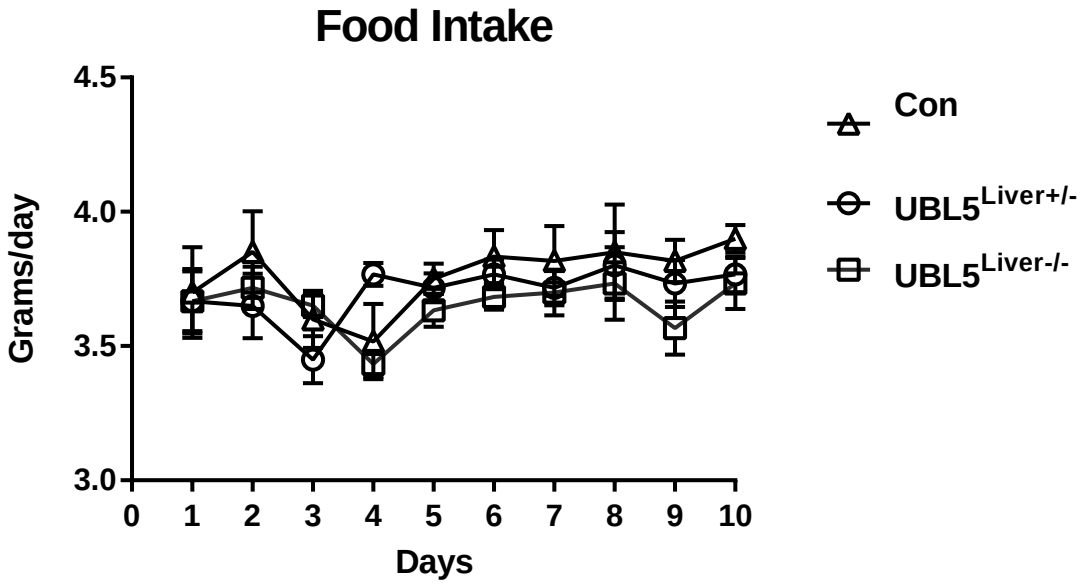

Figure 3.10: Daily food intake: A daily food intake (in grams) measure for control mice (Con) shown in green circle, heterozygous mice ($UBL5^{Liver+/-}$) shown in blue square and homozygous mice / UBL5 KO ($UBL5^{Liver-/-}$) shown in red triangle. Values presented as mean ± SEM. N=10.

3.4.3 Molecular Characterisation

3.4.3.1 Expression of *UBL5* in the liver of *UBL5* KO mice and littermates (10 days after the first tamoxifen gavage).

Real time PCR was used to assess the level of *UBL5* knockdown after tamoxifen administration in liver samples from UBL5 KO, heterozygous and the littermate control mice, 10 days following administration. Figure 3.11 shows that the KO mice have a significant (97%) reduction of *UBL5* gene in the liver compared with control mice. Whilst the heterozygous mice display an approximate 50% reduction (significant) in gene expression compared to littermate control mice.

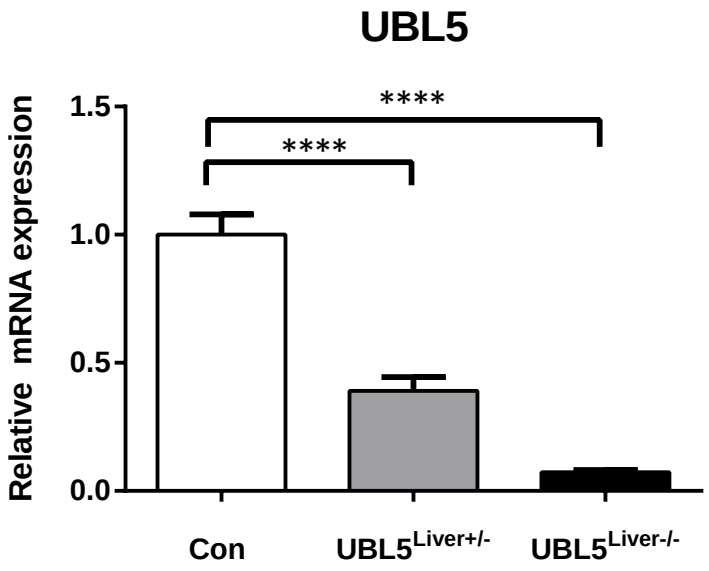

Figure 3.11: *UBL5* mRNA levels in the liver from *UBL5* KO mice and littermates 10 days after the first tamoxifen gavage: mRNA levels were expressed relative to the control (C57BL/6 wild type Cre positive mice) sample, $UBL5^{Liver+/-}$ is the heterozygous group and the $UBL5^{Liver-/-}$ is the homozygous. The ΔΔCt method was used to calculate relative quantification of gene expression with GAPDH rRNA as the housekeeper gene. Values presented as mean ± SEM. n=10. ****p ≤ 0.0001.

3.4.3.2 Expression of *UBL5* in other tissues

To confirm that *UBL5* was not supressed in other tissues, we measured the mRNA levels in heart, kidney, white adipose tissue, muscle and brain of the UBL5 KO, heterozygous and littermate control mice. As can be seen in (Figure 3.12), *UBL5* expression was not reduced in either the KO or heterozygous mice compared to the littermate control mice in any of the tissues examined (panels A – E).

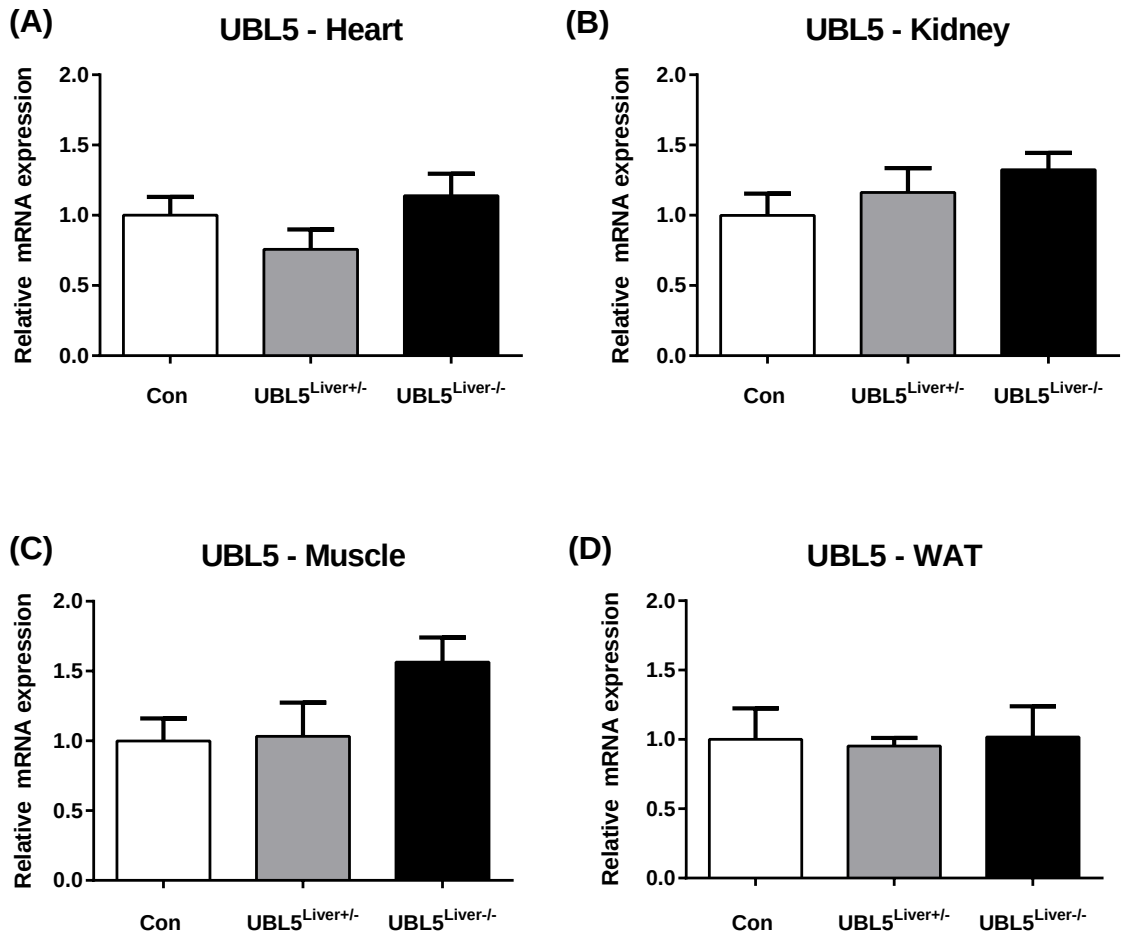

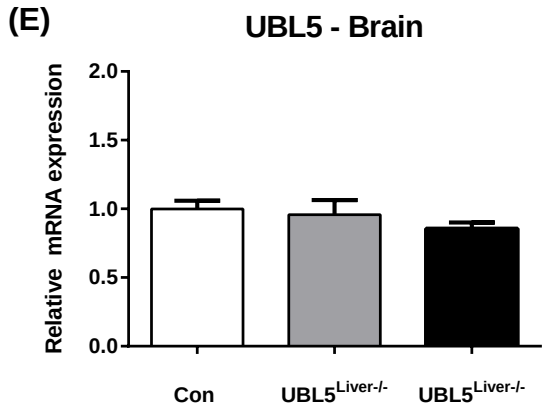

Figure 3.12: *UBL5* mRNA levels in various tissues from UBL5 KO mice and littermates 10 days after the first tamoxifen gavage: *UBL5* mRNA levels were expressed in **(A)** heart **(B)** kidney **(C)** muscle - right gastrocnemius **(D)** white adipose tissue **(E)** brain, all relative to the control (C57BL/6 wildtype Cre positive mice) sample, $UBL5^{Liver+/-}$ is the heterozygous group and the $UBL5^{Liver-/-}$ is the homozygous. The ΔΔCt method was used to calculate relative quantification of gene expression with GAPDH rRNA as the housekeeper gene. Values presented as mean ± SEM. n=10.

3.5 Discussion

Engineered mouse models are critical tools in research to study gene function and physiological contributions of gene products. In the present study, liver specific *UBL5* knockout mouse models were generated.

In an effort to elucidate the role of UPRmt and UBL5 in a mammalian system and more specifically in the liver, we pursued this work by generating a conditional liver specific UBL5 KO model. This work has not been undertaken previously and we are the first laboratory to generate and study these mice.

To generate UBL5 KO mice the Cre/lox recombination system was selected, where the Cre was controlled by tamoxifen. As it was shown in previous studies, mice that are flanked by loxP sites at the gene of interest can be crossed with other mice that express Cre activity under the control of specific tissue promoters providing total control of gene deletion, as the gene can be deleted via tamoxifen administration (Rajewsky et al., 1996; Ryding et al., 20010). There are other different systems that use other inducers to delete genes such as Flp/Frt (Brian Sauer, 1994). In our study, we chose the Cre/lox system, because this method provides flexibility in studying gene

function in various tissues, as mice with the gene of interest flanked by loxP sites can be crossed with mice expressing Cre under different tissue-specific promoters (Rajewsky *et al.*, 1996; Ryding *et al.*, 2001). Many studies have utilized this system in the past. For example, the insulin receptor (IR) knockout mice (Bruning *et al.*, 1998). To produce IR KO mice Bruning *et. al* generated the IR(lox/+) mice and crossed them with mice expressing Cre in several tissues such as liver, β-cell, skeletal muscle, heart, adipocytes, brown adipose tissue, brain and vascular endothelium (Bruning *et al.*, 1998; Kulkarni *et al.*, 1999; Bruning *et al.*, 2000; Michael *et al.*, 2000; Guerra *et al.*, 2001; Belke *et al.*, 2002; Bluher *et al.*, 2002; Bluher *et al.*, 2003; Vicent *et al.*, 2003). Additionally, Lin et.al generated the peroxisome proliferator - activated receptor gamma coactivator 1-alpha (PGC-1α) knockout mice and crossed with different Cre mice to generate whole-body, neuronal and muscle PGC-1α KO mice (Lin *et al.*, 2004; Handschin *et al.*, 2007; Ma *et al.*, 2010).

Tamoxifen is the essential substrate in inducible Cre gene deletion (Tannour-Louet et al., 2002; Y. Zhang et al., 1996). There are various ways of tamoxifen or 4-OHT administration in research to induce the Cre activity. The intraperitoneal (i.p) injection has been reported as the most frequently used method of administration in mice (Brocard et al., 1997; Indra et al., 1999; Imai, 2003; Zhang et al., 2005), although it has been reported to cause spontaneous death to 6% of subjects (Andersson, Winer, Mørk, Molkentin, & Jaisser, 2010; C. Guo, Yang, & Lobe, 2002; Kiermayer, Conrad, Schneider, Schmidt, & Brielmeier, 2007). To test this, our laboratory performed a comparison experiment between different tamoxifen administration routes in mice, using either oral gavage or i.p. injection. Ruan et al showed that mice treated with gavage had rate of 100% survival, while the mice treated with i.p injections had 62% rate of survival (Ruan et. al, unpublished observations “Andrikopoulos lab”). Additionally, repetitive i.p. injections caused irritation close to the injection site and sleet of tamoxifen on the skin, in that way dropping the rate of survival. Even though these problems can be solved by oral gavage, there are other limitations of this method. Oral gavage can stress mice as the needle could injure the throat causing discomfort during feeding. This could lead to eating and drinking disorders and consequently loss of weight and dehydration. To test this throughout the period of tamoxifen treatment, we were tracking daily the body weight and food intake. Mice did

not show significant decrease in these parameters, showing that the daily gavages did not compromise the welfare of the rodents.

The first approach to test the knockdown of *UBL5* in our mice was a real-time PCR in liver samples that we collected from UBL5 KO, heterozygous and control mice on the tenth day after the first tamoxifen gavage. At this time point we were not exactly sure that we would see the desirable results because we were still optimizing the time needed to achieve the knockdown in our mouse model. We found a significant reduction in gene expression in the UBL5 KO mice by 97%, whilst in the heterozygous mice there was a modest 60% reduction when compared to the control mice. It is known that the duration of tamoxifen treatment varies depending on the methods and protocols from 1 to 59 days depending on the dose and way of administration (Andersson et al., 2010). Achieving 97% *UBL5* gene reduction in KO mice 10 days after tamoxifen treatment was ideal for our study.

A limitation of this study was the absence of Western blot results. Western blot was a challenging aspect of this study as UBL5 is a small protein of approximate 9 kDa in size. In the past attempts were made using 15% and 20% polyacrylamide gel, 15-20% polyacrylamide gradient gels, 10-20% tris-tricine gradient gel (Bio-Rad® Laboratories) as well as running the gel at 4 ^{o}C but the aforementioned were unsuccessful in detecting a band. Furthermore there are no commercially available antibodies specific against UBL5 for Western blotting. Therefore we have had to rely on UBL5 mRNA levels for the gene expression pattern in the knockout mice.).

It is widely shown that the Cre recombinase system combined with an appropriate promoter shows high specificity in the tissue of interest without the issue of leakage to other tissues (Lewandoski, 2001; Santoro & Schultz, 2002). Furthermore, the TTR promoter has been demonstrated to be liver specific without affecting other organs/tissues (Tannour-Louet et al., 2002; Y. Wang, DeMayo, Tsai, & O'Malley, 1997). However, we wanted to confirm that in our mouse model, there was no other off target effects where *UBL5* was deleted in other tissues. The results clearly showed the specificity of the promoter with no reductions in gene expression in the tissues studied. Interestingly, there was a trend for an increase in *UBL5* gene expression in the muscle and heart of the KO mice, but these results did not reach statistical

significance. Taken together these results confirmed the liver specificity of our UBL5 KO mice model.

3.6 Conclusion

In conclusion, we have shown that the methodology chosen to generate the knockout model proved to be highly effective with little to no adverse effects of the use of the tamoxifen treatment. Furthermore, we have clearly shown that the KO mice have a near 100% deletion of UBL5 specifically in the liver with partial deletion detected in the heterozygous mice. We have now generated our working model to investigate the role of UBL5 in the UPRmt specifically in the liver.

In Chapter 4 we will study and describe in detail the phenotype of the UBL5 KO and heterozygous mice compared to control mice.

CHAPTER 4: PHENOTYPIC CHARACTERIZATION OF LIVER SPECIFIC INDUCIBLE *UBL5* KNOCKOUT MICE AND LITTERMATES

4.1 Introduction

In Chapter 3 we demonstrated the successful deletion of *UBL5* specifically in the liver using the MCM Cre Lox system and we generated the UBL5 KO mice ($UBL5^{Liver-/-}$), heterozygous ($UBL5^{Liver+/-}$) and control mice. Our model clearly confirmed the specificity of the *UBL5* deletion in the liver and not in other metabolic active organs. As we observed in the previous chapter on the 10th day the KO mice showed 97 % UBL5 gene deletion and heterozygous mice had approximately 65 % gene deletion. Approximately 15 days after the first tamoxifen gavage the homozygous mice seemed to suffer severe liver dysfunction and premature death, while the heterozygous and control mice did not suffer the same consequences (the death rate of homozygous was 100%). Where post-mortem analysis was conducted with the help of the resident veterinarian, livers from homozygous mice presented pale and had dark patches along with yellow fluid accumulation in the peritoneal cavity while the rest of the organs appeared normal. We assume that the homozygous mice died due to liver failure. Therefore, for this chapter we redesigned the protocol to study the mice at 5-days and 10-days post tamoxifen gavage. This Chapter will present and discuss the results obtained from phenotypic characterization of the liver specific UBL5 KO mouse model in order to understand the possible role of UBL5 in liver mitochondrial function.

As we described in detail in Chapter 1, the evidence that UBL5 is associated with the UPRmt came from studies in the *C. elegans* and mammalian cells (C. M. Haynes

et al., 2007). The UPRmt stress response is essential for the maintenance of the proper mitochondrial function (C. M. Haynes et al., 2007). Studies suggest that knockdown of *UBL5* by RNA interference inhibited the induction of heat shock proteins such as HSP60, leading to impaired mitochondrial function and the assembly of unfolded mitochondrial proteins (Benedetti et al., 2006). Moreover, nuclear and cytosolic *UBL5* gene expression becomes elevated as a consequence of mitochondrial stress, suggesting the ability for UBL5 to self-amplify to cope with stress (Haynes et al., 2007; Haynes et al., 2010). Benedetti et al showed that the mitochondrial matrix chaperones H*SP70* and *HSP60*, encoded by the *C. elegans* were triggered by distress that led to protein folding within the mitochondria (Takunari Yoneda et al., 2004). An early in vitro study showed the mammalian stress protein HSP70 (mitochondrial HSP70) networking with mitochondrial proteins (Mizzen et al., 1989; Mizzen et al., 1991; Wadhwa et al., 2002). A study in rat hepatoma cells depleted of mitochondrial DNA, showed elevated levels of HSP60 and HSP10 because of accumulation of unfolded proteins (Martinus et al., 1996). Further studies demonstrated that misfolded proteins within the mitochondrial matrix were recognized by the protease complex ClpP-1 that degraded misfolded proteins to peptides or release ligand and convey the UPRmt signal to the cytosol (Broadley & Hartl, 2008) (Takunari Yoneda et al., 2004). Also, a study on mammalian cells presented evidence that a UPRmt can be stimulated by *Clpx* protease (Al-Furoukh et al., 2015). As Al-Furoukh et,al showed in mammalian cells (myoblasts), that overexpression of *Clpx* upregulated the markers (such as CHOP, HSP10, HSP60 and HSP70) of the mitochondrial proteostasis pathway (the UPRmt) (Al-Furoukh et al., 2015). A transcription factor CHOP seemed to play a key role in triggering the UPRmt in mammals (Quan Zhao et al., 2002). Along with mammalian ATF5 that seems to act in place of DVE-1 (worms) in mammals and showed to induce transcription of mitochondrial proteostasis genes (Fiorese, 2016) (Al-Furoukh et al., 2015). Disturbance in the UPRmt pathway can lead to mitochondrial dysfunction and apoptosis (C. M. Haynes et al., 2007).

Mitochondrial dysfunction can be linked to several disorders in the liver (D. J. J. o. g. Pessayre & hepatology, 2007; Wei, Rector, Thyfault, & Ibdah, 2008). Hepatic steatosis and liver injury are caused because of the impaired mitochondrial function coming from depletion in mitochondrial DNA and increased ROS levels (Demeilliers

et al., 2002; Fromenty, Pessayre, & therapeutics, 1995). Recent evidence suggest that mitochondrial dysfunction may play a significant role in the pathogenesis of NAFLD, although the actual mechanism of fatty liver is still unclear (Caldwell et al., 1999; Ibdah et al., 2005; D. Pessayre & B. J. J. o. h. Fromenty, 2005; Sanyal et al., 2001b). NAFLD comprises of liver steatosis, non-alcoholic steatohepatitis (NASH) fibrosis and cirrhosis. It can progress towards liver failure and premature death. (McCullough, 2004). Pathogenesis of NAFLD most likely involves reduced capacity to oxidize fatty acids, increased hepatic fatty acid synthesis and increased delivery and passage of FFAs into the liver (Wei et al., 2008). The mitochondrial abnormalities related with NAFLD consist of impaired mitochondrial β-oxidation, reduces activity of respiratory chain complexes, increased ROS levels, diminished *PGC-1* (nuclear receptor pleiotropic regulators oxidative and glycolytic metabolism) and morphological abnormalities such as ultrastructural lesion (Mangelsdorf et al., 1995; Valerio et al., 2006; Wei et al., 2008). Studies in animal models and patients with NAFLD have shown morphological changes of mitochondria such as hypodense, bigger in size and fragmented mitochondria (Begriche, Igoudjil, Pessayre, & Fromenty, 2006; Caldwell et al., 1999; Ibdah et al., 2005; Sambasiva Rao & Reddy, 2004; Sanyal et al., 2001b; Sobaniec-Lotowska & Lebensztejn, 2003). Similar mitochondrial lesions were shown in liver biopsies from patients treated with agent (4,4' -diethylamino ethoxyhexestrol) that inhibits β-oxidation and mitochondrial respiratory chain activity (Berson et al., 1998). Extended treatment with this drug is related with steatosis in the liver that histologically resembles the NAFLD in humans (Berson et al., 1998). Also, decreased expression of mitochondrial DNA have shown in patients with NASH accompanied with reduced action of complexes I, III, IV and V (Pérez-Carreras et al., 2003; Santamaría et al., 2003).

Despite the evidence that UBL5 may have functional significance in the regulation of energy homeostasis and metabolism, the precise role of UBL5 in different mammalian tissues have not been thoroughly examined. This chapter will utilise our liver specific UBL5 knockout model and characterize the effects of the deletion in the UPRmt response and in mitochondria and liver function.

4.2 Chapter Aim

The overall aim of this Chapter is to investigate the function(s) of *UBL5 in vivo* and in *vitro* (primary hepatocytes extracted from our liver specific inducible *UBL5* mice model). This will be achieved by studying the phenotypic consequences of partial or complete *UBL5* deletion using the floxed (inducible) *UBL5* liver specific KO mice model.

4.3 Experimental Methods

The procedures used in this Chapter are detailed in the following sections. A general overview of laboratory materials and methods are described in (Chapter 2).

When we refer to UBL5 KO mice and littermates we include the following groups; UBL5 KO or homozygous inducible liver specific *UBL5* mice ($UBL5^{Liver-/-}$) and heterozygous inducible *UBL5* liver knockout mice ($UBL5^{Liver+/-}$) and controls, that were generated and identified as detailed in (Chapter 3).

4.3.1 Study design

Our findings in (Chapter 3) as we described above demonstrated that around 15 days after the first tamoxifen gavage some UBL5 KO homozygous mice presented with apparent liver failure and consequently death, while the heterozygous and control mice did not show signs of liver dysfunction. After our findings, we decided to reassess the timeline of tamoxifen administration and performed experiments on earlier days. Thus, we separated our study to two different groups one: which would be on the fifth day and the second group of experimental animals on the tenth day after the first tamoxifen gavage (Figure 4.1) and the following methods on each group were performed as described below.

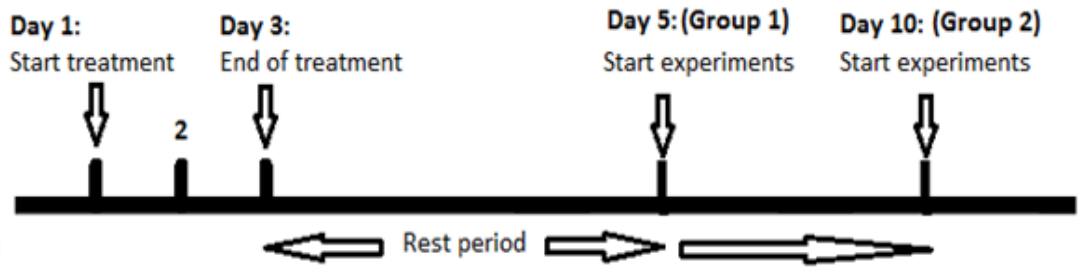

Figure 4.1: Timeline of tamoxifen induction of UBL5 KO mice and littermates.

4.3.2 Tamoxifen Administration

The same tamoxifen administration protocol was used as described in (Chapter 3).

4.3.3 Tissue Collection

Plasma, liver, brain (hypothalamus, cortex and cerebellum), heart, kidneys, skeletal muscles and white adipose tissues were collected as described in (Chapter 2).

4.3.4 Primary Hepatocyte Isolation

Hepatocytes were isolated from our liver specific inducible UBL5 knockout mouse model as described in (Chapter 2). To stain for mitochondria, MitoRed stain was used as described in (Chapter 2).

4.3.5 Gene Expression Studies

RNA was extracted from the various tissues (Chapter 2), treated with DNAse (Chapter 2) and reversed-transcribed to produce cDNA (Chapter 2). The gene expression of *UBL5* and several other genes that are thought to be involved in mitochondrial unfolded protein response such as *CHOP, ATF5, HSP70mt, HSP60, HSP10, Clpp, ClpX* and *lonp-1*, also *PGC1-α* (mitochondrial biogenesis gene) and also genes involved in several aspects of fatty acid synthesis and metabolism such as, *CPT1α, FASN, ACACA, PPARα* and *PPARγ*. All these genes were measured and the

housekeeper gene *GAPDG* rRNA by Real Time PCR utilising the SYBR Green chemistry (Chapter 2).

Primer and template concentrations were optimized for *UBL5* as detailed in Chapter 2). The optimal primer concentration was determined to be 150 nM for each of forward and reverse primer. The optimal cDNA template concentration was identified as 25 ng. The Comparative Ct (ΔΔCt) method was used to calculate relative quantification of gene expression.

4.3.6 Measurements of Plasma Parameters

Plasma was sent to the Department of Pathology, Austin Health for measurements of liver enzymes (Bilirubin, ALT, AST and AP), total protein levels, cholesterol, triglycerides and ketone levels.

4.3.7 Histology

Liver samples fresh and fixed (10% formaldehyde) were sent to the Department of Pathology, Austin Health for tissue processing and staining with hematoxylin & eosin, caspase 3 and 4-HNE (fixed liver tissues) and for Oil Red O (fresh liver tissues) as per manufacturers' instructions.

4.3.8 Oral Glucose Tolerance Test (OGTT)

The OGTT was performed as described in (Chapter 2). After the procedure, mice were sacrificed by cervical dislocation and plasma, liver, brain (hypothalamus, cortex and cerebellum) heart, kidneys, skeletal muscles (gastrocnemius), and white adipose tissues (subcutaneous, infra renal and gonadal) were excised, frozen in liquid nitrogen and stored at -80 °C until use for gene expression studies.

4.3.9 Mitochondrial Respiration Assessment (Oroboros)

Mitochondrial respiration experiment was performed on fresh liver samples as described in (Chapter 2) and all experiments were performed at Victoria University (Footscray Nicholson Campus).

4.4 Results

4.4.1 Phenotype of the liver specific UBL5 KO mice and littermates (5 days after first tamoxifen gavage)

4.4.1.1 Expression of UBL5 in the UBL5 KO mice and littermates

UBL5 gene expression in the livers collected from our groups is shown in Figure 4.2. Five days' post tamoxifen administration, both the heterozygous and homozygous mice showed a 70 percent reduction in the expression of UBL5 compared to control mice.

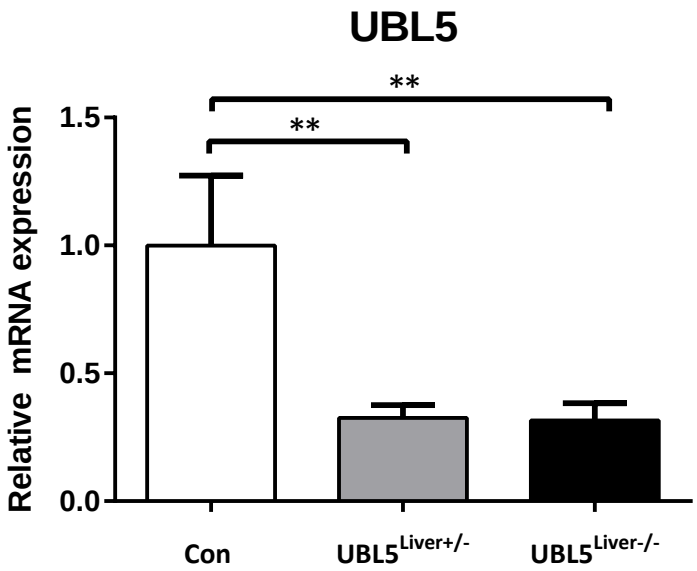

Figure 4.2: *UBL5* mRNA levels in the liver from UBL5 KO mice and littermates 5 days after the first tamoxifen gavage: mRNA levels were expressed relative to the control sample, UBL5Liver+/- is the heterozygous group and the UBL5Liver-/- is the homozygous. The ΔΔCt method was used to calculate relative quantification of gene expression with GAPDH rRNA as the housekeeper gene. Values presented as mean ± SEM. n=6-11. **p ≤ 0.01.

4.4.1.2 Physiological characteristics of UBL5 KO mice and littermates

On the 5th day after the first tamoxifen gavage, body weight (Figure 4.3) and liver weight (Figure 4.4) were measured. No significant differences were observed between groups.

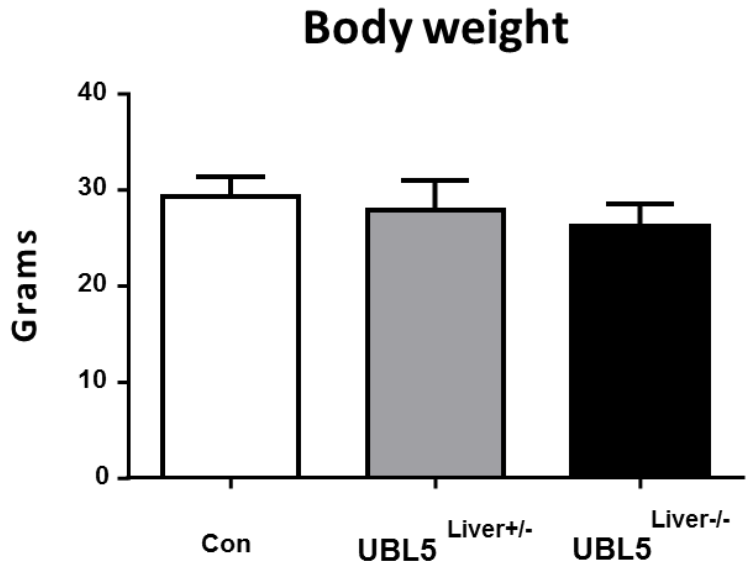

Figure 4.3: Body weight of UBL5 KO and littermates: Body weight of heterozygous ($UBL5^{Liver+/-}$), homozygous ($UBL5^{Liver-/-}$) and controls (Con) was measured on the 5th day after the first tamoxifen gavage. N=6-11.

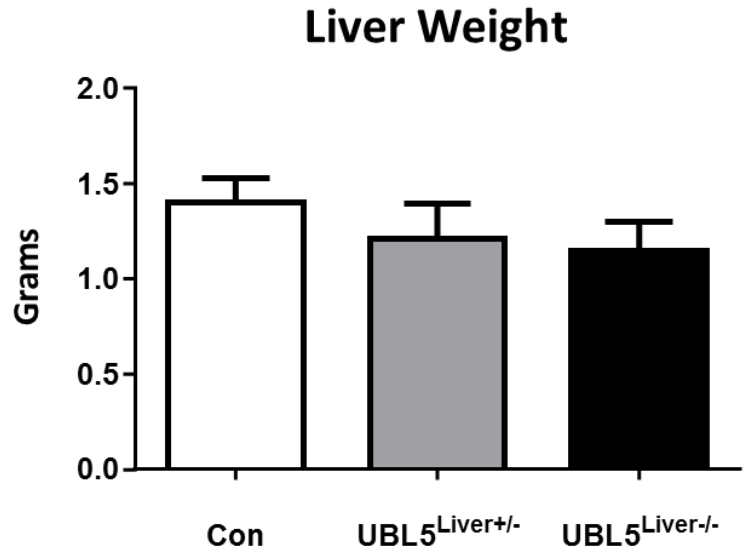

Figure 4.4: Liver weight of UBL5 KO and littermates: Liver weight of heterozygous ($UBL5^{Liver+/-}$), homozygous ($UBL5^{Liver-/-}$) and controls (Con) was measured on the 5th day after the first tamoxifen gavage. N=6-11.

4.4.1.3 Histology

Histology was performed fixed liver. We did a H&E stain in order to analyse morphology (Figure 4.5. A, B, C) which were sent to the Department of Anatomy and Neuroscience (histopathology and organ pathology service) of the University of Melbourne for blind evaluation and scoring. All mouse groups showed no cellular degradation and the morphology appeared normal. The Australian Phenomics Network (APN) staff used a grading scale from 0 to 5 to illustrate the histological changes. All groups were scored between of 0 to 2, which is considered normal (Chapter 2 Methods).

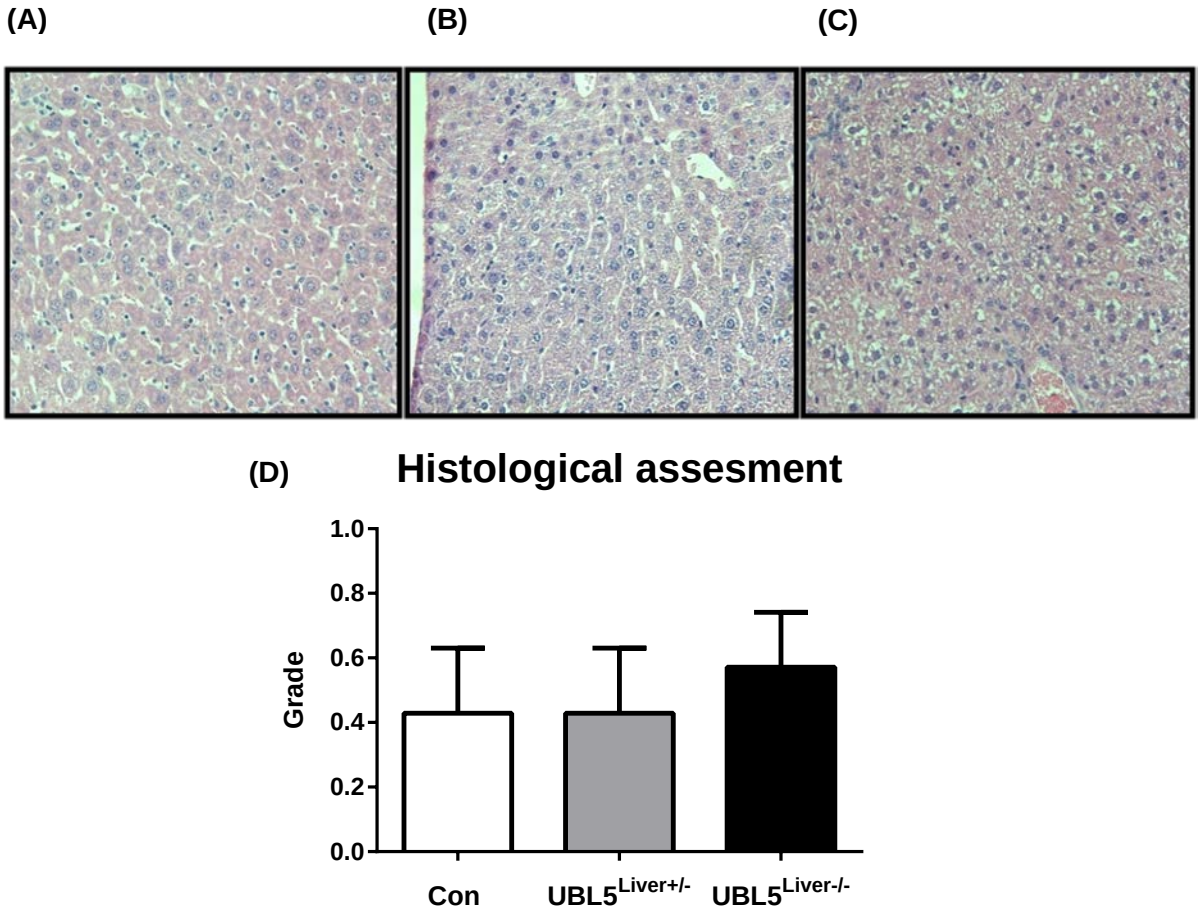

Figure 4.5: Hematoxylin and eosin stain on UKL5 KO mice and littermates 5 days after the first tamoxifen gavage: Hematoxylin and eosin (H&E) stain was done on fixed (in 10% formaldehyde) liver tissues taken from (A) controls, (B) UBL5Liver+/- (Heterozygous) and (C) UBL5Liver-/- (Homozygous – KO). All three pictures are times 20 under the microscope (x20). (D) A graph that represents histological grade in between of three groups compare to the controls. N=5.

4.4.1.4 Liver function test of UBL5 KO mice and littermates

Liver enzymes were measured in plasma collected from UBL5 KO homozygous, heterozygous and control mice. The bilirubin levels were shown as 1 mol/L in all the animals of each group, thus there is no error bar (Figure 4.6 A, B, C, D).

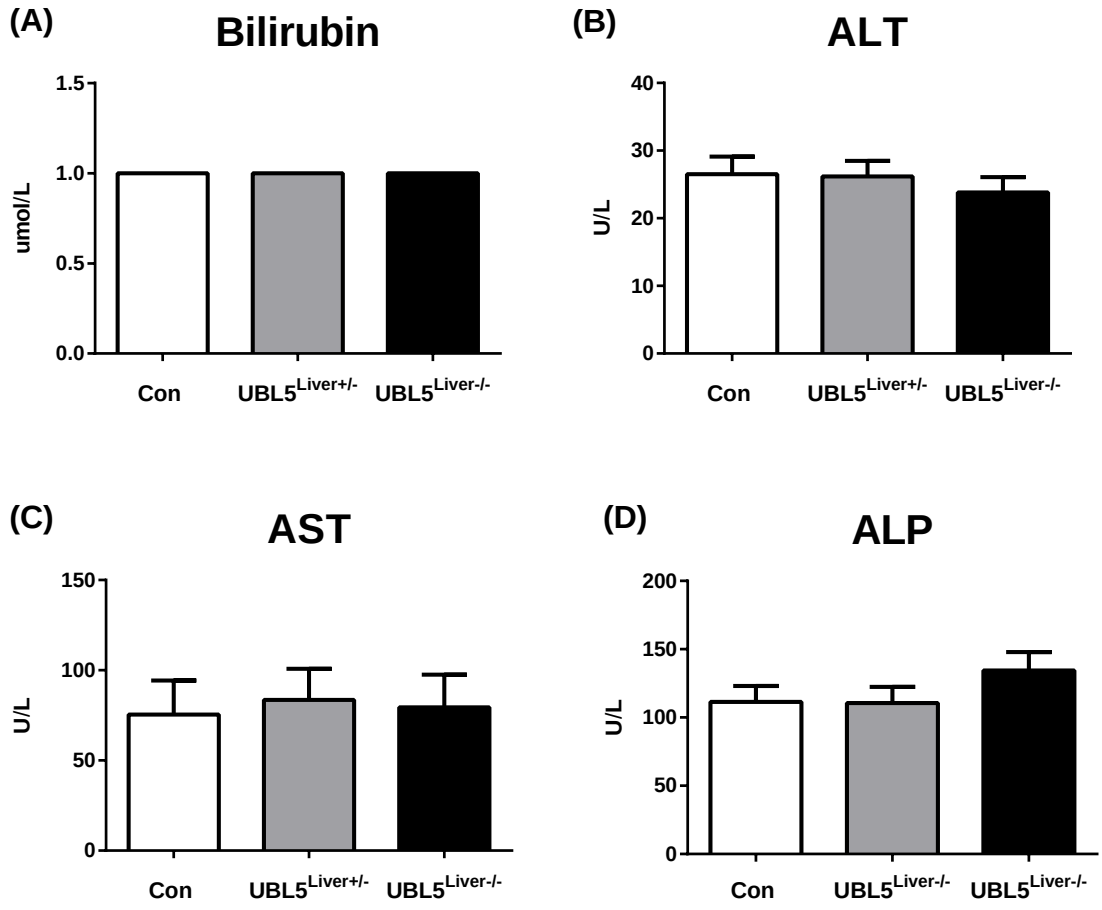

Figure 4.6: Liver plasma enzyme levels of KO mice and littermates: Liver function test, plasma enzymes were assessed in $UBL5^{Liver+/-}$ (Heterozygous), $UBL5^{Liver-/-}$ (homozygous – KO) and controls. **(A)** Bili = bilirubin, **(B)** ALT = Alanine transaminase, **(C)** AST = Aspartate aminotransferase, **(D)** ALP = Alkaline phosphatase). N=6-11.

4.4.1.5 Oral glucose tolerance tests in UBL5 KO mice and littermates

Oral glucose tolerance tests (OGTTs) were performed in conscious mice per the protocol in Chapter 2 with both male and female mice used for the assessment, UBL5 KO homozygous, heterozygous and control mice. There did not appear to be a strong glucose phenotype in the conscious mice. Glucose tolerance was not affected on the 5th day after the first tamoxifen gavage. (Figure 4.7).

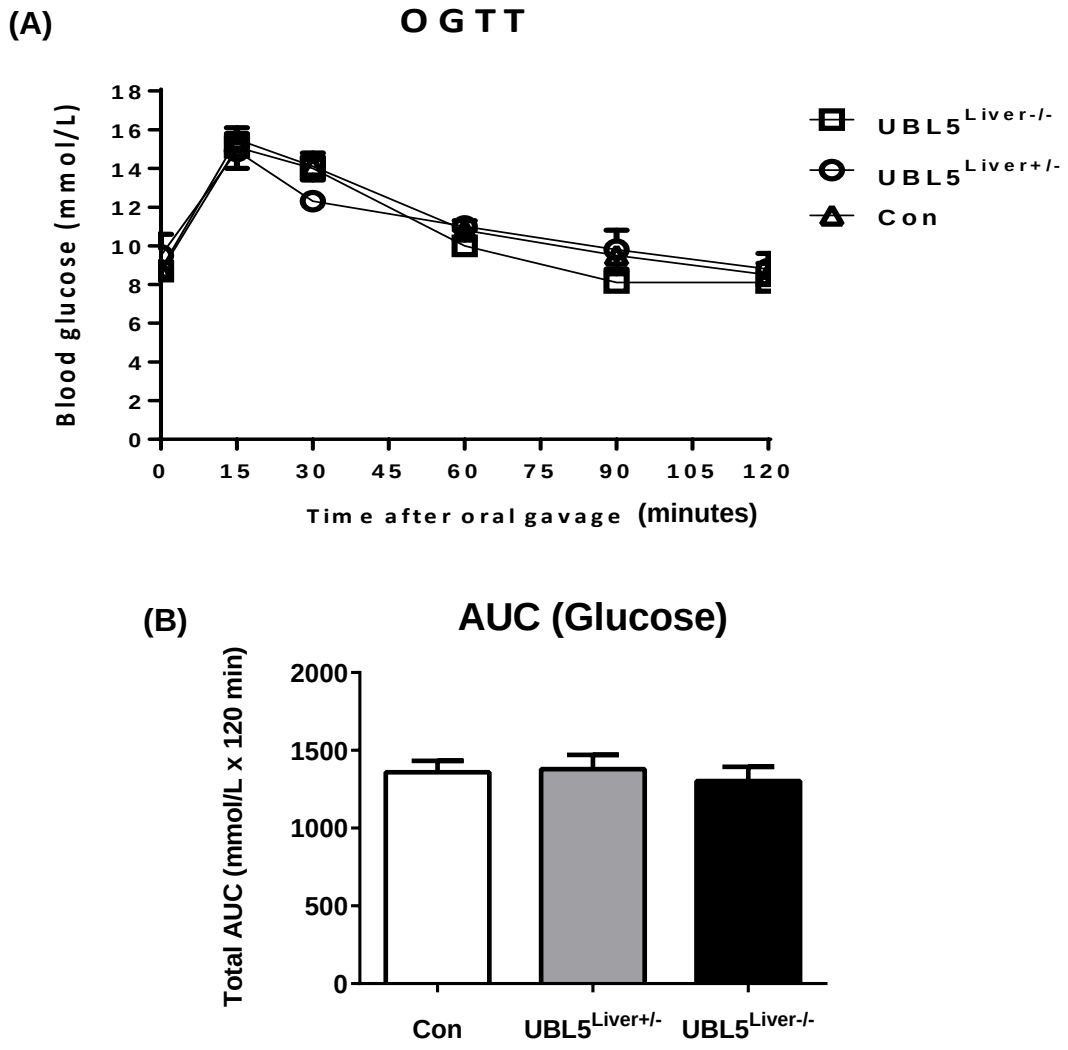

Figure 4.7: Oral glucose tolerance test (OGTT) of UBL5 KO mice and littermates. Oral glucose tolerance tests were performed on UBL5$^{Liver+/-}$ (Heterozygous), UBL5$^{Liver-/-}$ (Homozygous - KO) and controls **(A)** Plasma glucose levels were measured at various time points. **(B)** Plasma glucose levels during an OGTT expressed as Area Under Curve. N= 6 – 13.

4.4.1.6 Expression profile of UPR^{mt} genes in the liver of UBL5 KO mice and littermates

To check the expression of UPRmt genes in the UBL5 KO mice and littermates, we assessed the mRNA levels of *CHOP*, *Clpp* and *HSP60* genes (Figure 4.8). No difference in the levels of expression were observed between the groups.

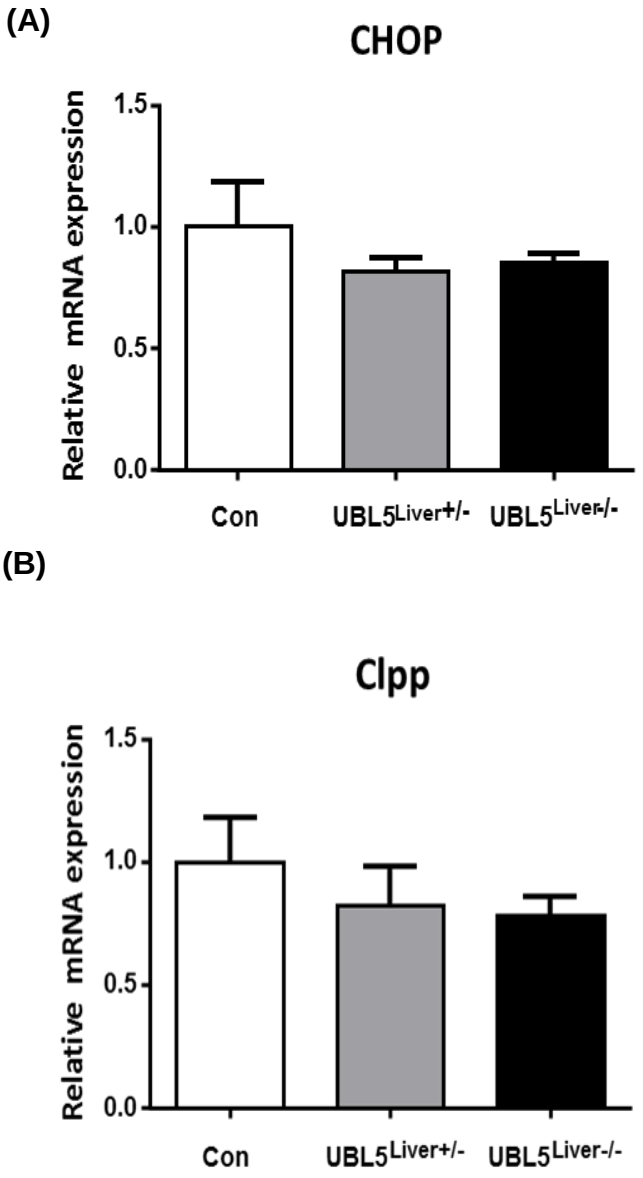

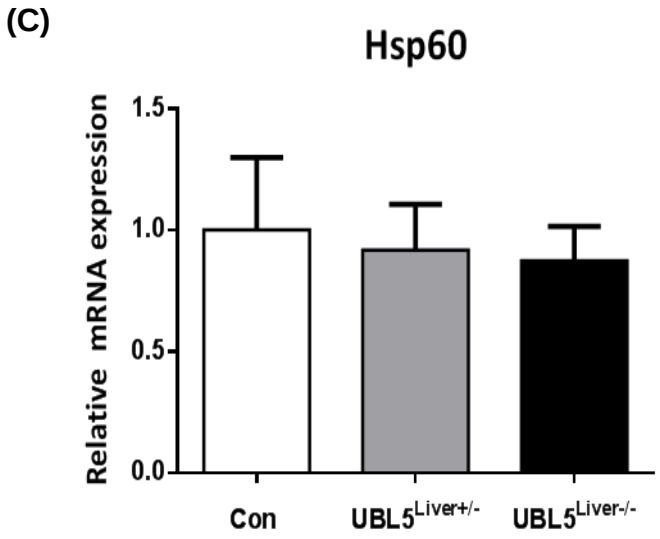

Figure 4.8: UPRmt genes mRNA levels in the liver from UBL5 KO mice and littermates 5 days after the first tamoxifen gavage: mRNA levels of **(A)** CHOP, **(B)** Clpp and **(C)** Hsp60 were expressed relative to the control sample, $UBL5^{Liver+/-}$ (Heterozygous) and $UBL5^{Liver-/-}$ (Homozygous – KO). The ΔΔCt method was used to calculate relative quantification of gene expression with GAPDH rRNA as the housekeeper gene. Values presented as mean ± SEM. n=5-10. NS P > 0.05.

4.4.2 Phenotype of the UBL5 KO mice and littermates (10 days after first tamoxifen gavage)

4.4.2.1 Expression of UBL5 in the UBL5UKO mice and littermates

Real Time PCR was performed to examine the *UBL5* gene expression pattern in the liver from UBL5 KO mice and littermates and the result is shown in Figure 4.9. There was a 65 percent reduction of *UBL5* gene in heterozygous mice and 95 percent reduction in KO mice compared to the littermate controls.

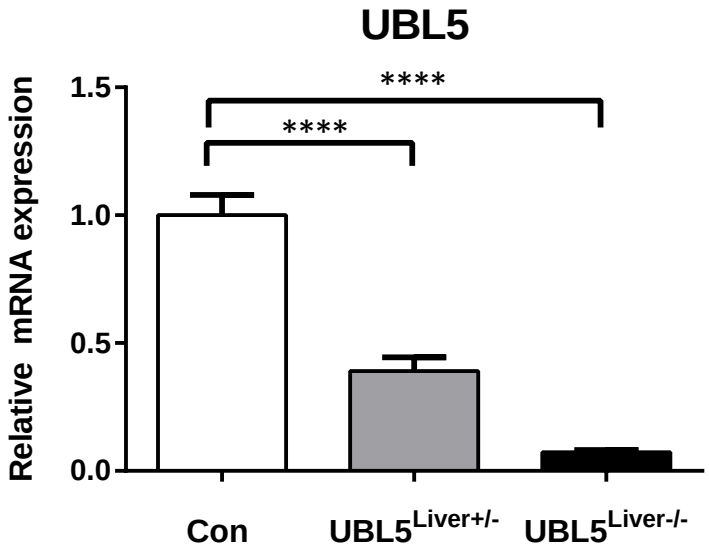

Figure 4.9: *UBL5* mRNA levels in the liver from UBL5 KO and littermates 10 days after the first tamoxifen gavage: mRNA levels were expressed relative to the control sample, $UBL5^{Liver+/-}$ (Heterozygous) and $UBL5^{Liver-/-}$ (Homozygous – KO). The ΔΔCt method was used to calculate relative quantification of gene expression with GAPDH rRNA as the housekeeper gene. Values represent mean ± SEM. n=12-22. ****p ≤ 0.0001.

4.4.2.2 Physiological characteristics of UBL5 KO mice and littermates

4.4.2.2.1 Body Wight, Liver Weight, Glucose and Insulin levels

Body weight (Figure 4.10) and liver weight (Figure 4.11) were measured in all groups of mice. There were no significant differences in body weight between the groups. However, liver weight was significantly lower in the UBL5 KO homozygous mice compare to both controls and heterozygous mice. Glucose levels by using glucometer and Insulin levels via ELISA kit were measured in plasma after 6 hours fasting in UBL5 KO mice and littermates. Glucose levels did not show any difference between groups while insulin levels found lower in UBL5 KO mice compare to controls and heterozygous (Table 4.1).

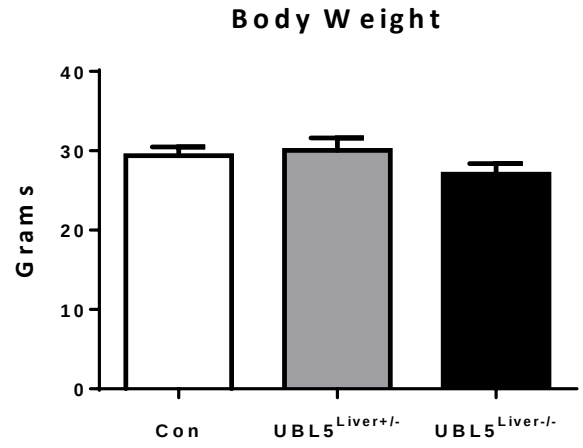

Figure 4.10: Body weight of UBL5 KO and littermates: Body weight of UBL5$^{Liver+/-}$ (Heterozygous), UBL5$^{Liver-/-}$ (Homozygous – KO) and controls was measured on the 10th day after the first tamoxifen gavage. N=12-22.

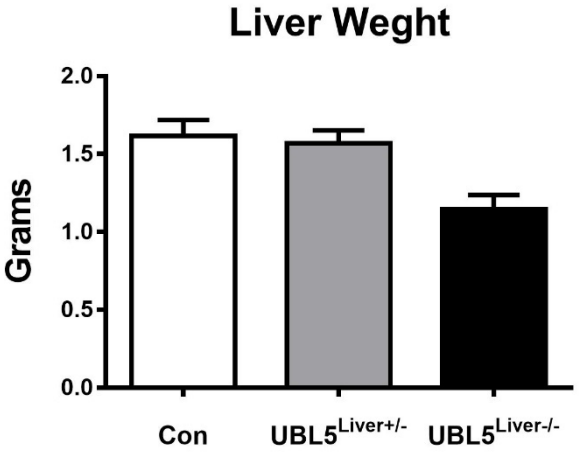

Figure 4.11: Liver weight of UBL5 KO mice and littermates: Liver weight of UBL5$^{Liver+/-}$ (Heterozygous), UBL5$^{Liver-/-}$ (Homozygous – KO) and controls was measured on the 10th day after the first tamoxifen gavage. N=12-22. ** P ≤ 0.01.

Table 4.1: Insulin and Glucose of UBL5 KO mice and littermates. UBL5$^{Liver+/-}$ (Heterozygous), UBL5$^{Liver-/-}$ (Homozygous – KO) plasma were collected on the 10th days after the first tamoxifen gavage. N=3. * P ≤ 0.05.

6 hours fasting	Con	UBL5$^{Liver+/-}$	UBL5$^{Liver-/-}$
Insulin (ng/ml)	2.6 ± 0.21	2.4 ± 0.23	1.4 ± 0.02 *
Glucose (mmol/l)	13.3 ± 0.3	14 ± 0.6	14 ± 1.5

4.4.2.2.2 Macroscopic observation

During dissection and tissue collection we observed differences in the liver morphology among the groups. Upon macroscopic examination of the liver we observed that UBL5 KO mice had bigger gallbladders compared to the controls and heterozygous mice and the liver looked pale and blotchy (Figure 4.12, A, B, C).

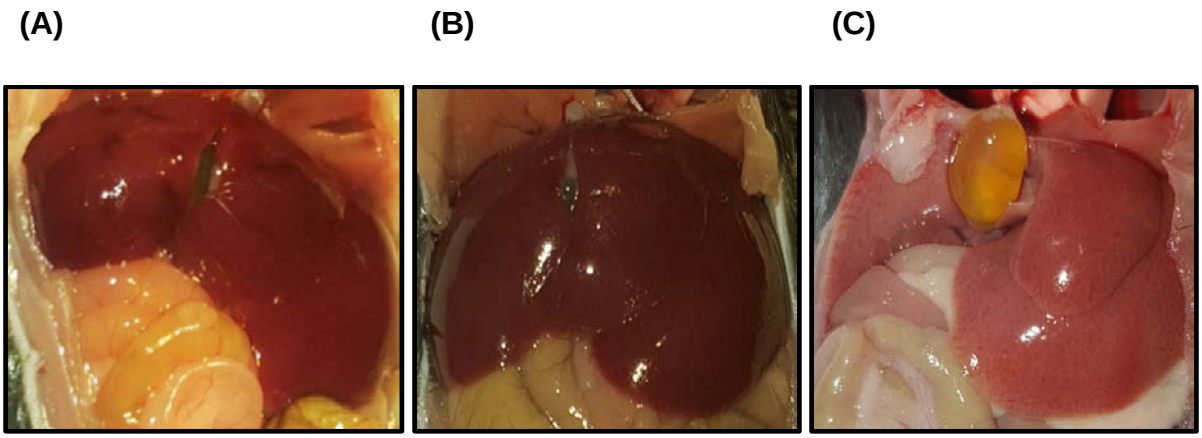

Figure 4.12: Macroscopic observation of the livers from UBL5 KO mice and littermates. **(A)** Controls, **(B)** $UBL5^{Liver+/-}$ (heterozygous) and **(C)** $UBL5^{Liver-/-}$ (Homozygous – KO).

4.4.2.3 Histology

Histology was performed on liver tissue of all mice and H&E staining was completed for morphological observation and assessment. We also performed a caspase 3 analysis for determination of apoptosis in our samples, 4-HNE staining for the assessment of oxidative damage as a marker for oxidative stress and Oil Red O for lipid deposits.

Our UBL5 KO mice stained with H&E stain showed multiple sections with severe and diffuse multifocal hepatocellular necrosis, cellular debris (organic waste left over after a cell dies by apoptosis or lysis) and angiectasis (abnormal dilation of blood vessels), haemorrhage (an outflow of blood from a burst blood vessel), vascularization (abnormal or excessive formation of blood vessels), shrunken hepatocytes, nuclear pyknosis or karyorrhexis (irreversible condensation of chromatin in the nucleus of a cell undergoing necrosis or apoptosis) compared with controls that presented with normal liver histology. No cellular damage was observed in the heterozygous mice. The grading scale from 0 to 5 was employed to illustrate the histological changes (Grade 0: Unremarkable tissue, Grade 1: Mild [1-2 foci], Grade 2: Mild to moderate [3-6 foci], Grade 3: Moderate [7-12 foci], Grade 4: Moderate to severe [multifocal], Grade 5: Severe [Diffuse]) (Chapter 2 Methods). The UBL5 KO group was graded between grade 4 to 5 indicating severe cellular damage/degradation, while the controls and heterozygous samples were scored between 0 and 2 which is considered normal (Figure 4.13).

To assess the degree of apoptosis, caspase 3 staining was significantly increased in the UBL5 KO mice compared to controls and heterozygous mice (Figure 4.14).

Oil RedO staining on fresh liver tissue showed severe macro vesicular and micro vesicular steatosis in the homozygous KO mice. With micro vesicular steatosis being surrounded around vesicles (Figure 4.15).

The 4-HNE staining was significantly increased in the UBL5 KO homozygous mice compared to heterozygous and controls (Figure 4.16).

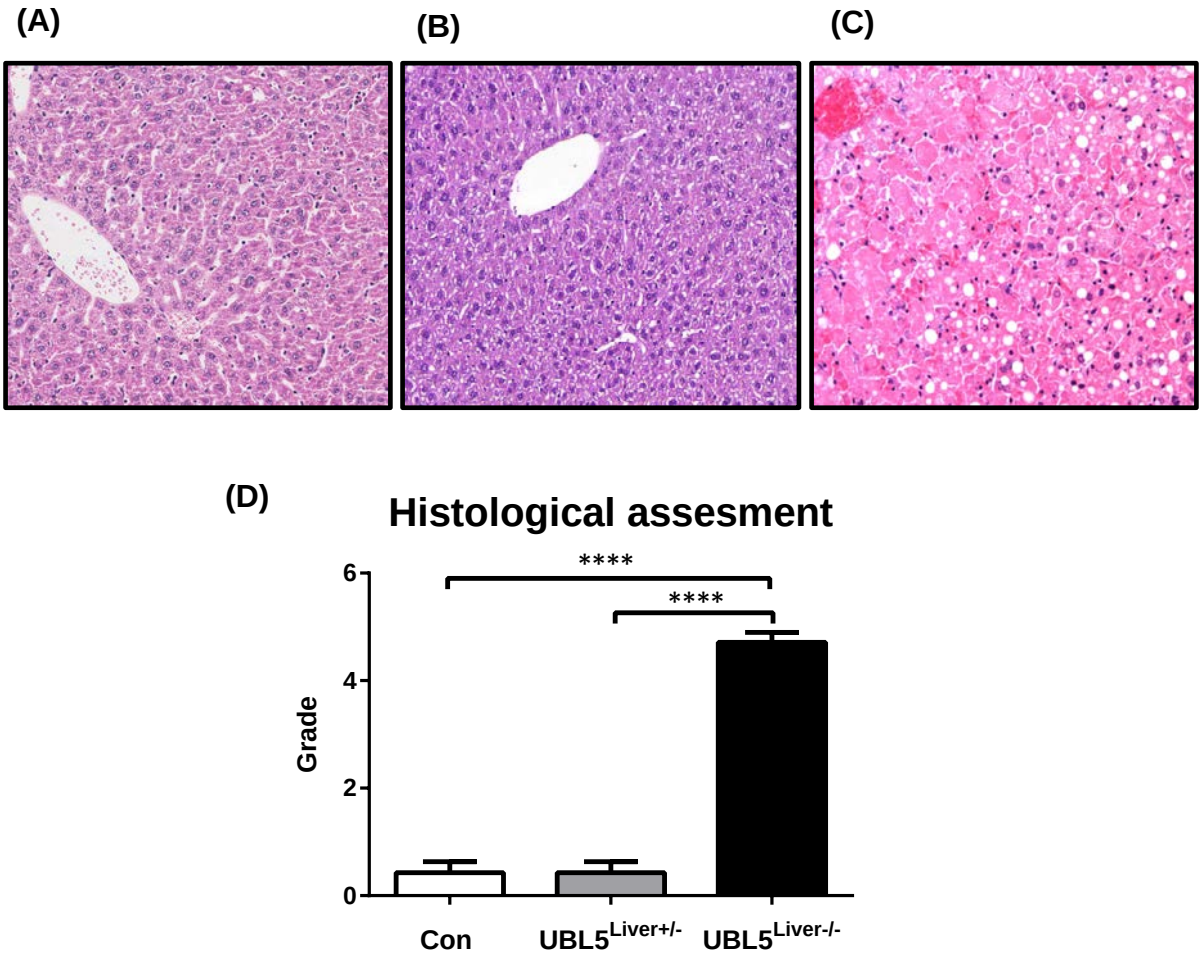

Figure 4.13: Hematoxylin and eosin (H&E) stain on UBL5 KO mice and littermates 10 days after the first tamoxifen gavage: Hematoxylin and eosin stain was done on fixed (in 10% formaldehyde) liver tissues from **(A)** controls, **(B)** $UBL5^{Liver+/-}$ (Heterozygous) and **(C)** $UBL5^{Liver-/-}$ (Homozygous – KO). All three pictures are times 20 under the microscope (x20). **(D)** A graph that represents histological grade in between of three groups compare to the controls. N=10. **** P<0.0001.

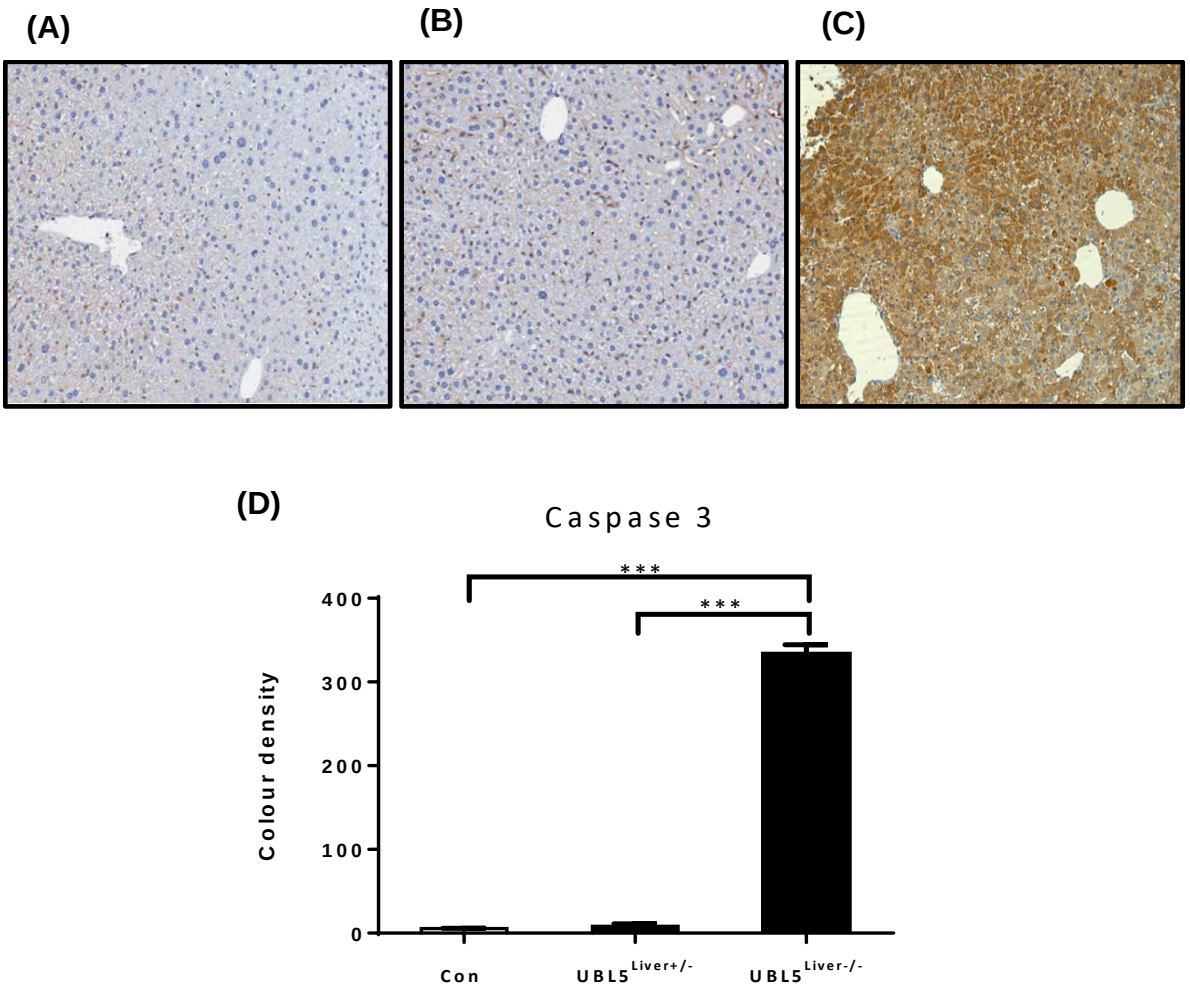

Figure 4.14: Caspase 3 stain on UBL5 KO and littermates 10 days after the first tamoxifen gavage: Caspase 3 antibody stain was done on fixed (in 10% formaldehyde) liver tissues from **(A)** controls, (B) $UBL5^{Liver+/-}$ (heterozygous) and **(C)** $UBL5^{Liver-/-}$ (Homozygous – KO). All three pictures are times 20 under the microscope (x10). **(D)** A graph that represents histological grade in between of three groups compare to the controls. N=4. *** P<0.001.

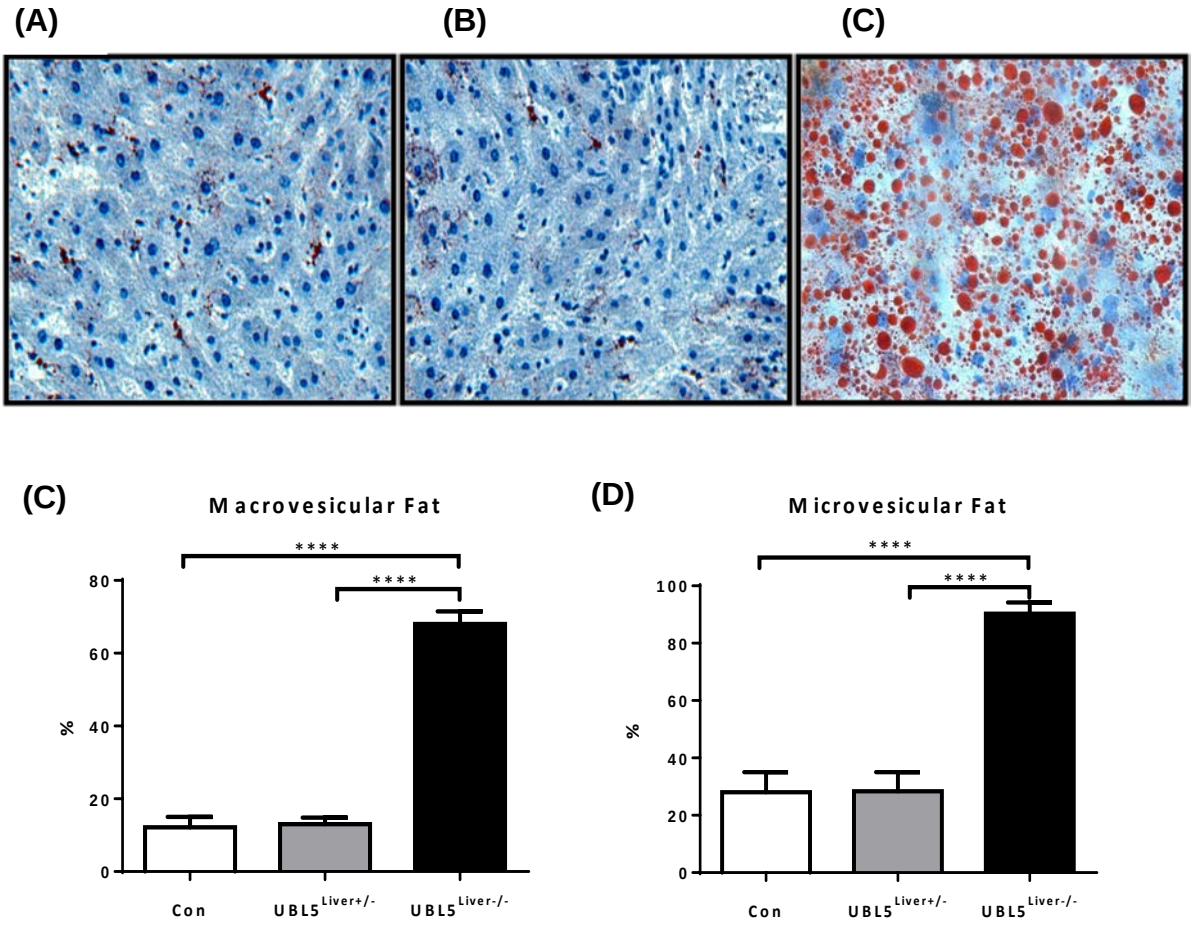

Figure 4.15: Oil RedO stain on UBL5 KO and littermates 10 days after the first tamoxifen gavage: Oil RedO stain was done on fresh liver tissues from **(A)** controls, (B) UBL5$^{Liver+/-}$ (heterozygous) and **(C)** UBL5$^{Liver-/-}$ (Homozygous – KO). All three pictures are times 20 under the microscope (x10). **(D)** A graph that represents histological grade in between of three groups compare to the controls. N=4. **** P<0.0001.

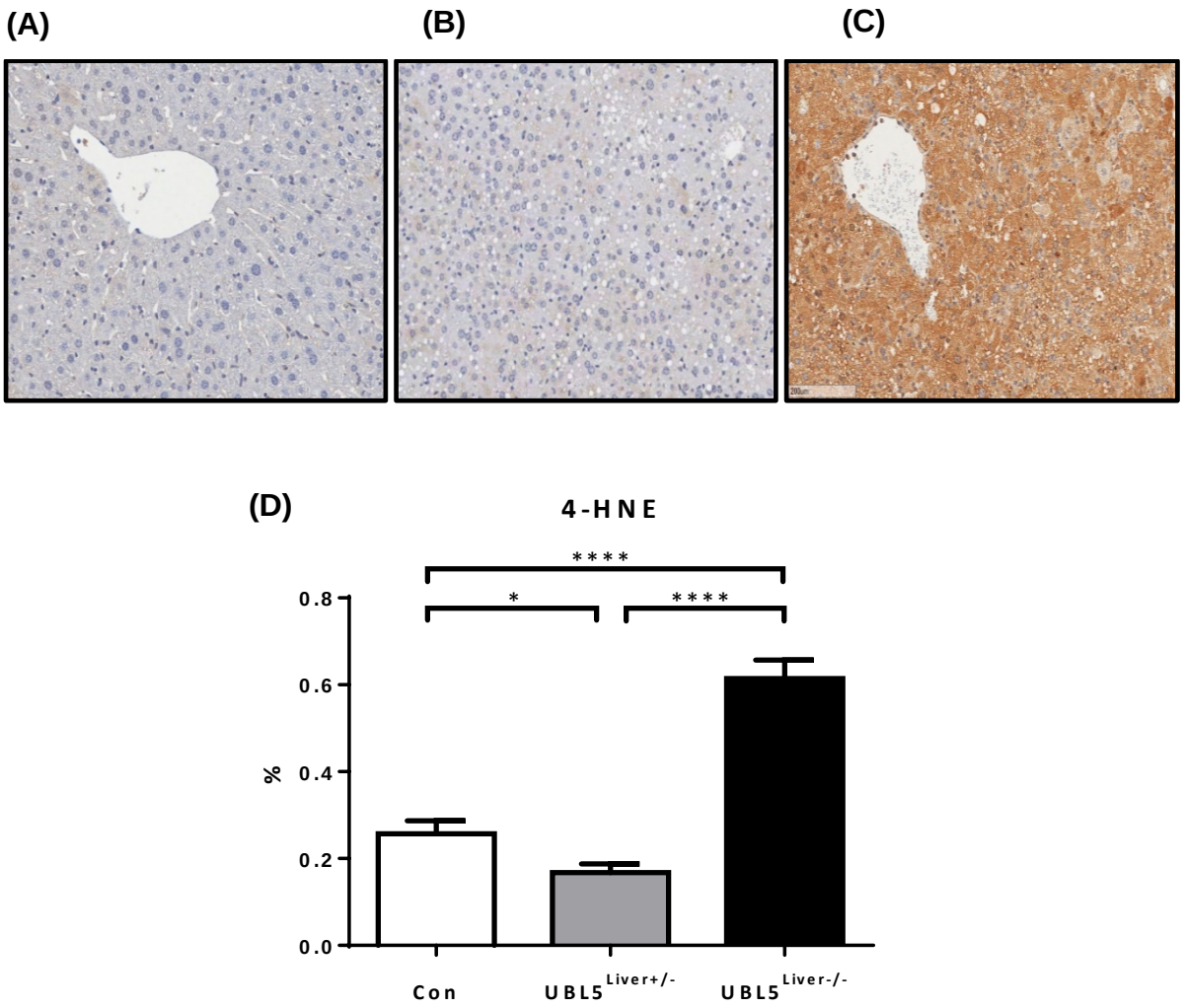

Figure 4.16: 4-HNE stain on UBL5 KO and littermates 10 days after the first tamoxifen gavage: 4-Hydroxynonenal (4-HNE) antibody stain was done on fixed (in 10% formaldehyde) liver tissues from **(A)** controls, **(B)** $UBL5^{Liver+/-}$ (Heterozygous) and **(C)** $UBL5^{Liver-/-}$ (Homozygous – KO). All three pictures are times 20 under the microscope (x20). **(D)** A graph that represents histological grade in between of three groups compare to the controls. N=4. **** P<0.0001.

4.4.2.4 Liver function test of UBL5 KO mice and littermates

Liver enzymes such as bilirubin, alanine transaminase, aspartate aminotransferase and alkaline phosphatase were significantly elevated in UBL5 KO mice that indicated severe liver damage in our model (Figure 4.17, A, B, C, D).

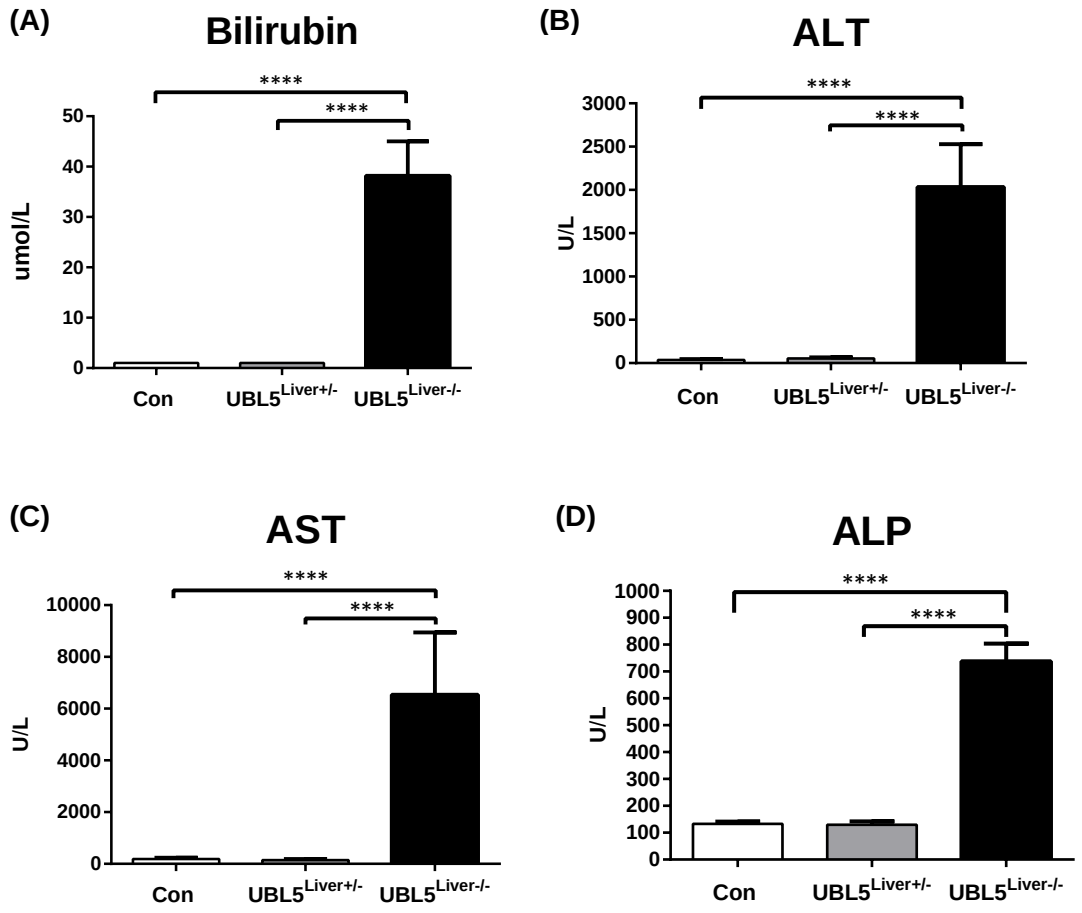

Figure 4.17: Liver plasma enzyme levels of UBL5 KO mice and littermates: (Liver function test) plasma enzymes were assessed in UBL5$^{Liver+/-}$ (Heterozygous), UBL5$^{Liver-/-}$ (Homozygous – KO) and controls 10 days after the first tamoxifen gavage. **(A)** Bili = bilirubin, **(B)** ALT = Alanine transaminase, **(C)** AST = Aspartate aminotransferase, **(D)** ALP = Alkaline phosphatase. N=12-22. **** P<0.0001.

4.4.2.5 Lipid profile of UBL5 KO mice and littermates

To assess the lipid profile of our animals we measured cholesterol, triglyceride and ketone (BHYB) levels in plasma collected from UBL5 KO, heterozygous and control mice. Cholesterol levels were significantly elevated in UBL5 KO mice compare to heterozygous and control mice (Figure 4.18, A). The triglyceride levels found diminished in UBL5 KO mice compare to heterozygous and controls (Figure 4.18, B). The ketone (BHYB) levels were significantly elevated in UBL5 KO mice compare to heterozygous and controls (Figure 4.18, C).

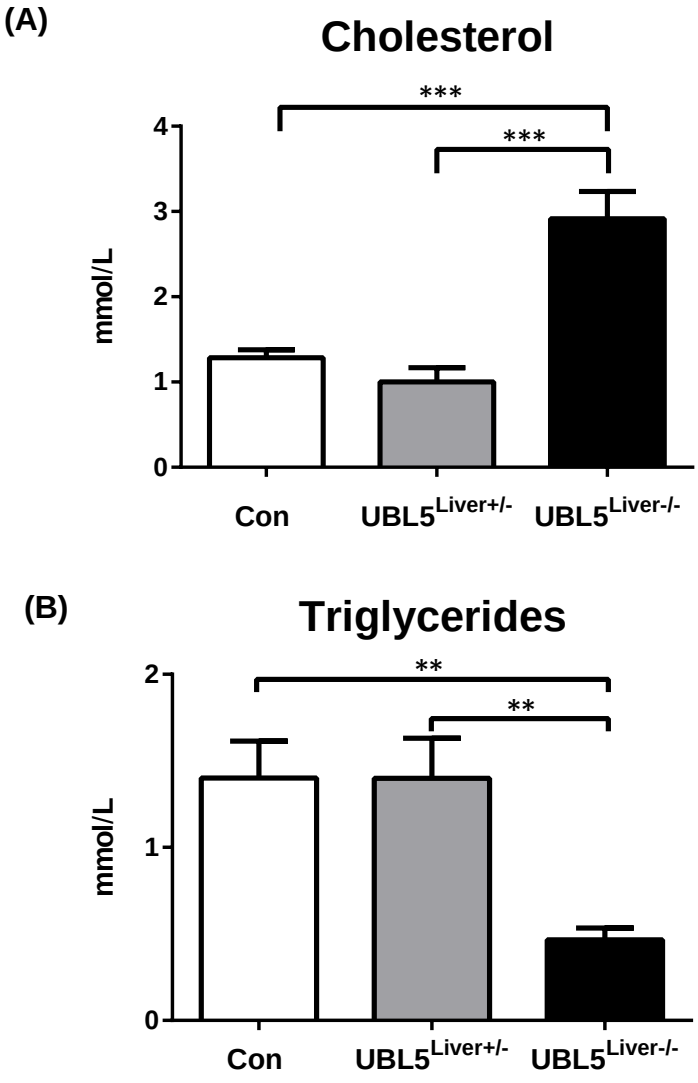

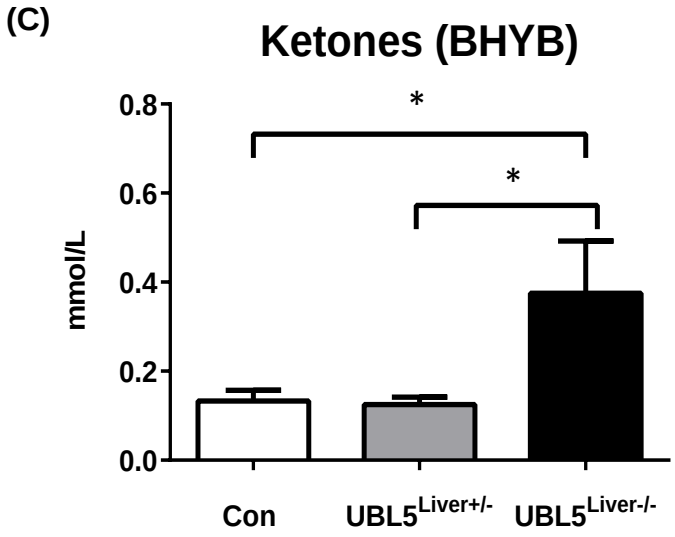

Figure 4.18: Lipid profile of UBL5 KO mice and littermates: plasma levels of **(A)** Cholesterol, **(B)** Triglycerides and **(C)** Ketones (BHYB) were assessed in $UBL5^{Liver+/-}$ (Heterozygous), $UBL5^{Liver-/-}$ (Homozygous – KO) and controls 10 days after the first tamoxifen gavage. N=5-10. * P ≤ 0.05, ** P ≤ 0.01.

4.4.2.6 Oral glucose tolerance tests in UBL5 KO mice and littermates

Glucose tolerance was assessed in all mice and presented in Figure 4.19. The UBL5 KO mice were significantly glucose intolerant compared to both the control and heterozygous groups as shown by the increased glucose levels throughout the 2-hour test (Figure 4.19, A). This is further shown by the total AUC of plasma glucose levels ((Figure 4.19, B). Also, we performed pyruvate tolerance test on a different cohort of mice (UBL5 KO, heterozygous and control mice). The UBL5 KO mice showed significantly lower plasma glucose levels during the pyruvate tolerance test compare to heterozygous and control mice (Figure 4.20, A). This is further shown by the total AUC of (after pyruvate i.p) glucose plasma levels (Figure 4.20, B).

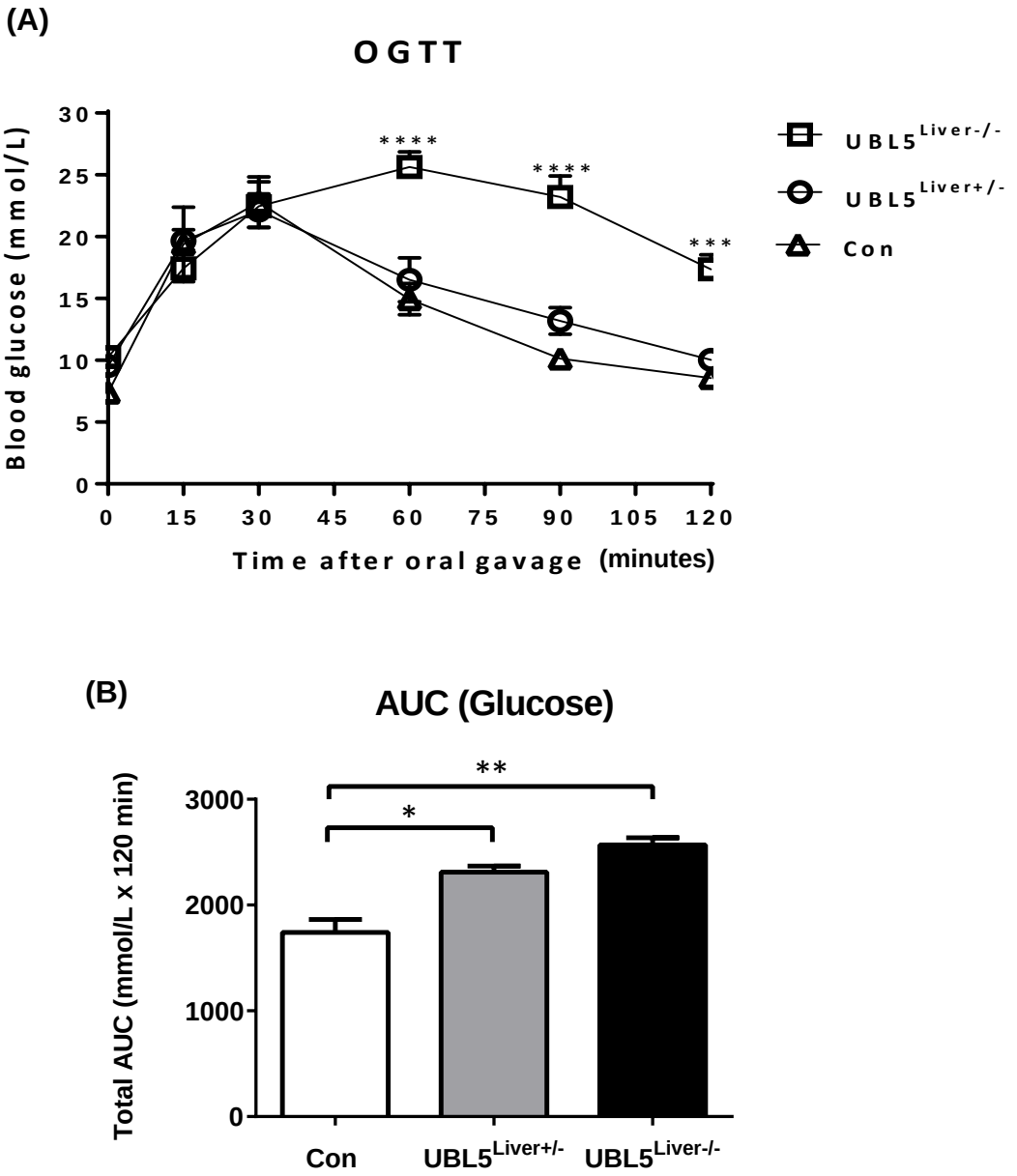

Figure 4.19: Oral glucose tolerance test (OGTT) of UBL5 KO mice and littermates. Oral glucose tolerance tests were performed on UBL5$^{Liver+/-}$ (Heterozygous), UBL5$^{Liver-/-}$ (Homozygous – KO) and controls 10 days after the first tamoxifen gavage. **(A)** Plasma glucose levels were measured at various time points. (B) Plasma glucose levels during an OFTT expressed as Area under Curve. N= 3 – 7. ** P ≤ 0.01, *** P ≤ 0.001, **** P ≤ 0.0001 (compare to controls).

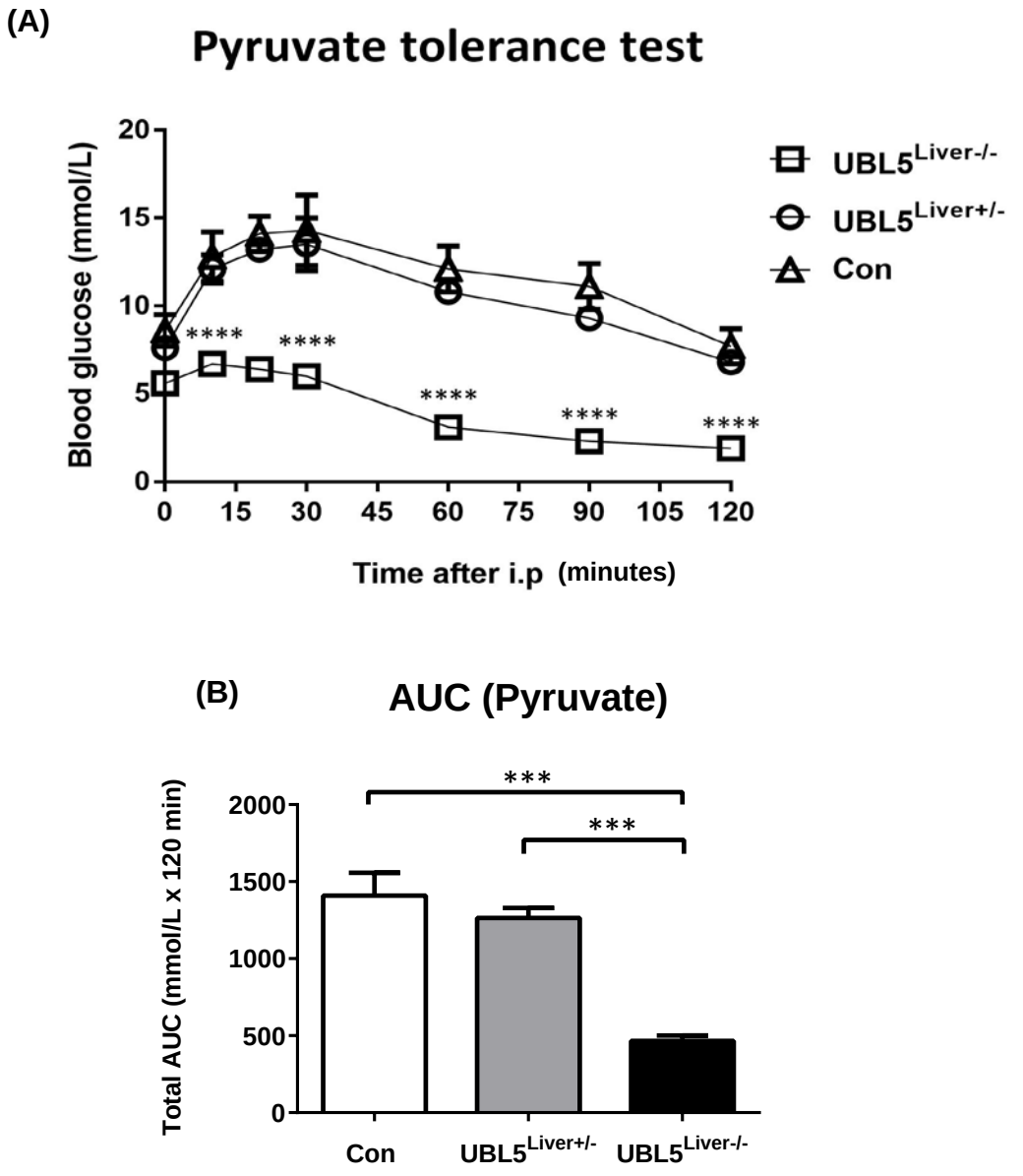

Figure 4.20: Pyruvate tolerance test of UBL5 KO mice and littermates. Intraperitoneal pyruvate tolerance tests were performed on UBL5$^{Liver+/-}$ (Heterozygous), UBL5$^{Liver-/-}$ (Homozygous – KO) and controls 10 days after the first tamoxifen gavage. **(A)** Plasma glucose levels were measured at various time points. **(B)** Plasma glucose levels during an OGTT expressed as Area under Curve. N= 4. *** P ≤ 0.001, **** P ≤ 0.0001 (compare to controls).

4.4.2.7 Mitochondrial function ten days after the first tamoxifen dose

4.4.2.7.1 MitoRed stain on isolated primary hepatocytes

To determine whether a reduction of UBL5 would affect mitochondrial function, hepatocytes were isolated as described in methods (Chapter 2) and stained with MitoRed (stains mitochondria with red colour as we describe in Chapter 2) analysed under fluorescence microscope (x100) (Figure 4.21). As can be seen in the figure, mitochondria were fragmented in hepatocytes from UBL5 KO mice compared to control mice. The figure 4.21 (D) shows significant increase in fluorescence colour density in UBL5 KO mice compared to control mice.

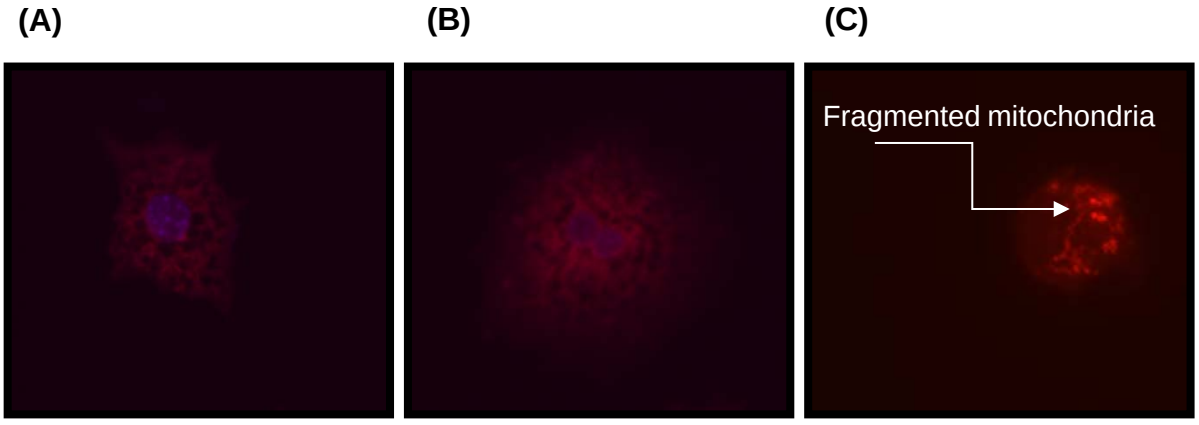

(D)

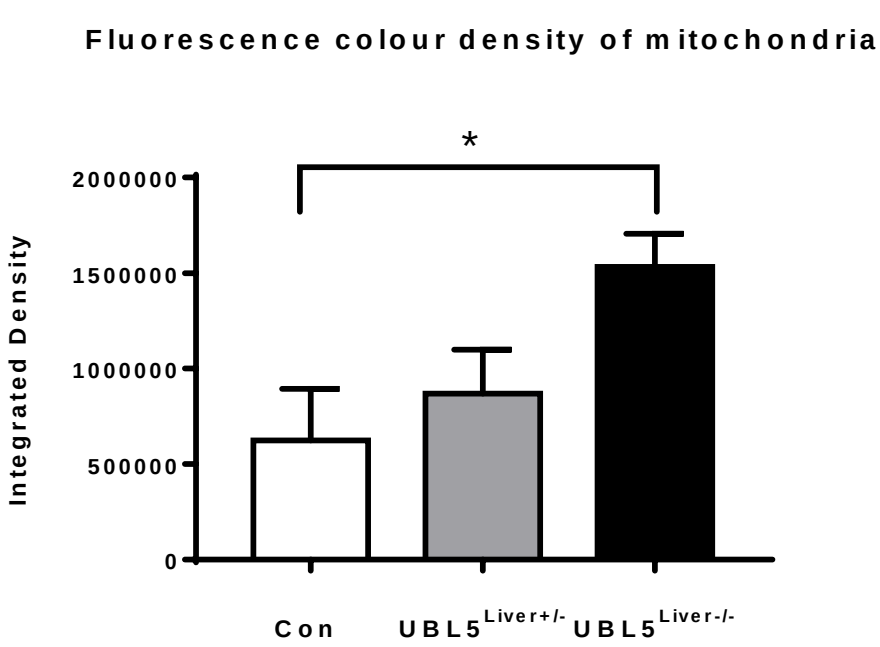

Figure 4.21: Primary hepatocytes stained with MitoRed. Isolated hepatocytes stained with MitoRed ten days after tamoxifen treatment. **(A)** Controls and **(B)** heterozygous **(C)** UBL5 KO ($UBL5^{Liver-/-}$) homozygous (D) a graph that represents the fluorescence colour density of mitochondria among the groups (analysed using FIJI software). N=3-4 * P ≤ 0.05.

4.4.2.7.2 Expression of mitochondrial biogenesis gene *PGC-1α*

To further check for the effect on mitochondrial function, mRNA levels of the inducer of mitochondrial biogenesis peroxisome proliferator-activated receptor gamma coactivator 1-alpha (*PGC-1α*) gene was assessed. The levels of *PGC-1α* was shown to be significantly lower in UBL5 KO mice compared to the controls (Figure 4.22).

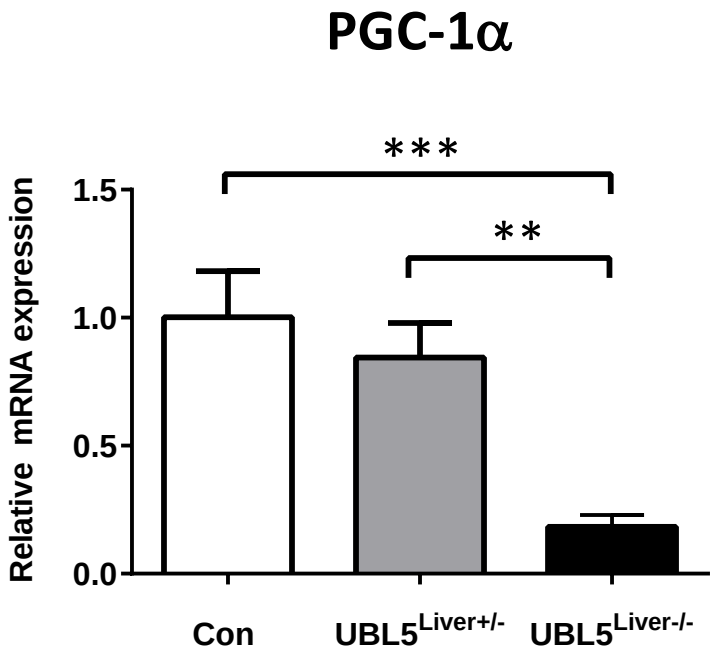

Figure 4.22: *PGC-1α* mRNA expression in UBL5 KO mice and controls. Mitochondrial biogenesis peroxisome proliferator-activated receptor gamma coactivator 1-alpha (*PGC-1α*) mRNA levels ten days after the first tamoxifen treatment in liver of UBL5Liver-/- (Homozygous – KO) and controls. N=4. ***P ≤0.001.

4.4.2.7.3 Assessment of mitochondrial respiration in UBL5 KO mice and littermates (OROBOROS)

To measure mitochondrial respiration and the levels of reactive oxygen species (ROS) we performed the respirometer experiment on livers taken from our UBL5 KO mice and their littermates. There was no leak (mitochondrial proton and electron leak) in respiratory Complex I (is the first large protein complex of the respiratory chains). During the maximum mitochondrial respiration that measures all the mitochondrial complexes, the KO mice showed significantly lower maximum respiration compared to the controls and heterozygous (Figure 4.23, A, B, C). After the challenge with FCCP (in mitochondria FCCP uncouples oxidative phosphorylation that disturbs the synthesis of ATP through transporting protons (D. Wilson, Merz, & biophysics, 1967)) our KO mice presented with reduced respiration until the end of the experiment. Also, ROS levels were found to be significantly increased in our UBL5 KO towards the whole experiment (Figure 4.23, D).

(A)

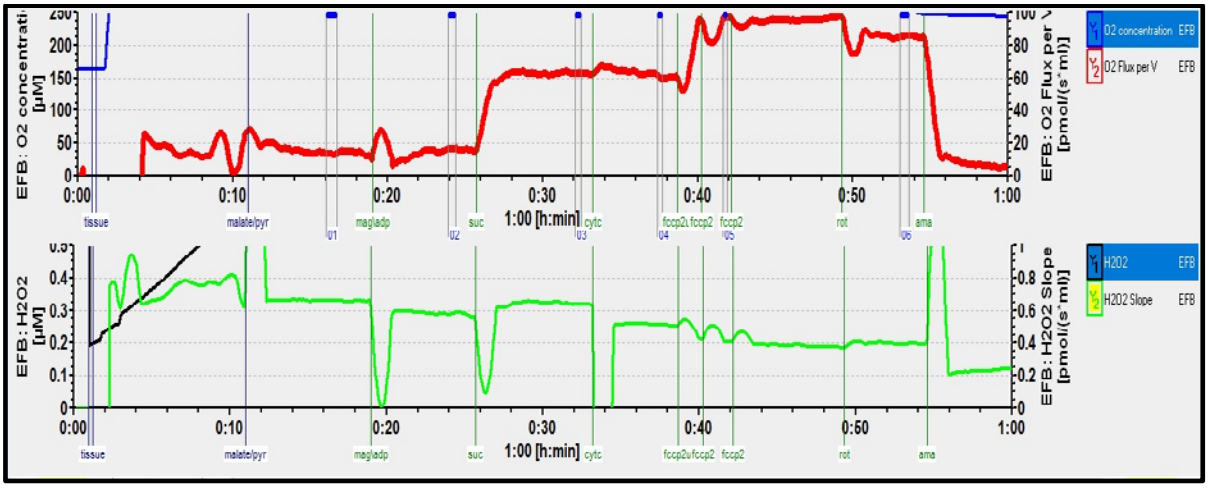
EFB: O2 concentrati [µM]
EFB: O2 Flux per V [pmol/(s*ml)]
O2 concentration EFB
O2 Flux per V EFB
tissue
malate/pyr
mag/adp
suc
1:00 [h:min]
cytc
fccp2i.fccp2
fccp2
rot
ama
EFB: H2O2 [µM]
EFB: H2O2 Slope [pmol/(s*ml)]
H2O2 EFB
H2O2 Slope EFB

(B)

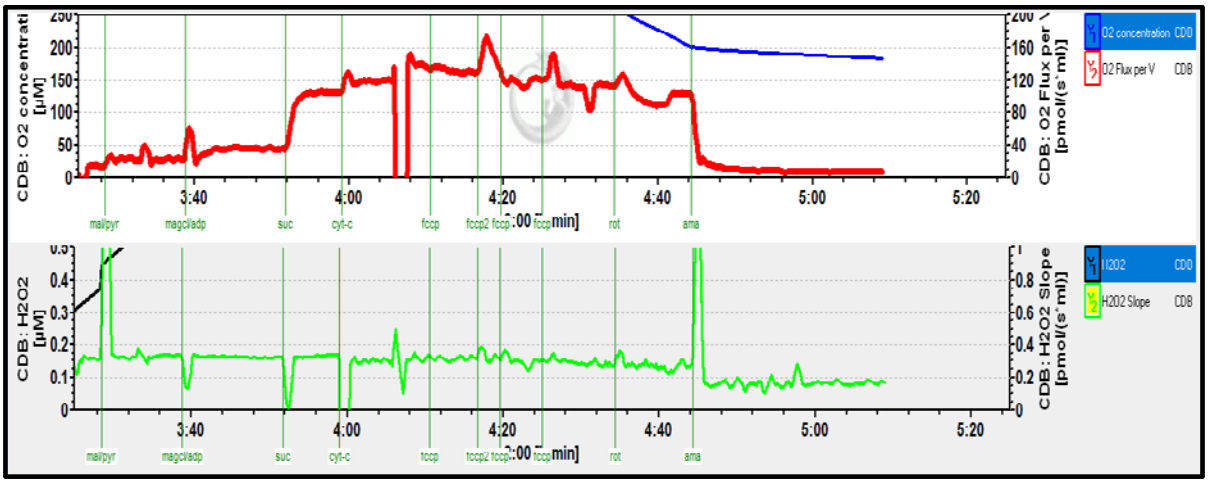
CDB: O2 concentrati [µM]
CDB: O2 Flux per V [pmol/(s*ml)]
O2 concentration CDB
O2 Flux per V CDB
mal/pyr
magcl/adp
suc
cyt-c
fccp
rot
ama
CDB: H2O2 [µM]
CDB: H2O2 Slope [pmol/(s*ml)]
H2O2 CDB
H2O2 Slope CDB

(D)

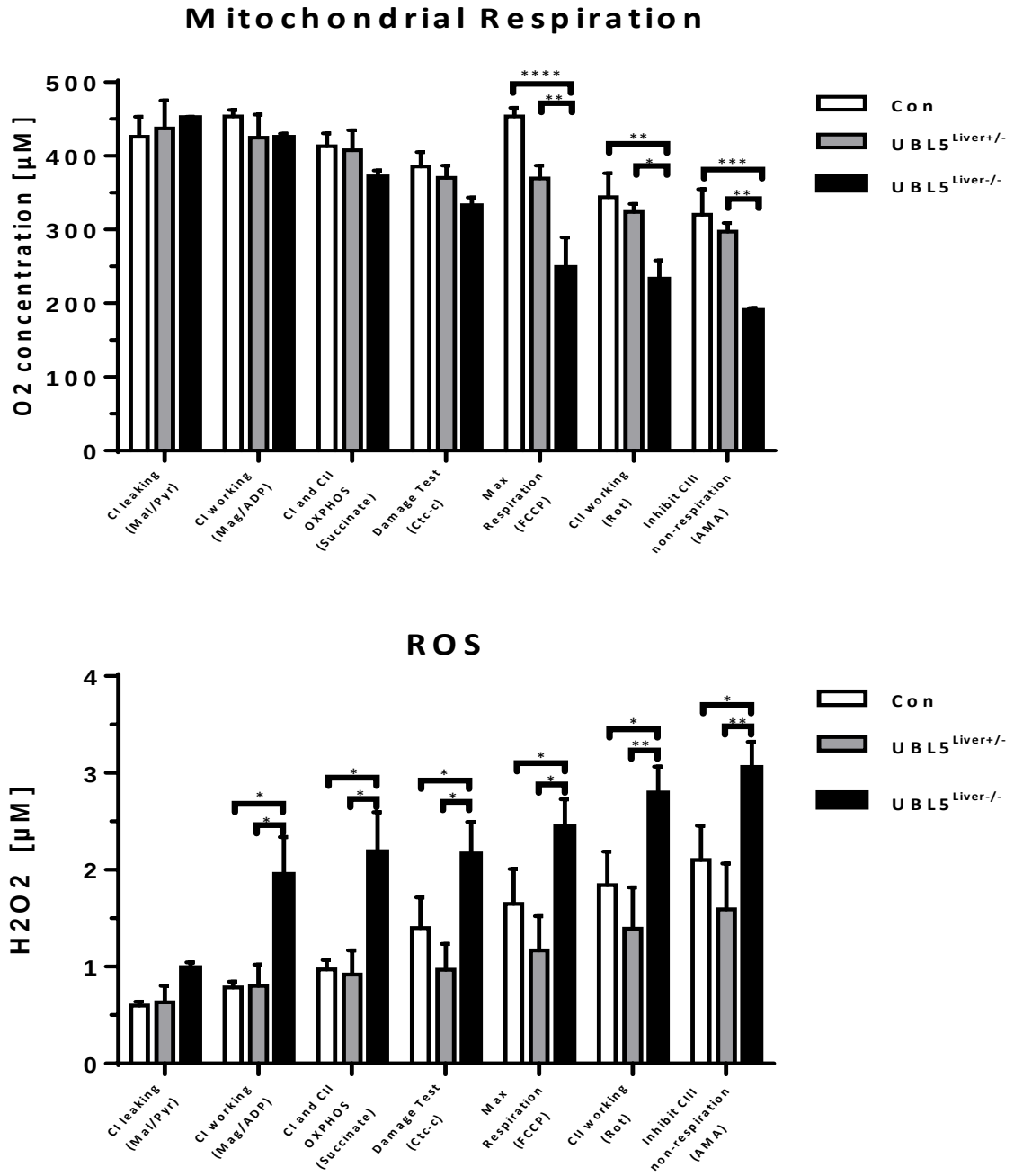

Figure 4.23: Mitochondrial respiration and ROS levels in UBL5 KO mice and littermates ten days after the first tamoxifen dose. (A) Representative picture of the respiration and ROS measurements in control mice (OROBOROS machine). **(B)** Representative picture of the respiration and ROS measurements in UBL5$^{Liver-/-}$ (homozygous - KO) mice (OROBOROS machine). **(C)** Collated data of mitochondrial respiration experiment showing all the mitochondrial complexes. **(D)** ROS levels during the mitochondrial respiration experiment. UBL5$^{Liver-/-}$ (Homozygous – KO), UBL5$^{Liver+/-}$ (Heterozygous) and controls. (CI = Complex I, CII = Complex II, CII = Complex III), (Mal/Pyr = Malate and Pyruvate. Mag/ADP = Magnesium chloride and Adenosine diphosphate. Succinate. Ctc-c = Cytochrome-C. FCCP = Carbonyl cyanide 4-(trifluoromethoxy) phenylhydrazone (mitochondrial oxidative phosphorylation uncoupler). (Rot = Rotenone. AMA = Antimycin-A). N=3-4, *P ≤0.05, **P ≤0.01, ***P ≤0.001, ****P ≤0.0001.

4.4.2.8 Fatty acid action in UBL5 KO mice and littermates

A real-time PCR was performed to assess the expression of genes involved in different aspects of fatty acid synthesis and metabolism.

The *carnitine-palmitoyl transferase 1 A (CPT1-α)* gene responsible for the mitochondrial uptake of long-chain fatty acids and their beta oxidation in the mitochondrion, did not show significant differences between groups (Figure 4.24).

The gene expression of fatty acid synthase (*FASN*) that catalyzes fatty acid synthesis was significantly lower in UBL5 KO mice compare to heterozygous and controls (Figure 4.25).

The gene expression of members of the peroxisome proliferator-activated receptor (PPARs) family *PPARα* and *PPARγ* were significantly downregulated in UBL5 KO mice compare to heterozygous and controls (Figure 4.26, A, B).

The acetyl-CoA carboxylase alpha (*ACACA*) gene responsible for fatty acid synthesis was found significantly downregulated in UBL5 KO mice (Figure 4.27).

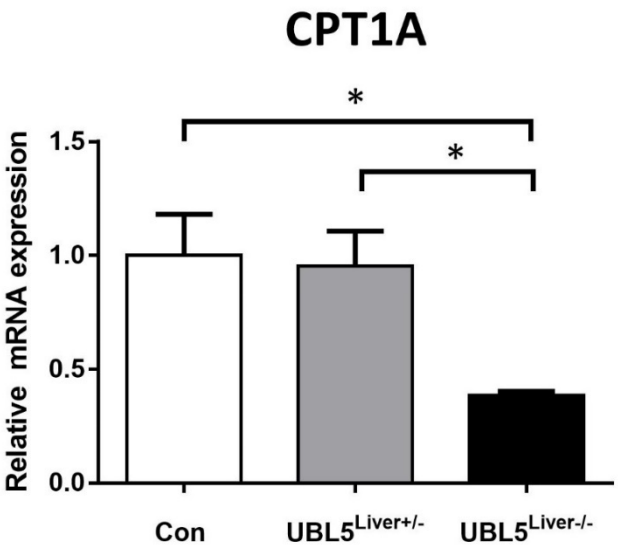

Figure 4.24: **mRNA levels of CPT1A gene in the liver from UBL5 KO mice and littermates 10 days after the first tamoxifen gavage:** mRNA levels of *the carnitine-palmitoyl transferase 1 A (CPT1A)* were expressed relative to the control sample, $UBL5^{Liver+/-}$ (heterozygous) and the $UBL5^{Liver-/-}$ (homozygous – KO). The ΔΔCt method was used to calculate relative quantification of gene expression with GAPDH rRNA as the housekeeper gene. Values presented as mean ± SEM. n=8. *P ≤0.05.

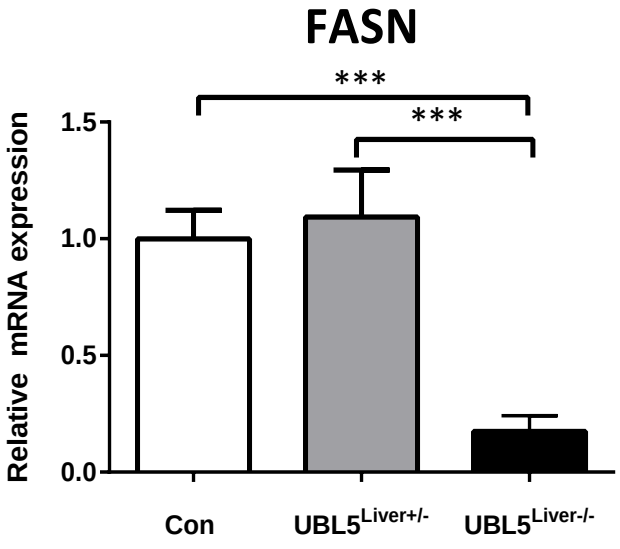

Figure 4.25: *FASN* gene mRNA levels in the liver from UBL5 KO mice and littermates 10 days after the first tamoxifen gavage: mRNA levels of fatty acid synthase (*FASN*) gene was expressed relative to the control sample, $UBL5^{Liver+/-}$ (heterozygous) and the $UBL5^{Liver-/-}$ (homozygous – KO). The ΔΔCt method was used to calculate relative quantification of gene expression with GAPDH rRNA as the housekeeper gene. Values presented as mean ± SEM. n=8 ***P ≤0.001.

(A)

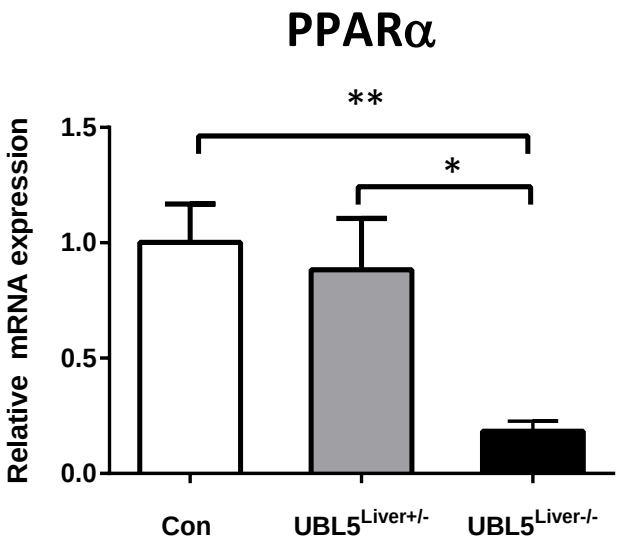

(B)

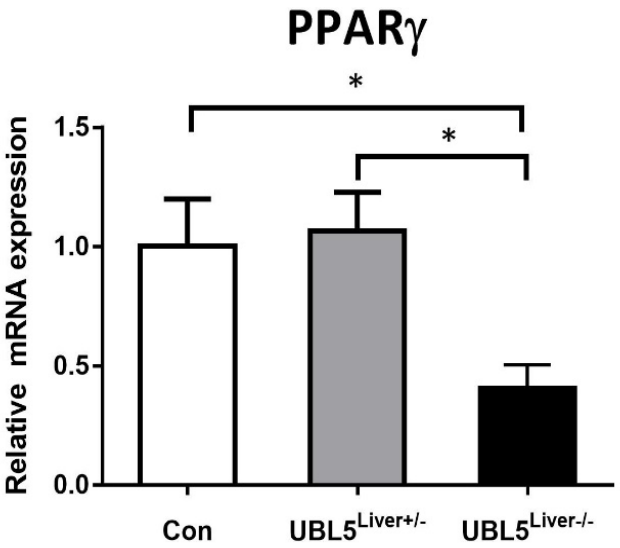

Figure 4.26: *PPARα and PPARγ* gene mRNA levels in the liver from UBL5 KO mice and littermates 10 days after the first tamoxifen gavage: mRNA levels of **(A)** *PPARα and* **(B)** *PPARγ* genes was expressed relative to the control sample, $UBL5^{Liver+/-}$ (heterozygous) and the $UBL5^{Liver-/-}$ (homozygous – KO). The ΔΔCt method was used to calculate relative quantification of gene expression with GAPDH rRNA as the housekeeper gene. Values presented as mean ± SEM. n=8 **P ≤0.01.

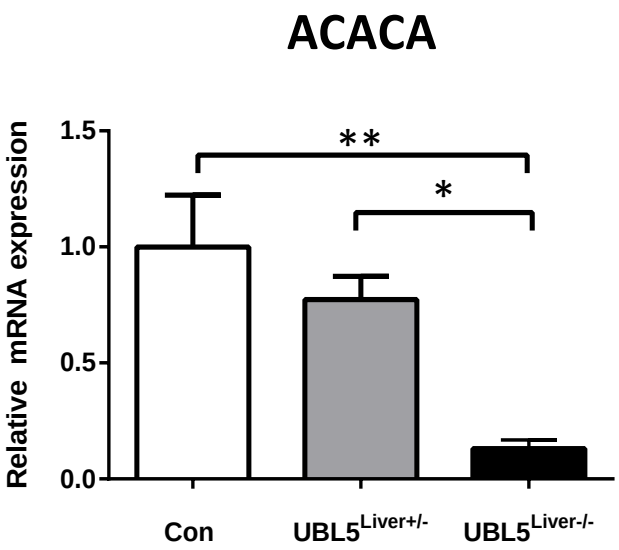

Figure 4.27: *ACACA* gene mRNA levels in the liver from UBL5 KO mice and littermates 10 days after the first tamoxifen gavage: mRNA levels of acetyl-CoA carboxylase alpha (*ACACA*) gene was expressed relative to the control sample, $UBL5^{Liver+/-}$ (heterozygous) and the $UBL5^{Liver-/-}$ (homozygous – KO). The ΔΔCt method was used to calculate relative quantification of gene expression with GAPDH rRNA as the housekeeper gene. Values presented as mean ± SEM. n=8 *P ≤0.05, **P ≤0.01.

4.4.2.9 Expression of UPR^{mt} genes in the liver of UBL5 KO mice and littermates

We performed Real Time PCR to assess the expression of UPRmt genes such as transcription factors *CHOP* and *ATF5*, heat shock protein *HSP60, HSP10*, and *HSP70mt* and proteases *Clpp*, *Clpx and lonp-1*.

The transcription factors *CHOP* and *ATF5* were found significantly downregulated in UBL5 KO mice compare to heterozygous and controls (Figure 4.28, A, B).

The Heat shock protein *HSP10* did not show differences between groups (Figure 4.28, C). The levels of *HSP60* was significantly reduced in the UBL5 KO mice compare to the littermates (Figure 4.28, D). The gene levels of mitochondrial specific heat shock protein *HSP70mt* were significantly upregulated in our UBL5 KO mice compare to heterozygous and controls (Figure 4.28, E).

The proteases C*lpp* and *Clpx* were significantly reduced in UBL5 KO mice compared to heterozygous and controls (Figure 4.28, F, G), with the lonp-1 showed a trend for reduction in UBL5 KO mice, although the result was not statistically significant (Figure 4.28, H).

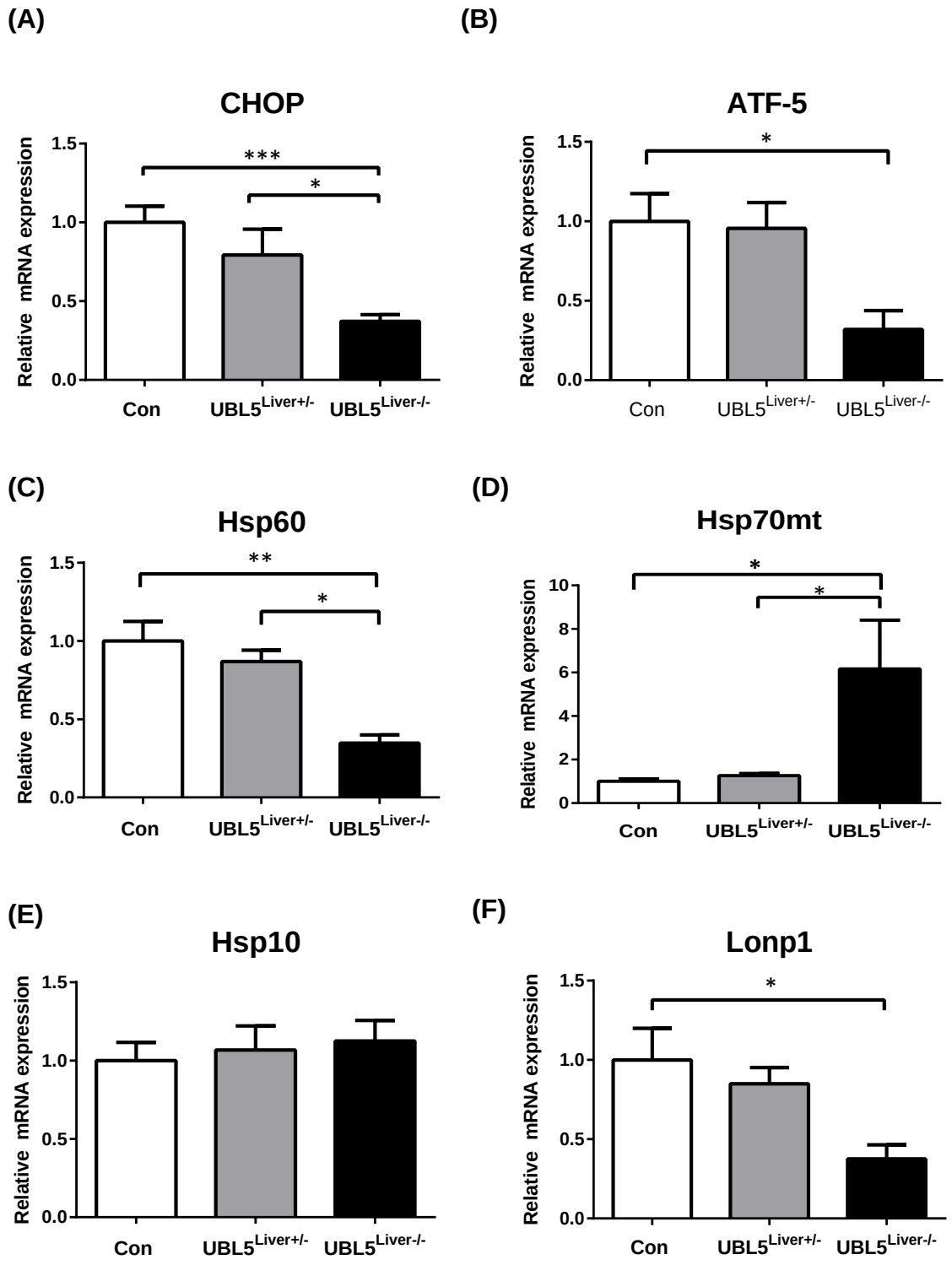

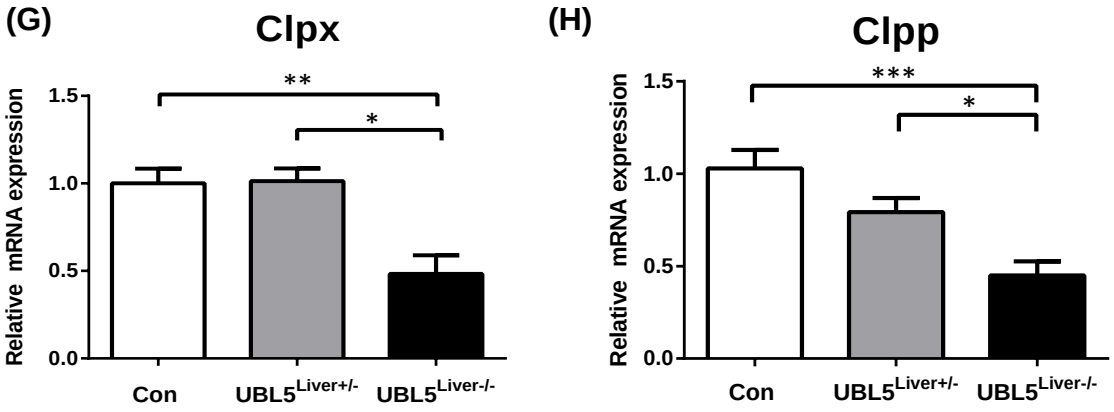

Figure 4.28: UPRmt genes mRNA levels in the liver from UBL5 KO mice and littermates 10 days after the first tamoxifen gavage: mRNA levels of **(A)** transcription factor CHOP, **(B)** transcription factor ATF-5 **(C),** heat shock protein Hsp60 **(D)** heat shock protein Hsp70mt, **(E)** heat shock protein hsp10 **(F),** protease lonp1 **(G)** protease ClpX, **(H)** protease Clpp, were expressed relative to the control sample, UBL5Liver+/- (heterozygous) and the UBL5Liver-/- (homozygous – KO). The ΔΔCt method was used to calculate relative quantification of gene expression with GAPDH rRNA as the housekeeper gene. Values presented as mean ± SEM. n=12-22. *P ≤0.05, **P ≤0.01, ***P ≤0.001, ****p< 0.0001.

4.5 Discussion

In this chapter, we performed various phenotypic assessments of our UBL5 KO mice at two timepoints: 5 -days and 10 -days post first tamoxifen gavage. As discussed in Chapter 3, the UBL5 KO mice have severe liver failure at 15 -days post gavage. Therefore, these earlier timepoints were chosen to more accurately investigate the biological effects of UBL5 deletion.

Five days after the first tamoxifen gavage, *UBL5* gene expression was reduced to 65% in both KO mice and heterozygous mice (i.e reduced by 35%). Both the heterozygous and KO mice have not reached full gene deletion at this stage, though this shows that both genotypes lose *UBL5* mRNA to the same level. Despite this ~35% reduction of *UBL5* mRNA, they displayed normal physiological characteristics such as body weight and liver weight. Also, there was no difference between the groups in glucose tolerance, liver histology, and circulating liver enzyme levels.

Establishing whether a 35% reduction in *UBL5* was enough to trigger the UPRmt we measured three key genes: the transcription factor *CHOP*, the heat shock protein *Hsp60* and a protease *Clpp* (Al-Furoukh et al., 2015; Fiorese et al., 2016; Schulz & Haynes, 2015). However, expression of all the UPRmt genes measured were unaffected. These results imply that a 35% reduction in *UBL5* was not sufficient enough to cause a difference in phenotype and mice remained metabolically normal because the UPRmt was not activated due to a lack of stress in the system. Therefore, we extended the timepoint out to 10 days' post-tamoxifen injection (as described in Chapter 3) given that we saw a ~50% knockdown in the heterozygous mice and ~97% knockdown in UBL5 KO mice.

At the 10 day timepoint, the 50% reduction in the heterozygous mice was not enough to see any differences in the UPRmt compared to controls. However, the almost complete reduction in *UBL5* seen in the KO mice greatly reduced the UPRmt pathway, demonstrating the essential requirement for *UBL5* in activating the UPRmt. The only exception was the mitochondrial *HSP70* that was elevated in our UBL5 KO mice. HSP70 assists in the folding of non-active proteins during stress, but the actual mechanism of its activation is still unclear (Mayer, Bukau, & sciences, 2005). Therefore, it could have some redundancy in its transcription, which could be the

reason that it is increased despite the global decrease in UPRmt mRNA. However, this increase in *HSP70* mRNA does help to reinforce that there is mitochondrial stress occurring in the KO mice. Very similar findings were seen in *C.elegans*, where the knockdown of *UBL5* using RNAi prevented the activation of the UPRmt (Benedetti et al., 2006).

Haynes also found that when subjecting mammalian 293T cells to mitochondrial stress by SPG7 RNAi treatment leads the UBL5 to form a complex with SATB2, the mammalian homologue of DVE-1 (C. M. Haynes et al., 2007). This shows us that UBL5/SATB2 complex formation is also essential for the activation of mammalian UPRmt. These findings support our hypothesis that UBL5 regulates the UPRmt and in its absence, it cannot activate properly even under severe mitochondrial stress.

This considerable decrease seen in the UPRmt significantly impacted hepatic mitochondrial integrity and function in the KO mice. ROS levels were markedly increased and were accompanied by a decrease in mitochondrial respiration rates (ROS was directly measured during mitochondrial respiration using Oroboros). The KO mice showed large increases in 4HNE, which is a marker of lipid peroxidation and proportionally indicates levels of oxidative stress. Sangle et al showed in cultured porcine aortic endothelial cells treated with LDL that oxygen consumption was impaired in Complexes I, II/III, and IV and significantly increased the release of ROS that led to attenuation of the mitochondrial electron transport chain pathway (Sangle et al., 2010). The findings suggest that, decreased mitochondrial oxygen consumption reduces mitochondrial function, increases ROS generation, that can potentially contribute to mitochondrial dysfunction. Staining the isolated hepatocytes from the UBL5 KO mice with MitoRed revealed fragmented mitochondria, further supporting diminished mitochondrial respiratory ability and mitochondrial damage in UBL5 KO mice.

On a physiological level, both pyruvate tolerance and glucose tolerance in the KO mice were significantly impaired. Which could indicate a failure of hepatic gluconeogenesis. However further studies are required to confirm it. Also, UBL5 KO mice had decreased mRNA of acetyl CoA carboxylase alpha (*ACACA*), *PPARα* and *PPARγ* (that regulates peroxisomal and mitochondrial fatty acid β-oxidation), *CPT-1α* (that regulates free fatty acid transport into mitochondria for β-oxidation) and fatty acid

synthase (FASN). The decrease in expression of many genes involved in OXPHOS and the TCA cycle further shows that there is unrecoverable mitochondrial damage occurring in UBL5 KO mice. As it is known mitochondria are essential in metabolism by producing ATP, lipids, nuclear acids and amino acids (McBride et al., 2006). Therefore, it is not surprising to see the expression of many metabolic genes to be altered during mitochondrial dysfunction. For instance, Nargund et al in 2015 reported that a lack of the UPRmt signalling molecule ATFS-1 in *C. elegans* caused a reduction in respiratory capacity and OXPHOS complex assembly (Amrita M. Nargund, Christopher J. Fiorese, Mark W. Pellegrino, P. Deng, & Cole M. Haynes, 2015). Normally ATSF-1 binds the promoters of many TCA cycle and OXPHOS genes. Although during mitochondrial stress it represses or limits their transcription and induces the promoters of all glycolysis genes (Amrita M. Nargund et al., 2015). Possibly this happens to allow the cell to maintain the ATP levels, independent of mitochondrial function. This is very similar to our findings in the UBL5 KO mice where it was found that the mammalian analogue for ATFS-1, *ATF5* was also reduced. The reduction in *ATF5* could also further explain the decrease in mitochondrial respiration and increased ROS generation due to similar defects in mitochondrial complex assembly, though further investigation is needed to confirm this. The severe micro and macro vesicular fat build up that we see in the histology of our KO mice indicates that since the pathway for lipid metabolism is dysfunctional the fat is built up in the liver. Micro vesicular steatosis occurs as a consequence of severe impairment of mitochondrial β-oxidation, which prevents the fatty acid molecules from being broken down leading them to being stored in the cell instead (D Pessayre, Mansouri, Haouzi, Fromenty, & toxicology, 1999). Increased presence of micro vesicular steatosis in the UBL5 KO mice is resulting from impaired mitochondrial function. Previous studies have shown appearance of micro vesicular steatosis in the presence of mitochondrial dysfunction. For example, Natarajan and colleagues in 2006 studied rats that were induced micro vesicular steatosis via i.p injections of sodium valproate displayed severe mitochondrial damage with presence of oxidative stress in liver, accompanied by changes in mitochondria (structural and functional) (Natarajan, Eapen, Pullimood, & Balasubramanian, 2006). Similarly, another study showed rats fed with high fat diet plus fructose displayed severe micro vesicular steatosis in the liver with inflammation, accompanied with decreased mitochondria respiration and increased ROS generation

and disturbed mitochondrial lipid peroxidation (García-Berumen et al., 2019). Similar histological and mitochondrial pattern was also observed in patients with acute fatty liver failure in pregnancy (Sherlock, 1983) and in patients with alcohol abuse (Mansouri et al., 1997). Reduction in *PPARα* levels could also explain the increased levels of ketones in our UBL5 KO mice, since PPARα is one of the main regulators of ketolysis and fatty acid catabolism (Grabacka, Pierzchalska, Dean, & Reiss, 2016).

The mitochondrial damage caused by reduced UPRmt levels led to severe apoptosis in UBL5 KO mice that was confirmed via cleaved caspase-3 histological stain. Mitochondrial derived apoptosis can be caused by ROS build up from oxidative stress leading to damaged proteins (Yee, Yang, & Hekimi, 2014). Once there is severe enough mitochondrial damage, cytochrome-c is released from the mitochondria and activates caspase-9. This causes a cascade that leads to the cleaving of caspase-3 which is a direct transcription factor for apoptosis (Nieminen, 2003; Yee et al., 2014). This makes cleaved caspase 3 one of the best measures for mitochondrial derived apoptosis and further shows the extent of the mitochondrial damage caused by the removal of UBL5 and the subsequent reduction in the UPRmt.

UBL5 KO mice displayed severe liver failure. Liver enzymes such as bilirubin (Bili), alanine aminotransferase (ALT), alkaline phosphatase (ALP), serum albumin and aspartate aminotransferase (AST) showed significant elevation in our UBL5 KO. A combination of elevated levels of these enzymes usually indicates liver disease (Johnston, 1999; M. Lee, 2009). The increase of these enzymes in our KO mice indicates that they suffer from severe liver damage. Macroscopically the livers of UBL5 KO mice were pale, possibly due to the increased fat accumulation that we mentioned above and were significantly smaller compared to the heterozygous and control mice. The increase in plasma cholesterol levels is indicative of the failure of the liver to break down cholesterol.

Previous studies have reported similar defects (in mitochondrial function, liver function and gene expression) in models of liver specific mitochondrial dysfunction. For example, Ghandi et al in 2015 showed that reduction of a hepatic growth factor caused lower ATP levels, oxidative stress and reduced mitochondrial respiratory function that led to decreased *ACACA, PPARα* and *CPT-1α* mRNA levels, increased hepatic steatosis and apoptosis (Gandhi et al., 2015). Although the mouse model used

in this published work is different than the mouse model used here (since they had a growth factor liver specific knockdown mouse model and we use a liver specific knockdown model of a *UBL5* gene (essential for mitochondrial UPRmt)). Nonetheless the pattern of defects caused by mitochondrial dysfunction is similar in both models (such as increased fat accumulation in the liver, oxidative stress, reduced mitochondrial respiration, decreased genes such as *ACACA*, *PPARα* and *CPT-1α*). Similar effects have also been reported in patients with acute kidney failure. In this cohort of patients, there was an increase in ROS levels and decreased *PGC-1α* which caused them persistent mitochondrial injury that led to kidney failure (Stallons, Funk, & Schnellmann, 2013). Even though this study refers to different tissue we see that mitochondrial dysfunction can lead to organ failure. Similarly, to what we see in our KO mice where they suffer from severe liver dysfunction caused by mitochondrial disturbance.

4.6 Conclusion:

In conclusion, based on the findings from this study, the phenotypic characteristics of the UBL5 KO mice demonstrate the importance of UBL5 and UPRmt in mitochondrial and liver physiological function. Absence of UBL5 decreases UPRmt that leads to impaired mitochondrial function, apoptosis and liver failure.

In the next chapter, we will be investigating the stress response under high fat diet rich in cholesterol in heterozygous mice. The heterozygous mice showed no discernible phenotype compared to the control animals on chow. Therefore, we aimed to see if these mice, with a partial deletion of UBL5, would have a worsened phenotype in response to the high fat diet.

CHAPTER 5: HIGH-FAT DIETARY CHALLENGE: HETEROZYGOUS (UBL5$^{LIVER+/-}$) MICE VERSUS CONTROLS

5.1 Introduction

In Chapter 4 we described the phenotype of our homozygous KO (UBL5$^{Liver-/-}$) mice. We found that there was a 97% reduction in UBL5 in the liver and the mice had liver dysfunction, glucose intolerance, severe hepatic steatosis, and apoptosis. Mitochondrial respiration was reduced coupled with an increase in ROS levels and oxidative stress. Mechanistically, expression levels of key genes in the UPRmt were significantly reduced. Interestingly, the heterozygous (UBL5$^{Liver+/-}$) mice with 60% reduction of UBL5 did not show any discernible phenotype when on a normal chow diet. Therefore, we concluded that a partial reduction in UBL5 expression in the liver still renders the mice healthy whilst a near complete reduction elicits liver specific defects that ultimately leads to death.

It is well established that mitochondrial dysfunction plays a key role in several disorders such as obesity, insulin resistance and type 2 diabetes (Mary-Elizabeth Patti, et al, 2010; Neuschwander-TetriBA, et al, 2003; Wei Y. et al. [World J Gastroenterol] 2008). Mitochondrial damage can impair β-oxidation of fatty acids that leads to the formation of intracellular micro-vesicular steatosis (small lipid-consecrating vesicles) (Fromenty & Pessayre, 1995). Impairment in β-oxidation causes fatty acids to form into triglycerides that are usually exported from the cell as lipoproteins (Very low density lipoproteins (VLDLs)) or are stored within the cell as lipid vesicles. The cause of triglyceride build-up is unclear. Furthermore, toxicity may occur due to the increased levels of the remaining vacant fatty acids that can form micelles with the neutral triglycerides, preventing their export from the cell (Fromenty & Pessayre, 1995).

Chronic consumption of a diet rich in fat and cholesterol can lead to glucose intolerance (Hansen et al., 1998) and progress toward obesity, type 2 diabetes (Tang, Wei, Chen, & Liu, 2006) and NAFLD (Leung et al., 2016; Samuel et al., 2004) through increasing intracellular fatty acid products (Chavez et al., 2003; Samuel et al., 2004). Multiple metabolic pathways may be affected by these lipid metabolites leading to reduced insulin signalling, impaired glucose oxidation (Borkman et al., 1989; Kraegen, James, Storlien, Burleigh, & Chisholm, 1986) and elevated levels of oxidative stress (Harper, Bevilacqua, Hagopian, Weindruch, & Ramsey, 2004; Sreekumar et al., 2002). Mitochondrial dysfunction may be induced by chronic exposure to a high fat diet (Ritov et al., 2005; Sparks et al., 2005) with several studies showing its deleterious effects in rodents (Jove et al., 2004; Sparks et al., 2005; Lionetti et al., 2007; Bonnard et al., 2008) and humans (Richardson et al., 2005; Sparks et al., 2005; Brehm et al., 2006; Hoeks et al., 2006; Szendroedi and Roden, 2008). For example, insulin sensitive individuals consuming an isoenergetic HFD for 3 days showed reduced mRNA levels of PGC-1α, subunits for Complex I and Complex II (NDUFB3, NDUFB5, NDUFS1, NDUFV1 and SDHB) and several other mitochondrial genes associated with OXPHOS and ATP synthesis (Sparks et al., 2005;) In the same study (separate experiment) the authors fed mice (C57Bl/6J) with the same HFD for 3 weeks and found similar results (downregulated OXPHOS and PGC1-α mRNAs by ~90%, cytochrome C and PGC1-α protein by ~40%) (Sparks et al., 2005;) Mice that were fed a HFD containing 71% fat for 16 weeks which induced a NASH-like pathology, showed similar results with decreased mitochondrial gene and protein expression, mitochondrial respiration and mitochondrial membrane potential in the liver (Mantena et al., 2009). Similarly, Guo et al showed that mice fed with HFD (60% calorie from fat) had upregulated proteins involved in fatty acid oxidation, amino acid degradation, TCA-cycle, oxidative phosphorylation and Tim proteins (important for protein import) in the liver. Also, the structural analysis of mitochondria showed condensed mitochondria with disturbed respiratory function in HFD fed group (Y. Guo et al., 2013). Leung et al showed in 2016 that mice (C57Bl6) fed with 21% fat, 2% cholesterol diet for 33 weeks developed significant steatohepatitis and fibrosis. The same mice also showed hepatic 4-hydroxynonenal content (a marker of oxidative stress; (Leung et al., 2016). Finally, a study in mice showed that restricting mitochondrial biogenesis, with increased oxygen consumption and adenosine triphosphate production, increased mitochondrial oxygen

consumption and ATP production (Nisoli et al., 2005; Civitarese et al., 2007). Together, these studies suggest that exposure to a HFD negatively affects the bioenergetics of liver mitochondria (OXPHOS and mitochondrial biogenesis) and this probably contributes to hypoxic stress, poor mitochondrial respiration and deleterious changes of mitochondrial proteins/genes.

Given our results from the previous chapter showed a protective nature from the heterozygous mice and we know that HF feeding is detrimental to mitochondrial function, this chapter explored the extent of the protective nature of a partial reduction in UBL5, by challenging the heterozygous mice with a 60% high-fat diet. Furthermore, given the UBL5 KO mice (with 97% reduction in UBL5 gene expression) displayed a severe liver phenotype made us wonder if human patients with liver disease (such as fatty liver) would have altered UBL5 expression levels.

5.2 Chapter hypothesis

The hypothesis for this chapter is in two parts:
Hypothesis 1: Patients with liver disease (such as fatty liver) would have altered UBL5 expression compared to healthy individuals.

Hypothesis 2: The heterozygous mice will display a worsened phenotype under HFD compared to control mice due to the lower amount of UBL5, making the mice less able to activate the UPRmt leading to more severe mitochondrial damage.

5.3 Chapter aims

To address the hypotheses above, this chapter has two specific aims:

Aim 1: To confirm the levels of UBL5 expression in human patients with liver disease (fatty liver and cirrhosis).

Aim 2: To investigate the physiological consequences of feeding a high cholesterol/high fat diet to our heterozygous mice.

5.4 Specific chapter methods.

The general material and methods for the experimental procedures utilised and discussed in this chapter are described in detail in (Chapter 2).

5.4.1 Human study:

We accessed human livers from the tissue bank (Austin Health, Victorian cancer biobank). For the controls the samples were taken from patients (males and females) suffering from carcinoma but with no obvious liver disease, therefore, all the livers that were collected had no fat accumulation or signs of cirrhosis. While all the cirrhotic and fatty liver samples were also collected from patients (males) suffering from cancer but they also had severe liver disease (Table 5.1 A) (Ethics/project number LNR/13/Austin/163). Real time PCR was performed using the same protocol (described in Chapter 2).

5.4.2 Mice study:

As shown in (Figure 5.1) male mice were tamoxifen treated at six weeks of age as mentioned in previous chapters, and a week later they were randomised to receive either a 21% fat, 2% cholesterol semi pure rodent diet (HFD) (Appendix II) or a 3% fat standard laboratory chow diet (Appendix I). As discussed above, prolonged treatment with a HFD causes fatty liver and mitochondrial dysfunction (Y. Guo et al., 2013; Leung et al., 2016; Mantena et al., 2009). Based on these studies we decided to feed the mice with the HFD for 2 and 5 months to establish these defects. At the end of HF-feeding (2 and 5 months respectively) we performed GTT, and the next day we culled the animals for plasma and tissue (livers) collection. All the protocols and statistical analysis are described in greater detail in chapter 2.

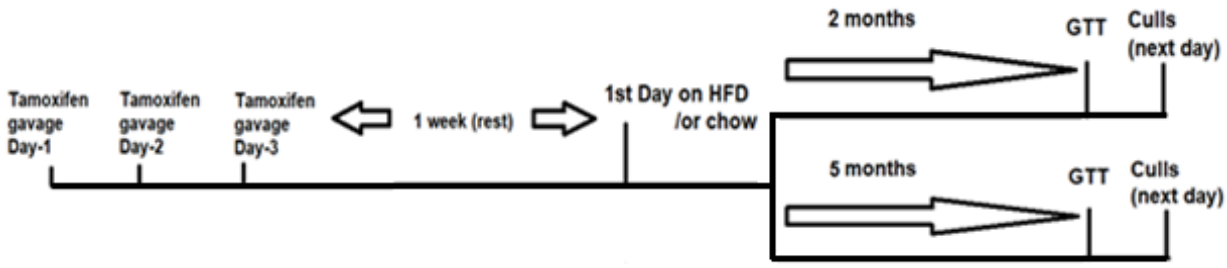

Figure 5.1: Illustration of HFD treatment (2 and 5 months).

5.5 Results

5.5.1 *UBL5* mRNA levels in Humans with liver disease

The baseline characteristics of the patient population are shown in (Table 5.1 A) Control patients and those with liver dysfunction (fatty liver and cirrhosis) had a history of smoking and alcohol consumption. The average age of the control patients was around 48 years of age while patients with liver disease were around 60 years old. Patients with fatty liver and cirrhosis had higher BMI that the controls (Table 5.1 A, B).

The Real-Time PCR results, as shown in Figure 5.2, showed elevated gene expression levels of *UBL5* in patients with fatty liver disease and cirrhosis compared to the healthy livers from controls. When we analysed the results separately for patients with fatty liver, patients with cirrhosis and compared them to controls, we found that *UBL5* gene expression remained upregulated in both the cirrhotic and fatty liver groups. Importantly, both males and the females showed same level of increased expression (Appendix III).

Table 5.1: Human liver samples collected from Victorian cancer tissue bank (Austin Health). (A) List of patients and all the details (marked as blue are the patients with liver disease, yellow are the control patients). **(B)** Sum up table of all the patient's details, gender, age and BMI.

(A)

Co-morbidity	Sex	Age	Diagnosis	Clinical Status	Weight (or BMI) n time of extractio
Fatty liver	Male	46	8140/6 Adenocarcinoma, metastatic, NOS	Metastasis (Secondary)	BMI: 31.4 188cm, 111kg
Fatty liver	Male	52	8160/3 Cholangiocarcinoma	Primary	BMI: 29.7
Liver cirrhosis	Male	67	8170/3 Hepatocellular carcinoma, NOS	Primary	BMI: 41.7 182cm, 137.6kg
Liver cirrhosis	Male	65	8170/3 Hepatocellular carcinoma, NOS	Primary	BMI: 53.3 165cm, 145kg
Liver cirrhosis	Male	64	8170/3 Hepatocellular carcinoma, NOS	Primary	BMI: 35.4 173cm, 106kg
Liver cirrhosis, Fatty liver	Male	71	8170/3 Hepatocellular carcinoma, NOS	Primary	BMI: 32 163cm, 85kg
Liver Cirrhosis, Fatty liver	Male	41	8170/3 Hepatocellular carcinoma, NOS	Primary	BMI: 23.2 176cm, 72kg
Liver cirrhosis, Fatty liver	Male	79	8170/3 Hepatocellular carcinoma, NOS	Primary	BMI: 29.7 176cm, 92kg
Liver cirrhosis, Fatty liver	Male	63	8160/3 Cholangiocarcinoma	Primary	BMI: 36.2 175cm, 111 kg
No hx of fatty liver or cirrhosis	Male	75	8170/3 Hepatocellular carcinoma, NOS	Primary	BMI: 37.4 (11 months surgery) 170cm, 108kg
No hx of fatty liver or cirrhosis	Male	67	9120/0 Hemangioma, NOS	Benign	BMI: 29.1 171cm, 85kg
No hx of fatty liver or cirrhosis	Male	45	8890/0 Leiomyoma, NOS	Benign	BMI: 21 180cm, 68.65kg
No hx of fatty	Male	42	9121/0 Cavernous hemangioma	Benign	

(B)

	Patients	Sex	Age	BMI
Controls	N = 10	Male / Female	47.9 ± 7.8	26.5 ± 2.5
Fatty liver / Cirrhosis	N = 9	Male	60.89 ± 3.9	34.7 ± 2.9

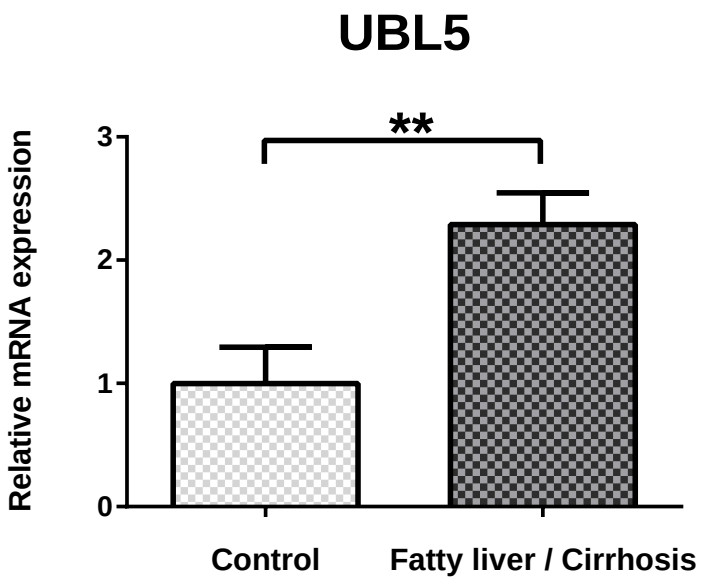

Figure 5.2: *UBL5* mRNA levels in human livers from patients with fatty liver and cirrhosis and controls: mRNA levels were expressed relative to the control sample. The ΔΔCt method was used to calculate relative quantification of gene expression with 18s rRNA as the housekeeper gene. Values presented as mean ± SEM. n=9-10. ** P ≤ 0.01.

5.5.2 Effect of two months on a HFD in heterozygous and control mice.

5.5.2.1 *UBL5* gene expression in heterozygous and controls fed with either HFD or chow for two months

Gene expression levels of *UBL5* were measured in the livers of heterozygous and control mice as shown in (Figure 5.3). Expression levels of *UBL5* were significantly elevated in HF-fed control mice compared to the chow fed controls. Chow-fed heterozygous mice showed the same degree of reduction in UBL5 gene expression levels (50%) as previously found. When challenged with a HFD, the heterozygous mice had significantly more *UBL5* expression than the chow-fed heterozygous mice and were normalised back to the levels seen in control mice on the chow diet. The control HF-fed mice have significantly higher expression than the HF-fed heterozygous.

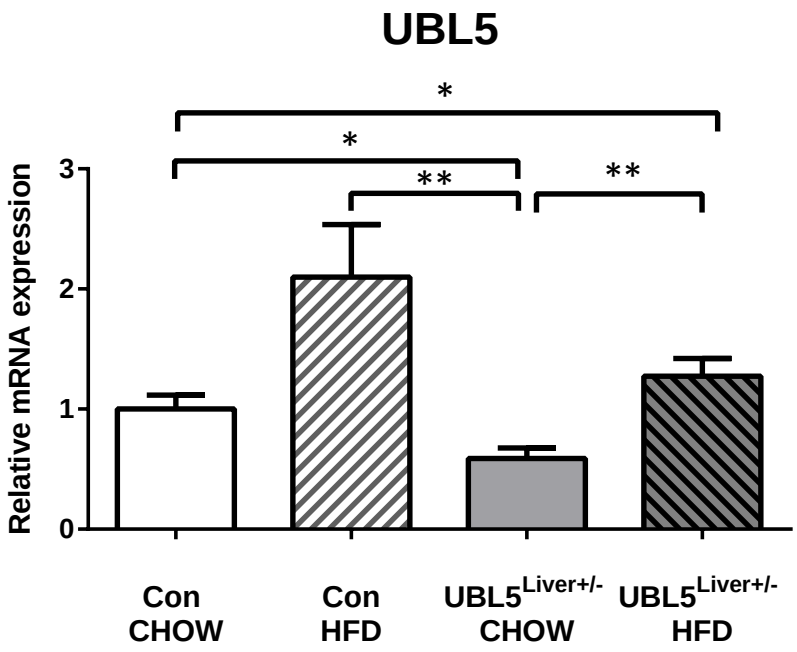

Figure 5.3: *UBL5* mRNA levels in the liver from heterozygous and control mice 2 months on HFD and CHOW: mRNA levels were expressed relative to the control sample. $UBL5^{Liver+/-}$ is the heterozygous group and the Con is the control. The ΔΔCt method was used to calculate relative quantification of gene expression with GAPDH rRNA as the housekeeper gene. Values presented as mean ± SEM. n=5-10. *P ≤0.05, ** P ≤ 0.01.

5.5.2.2 Food intake, body weight and liver weight

Body weight and food intake were measured weekly for 9 weeks and illustrated in (Figure 5.4 and Figure 5.5.). At the commencement of the diet, body weights were similar between all groups either on the HFD or chow diet. Throughout the study period, both heterozygous mice and controls on HFD significantly increased their body weight compared to the chow-fed groups (Figure 5.4).

Heterozygous mice on HFD consumed more grams of food at the beginning of the study while the controls on HFD were eating less. However, by the end of the study there were no significant differences in food intake between the groups (Figure 5.5).

The liver weight was significantly higher in controls fed with HFD compared to the rest of the groups (Figure 5.6). No differences were seen between the heterozygous and control mice when consuming either a HF or chow diet.

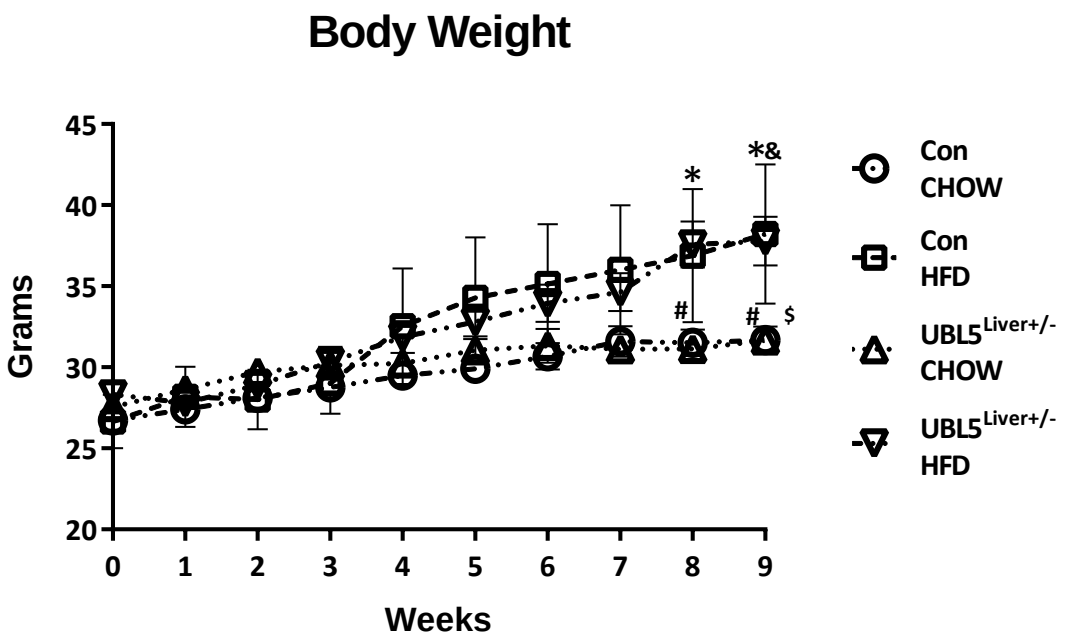

Figure 5.4: Body weight 2 months on 21% Fat, 2% cholesterol semi pure rodent diet (HFD). Body weight of controls on chow (circle), a control on HFD (square), a heterozygous ($UBL5^{Liver+/-}$) on CHOW (triangle) and Heterozygous ($UBL5^{Liver+/-}$) on HFD (reversed triangle) was measured every week throughout the 2 months' period. N=5-10. *****= Con CHOW vs Con HFD, **#=** $UBL5^{Liver+/-}$ CHOW vs $UBL5^{Liver+/-}$ HFD, **&=** Con CHOW vs $UBL5^{Liver+/-}$ HFD, **$=** Con HFD vs $UBL5^{Liver+/-}$ CHOW (P ≤0.05).

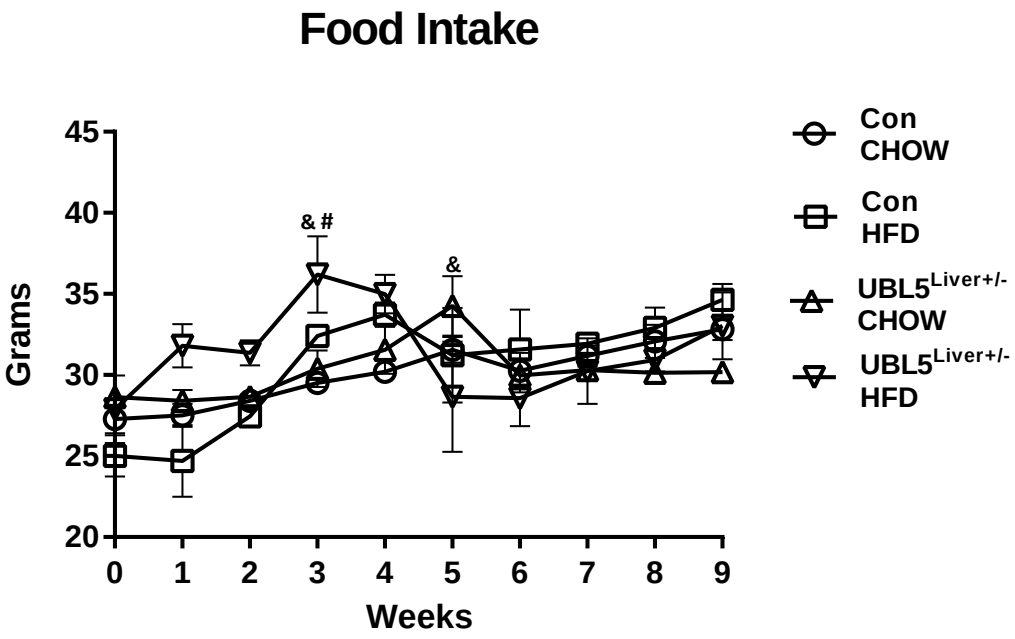

Figure 5.5: Food intake (grams) of high fat-fed heterozygous mice and controls. Food intake of controls on chow (circle), a control on HFD (square), a heterozygous ($UBL5^{Liver+/-}$) on CHOW (triangle) and Heterozygous ($UBL5^{Liver+/-}$) on HFD (reversed triangle) was measured every week throughout the 2 months' period. N=5-10. **# =** UBL-$5^{Liver+/-}$ CHOW vs $UBL5^{Liver+/-}$ HFD, **& =** Con CHOW vs $UBL5^{Liver+/-}$ HFD, (P ≤0.05).

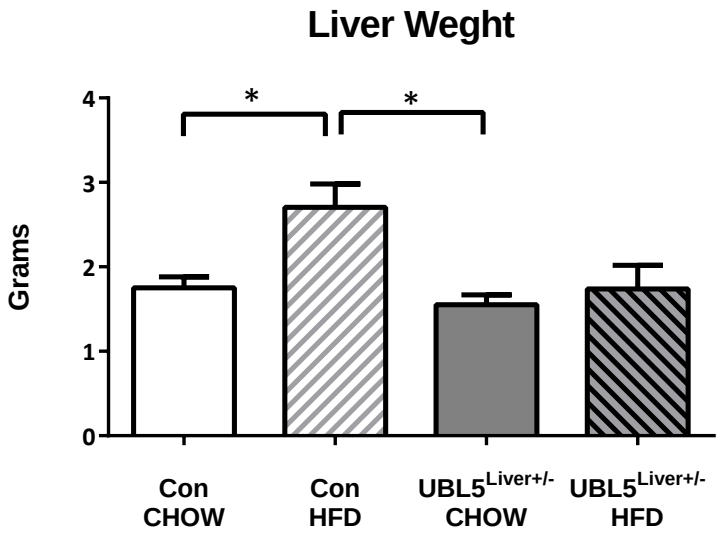

Figure 5.6: Liver weight of high fat-fed heterozygous mice and controls. Liver weights of heterozygous (UBL5$^{Liver+/-}$) mice and littermates were measured at the end of 2 months. N=5-10. *****P ≤0.05.

5.5.2.3 Glucose tolerance test

Glucose tolerance was assessed at the end of two month feeding period by OGTT and shown in (Figure 5.7, A). Both chow-fed groups showed normal glucose tolerance during the test while control mice on the HFD were significantly glucose intolerant. Surprisingly, the heterozygous mice had normal glucose tolerance on the HFD compared to the control mice on both diets and the chow-fed heterozygous mice. Figure 5.7, B Illustrates this response as an Area Under Curve (AUC) of the glucose curves. The body weight at the time of the test was significantly increased for both HF-fed groups (control and heterozygous mice) compared to the chow-fed groups (control and heterozygous mice) (Figure 5.8).

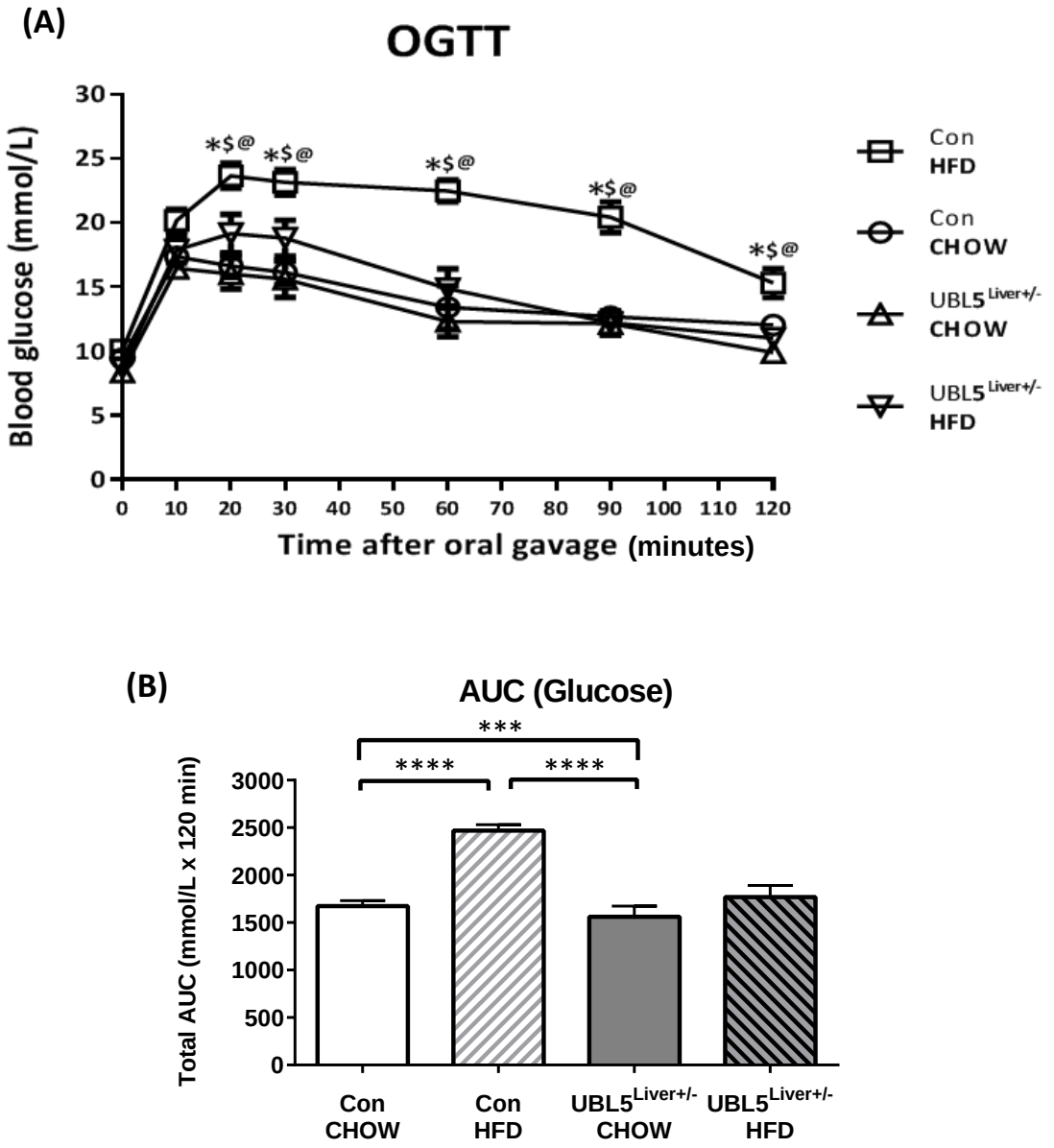

Figure 5.7: Oral glucose tolerance test (OGTT) of heterozygous (UBL5$^{Liver+/-}$) and controls 2 months on HFD and CHOW. Oral glucose tolerance test was performed on controls and heterozygous (UBL5$^{Liver+/-}$) on HFD and CHOW (2months). **(A)** Plasma glucose levels were measured at various time points, ***** = Con CHOW vs Con HFD, # = UBL5$^{Liver+/-}$ CHOW vs UBL5$^{Liver\ +/-}$ HFD, & = Con CHOW vs UBL5$^{Liver+/-}$ HFD, $ = Con HFD vs UBL5$^{Liver+/-}$ CHOW, @ = Con HFD vs UBL5$^{Liver+/-}$ HFD ($P \leq 0.05$). **(B)** Plasma glucose levels during an OGTT expressed as Area under Curve. N= 5 – 10. ** $P \leq 0.01$, *** $P \leq 0.001$, **** $P \leq 0.0001$.

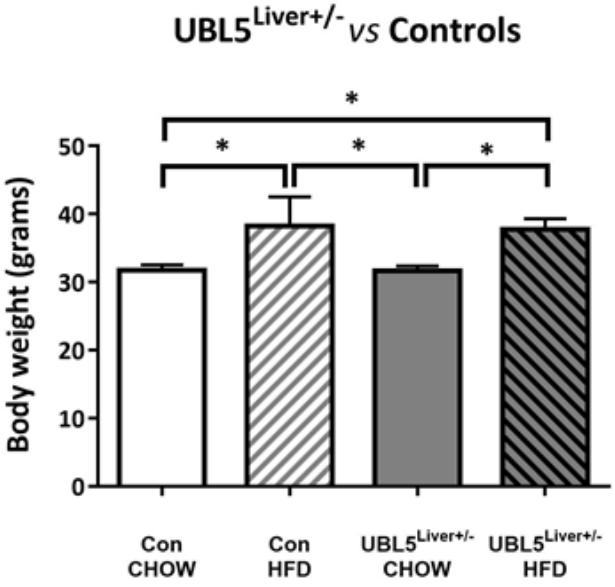

Figure 5.8: Body weight 2 months on 21% Fat, 2% cholesterol semi pure rodent diet (HFD). Body weight (before OGTT) of controls on chow., a control on HFD, a heterozygous ($UBL5^{Liver+/-}$) on CHOW and Heterozygous ($UBL5^{Liver+/-}$) on HFD was measured on the day of GTT. N=5-10. *****P ≤0.05.

5.5.2.4 Histological assessment of liver tissue

Histology was performed on the livers collected following the feeding period. H&E stain on the section were performed to observe potential morphological changes (Figure 5.9, A, B). In Figure 5.9, A are representative H&E slides for each group. HF-fed control mice showed liver parenchyma with severe vacuolation and diffuse macro/ micro-vesicular steatosis (increased fatty deposits). Furthermore, the sections showed focal mononuclear cellular infiltrates (characteristic of inflammatory lesions, where the white blood cells gather at the site of injury) and accompanying necrosis with mildly dilated central and portal veins. The Heterozygous mice on the HFD showed liver parenchyma including hepatocytes, Kupffer cells, portal triads and central veins with moderate, multifocal macro/micro-vesicular steatosis. Occasional displaced nucleus and numerous intracytoplasmic vacuoles. Both chow groups showed normal livers, with H&E sections showing typical liver parenchyma including hepatocytes, Kupffer cells, portal triads and central veins. There were no lesions of significance. Figure 5.9, B demonstrates the grading of the slides (from 0-5) denoting the levels of cellular degradation observed. Control mice on chow had grade 0-1 which is considered as normal histology where grade cannot be assessed/well differentiated, the control mice on HFD were graded as 4-5 which is undifferentiated (anaplastic) and signifies poor

histology, the heterozygous on chow mice were graded as 0-2 that is well differentiated/ moderately differentiated and the heterozygous on HFD were grated between 1-3 that is moderately/poor differentiated histology.

(A)

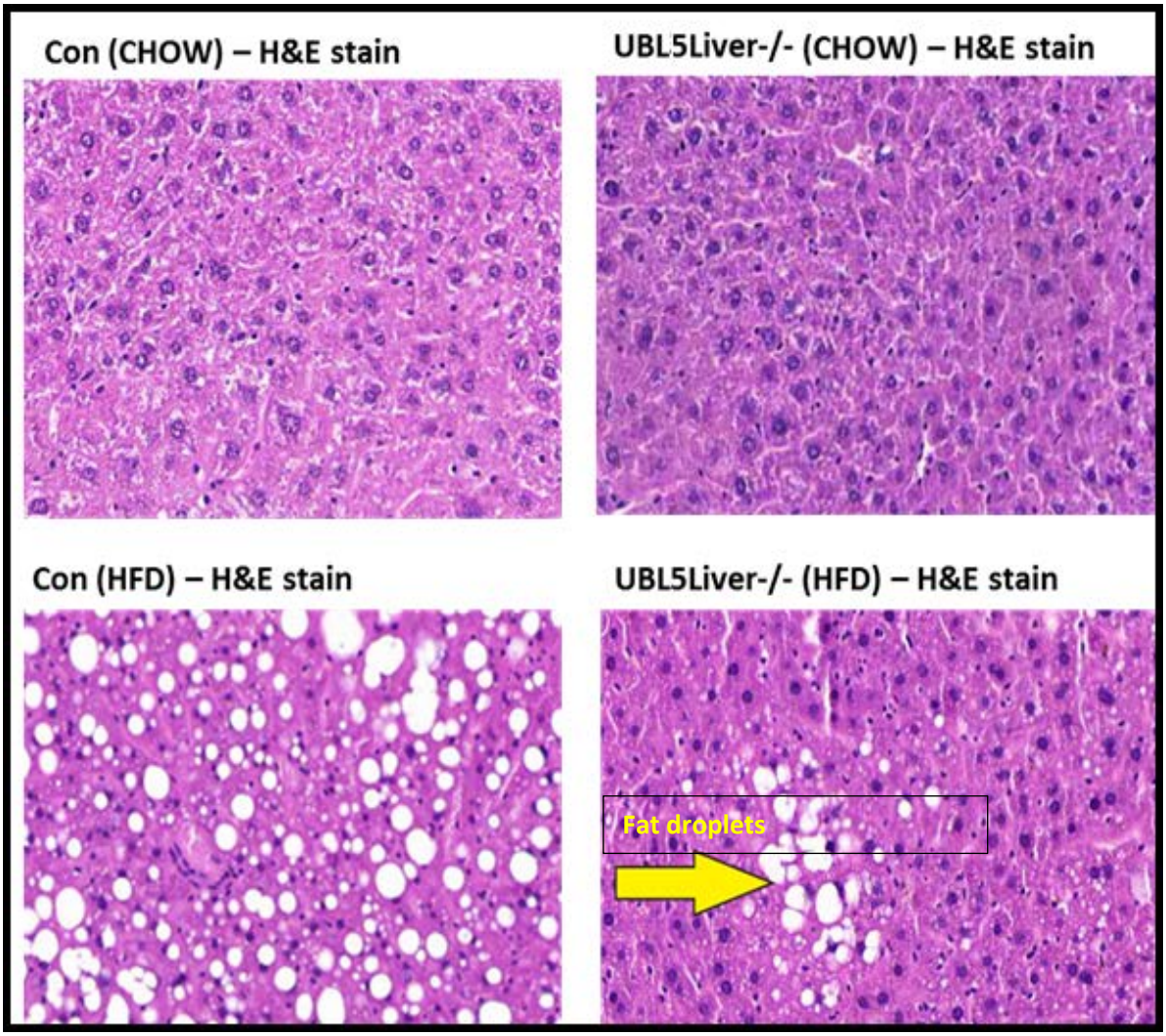

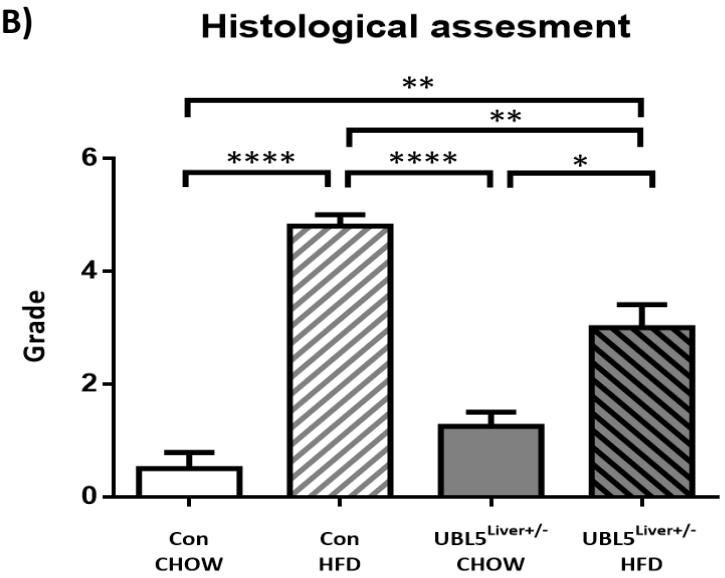

Figure 5.9: Hematoxylin and eosin (H&E) stain on livers samples from heterozygous and controls 2 months on HFD and CHOW: Hematoxylin and eosin stain was done on fixed (in 10% formaldehyde) liver tissues from **(A)** controls and heterozygous ($UBL5^{Liver+/-}$) on HFD and CHOW. Yellow arrow points at fat droplets. **(B)** A graph that represents histological grade in between of four groups compare to the controls. N=5-10. *=P ** P ≤ 0.01, *** P ≤ 0.001, **** P ≤ 0.0001.

5.5.2.5 Liver function test analysis

Liver enzymes such as alanine transaminase (ALT), alkaline phosphatase (ALP) and bilirubin (Bili) were measured in plasma from all feeding groups. The results are illustrated in (Figure 5.10, A, B, C). ALT was significantly elevated in controls fed a HFD compared to the chow-fed groups, the levels of ALT in the heterozygous mice HF-fed did not change compared to the chow-fed groups (Figure 5.10, A). The ALP (Figure 5.10, B) and Bili (Figure 5.10, C) did not show any significant differences across the groups.

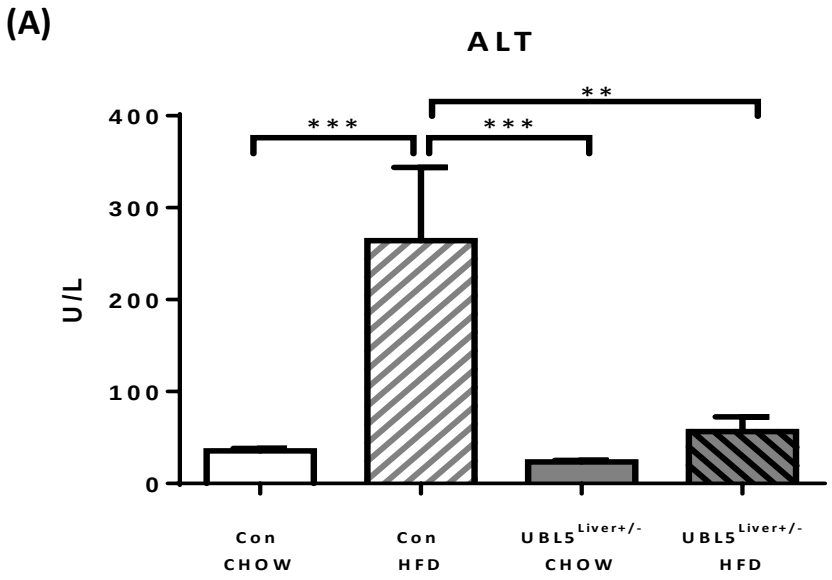
(A)
ALT
U/L
400
300
200
100
0
***
***
**
Con CHOW
Con HFD
UBL5Liver+/- CHOW
UBL5Liver+/- HFD

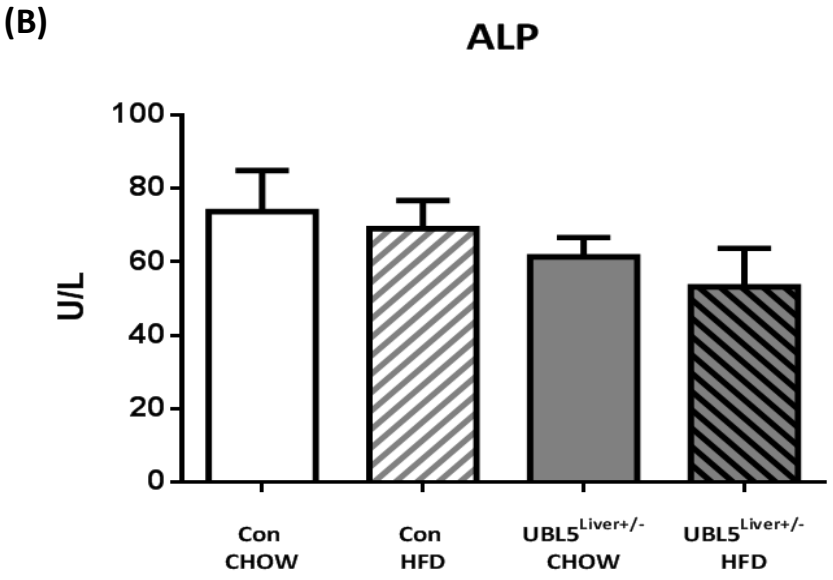
(B)
ALP
U/L
100
80
60
40
20
0
Con CHOW
Con HFD
UBL5Liver+/- CHOW
UBL5Liver+/- HFD

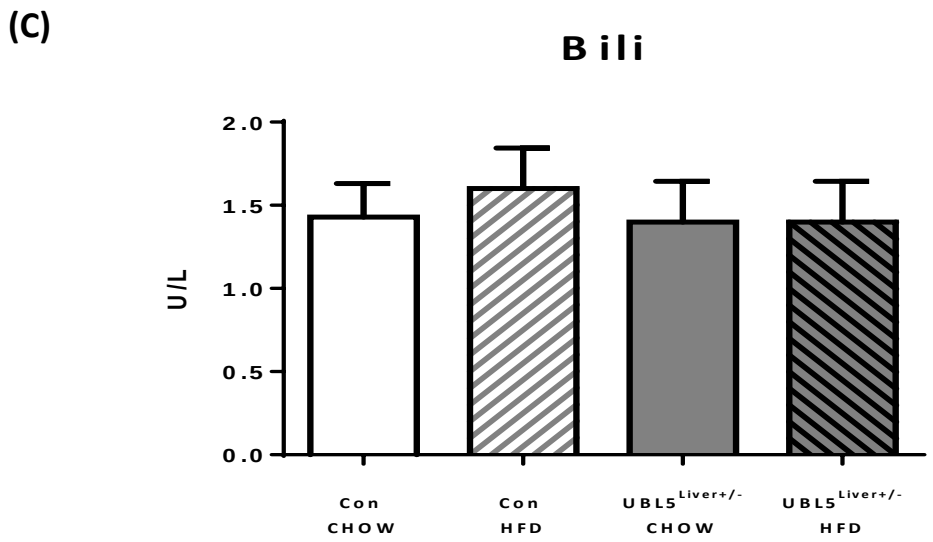

Figure 5.10: Liver plasma enzyme alanine transaminase (ALT), alkaline phosphatase (ALP) and bilirubin (Bili) levels from heterozygous and controls 2 months on HFD and CHOW: Liver function test, **(A)** ALT levels, **(B)** ALP levels and **(C)** Bili levels were assessed in UBL5$^{Liver+/-}$ on CHOW, UBL5$^{Liver+/-}$ on HFD and controls on CHOW and controls on HFD at the end of the study (2 months). N=5-10. ** P ≤ 0.01, *** P ≤ 0.001.

5.5.2.6 Plasma lipid profile

To further understand what the effects of a HFD are on the lipid profile of the mice, we measured circulating levels of total cholesterol, triglycerides and ketones / b-hydroxybutyrate (BHB). The circulating cholesterol levels were significantly elevated in the control mice fed a HFD compared to the chow groups. The heterozygous mice on a HFD had a trend for increased cholesterol levels but it was not statistically significant compared to the chow groups. Interestingly, levels were significantly reduced when compared to the controls fed a HFD (Figure 5.11, A). The circulating levels of triglycerides and ketones were not significantly different between the groups after two months on HFD versus chow diet (Figure 5.11, B, C).

(A)

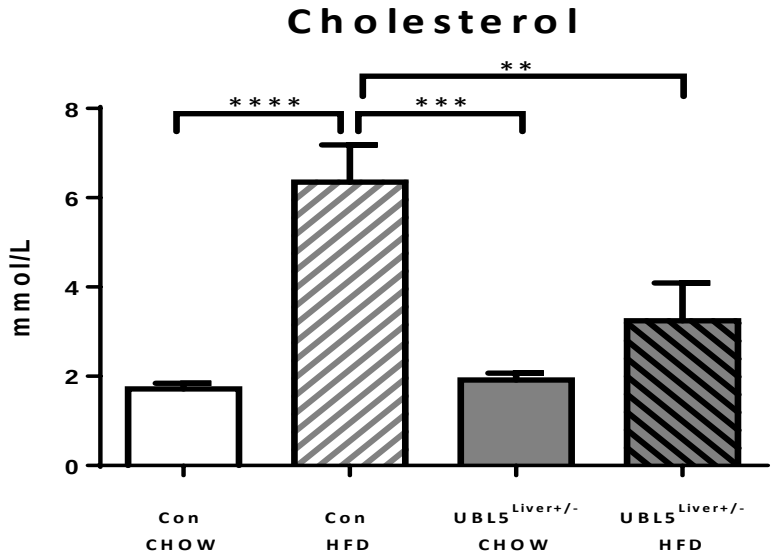
Cholesterol
****
***
**
mmol/L
8
6
4
2
0
Con CHOW
Con HFD
UBL5Liver+/- CHOW
UBL5Liver+/- HFD

(B)

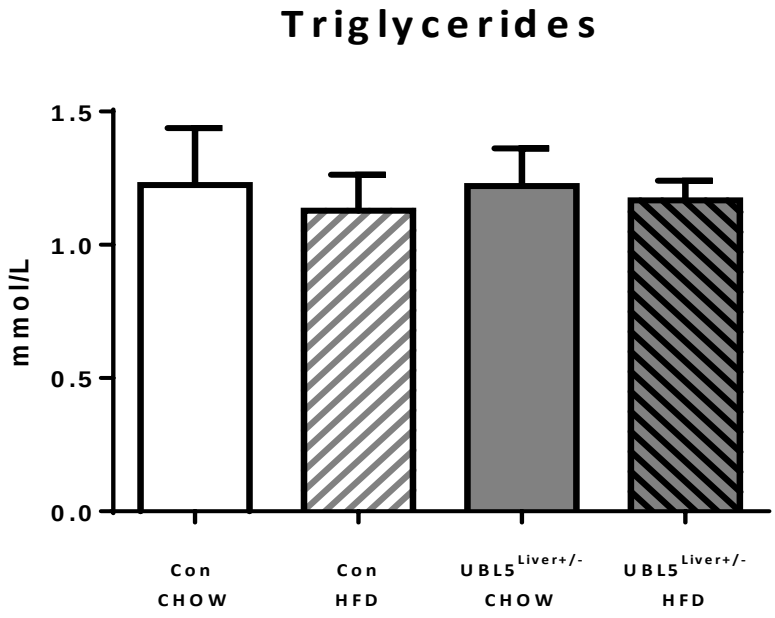
Triglycerides
mmol/L
1.5
1.0
0.5
0.0
Con CHOW
Con HFD
UBL5Liver+/- CHOW
UBL5Liver+/- HFD

(C)

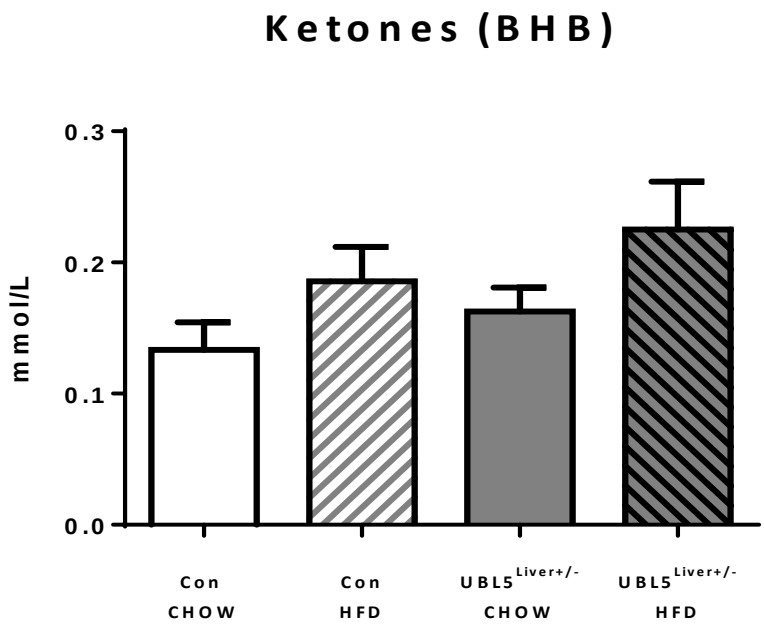

Figure 5.11: Cholesterol, triglycerides and ketone (BHB) levels from plasma of heterozygous and controls 2 months on HFD and CHOW diet: (A) Cholesterol, **(B)** triglycerides and **(C)** ketone (BHB) levels were assessed in heterozygous ($UBL5^{Liver+/-}$) on CHOW, heterozygous on HFD and controls on CHOW and controls on HFD at the end of the study (2months). N=5-10. ** P ≤ 0.01, *** P ≤ 0.001, **** P ≤ 0.0001.

5.5.2.7 Expression profile of genes involved in the UPRmt

In Figures 5.12 (A, B, C) we assessed the gene expression profile of several genes important in the UPRmt. We found that the transcription factor *CHOP* was significantly elevated in our heterozygous mice fed a HFD compared to the chow-fed heterozygous groups and to the control mice on a HFD. The controls on a HFD had elevated levels of *CHOP* as well though it was significantly lower than in the heterozygous on HFD (Figure 5.12, A). The expression levels of the proteases *Clpp* and *ClpX* were significantly upregulated in the heterozygous mice on HFD compared to the controls (Figure 5.12, B).

Correspondingly, both heat shock proteins (Hsp60, Hsp70mt) were significantly higher in our heterozygous mice on HFD. Hsp10 was upregulated in both groups on HFD (Figure 5.12, C).

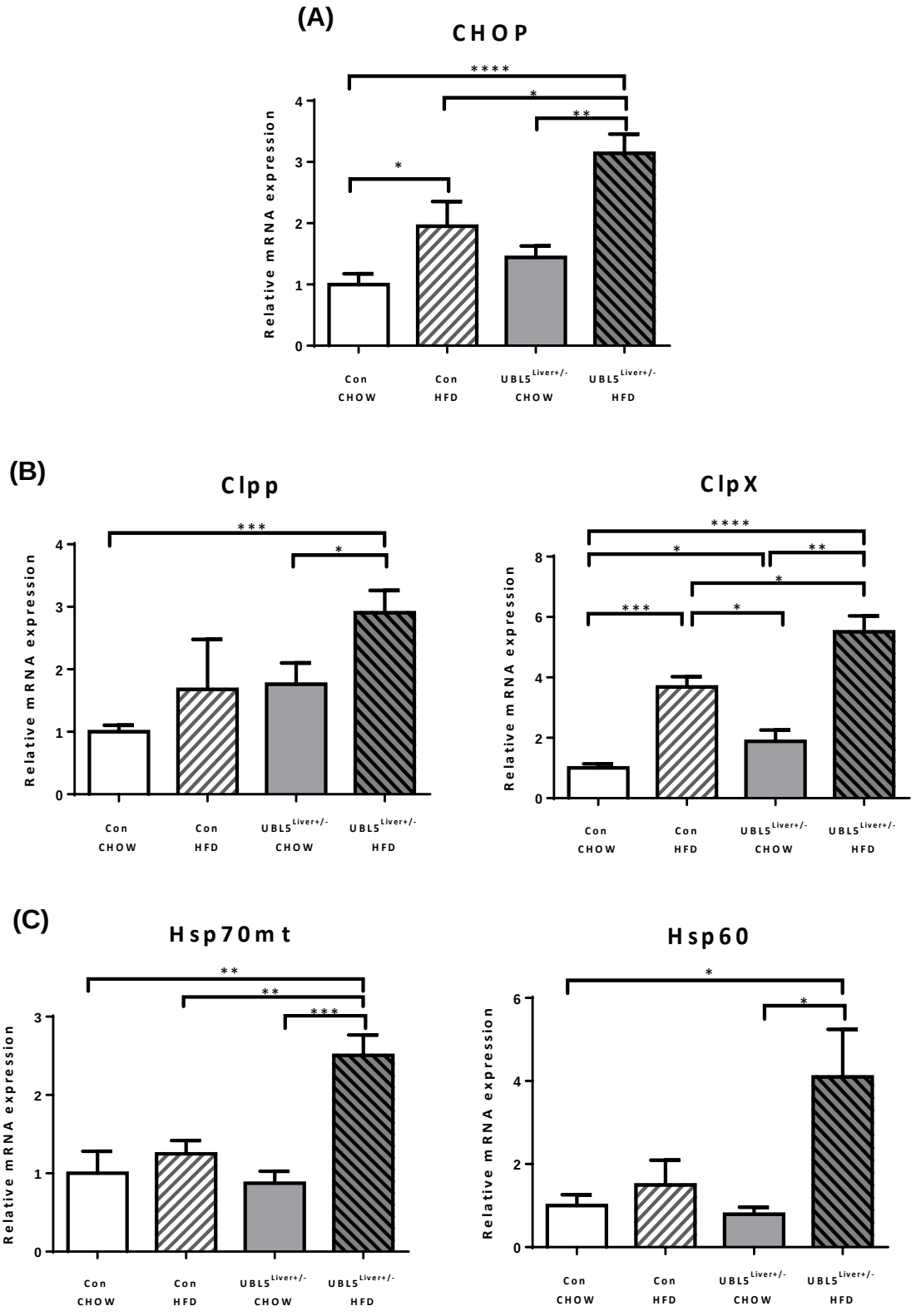

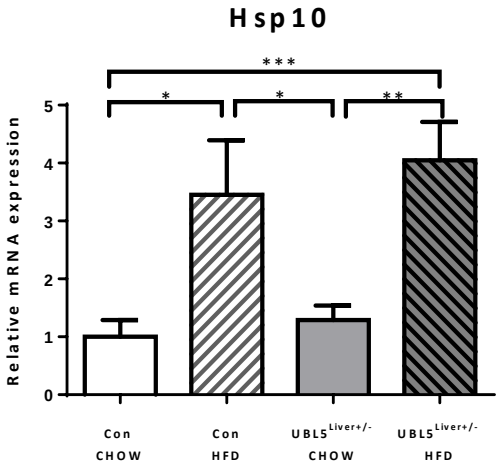

Figure 5.12: UPRmt genes mRNA levels in the liver from heterozygous and controls 2 months on HFD and CHOW: mRNA levels of **(A)** transcription factor *CHOP*, **(B)** proteases *Clpp* and *Clp*X **(C)** heat shock protein *Hsp60*, *Hsp70mt* and *Hsp10*, were expressed relative to the control and heterozygous ($UBL5^{Liver+/-}$). The ΔΔCt method was used to calculate relative quantification of gene expression with GAPDH RNA as the housekeeper gene. Values presented as mean ± SEM. n=5-10. *P ≤0.05, **P ≤0.01, ***P ≤0.001, ****p< 0.0001.

5.5.3 Effects of five months on HFD in heterozygous and control mice

Our two-month dataset demonstrated a protective nature of the heterozygous mice on a HFD. To determine whether this protective effect would, continue, we completed another cohort with 5 months of HFD feeding (Figure 5.1).

5.5.3.1 *UBL5* gene expression

UBL5 gene expression levels were measured in the livers of the HF-fed and chow-fed heterozygous and control mice after 5 months on the diets (Figure 5.13). Expression levels of *UBL5* were significantly elevated in controls fed a HFD compared to the controls on a chow diet. Heterozygous mice on chow showed 50% reduction of *UBL5* levels compared to the control mice on the chow diet. HF-fed heterozygous mice had significantly elevated levels of *UBL5* compared to the chow-fed heterozygous mice. Although it seems that the HF-fed heterozygous mice have higher expression compared to control mice on chow, this was not statistically significant.

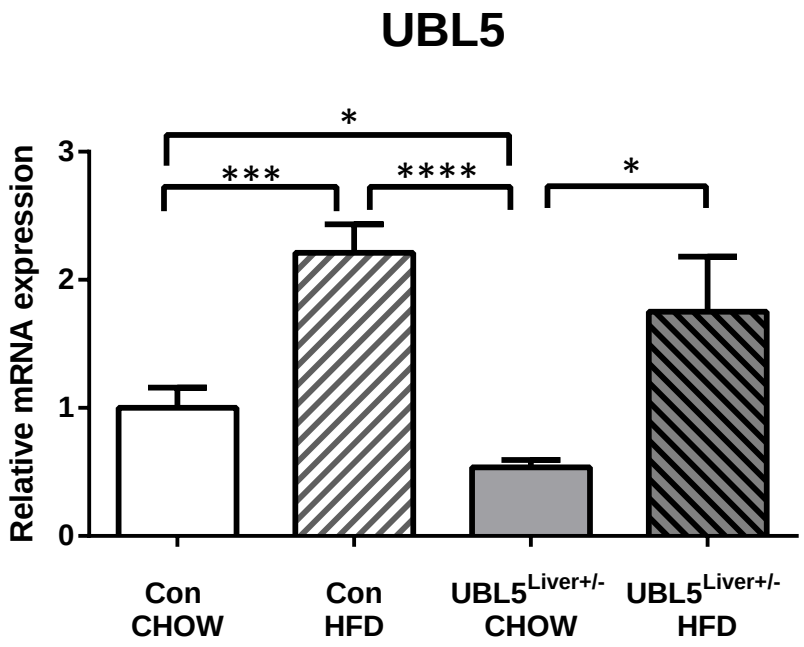

Figure 5.13: Ubl-5 mRNA levels in the liver from heterozygous and controls 5 months on HFD and CHOW: mRNA levels were expressed relative to the control sample, heterozygous ($UBL5^{Liver+/-}$) and the controls (Con). The ΔΔCt method was used to calculate relative quantification of gene expression with GAPDH rRNA as the housekeeper gene. Values are presented as mean ± SEM. n=5-10. *P ≤0.05, ***P ≤0.001, ****p< 0.0001.

5.5.3.2 Food intake, body weight and liver weight

Body weight and food intake were measured weekly for 22 weeks and shown in (Figure 5.14 and Figure 5.15 respectively). At the beginning of the study, the body weights were similar between groups either on HFD or chow diet. Throughout the study period both groups on HFD significantly increased their body weight compared to the chow groups (Figure 5.14).

Heterozygous mice on a chow diet consumed more grams of food at the beginning of the study while the remaining groups were consuming less. However, by the end of the study, the heterozygous mice on a chow diet were eating significantly less than the controls on HFD and heterozygous on HFD (Figure 5.15).

Liver weight was significantly elevated in both controls and heterozygous mice on HFD compared to the chow groups (Figure 5.16).

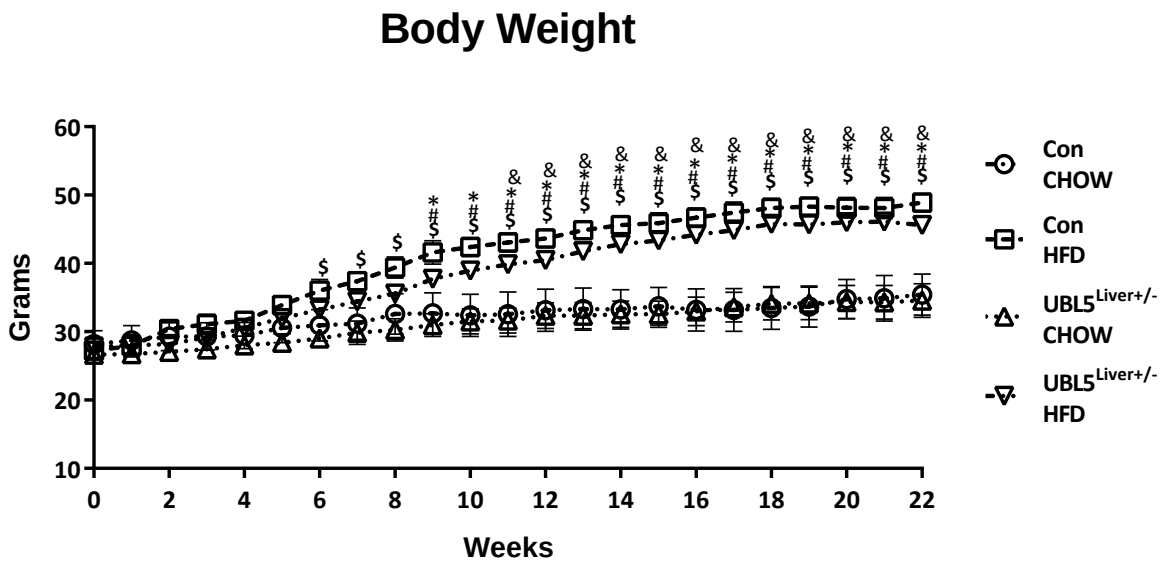

Figure 5.14: Body weight 5 months on 21% Fat, 2% cholesterol semi pure rodent diet (HFD). Body weight of controls (Con) on CHOW (circle), a control on HFD (square), a heterozygous ($UBL5^{Liver+/-}$) on CHOW (triangle) and heterozygous on HFD (reversed triangle) was measured every week through the period of 5 months. N=5-10. ***** = Con CHOW vs Con HFD, **# =** $UBL5^{Liver+/-}$ CHOW vs $UBL5L^{iver+/-}$ HFD, **& =** Con CHOW vs $UBL5^{Liver+/-}$ HFD, **$ =** Con HFD vs $UBL5^{Liver+/-}$ CHOW (P ≤0.05).

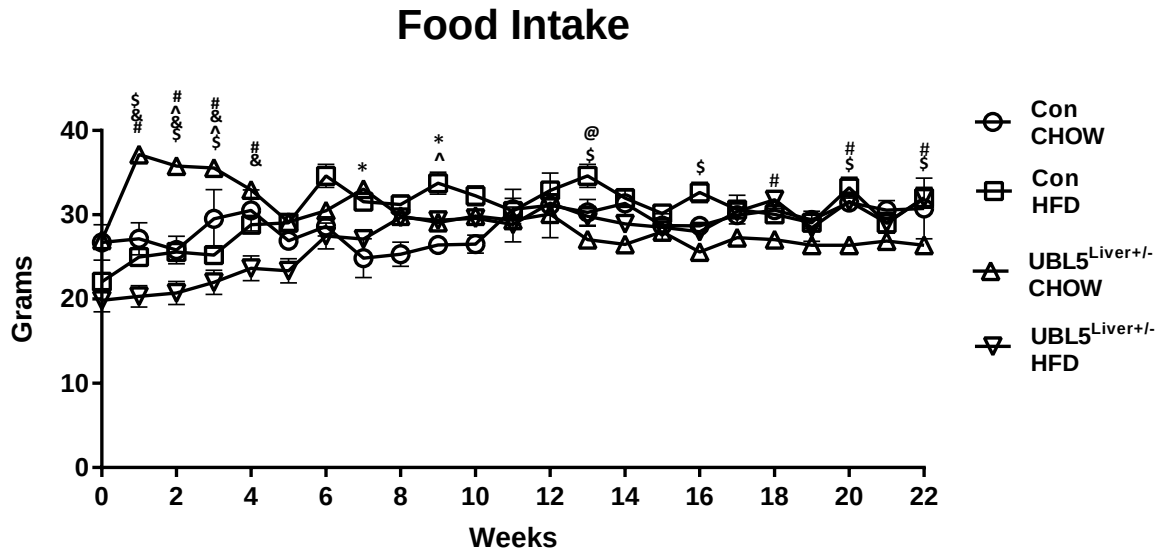

Figure 5.15: Food intake (grams) of high fat-fed heterozygous mice and controls. Food intake of heterozygous ($UBL5^{Liver+/-}$) mice and controls (Con) were measured over 5 months. N=5-10. ***** = Con CHOW vs Con HFD, **# =** $UBL5^{Liver+/-}$ CHOW vs $UBL5^{Liver+/-}$ HFD, **&** = Con CHOW vs $UBL5^{Liver+/-}$ HFD, **$=** Con HFD vs $UBL5^{Liver+/-}$ CHOW (P ≤0.05), **^** =Con CHOW vs $UBL5^{Liver+/-}$ CHOW, @ = Con HFD vs $UBL5^{Liver+/-}$ HFD.

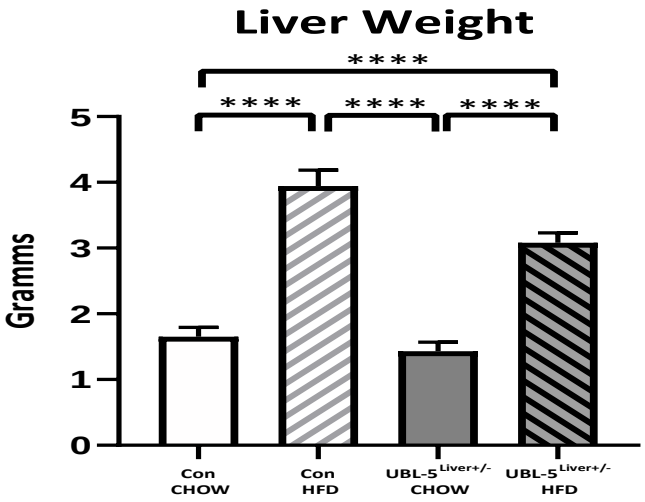

Figure 5.16: Liver weight 5 months on 21% Fat, 2% cholesterol semi pure rodent diet (HFD). Liver weight of controls on CHOW, a controls (Con) on HFD, a heterozygous ($UBL5^{Liver+/-}$) on CHOW and heterozygous on HFD was measured at the end of 5 months. N=5-10. ****p< 0.0001.

5.5.3.3 Glucose tolerance

Glucose tolerance, as assessed by an OGTT, was completed at the end of the five-month feeding protocol and the results shown in (Figure 5.17). With chow feeding, both the heterozygous and control mice showed normal glucose tolerance during the test while the HF-fed controls were glucose intolerant. The heterozygous mice on the HFD were glucose intolerant for the first 60 minutes of the experiment but then normalised their glucose levels at the conclusion (Figure 5.17, A). The Area Under Curve (AUC) of the glucose excursions were significantly increased for the controls on HFD, and we see a trend for an increase for heterozygous mice on HFD although it was not significant (Figure 5.17, B). The body weight was equally increased in both HF-fed groups (Figure 5.18).

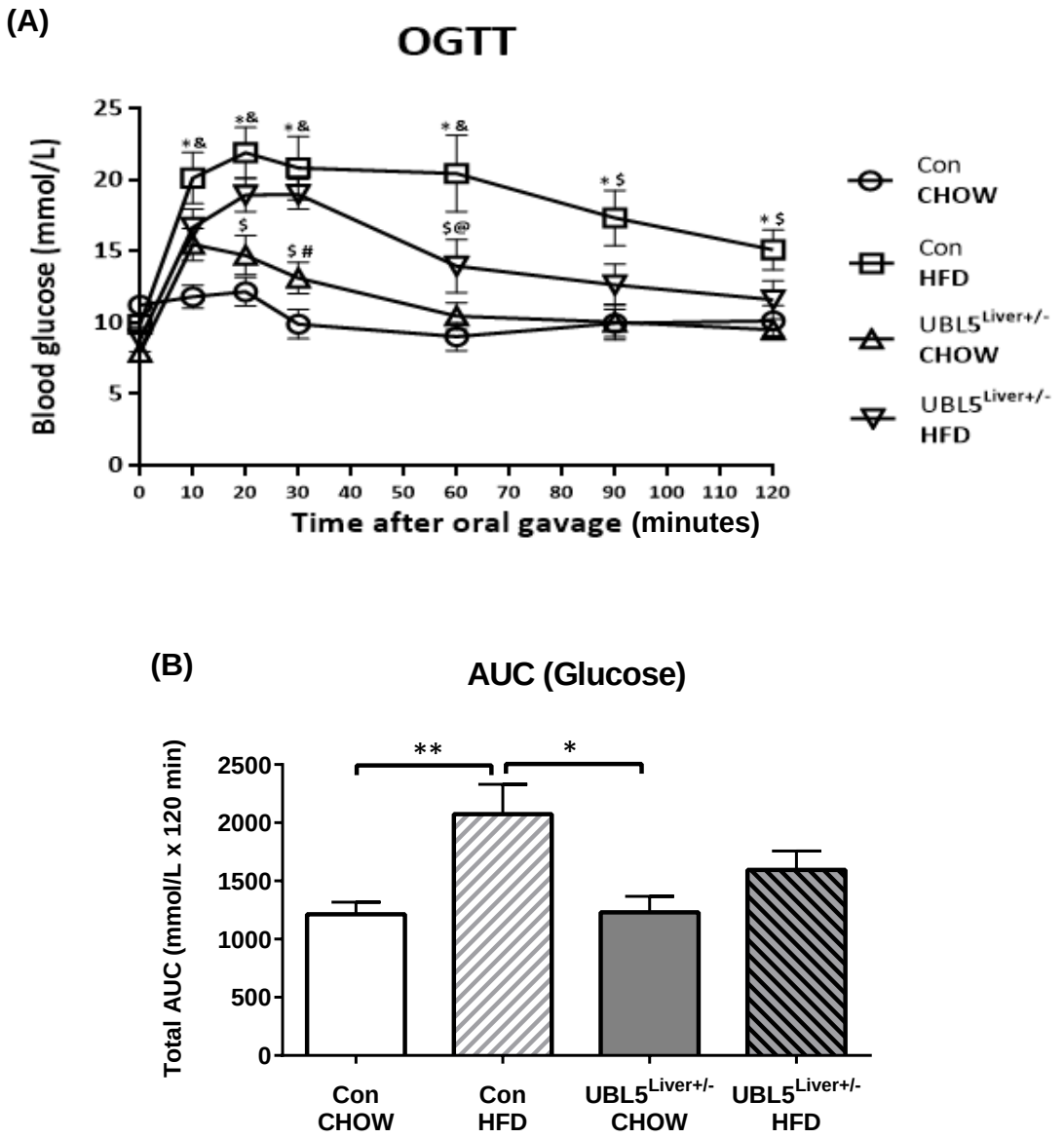

Figure 5.17: Oral glucose tolerance test (OGTT) of heterozygous and controls 5 months on HFD and CHOW. (A) Plasma glucose levels were measured at various time points, ***** = Con CHOW vs Con HFD, # = UBL5$^{Liver+/-}$ CHOW vs UBL5$^{Liver+/-}$ HFD, **&** = Con CHOW vs UBL5$^{Liver+/-}$ HFD, **$** = Con HFD vs UBL5$^{Liver+/-}$ CHOW, @ = Con HFD vs UBL5$^{Liver+/-}$ HFD. **(B)** Plasma glucose levels during an OGTT expressed as Area under Curve. Heterozygous are (UBL5$^{Liver+/-}$) and controls are (Con). N= 5 – 10. ** P ≤ 0.01, *** P ≤ 0.001, **** P ≤ 0.0001.

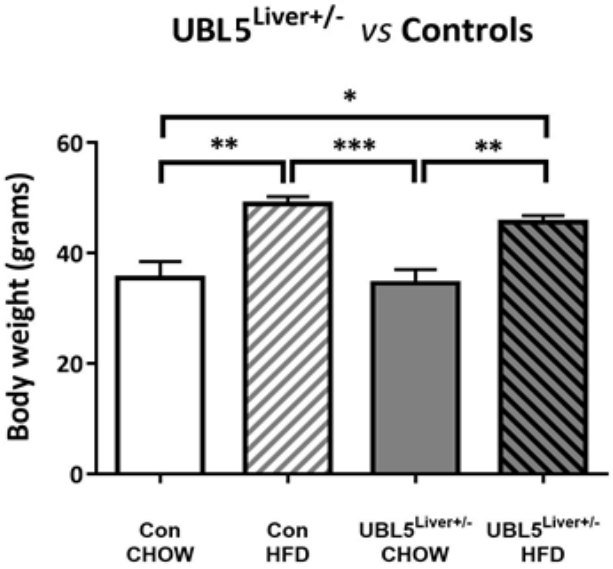

Figure 5.18: Body weight 5 months on 21% Fat, 2% cholesterol semi pure rodent diet (HFD). Body weight of controls on chow, a control on HFD, a heterozygous ($UBL5^{Liver+/-}$) on CHOW and Heterozygous ($UBL5^{Liver+/-}$) on HFD was measured on the day of GTT. N=5-10. *****P ≤ 0.05, **P ≤ 0.01, ***P ≤ 0.001.

5.5.3.4 Histological assessment of liver tissue

Histology was performed on the livers we collected from our mice at the conclusion of the feeding period. Morphological changes were assessed using H&E staining (Figure 5.19 A, B) with a representative picture shown in (Figure 5.19, A). The control mice on a HFD showed liver parenchyma with severe vacuolation, diffuse macro/ micro-vesicular steatosis (fatty change). Focal mononuclear cellular infiltrates and accompanying necrosis. The heterozygous mice on HFD showed similar results with the controls on HFD. All the controls on HFD were graded as grade 5 undifferentiated (anaplastic) while some of the heterozygous were grade 3 to 5 poor differentiated histology. Both chow groups showed normal liver histology (grade 0-1 cannot be assessed/well differentiated), with H&E sections showing typical liver parenchyma including hepatocytes, Kupffer cells, portal triads and central veins. No lesions of significance were observed.

The grading of cellular degradation is shown in (Figure 5.19, B) with both HF-fed groups showing significantly worse histology grading than the chow groups.

(A)

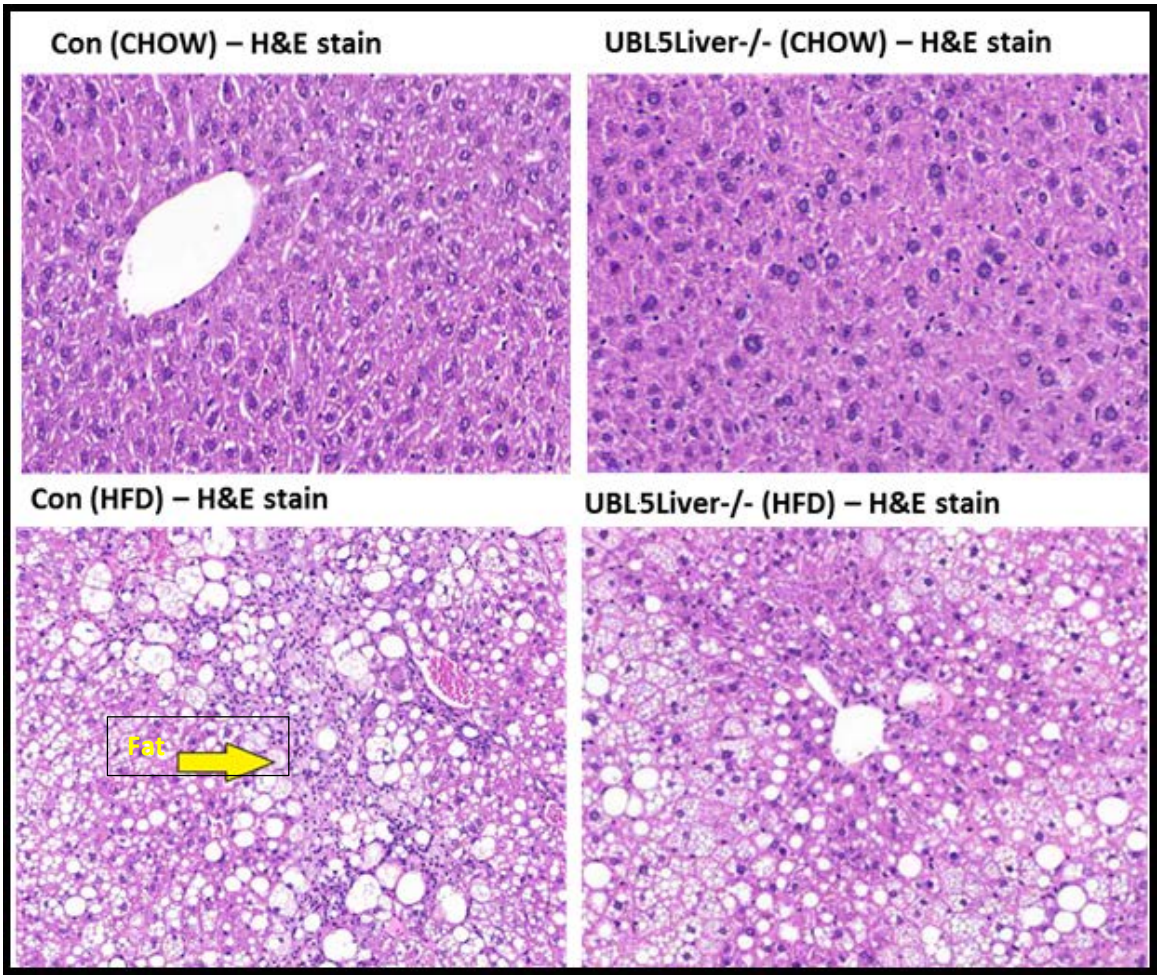

(B)

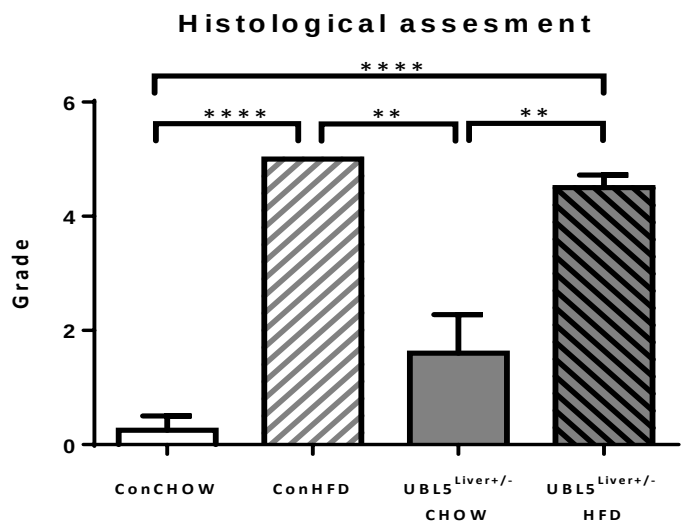

Figure 5.19: Hematoxylin and eosin (H&E) stain on livers samples from heterozygous and controls 5 months on HFD and CHOW: Hematoxylin and eosin stain was done on fixed (in 10% formaldehyde) liver tissues from **(A)** controls (Con) and heterozygous ($UBL5^{Liver+/-}$) on HFD and chow. Yellow arrow point to fat droplets. **(B)** A graph that represents histological grade in between of four groups compare to the controls. N=5-10. ** P ≤ 0.01, **** P ≤ 0.0001.

5.5.3.5 Liver function test analysis

The results from the liver enzyme profiling are illustrated in (Figure 5.20, A, B, C). ALP (Figure 5.20, A) and ALT (Figure 5.20, B) levels were significantly elevated in HF-fed controls when compared to both the chow groups and to the heterozygous mice fed a HFD. Importantly, heterozygous mice on the HFD showed significantly elevated levels of both these enzymes when compared to the chow groups. Bilirubin levels did not show significant difference across any of the groups (Figure 5.20, C).

(A)

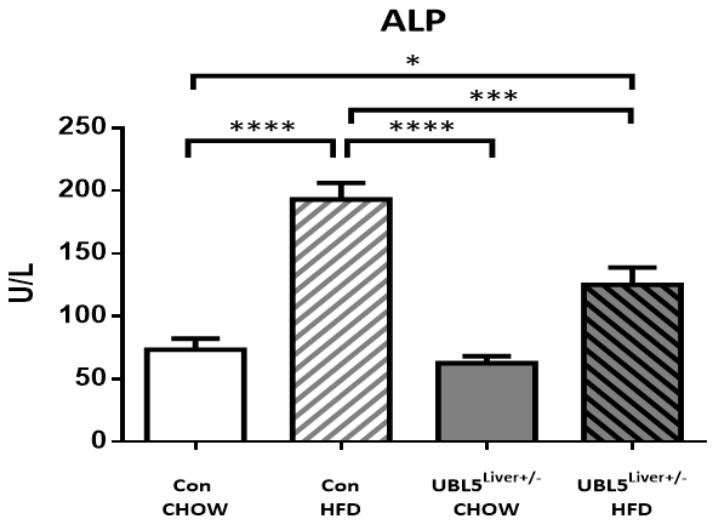

(B)

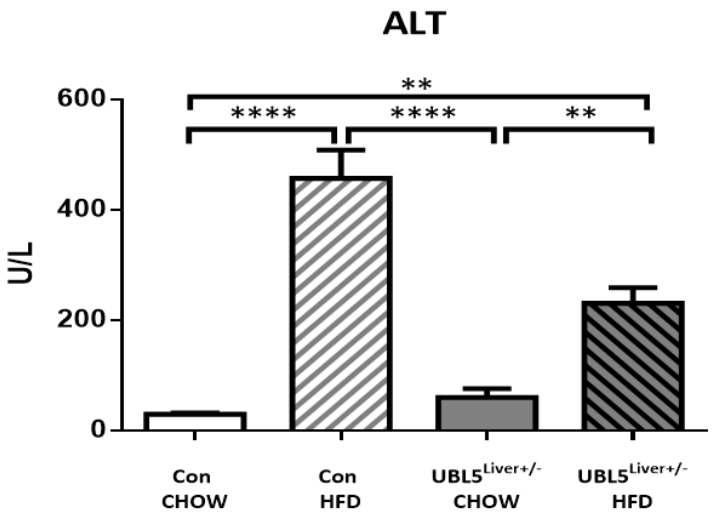

(C)

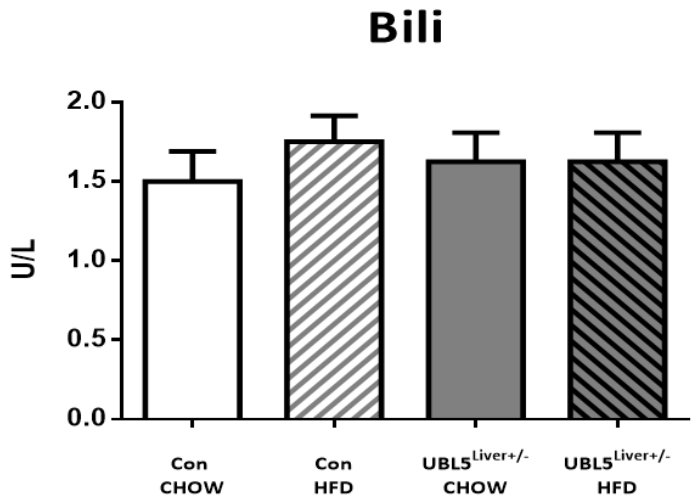

Figure 5.20: Liver plasma enzyme alanine transaminase (ALT), alkaline phosphatase (ALP) and bilirubin (Bili) levels from heterozygous and controls 5 months on HFD and CHOW: Liver function test, **(A)** ALT levels, **(B)** ALP levels and **(C)** Bili levels were assessed in heterozygous on CHOW, heterozygous on HFD and controls on CHOW and controls on HFD at the end of the study (5 months). Heterozygous are ($UBL5^{Liver+/-}$) and controls are (Con). N=5-10. *****P ≤0.05, **P ≤0.01, ***P ≤0.001, ****p< 0.0001.

5.5.3.6 Lipid profiling

To assess the lipid profile at five months in our animals, we measured circulating cholesterol, triglyceride and ketones / β-hydroxybutyrate (BHB) levels in plasma of non-fasted mice. The cholesterol levels were significantly elevated in controls fed a HFD compared to the chow-fed control group, which had baseline levels of cholesterol in their plasma. The heterozygous mice on a HFD had increased cholesterol levels compared to the chow groups, although the levels of cholesterol were significantly lower compared to the controls fed with HFD (Figure 5.21, A). Levels of both triglycerides and ketones were not significantly different between the groups after five months on a HFD compared to the chow diet (Figure 5.21, B, C).

(A)

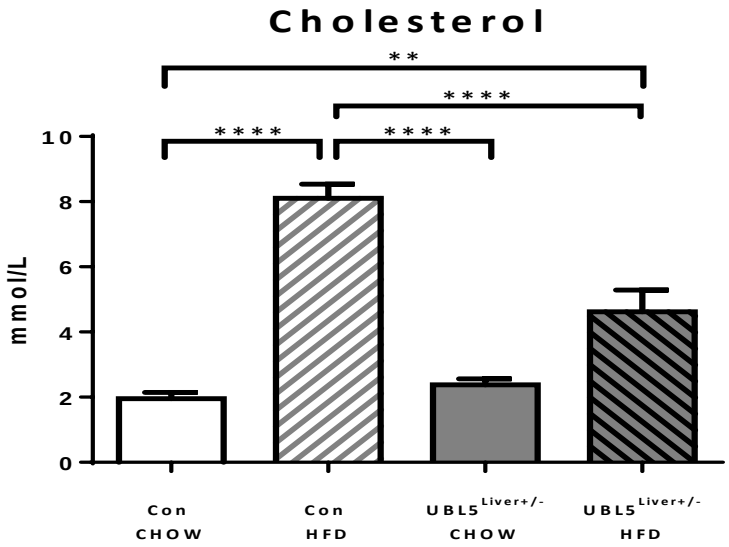
Cholesterol
**
****
****
****
10
8
6
4
2
0
mmol/L
Con CHOW
Con HFD
UBL5Liver+/- CHOW
UBL5Liver+/- HFD

(B)

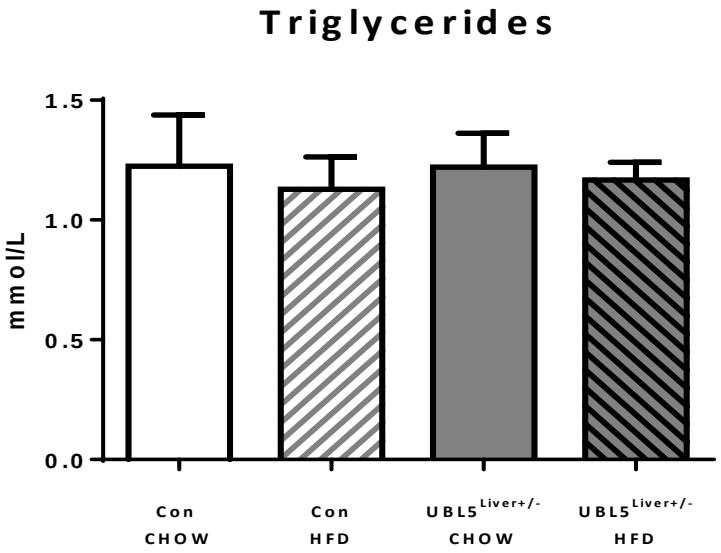
Triglycerides
1.5
1.0
0.5
0.0
mmol/L
Con CHOW
Con HFD
UBL5Liver+/- CHOW
UBL5Liver+/- HFD

(C)

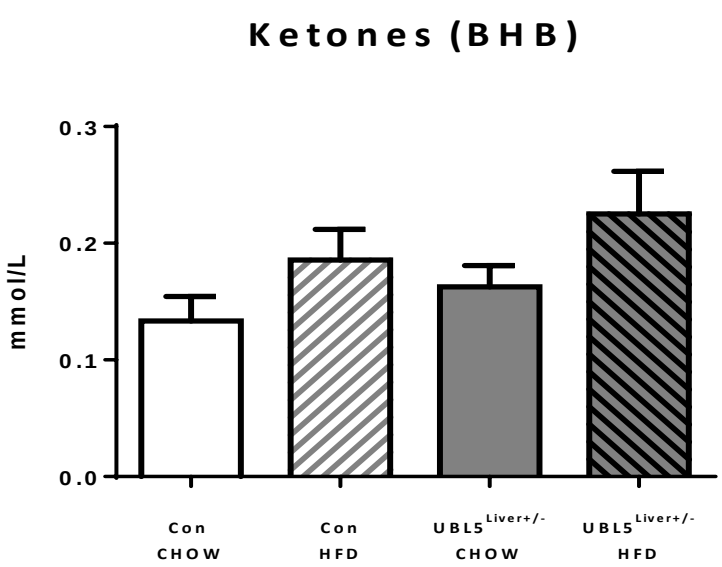

Figure 5.21: Cholesterol, triglycerides and ketone (BHB) levels from plasma of heterozygous and controls 5 months on HFD and CHOW: (A) Cholesterol, **(B)** triglycerides and **(C)** ketone (BHB) levels were assessed in Heterozygous (UBL-5Liver+/-) and controls (Con) on CHOW and HFD at the end of the study (5 months). N=5-10. ** P ≤ 0.01, *** P ≤ 0.001, **** P ≤ 0.0001.

5.5.3.7 Expression profile of genes involved in the UPRmt

Gene expression levels of the transcription factor *CHOP* was significantly elevated in our heterozygous mice fed with HFD compared to both chow groups and to the control mice fed a HFD. The controls on HFD also had elevated levels of *CHOP* though it was significantly lower than in the heterozygous on HFD (Figure 5.22, A).

Expression of the proteases (*Clpp* and *Clpx*) showed diverse results. The catalytic subunit of the *ClpPX*, the *ClpX* significantly elevated in heterozygous mice on HFD compared to the chow groups, while the proteolytic subunit *Clpp* did not show significant differences between the groups (Figure 5.22, B).

Expression of the heat shock proteins (*Hsp60, Hsp70m*t) were significantly higher in the heterozygous mice on HFD compared to chow-fed groups and controls on HFD, whilst *Hsp10* was upregulated in both HF-fed groups compared to chow-fed groups (Figure 5.22, C).

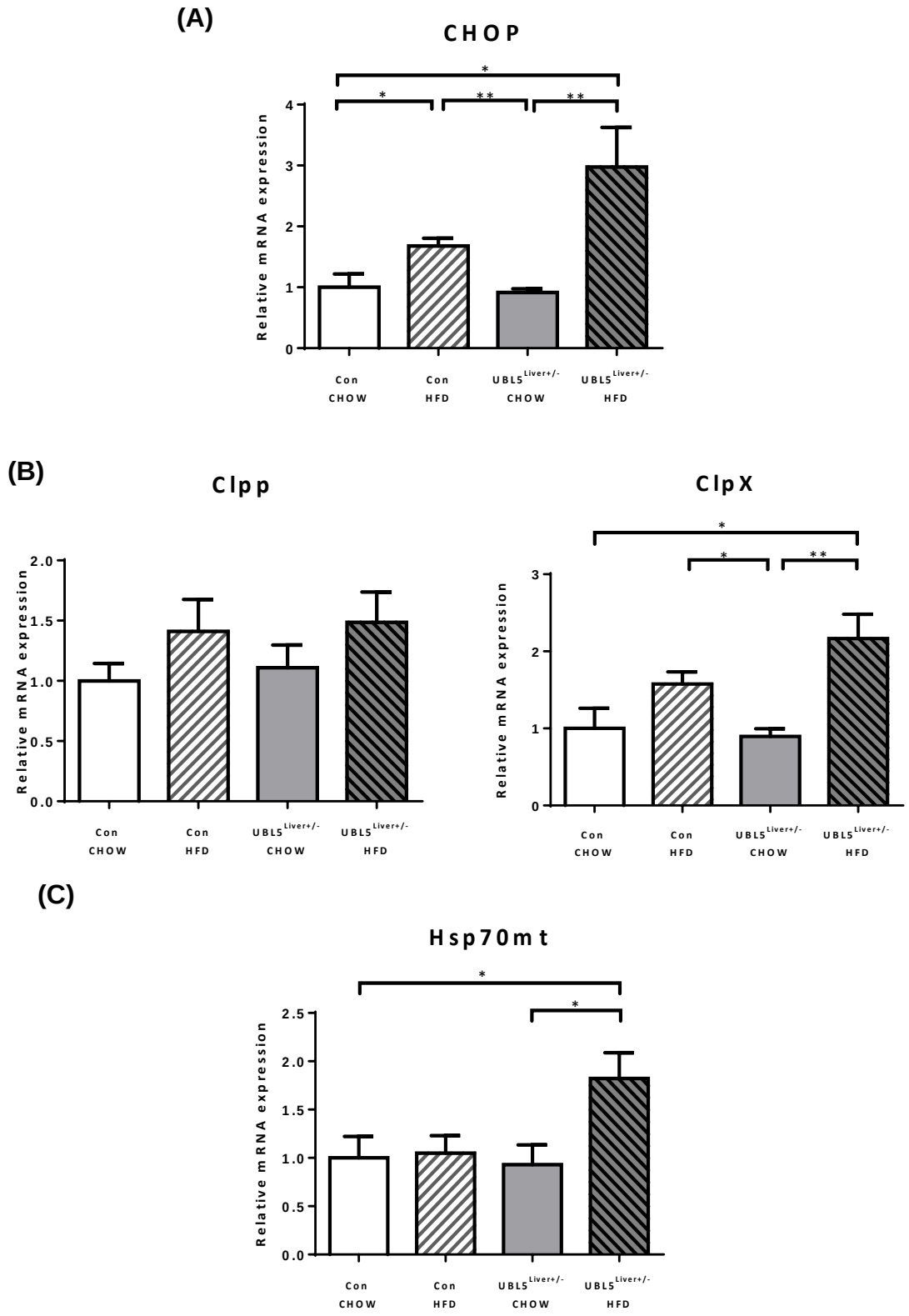
(A)
CHOP
Relative mRNA expression
0
1
2
3
4
*
*
**
**
Con CHOW
Con HFD
UBL5 Liver+/- CHOW
UBL5 Liver+/- HFD
(B)
Clpp
Relative mRNA expression
0.0
0.5
1.0
1.5
2.0
Con CHOW
Con HFD
UBL5 Liver+/- CHOW
UBL5 Liver+/- HFD
ClpX
Relative mRNA expression
0
1
2
3
*
*
**
Con CHOW
Con HFD
UBL5 Liver+/- CHOW
UBL5 Liver+/- HFD
(C)
Hsp70mt
Relative mRNA expression
0.0
0.5
1.0
1.5
2.0
2.5
*
*
Con CHOW
Con HFD
UBL5 Liver+/- CHOW
UBL5 Liver+/- HFD

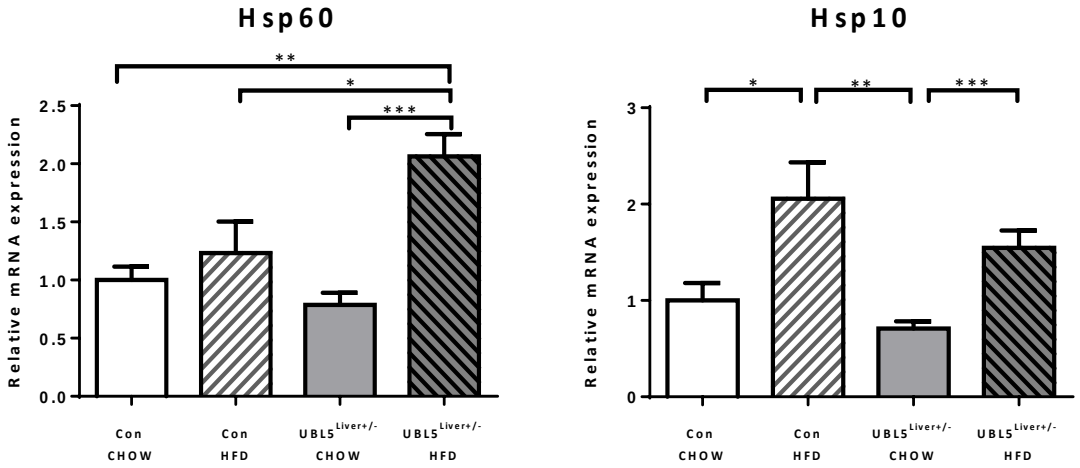

Figure 5.22: UPRmt genes mRNA levels in the liver from heterozygous and controls 5 months on HFD and CHOW: mRNA levels of **(A)** transcription factor *CHOP*, **(B)** proteases *Clpp* and *ClpX* **(C)** heat shock protein *Hsp60, Hsp70mt* and *Hsp1*0, were expressed relative to the control (Con) and heterozygous ($UBL5^{Liver+/-}$). The ΔΔCt method was used to calculate relative quantification of gene expression with GAPDH RNA as the housekeeper gene. Values presented as mean ± SEM. n=5-10. *P ≤0.05, **P ≤0.01, ***P ≤0.001, ****p< 0.0001.

5.6 Discussion

In Chapter 4, we demonstrated that our heterozygous mice (with 60% reduction in *UBL5* gene expression) did not show any deleterious phenotypes on a chow diet and remained healthy to that of the control mice.

We decided to induce stress on the livers of these mice that possibly would make them worse than controls because of their partial knockdown of UBL5. Therefore, based on previous literature, we chose to stress the heterozygous mice with a diet high in cholesterol and fat as high cholesterol diets have been shown to induce fatty liver in mice (Leung et al., 2016; Rivera et al., 2014). We investigated the variations in UBL5 levels in human patients with fatty liver disease to see if they were equivalent to our mouse model. In this chapter, we investigated the effects of the HFD in the heterozygous mice after two and five months of feeding. These timepoints were chosen to assess both the short and long term adverse effects of the high cholesterol diet on the heterozygous mice.

5.6.1 *UBL5* levels are increased in patients with fatty liver and cirrhosis.

There is no literature showing levels of *UBL5* in patients suffering from liver disease. We wanted human relevance in our study therefore we obtained human liver samples from patients with cirrhosis and fatty liver and measured *UBL5* gene expression levels. Our findings showed upregulation of *UBL5* in liver samples from both diseased states compared to controls. This increase could be due to the impact of liver disease on the hepatocytes and not the initial cause. The average age of control group was ~50 years old and of the patients with liver disease ~60 years old. BMI of the control patients was ~26.5 which is considered overweight with moderate health risks. While the patients with liver disease had ~34.7 BMI which is considered obese with higher health problems. This is an important observation as there have been previous studies of UBL5 linked to several metabolic syndrome related phenotypes in humans. For example, a study in a Mexican/American population showed a significant association of five single nucleotide polymorphisms (SNPs) of

UBL5 with increased waist-to-hip ratio, obesity and increased cholesterol levels in fasted individuals (Bozaoglu et al., 2006a). Additionally, Jowett et al studied a Mauritian and Nauruan population and found *UBL5* variants to be related to several metabolic-syndrome related phenotypes (Jowett et al., 2004). The exact link between UBL5 and these defects have not been determined. In our study, it is possible that this difference in BMI could add to the fatty liver/cirrhosis defect and additionally affect the *UBL5* expression levels. However, knowing the role of UBL5 in the stress response, we speculate that it was increased in patients with fatty liver and cirrhosis (and high BMI) due to the increased liver damage these patients had.

Having found that *UBL5* is indeed increased in the humans with fatty liver and cirrhosis we wanted to extend these findings to work out the mechanisms at play. Therefore, as we clearly showed in the previous chapter, the heterozygous mice are healthy under normal conditions (even with half the amount of *UBL5*), we wanted to explore the effects of a fatty liver inducing diet has on the animal and in particular on the UPRmt pathway.

5.6.2 UPRmt acts as a protective response against HFD in mice with severe liver dysfunction.

As previous studies have demonstrated, the high cholesterol/high fat diet is able to cause severe fat accumulation in the liver (Leung et al., 2016) (Rivera et al., 2014). Enduring consumption of a diet rich in fat and cholesterol can lead to liver dysfunction, oxidative stress and eventually NAFLD because of increased intracellular fatty acid products building up in the liver (Hansen et al., 1998) (Samuel et al., 2004) (Leung et al., 2016) (Chavez et al., 2003). We were interested to see if this HFD would cause our heterozygous mice to be more prone to fat accumulation, oxidative stress and liver dysfunction. For these reasons, we chose to treat our mice with high cholesterol diet to challenge specifically the liver and to induce fat accumulation and oxidative stress.

Upon finishing the two - month study we measured several parameters to evaluate the integrity of the liver in our different cohorts of mice. To our surprise, the

heterozygous mice were healthier than the controls on HFD. It is well known that consuming a HFD can alter the circulating lipid profile (Srinivasan, Viswanad, Asrat, Kaul, & Ramarao, 2005). We saw an increase in circulating cholesterol levels in control mice on HFD while the heterozygous mice on HFD were not affected. The triglycerides and ketones did not show any differences between our groups. Possibly because the diet we used was not sufficient to significantly elevate these lipids. Previous human studies have shown that subjects displayed lower serum triglyceride concentrations after consuming high-fat diets, compared with low-fat diets (Jacobs, De Angelis-Schierbaum, Egert, Assmann, & Kratz, 2004; G. Liu, Coulston, Hollenbeck, Reaven, & Metabolism, 1984; G. C. Liu, Coulston, & Reaven, 1983). Alternatively, serum triglyceride levels have been reported to increase during low-fat high-carb diet consumption rather than high-fat-diet (Demol et al., 2009) (Hellerstein, 2002) (Parks, Krauss, Christiansen, Neese, & Hellerstein, 1999). Although all these diets are different, we cannot make a direct comparison. Also, we measured the circulating triglyceride levels only and not the hepatic triglycerides that could explain why we see no difference in levels.

The heterozygous mice showed no decline in liver function at two months of HF-feeding and nor was there any effect on glucose tolerance compared to the chow control mice. LFTs was not significantly different compared to chow controls yet significantly improved compared to the HFD control. Increased levels of these enzymes indicate liver damage or injury and correlates with several liver diseases such as NAFLD and NASH (Johnston, 1999; M. Lee, 2009). Bilirubin did not show any difference between groups which is supported by early reports showing that bilirubin levels are not increased by a high fat diet (Barrett, 1971). Body weight on the HFD could not be differentiated between the heterozygous and control mice during the feeding period. Both groups put on the same amount of weight when compared to their chow-fed groups. This consumption of HFD has been shown in a previous study in mice to have similar increases in body weight (Leung et al., 2016). This study also showed that liver weight increases in these mice. However, only the HF-fed control mice showed an increase in liver weight, while the HF-fed heterozygous mice had no such increase. This could possibly be in response to less fat accumulation in the liver. This was confirmed by histology where we saw less micro- and macro- vesicular fat accumulation in the livers of HF-fed heterozygous mice compare to controls on HFD.

Since the heterozygous mice on this diet had better liver function, glucose tolerance was not affected and in fact was significantly better than in the controls fed with HFD. Under normal conditions (when the liver is healthy), liver stores and manufactures glucose depending on the energy requirements. Having better glucose tolerance may suggest that the HF-fed heterozygous mice may have better liver function. However we need to acknowledge that many factors can influence glucose tolerance directly and indirectly (e.g time of the meal or type etcetera) (Andrikopoulos, Blair, Deluca, Fam, Proietto, et al., 2008).

UBL5 expression in the heterozygous mice was found to be normalized back to those of the chow-fed control mice. It appears that feeding such a diet can increase UBL5 expression because of the stresses these diets impose on the liver. While the heterozygous mice could not increase the levels of UBL5 higher than basal likely due to there being less liver stress/damage than the control HFD group. As we will describe in the next paragraph because of the partial expression of *UBL5* in the livers of these mice, the UPRmt response possibly activates under less stress which in turn has a protective effect of the mitochondria.

Following the changes, we saw in *UBL5* levels we were interested to see how the UPRmt genes were affected. The UPRmt was increased in the HF-fed heterozygous mice compared to controls on HFD, even though both groups were exposed to HFD. As we described in greater detail in previous chapters having activated heat shock proteins and generally the UPRmt defends the cell against stress and injury. Through maintaining mitochondrial proper function and cellular structure and function (Lin & Haynes, 2016; Petrof, Ciancio, & Chang, 2004). These increased levels of UPRmt (heat shock proteins, proteases and transcription factor) we saw in HF-fed heterozygous mice, perhaps protected them from the deleterious effects of HFD. The difference we see in UPRmt levels between groups is possibly due differences in *UBL5* expression levels between control and heterozygous mice. Likely we did not see the UPRmt increasing in the HF-fed controls to the extent of HF-fed heterozygous mice due to the severely damaged livers that were blocking the transcription. We can speculate that having half the copy of *UBL5* made the heterozygous mice more sensitive to a stress response. Therefore, the HF-fed heterozygous mice triggered the UPRmt earlier than controls which led them to preserve more healthier mitochondria in their livers. As we described previously, when

mitochondria are under stress the UPRmt activates and restores proper mitochondrial function. Possessing more healthier mitochondria possibly helped the heterozygous mice maintain better metabolism and liver function. Perhaps if we would have checked the gene expression at an earlier time point, we would have seen these genes increase in controls as well.

Evidence is mounting demonstrating how having more and healthier mitochondria is essential for better health, metabolism and longevity (Bratic & Trifunovic, 2010; Johannsen & Ravussin, 2009; Pizzorno, 2014). Improved mitochondrial capacity promotes longevity of the cell due to decreased apoptosis (Bratic & Trifunovic, 2010). Speakman et al observed that the MF1 (albino) female mice, that lived longer, had higher metabolic intensities via higher proton conductance across the inner mitochondrial membrane of skeletal muscles (Speakman et al., 2004). It is possible that our heterozygous mice had better metabolism because they had more and healthier mitochondria, although further investigation is required. Previous studies also showed that different models of heterozygous mice can display better health than the full KO or controls. For instance, Penn et al showed in 2002 that the heterozygous mice for “major histocompatibility complex” (set of genes essential in immune system) infected with Salmonella (three virulent strains), had a better survival rate than the knockouts and control mice (Penn, Damjanovich, & Potts, 2002). Furthermore, Lapointe and colleagues showed in 2008 that a homozygous knockout mouse of *Mclk1* gene (the mouse homologue of clk-1 aging enzyme) led to a severe under-development and embryonic lethality, while the partial deletion of *Mclk-1* gene increased the lifespan in mice by 31% (Lapointe & Hekimi, 2008). Similarly, partial inactivation of *Surf1* gene (encoding for cytochrome-c oxidase assembly factor of complex IV), in mice increased their lifespan and protected the mice from induced neurodegeneration (Dell'Agnello et al., 2007). Finally, a study in Drosophila showed that partial deficiency of *Surf1* in the central nervous system did not affect the flies and increased their lifespan while a complete knockdown of *Surf1* led to embryonic lethality (Zordan et al., 2006). Though these studies are different to the one we performed in this thesis, the overall conclusion is that models with partial gene reduction are beneficial for longevity compared to the complete knockdown mouse models.

Our data clearly showed that after two months of HF-feeding, the heterozygous mice had increased expression of genes associated with the UPRmt, better metabolism and liver function than the control mice. Therefore, to extend these findings, we completed another feeding cohort where we exposed the mice to the HFD for 5 months to determine if this protective effect could continue.

Our findings showed that when both the heterozygous and control mice were on the HFD, both groups gained the same weight compared to the chow-fed groups that remained as expected, lean (Leung et al., 2016). The liver weight of heterozygous mice on HFD was significantly increased similarly to controls on HFD, likely due to the increase in fat found within the livers as evidenced by the presence of severe micro- and macro- vesicular steatosis and inflammation. Glucose tolerance at the five-month time point showed the heterozygous mice unable to maintain normal response to high glucose, and becoming glucose intolerant in the early stages of the test. Although by the end of the experiment the HF-fed heterozygous managed to recover while controls on HFD remained glucose intolerant. We did not assess insulin levels due to lack of plasma. Although our model is liver specific and we do not expect the pancreas to be affected, therefore any changes we see are primarily driven by the liver. Liver function was also equally disturbed in the HF-fed heterozygous mice compared to the HF-fed controls with the LFT enzyme significantly increased in both groups compared to the chow-fed groups, although the HFD heterozygous mice displayed significantly lower enzyme levels than the HF-fed controls. Furthermore, cholesterol levels were elevated in the HF-fed heterozygous mice compared to the chow groups, but was still significantly lower compared to the controls on HFD. The data informs us that the heterozygous mice are still maintaining some level of protection despite being on the HFD for the extended period.

The *UBL5* levels increased in HF-fed heterozygous almost similarly to the *UBL5* expression levels of the HF-fed control mice. The HF-fed heterozygous mice still had higher levels of UPRmt gene expression than the controls on HFD. Possibly that is why they still had better glucose tolerance than controls on HFD because the protective response is still activated (for similar reasons as we discussed in two months). Although overall long-term consumption of HFD proved to be deleterious and affected negatively both of our groups.

5.7 Conclusion

In conclusion, this chapter demonstrated that UBL5 and the UPRmt helps to protect against the negative effects of a HFD in the liver, when on this diet for two months. After 5 months of exposure to HFD the positive effects in liver function from the increase in UPRmt begin to diminish. This demonstrates the increasing expression of UPRmt genes can have a protective effect on the cellular function of the liver.

In chapter 6 we will be investigating the severe liver failure seen in the UBL5 KO mice and attempting to discover ways to prevent the phenotype by preventing oxidative stress and fat accumulation. To investigate this, we will attempt both a pharmacological and gene therapy.

CHAPTER 6: THERAPEUTIC INTERVENTION STUDIES

6.1 Introduction

The previous result chapters comprehensively showed that the UBL5 KO mice (97% KD) developed liver dysfunction with severe steatosis, apoptosis, oxidative stress, increased ROS, mitochondrial dysfunction and decreased UPRmt. Initially the heterozygous mice did not show any phenotype under normal chow diet conditions, therefore we stressed them with a high cholesterol (2%) and high fat (21%) diet. Surprisingly the HF-fed heterozygous mice showed a better metabolic profile than the HF-fed control mice which was associated with an increased UPRmt response.

Overall, the results of the study clearly demonstrate that functional UBL5 and UPRmt are an absolute requirement for normal mitochondrial action and overall liver health. When UBL5 and UPRmt are completely absent, the mitochondrial dysfunction leads to metabolic complications with excessive deposition of lipids in the liver, that ultimately leads to severe liver damage and death. Targeting mitochondrial function directly could provide novel ways to treat these types of metabolic dysfunctions and complications. A few therapies have shown that they can improve mitochondrial function, ROS levels and resolve oxidative stress. For example, agents enhancing electron transport chain function, amino acid restoring, antioxidants, energy buffers, agents that enhance mitochondrial biogenesis and gene therapies (El-Hattab, Zarante, Almannai, Scaglia, & metabolism, 2017). Currently there are no available mitochondrial specific therapies, however, there are a diverse range of drugs and gene therapies being tested, including angiotensin-converting enzyme 2 (ACE2) (Mak et al., 2015b; B. A. Wilson, Nautiyal, Gwathmey, Rose, & Chappell, 2016), CoenzymeQ_{10} (Beal & biomembranes, 2004), creatinine (Tarnopolsky, 2008) and vitamin C (Dikalova et al., 2010).

Treatments for liver disease, such as NASH, involve exercise, healthy diet and weight loss, controlling blood sugar levels and in certain cases drugs that reduce high

cholesterol (Leoni et al., 2018). At present, there is no drug that has been approved for the specific treatment of NASH by the US Food and Drug Administration, Australian Therapeutic Goods Administration or the European Medicines Agency (Leoni et al., 2018). Of the currently available drugs used for other disease states, several have been trialled to determine their effectiveness in treating NASH; pioglitazone (Belfort et al., 2006b), vitamin E (Sanyal et al., 2010b), glucagon-like peptide-1 (GLP-1) analogues (Armstrong et al., 2016), statins (Cohen, Anania, & Chalasani, 2006) and Silymarin (Kheong, Mustapha, Mahadeva, & Hepatology, 2017). Also, imeglimin an oxidative phosphorylation blocker, has been shown to improve glucose tolerance, hepatic gluconeogenesis and decrease beta-cell apoptosis in diabetic patients (Vial et al., 2015). Furthermore, imeglimint has been shown to significantly reduce HbA1c (glycated haemoglobin) and it been considered as a treatment for NASH (Sumida et al., 2020). Moreover, the use of ACE2 overexpression has also been tested as a novel therapy (Mak et al., 2015b).

Pioglitazone is a drug that belongs to a family of insulin sensitizers named thiazolidinediones or also known as glitazones (Hulin, McCarthy, & Gibbs, 1996). Thiazolidinediones act through PPARγ activation/binding. PPARγ is a nuclear receptor that acts in glucose regulation and lipid metabolism (Braissant, Foufelle, Scotto, Dauça, & Wahli, 1996; Vidal-Puig et al., 1997). PPARγ is the third member of the PPAR family of nuclear receptors. PPARs are ligand-activated transcription factors that are responsible for the expression of numerous genes, and affect several metabolic processes, such as glucose and lipid homeostasis (metabolism and storage via FA regulation) (Duszka, Oresic, Le May, König, & Wahli, 2017; Rosen et al., 2002; Willson, Brown, Sternbach, & Henke, 2000). Pioglitazone targets tissues such liver, muscle and adipose for insulin action. The transcription of insulin-reactive genes that control glucose production is induced after the activation of PPARγ receptor (Berger & Moller, 2002).

Recent evidence supports the role of pioglitazone in improving steatosis, inflammation and fibrosis in NASH (Boettcher, Csako, Pucino, Wesley, & Loomba, 2012). Several trials demonstrated the ability of pioglitazone to increase adiponectin levels (promotes fatty acid uptake to adipose tissue) and reduce aminotransferases in

the serum. Liver enzymes (AST, ALT and ALP), cholesterol, LDL and HDL levels, hepatic inflammation, fibrosis and liver injury in patients with NAFLD are also improved following pioglitazone treatment (Aithal et al., 2008; Al Gharabally & ACOSTA, 2007; Belfort et al., 2006a; Lutchman et al., 2007; Promrat et al., 2004; Sanyal et al., 2004). Bajaj et al. showed improved ALT levels and reduced hepatic fat accumulation in patients with type 2 diabetes also treated with pioglitazone (Bajaj et al., 2003). The PIVENS study showed significant improvement in steatohepatitis in patients that received pioglitazone (Sanyal et al., 2010a). In 2006 Belfort et al. also published evidence showing an improvement of NASH with pioglitazone (Belfort et al., 2006a). Also, published evidence in studies in rodents suggest that pioglitazone may have anti-oxidant effects that can help with oxidative stress. For example, in alloxan-induced diabetic rabbits treatment for 8 weeks reduced oxidative stress. Animals after 8 weeks treatment showed significant reduction in Cu,Zn-SOD (superoxide dismutase) activity in their kidneys and in LPO (lipid peroxidation) levels(Gumieniczek, 2003). Similarly, in a rat model of ischemia, there was reduced oxidative stress and inflammation following treatment (rats were administered with 1 mg/kg pioglitazone 30 min prior to ischemia) (Collino et al., 2006). Obese Sprague-Dawley rats (12 weeks on HFD) showed that treatment with pioglitazone increased nitrate/nitrite excretion and expression of renal endothelial and neuronal nitric oxide synthase. Overall, this study showed that pioglitazone prevented oxidative stress by reducing free-radical production and by increasing nitric oxide production (Dobrian, Schriver, Khraibi, & Prewitt, 2004). Importantly in patients with newly diagnosed type 2 diabetes (randomized clinical trial), oxidative stress and lipid metabolism was significantly improved following pioglitazone treatment. This was shown by assessing lipid peroxidation, and SOD levels in patients' blood (Mirmiranpour et al., 2013).

Another avenue for fatty liver and oxidative stress treatment that has been proposed in animal studies is ACE2 overexpression (Mak et al., 2015b). ACE2 is the first known human homologue of ACE (zinc-metalloproteinase type-1 transmembrane protein) and was first discovered in 2000 (Donoghue et al., 2000; Tipnis et al., 2000). ACE2 is implicated in the non-classic/alternative renin-angiotensin system (RAS) (Chappell, 2012; Lubel, Herath, Burrell, & Angus, 2008); where ACE2 generates Ang(1-7) from Ang II directly, or indirectly via cleavage of Ang I to Ang (1–9) that can be converted into heptapeptide Ang-(1-7) by ACE (Donoghue et al., 2000; Vickers et

al., 2002). RAS is separated into two arms: classic and non-classic or alternative pathways. Classic RAS can be determined as the ACE-Ang II AT1R axis that stimulates water intake, vasoconstriction, sodium preservation, increased fibrosis, oxidative stress (generation of ROS), inflammation and cellular growth. The alternative RAS (ACE2/Ang-(1-7)/Mas) reduces oxidative stress, inflammation and fibrosis and mediates diuresis, vasodilation and natriuresis (Chappell, 2012; Lubel et al., 2008).

A study in which overexpression of recombinant ACE2 liver specific adeno-associated viral genome 2 serotype 8 vector (rAAV2/8-ACE2) were performed in various mouse models of liver disease showed significant improvements in the level of fatty liver, liver injury and oxidative stress (via 4-HNE stain) (Mak et al., 2015a). When ACE2 was overexpressed in *db/db* mice, hepatic steatosis was improved and associated with upregulation of fatty acid oxidation-related gene expression (Cao et al., 2016). In the same study, *in vitro* studies with HepG2 cells exposed to free fatty acids saw a reduction in cellular fat accumulation, oxidative stress and inflammation after treatment with Ang-(1-7)/ACE2 (Cao et al., 2016). In addition, the ACE2(-/y) mice, a whole-body knockout of ACE2, developed liver steatosis accompanied with oxidative stress and inflammation. These mice also showed increased levels of hepatic lipogenic genes and decreased expression of fatty acid oxidation-related genes in the liver (Cao et al., 2016).

Based on what is known in the literature of how these drugs work, we wanted to utilize these therapies in our UBL5 KO mice to determine whether specifically targeting reductions in fatty liver and oxidative stress, could protect these mice from liver failure and whether there are direct actions on the UPRmt even in the absence of UBL5.

6.2 Hypothesis

Pioglitazone and ACE2 gene therapy treatment will minimize some or all defects (such as fatty liver) in UBL5 KO mice and will improve their metabolic status.

6.3 Chapter Aim

The overall aim of this chapter is to determine whether pre-treatment with either (A) Pioglitazone and/or (B) overexpression of ACE2 in our UBL5 KO mice can overcome the mitochondrial stress and protect the mice against liver failure.

6.4 Pioglitazone treatment

6.4.1 Methods:

Our rationale for this study was to pre-treat our mice for 4 weeks prior to tamoxifen treatment to determine whether we can prevent to the onset of liver failure as a result of the deletion of UBL5. Methods used in this chapter including Real time PCR, histology, tamoxifen treatment, plasma analysis are described in detail in Chapter 2**.**

6.4.1.1 Protocol of pioglitazone treatment:

Figure 6.1, illustrates the protocol used for the Pioglitazone treatment study. At six weeks of age and one week of acclimatisation, mice were separated into the following treatment groups; 1) controls treated with vehicle/ placebo, 2) UBL5 KO ($UBL5^{Liver-/-}$ / homozygous) treated with placebo and 3) UBL5 KO ($UBL5^{Liver-/-}$ /homozygous) treated with pioglitazone. Mice were gavaged with either placebo (Methylcellulose 1.5%) or 3 mg/kg pioglitazone in 1.5% methyl-cellulose per day for four weeks. After this period, we gavaged all our animals with tamoxifen to induce deletion of UBL5 (as in Chapter 2). At 10 days following tamoxifen treatment, mice were sacrificed for tissue collection for histological and gene expression analysis and blood collection for plasma analysis of liver function. We also measured body weight and liver weight.

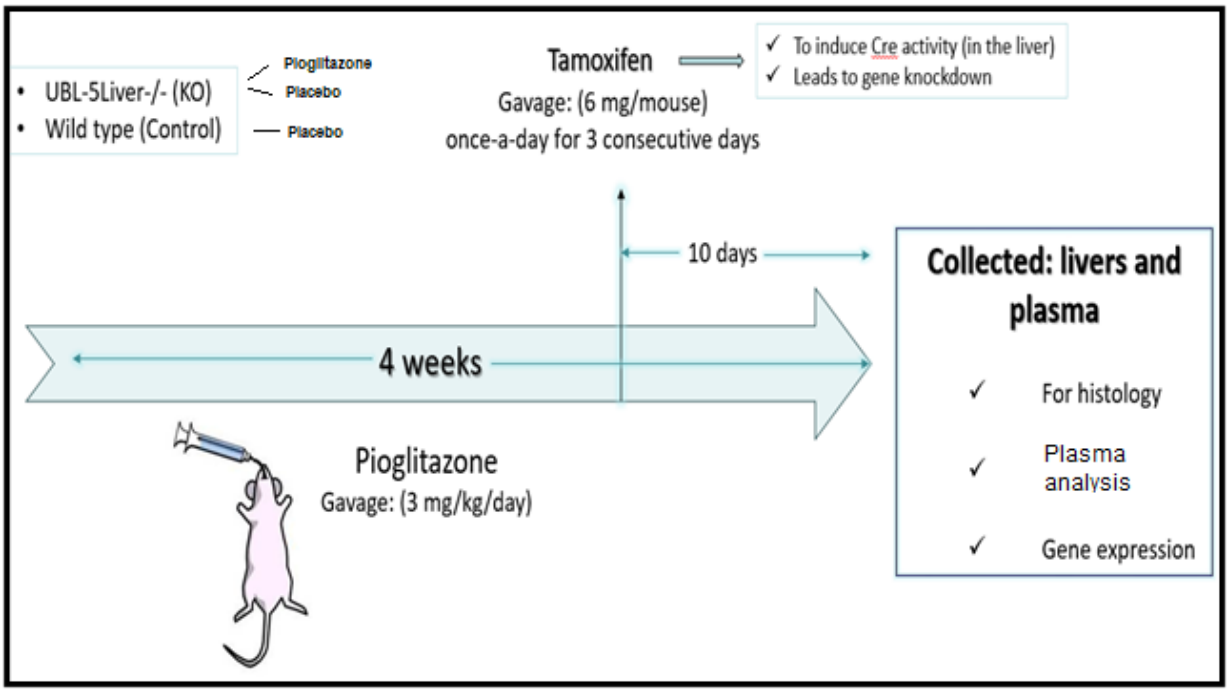

Figure 6.1: Schematic of protocol for the pioglitazone treatment.

6.4.2 Results

6.4.2.1 UBL5 and PPARγ gene expression in liver of treated mice

UBL-5 gene and *PPARγ* expression was assessed in the liver of all treated mice. Our results showed that both the pioglitazone and placebo treated UBL5 KO mice had significantly reduced *UBL5* gene expression levels (Figure 6.2) when compared to the placebo treated control mice.

The *PPARγ* gene expression levels were significantly elevated in the pioglitazone treated UBL5 KO group compared to groups treated with placebo (control and UBL5 KO mice) (Figure 6.3).

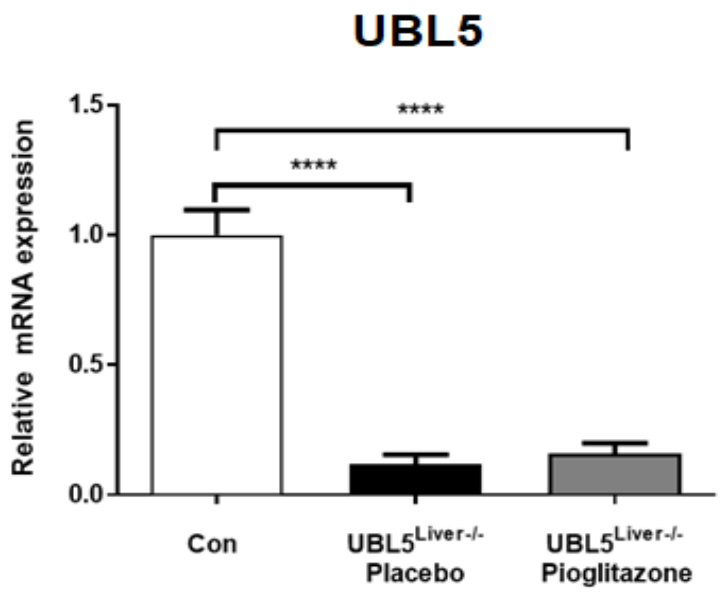

Figure 6.2: *UBL5* mRNA levels in the liver from UBL5 KO mice treated with placebo or pioglitazone: mRNA levels were expressed relative to the control sample, UBL5$^{Liver-/-}$ is the homozygous / KO mice. The ΔΔCt method was used to calculate relative quantification of gene expression with GAPDH rRNA as the housekeeper gene. Values presented as mean ± SEM. n=5-10. **** P<0.0001.

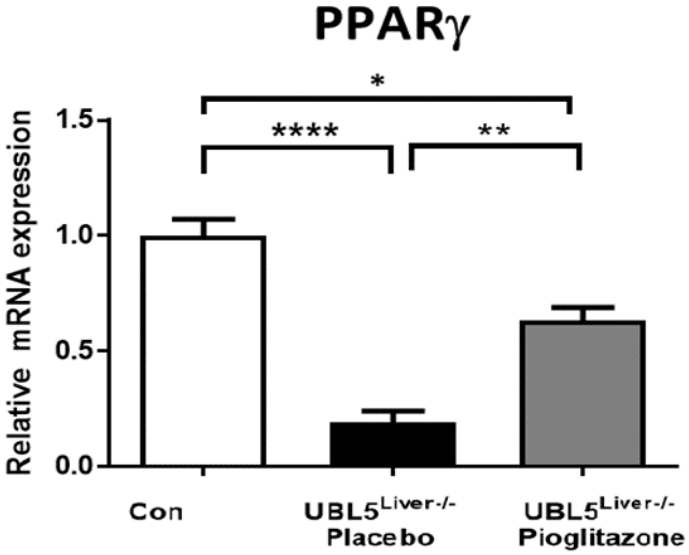

Figure 6.3: *PPARγ* mRNA levels in the liver from UBL5 KO mice and controls treated with placebo or pioglitazone: mRNA levels were expressed relative to the control sample, UBL5$^{Liver-/-}$ is the homozygous / KO mice. The ΔΔCt method was used to calculate relative quantification of gene expression with GAPDH rRNA as the housekeeper gene. Values presented as mean ± SEM. n=6-10. * P≤0.05, **p ≤ 0.01, **** P<0.0001.

6.4.2.2 Body weight and liver weight

Figure 6.4, demonstrates that body weights did not significantly change between the pioglitazone treated and placebo treated groups over the 4 weeks of treatment. Liver weights (Figure 6.5) were significantly lower in UBL5 KO mice treated with either placebo or pioglitazone. The images in Figure 6.6, show representative pictures of livers taken from: (figure 6.6, A) in the control mice treated with placebo visually the livers looked dark red, (figure 6.6, B) the UBL5 KO mice treated with placebo had pale pink/whitish looking livers and (figure 6.6, C) the UBL5 KO mice treated with pioglitazone had red livers, slightly patchy, paler than the livers of the control mice.

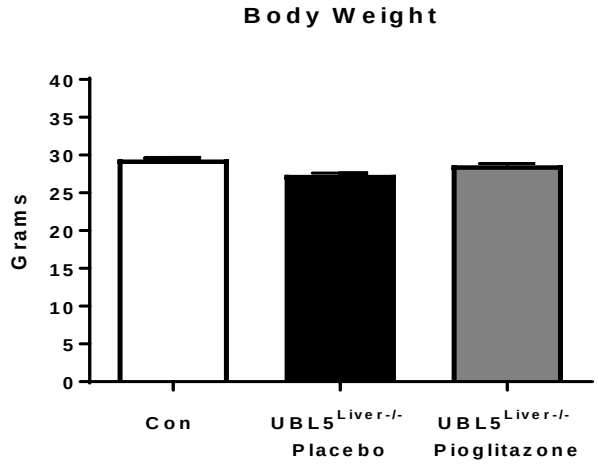

Figure 6.4: Final body weight of UBL5 KO mice and controls after four weeks on pioglitazone or placebo: Body weight of controls on placebo, UBL5 KO mice (UBL-5$^{Liver-/-}$) on placebo (Methylcellulose 1.5%) and UBL5 KO mice (UBL5$^{Liver-/-}$) on pioglitazone. N=6-10.

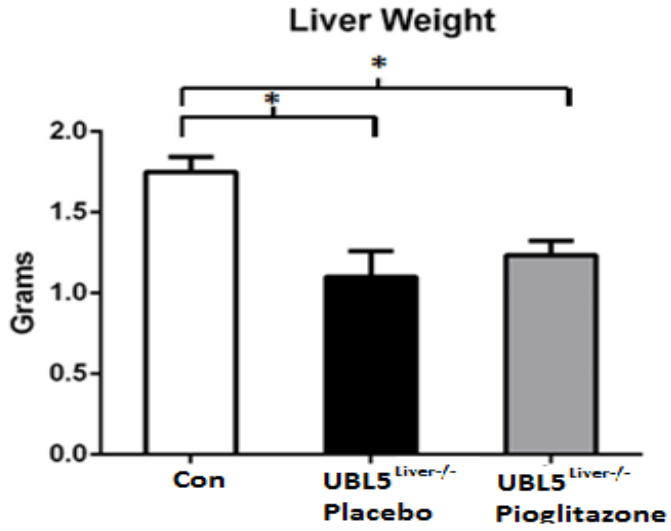

Figure 6.5: Liver weight of UBL5 KO mice and controls on placebo and pioglitazone and controls. Liver weights of UBL5 KO (UBL5$^{Liver-/-}$) mice and littermates were measured at the end of four weeks of treatment. N=5-10. *****P ≤0.05.

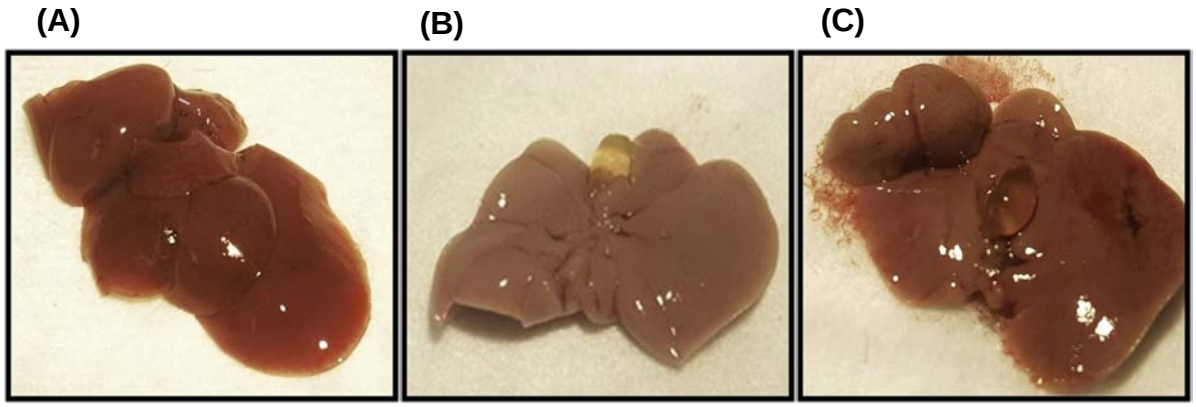

Figure 6.6: Liver appearance after culls from controls and UBL5 KO mice treated either with placebo or pioglitazone: (A) Control mice treated with placebo, **(B)** UBL5 KO (UBL5$^{Liver-/-}$) mice treated with placebo, **(C) UBL5 KO (**UBL5$^{Liver-/-}$) mice treated with pioglitazone. (Placebo = methylcellulose 1.5%).

6.4.2.3 Liver histology

Figure 6.7 illustrates the H&E staining of liver sections collected from the three treatment groups. As can be seen, there was an equal distribution of cellular degradation between the placebo and pioglitazone treated UBL5 KO mice (Figure 6.7 panels B and C), while the control mice had normal histology (Figure 6.7, A). The grading of slides (necrosis) is presented in (Figure 6.7, D) where the grade ranged between 0 to 5 (from healthy liver to severely degraded). Control mice had grade 0-1 which is considered as normal histology, the placebo treated UBL5 KO mice were graded as 5 which is undifferentiated and the pioglitazone treated UBL5 KO mice were graded as 3 to 4 that is moderately/poorly differentiated.

Oil RedO staining is presented in (Figure 6.8). The controls showed no fat accumulation (Figure 6.8, A). The representative pictures of placebo treated UBL5 KO and pioglitazone treated KO mice are shown in (Figure 6.8, panel B and C). There was a significant reduction in macro vesicular fat accumulation (percentage) in the pioglitazone treated UBL5 KO mice compared to the placebo treated UBL5 KO group (Figure 6.8, D). The percentage of micro vesicular fat was equally presented in both groups (Figure 6.8, E).

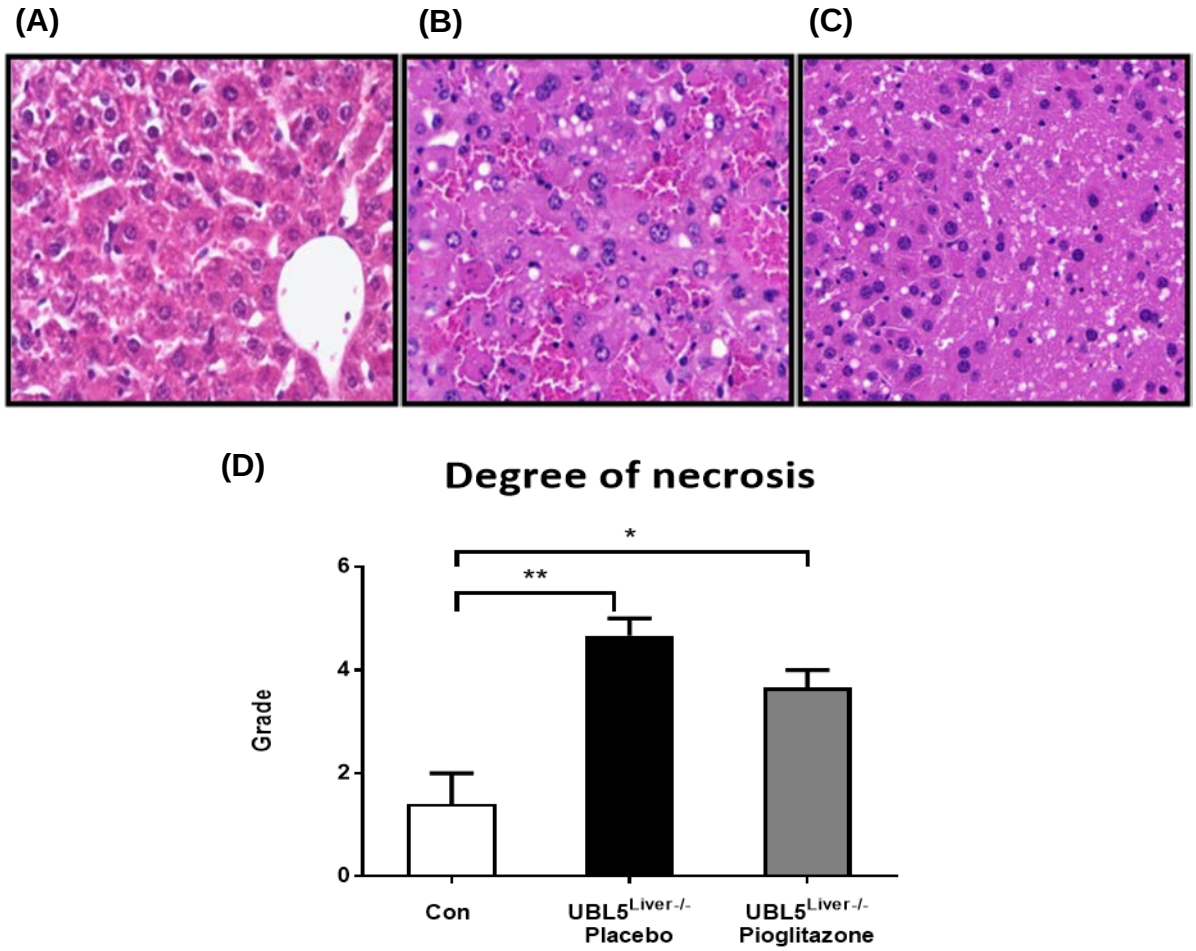

Figure 6.7: Hematoxylin and eosin (H&E) stain on livers samples from UBL5 KO and control mice 4 weeks on placebo or pioglitazone: Hematoxylin and eosin stain was done on fixed (in 10% formaldehyde) liver tissues from **(A)** Control mice treated with placebo, **(B) UBL5 KO** ($UBL5^{Liver-/-}$) mice treated with placebo, **(C) UBL5 KO (**$UBL5^{Liver-/-}$) treated with pioglitazone. **(D)** A graph that represents histological grade in between of groups compare to the control mice. N=5-*=P ** P ≤ 0.01. (Placebo = methylcellulose 1.5%).

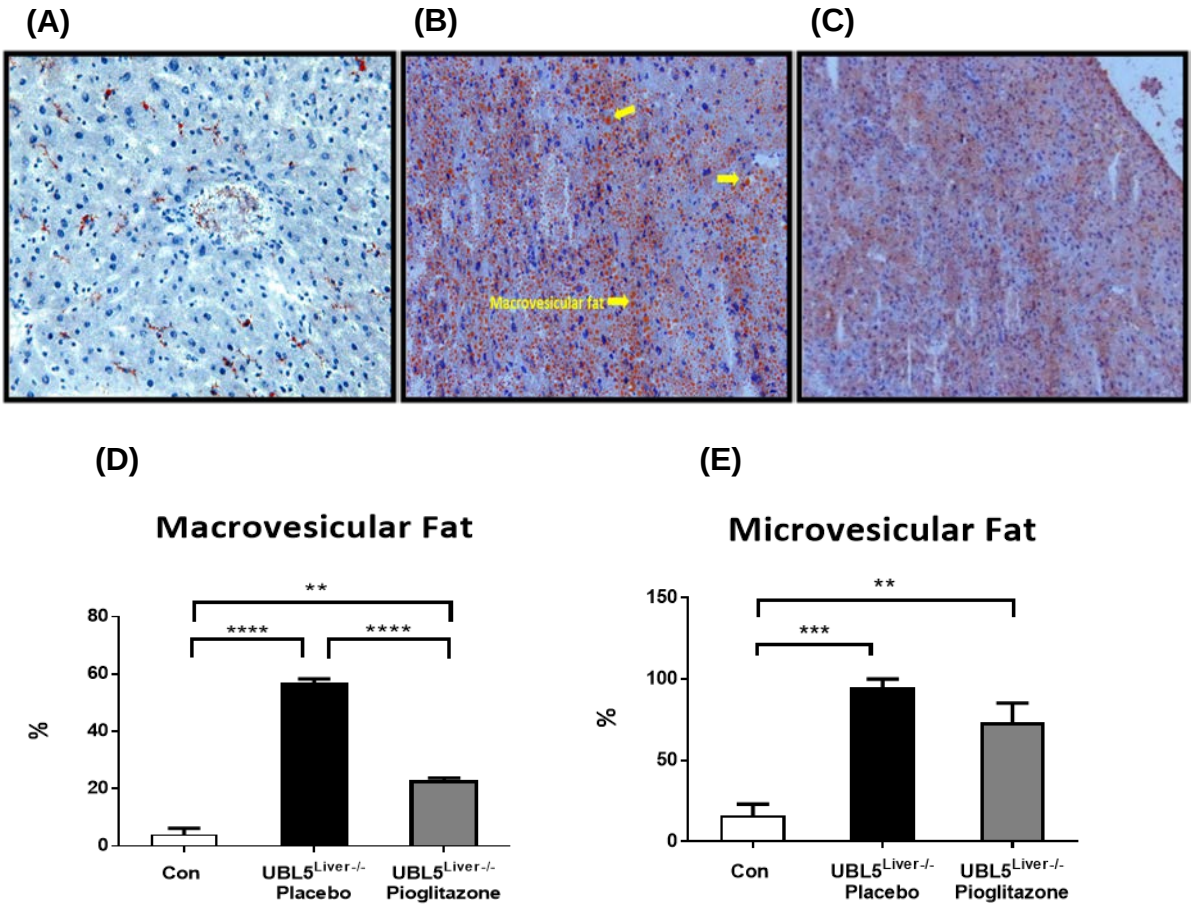

Figure 6.8: Oil RedO staining of fresh liver tissue from control mice and UBL5 KO treated either with placebo or pioglitazone. (A) Control mice treated with placebo, **(B)** UBL5 KO (UBL5$^{Liver-/-}$) mice treated with placebo, **(C)** UBL5 KO (UBL5$^{Liver-/-}$) treated with pioglitazone. **(D)** A graph that represents the percentage of macro vesicular fat in between of groups compare to the control mice. **(E)** A graph that represents the percentage of micro vesicular fat accumulation N=5. ** P ≤ 0.01, *** P ≤ 0.001, **** P<0.0001. (Placebo = methylcellulose 1.5%).

6.4.2.4 Liver enzyme levels (liver function test)

Specific liver enzymes to assess liver function were measured in plasma that was collected from all treatment groups. Bilirubin was shown to be significantly elevated in placebo treated UBL5 KO mice compared to controls, while the UBL5 KO mice treated with pioglitazone had lower levels of this enzyme compare to placebo-treated KO mice (Figure 6.9, A).

The ALT levels were increased in UBL5 KO treated with placebo compared to control mice. The pioglitazone-treated UBL5 KO mice displayed lower ALT levels compared to placebo treated KO mice (Figure 6.9, B).

AST was significantly elevated in UBL5 KO placebo-treated mice compared to controls. While the pioglitazone treated UBL5 KO mice showed reduced levels compare to placebo treated KO mice (Figure 6.9, C).

AP enzyme levels were significantly elevated in placebo treated KO mice compared to placebo treated control mice. While the pioglitazone treated UBL5 KO mice showed significantly lower enzyme levels compared to the placebo group (Figure 6.9, D).

All enzymes when compared to control mice were significantly elevated.

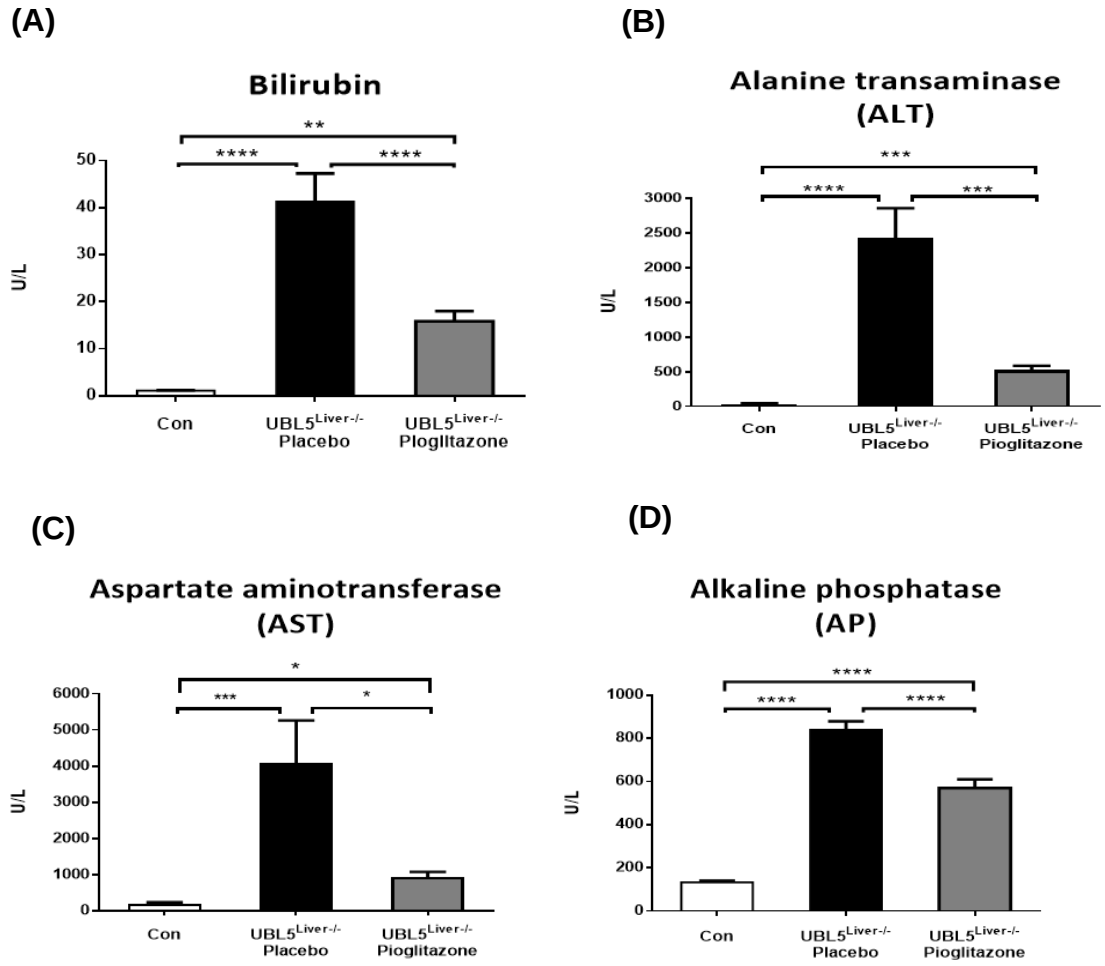

Figure 6.9: Liver plasma enzymes and bilirubin (Bili) levels from UBL5 KO and control mice: Liver function test, **(A)** Bilirubin, **(B)** alanine transaminase, **(C)** aspartate aminotransferase **(D)** alkaline phosphatase levels were assessed in UBL5 KO (UBL5$^{Liver-/-}$) and control mice treated with either placebo or pioglitazone for four weeks. N=5-10. * P≤0.05, **p ≤ 0.01, *** P ≤ 0.001, **** P<0.0001.

6.4.2.5 Lipid profile

To assess the lipid profile of our animals, we measured cholesterol, triglycerides and ketones (BHB) in plasma from non-fasted mice (Figure 6.10).

Cholesterol levels were significantly elevated in placebo treated KO mice compared to placebo treated control mice. Pioglitazone treated KO mice showed reduced levels of cholesterol compared to the placebo group, although it was elevated compared to the controls (Figure 6.10, A).

Triglyceride levels were reduced in both placebo and pioglitazone treated groups compared to placebo treated control mice (Figure 6.10, B).

BHB (ketones) levels were significantly elevated in placebo treated KO mice compare to both placebo treated controls and pioglitazone treated UBL5 KO mice (Figure 6.10, C).

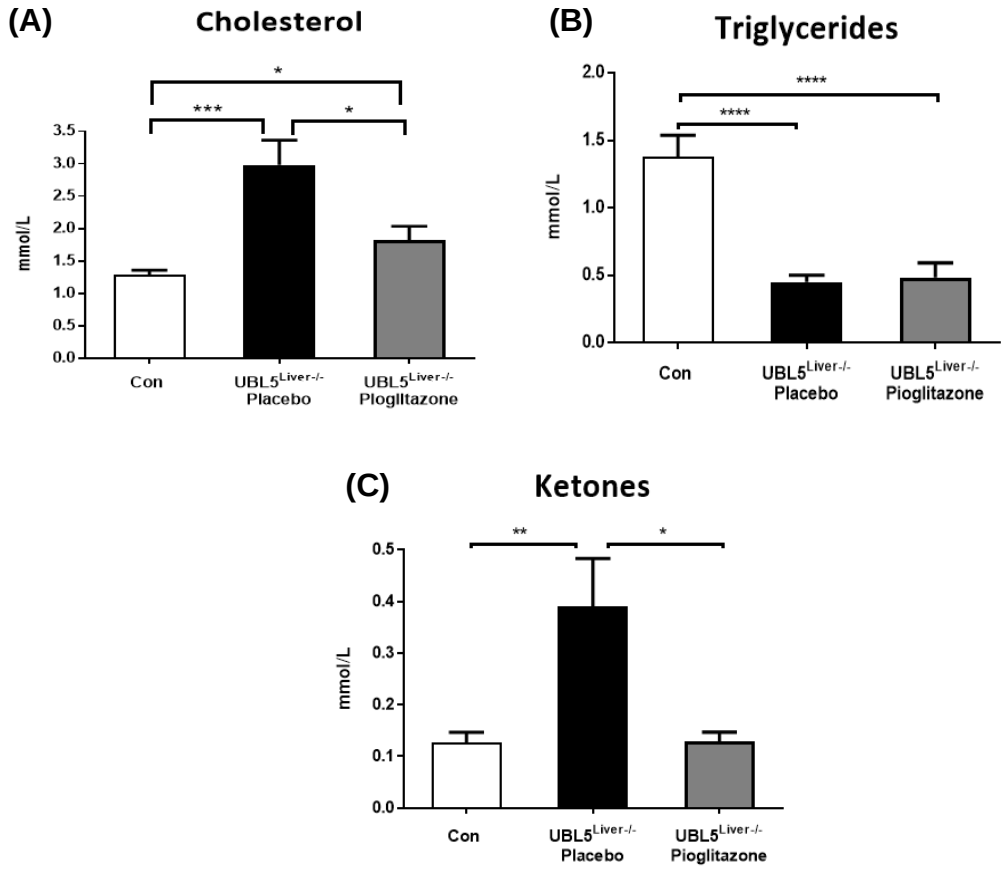

Figure 6.10: Cholesterol, triglycerides and ketone (BHB) levels from plasma of UBL5 KO and control mice treated with vehicle or ACE2: (A) Cholesterol, **(B)** triglycerides and **(C)** ketone (BHB) levels were assessed in UBL5 KO ($UBL5^{Liver-/-}$) and control mice. N=5-10. * P≤0.05, ** P ≤ 0.01, *** P ≤ 0.001, **** P ≤ 0.0001.

6.4.2.6 Expression of UPRmt genes

Figure 6.11 shows the mRNA expression of the key genes involved in the UPRmt. Expression levels of the transcription factor *CHOP* were significantly elevated in pioglitazone treated UBL5 KO mice compared to placebo treated KO mice. There was a trend for an increase compared to placebo treated control mice, however this

did not reach statistical significance. The placebo treated UBL5 KO mice had lover gene expression levels than the placebo treated control mice (Figure 6.11, A).

Pioglitazone treatment of the UBL5 KO mice significantly elevated the *ATF-5* expression levels compared to the placebo treated KO mice with *ATF-5* levels further increased compared to the placebo treated control mice (Figure 6.11, B). When compared to the placebo treated control mice, expression of *ATF-5* was again significantly reduced (as expected and as shown in Chapter 4).

The heat shock protein *HSP70mt* was elevated in placebo treated UBL5 KO mice compared to the placebo treated control and pioglitazone treated KO mice (Figure 6.11, C). The *HSP60* heat shock protein has not been shown in the figure because the expression level was undetectable in both the pioglitazone and placebo treated KO mice.

The proteases *Lonp-1*, *ClpX* and *ClpP* were significantly elevated in the pioglitazone treated KO mice compared to the placebo treated KO mice (panels D-F), with only ClpP significantly increased compared to the placebo-treated control group (panel F).

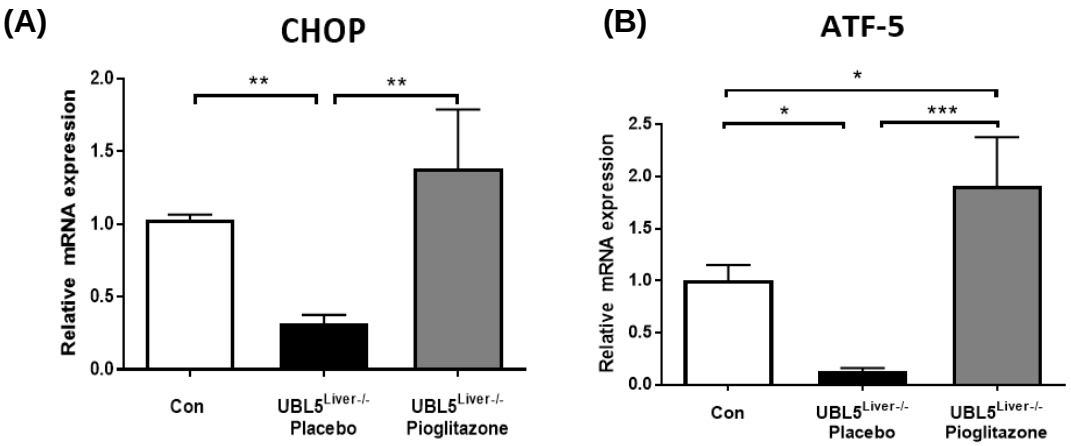

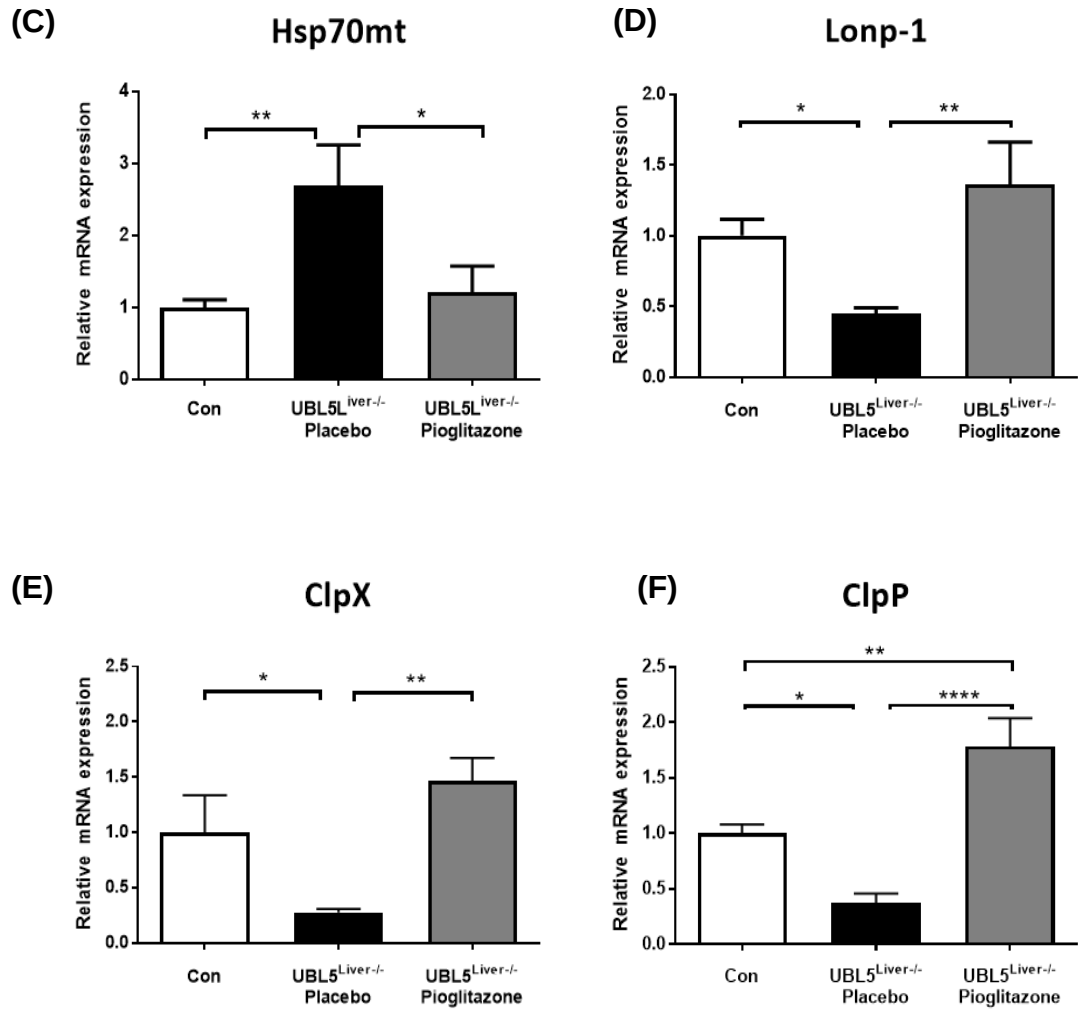

Figure 6.11: mRNA levels of UPRmt genes in the liver from UBL5 KO and control mice four weeks on placebo or pioglitazone: mRNA levels of **(A)** transcription factor *CHOP*, **(B)** *ATF-5,* **(C)** heat shock protein *Hsp70mt* and **(D)** proteases *lonp-1*, **(E)** *ClpX* and **(F)** *ClpP* were expressed relative to the control and UBL5 KO (UBL5$^{Liver-/-}$) mice. The ΔΔCt method was used to calculate relative quantification of gene expression with GAPDH RNA as the housekeeper gene. Values presented as mean ± SEM. n=5-10. *P ≤0.05, **P ≤0.01, ***P ≤0.001, ****p< 0.0001.

6.5 *ACE2* overexpression

6.5.1 Methods:

For the overexpression of *ACE2* gene we obtained the virus recombinant adeno-associated viral vector serotype 2/8 with *ACE2* (rAAV2/8-ACE2) and the vehicle vector (rAAV2/8+ Human serum albumin (HAS)) from our collaborator Dr Chandana Herath (Mak et al., 2015a). The ACE2 adenovirus was under the transcriptional control of a liver-specific promoter, a polyprotein E/human α1-antitrypsin, as previously described (Cunningham, Dane, Spinoulas, & Alexander, 2008). AAV serotype 8 (AAV8) is a part of the AAV family isolated from non-human primate. It was shown to only provoke negligible immune response and has high transduction efficiency in the liver (Y. Lu & Song, 2009) (Dane, Wowro, Cunningham, & Alexander, 2013), so this makes it preferable for hepatic gene transfer application. One dose of rAAV2/8-*ACE2* vector can achieve overexpression of ACE2 in the liver.

Figure 6.12 illustrates the protocol used for this second treatment study. As with the Pioglitazone study, adult mice were acclimatised in our facility for 1 week after-which mice were randomly separated into the following treatment groups: 1) controls treated with vehicle, 2) UBL5 KO ($UBL5^{Liver-/-}$) treated with vehicle and 3) UBL5 KO treated with ACE2 virus. Mice were intraperitoneally injected with a single dose of either vehicle or 100 µl of the ACE2 virus (which represents 1011 genomic copies of ACE2) and left for a week (incubation period) prior to tamoxifen treatment. Mice were then left for 10 days, with an OGTT performed on the 9^{th} day. On the 10^{th} day mice were culled for blood and tissue collection.

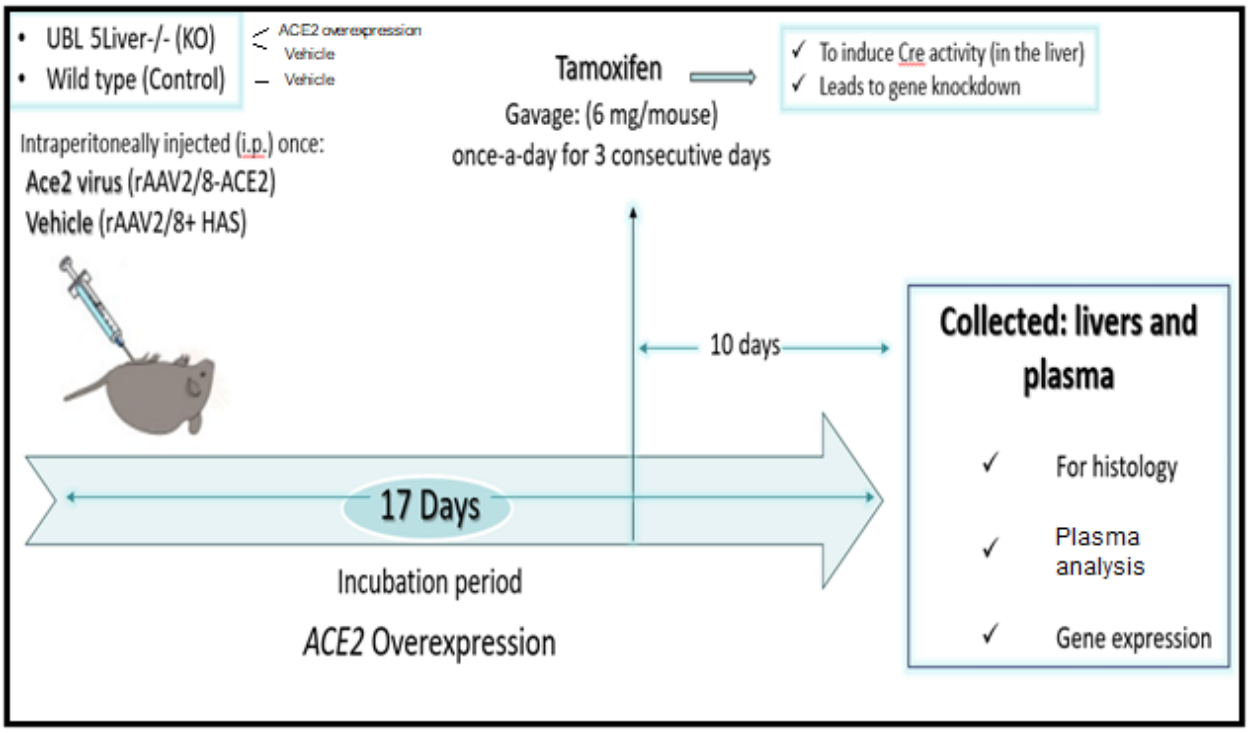

Figure 6.12: Schematic of the ACE2 overexpression treatment protocol.

6.5.2 Results:

6.5.2.1 *UBL5* and *ACE2* expression in liver

To confirm the UBL5 knockdown and the ACE2 overexpression in the KO mice, we assessed the *UBL5* and *ACE2* gene expression levels in the liver. Both the vehicle and ACE2 treated UBL5 KO mice showed significantly reduced *UBL5* mRNA levels compared to controls treated with Vehicle (Figure 6.13, A).

The ACE2 treated UBL5 KO mice displayed significantly increased levels of *ACE2,* while the KO mice on vehicle showed decreased levels of *ACE2* compare to the vehicle treated control mice (Figure 6.13, B).

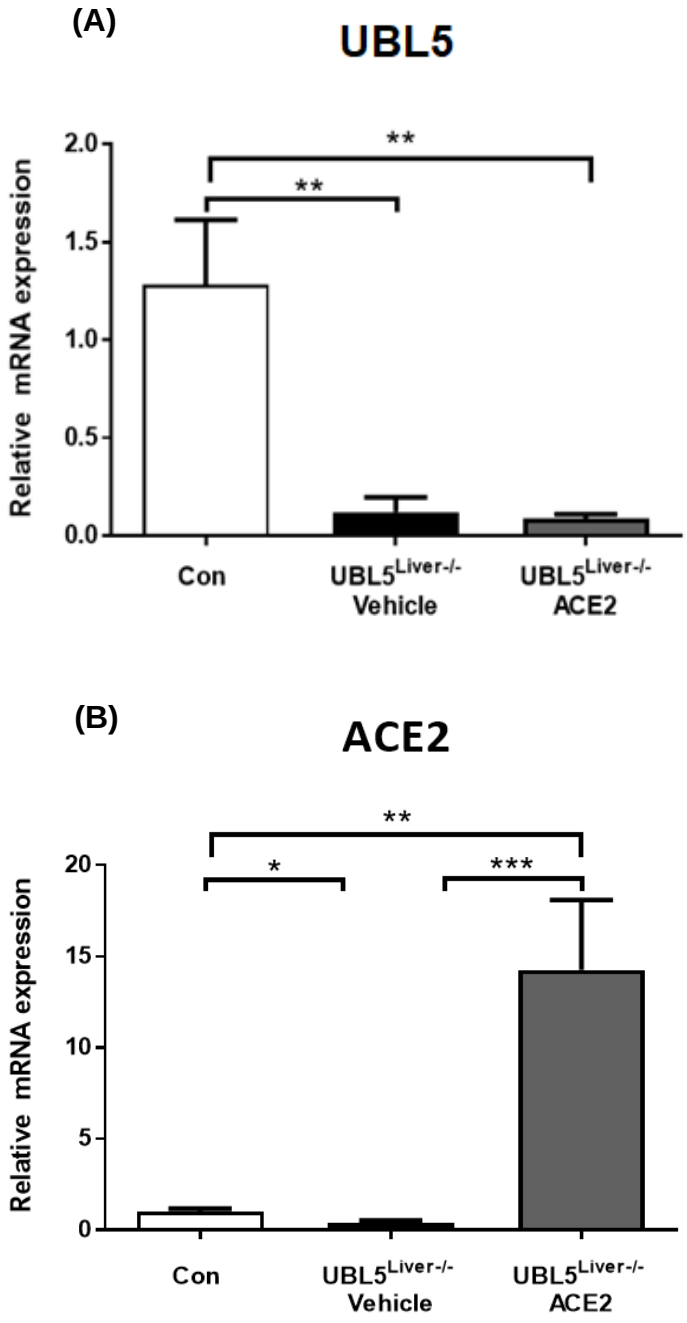

Figure 6.13: *UBL5* and *ACE2* mRNA levels in the liver from UBL5 KO mice treated with vector vehicle or vector with *ACE2* gene: mRNA levels were expressed relative to the control sample, UBL5 KO ($UBL5^{Liver-/-}$) is the homozygous mice. **(A)** *UBL5* gene expression, **(B)** *ACE2* gene expression. The ΔΔCt method was used to calculate relative quantification of gene expression with GAPDH rRNA as the housekeeper gene. Values presented as mean ± SEM. n=4-5. * P≤0.05, **p ≤ 0.01, *** P ≤ 0.001.

6.5.2.2 Body weight and liver weight

As illustrated in (Figure 6.14) the body weight was not different between groups at the end of the treatment. The liver weight was significantly lower in UBL5 KO mice treated with vehicle compared to the vehicle treated control mice. The *ACE2* treated UBL5 KO mice showed normal liver weight compared to the control mice (Figure 6.15). In (Figure 6.16), representative images of livers taken from controls treated with vehicle (Figure 6.16, A) were dark-red in colour indicating normal livers. UBL5 KO mice treated with vehicle (Figure 6.16, B), presented with pale whitish livers whilst those from the UBL5 KO ACE2 treated mice (Figure 6.16, C) had similar red colouration to the control mice.

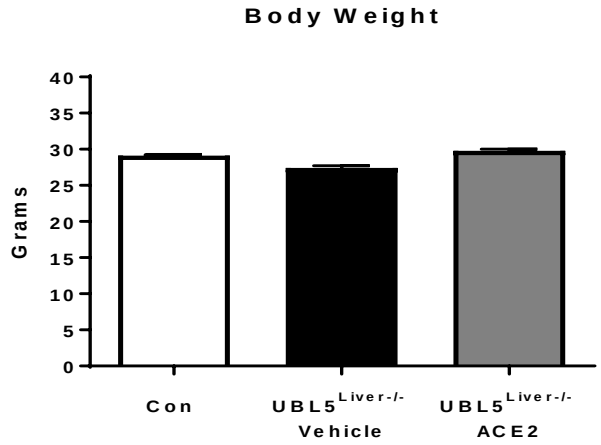

Figure 6.14: Final body weight of control and UBL5 KO mice treated with vehicle or ACE2: Body weight of control mice on vehicle, UBL5 KO ($UBL5^{Liver-/-}$) homozygous mice on vehicle and UBL5 KO ($UBL5^{Liver-/-}$) homozygous mice on *ACE2* treatment. N=4-5.

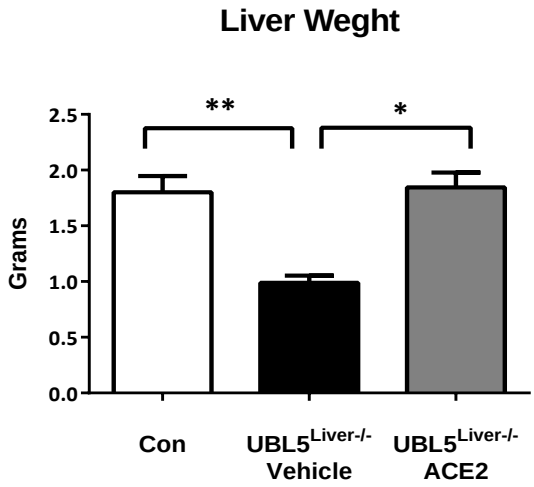

Figure 6.15: Liver weight of control and UBL5 KO mice treated with vehicle or *ACE2*. Liver weights of UBL5 KO (UBL5$^{Liver-/-}$) homozygous mice and littermates were measured at the end of treatment. N=4.5. *P ≤0.05, **P ≤0.01.

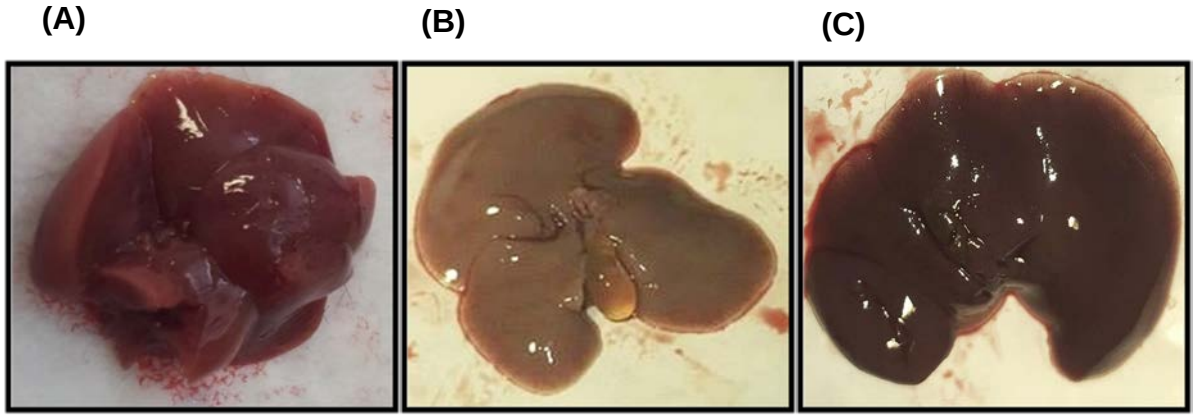

Figure 6.16: Liver appearance after culls from control and UBL5 KO mice treated either with vehicle vector or *ACE2*: (A) Control mice treated with vehicle, **(B)** UBL5 KO (UBL5$^{Liver-/-}$) homozygous mice with vehicle, **(C) UBL5 KO (**UBL5$^{Liver-/-}$) homozygous mice treated with *ACE2*.

6.5.2.3 Liver histology

The H&E stain is shown in (Figure 6.17). As can be seen, there are increased levels of cellular degradation in vehicle treated UBL5 KO mice (Figure 6.17, B), while the *ACE2* treated mice (Figure 6.17, C) and controls (Figure 6.17, A) had normal-looking liver histology. The controls ranged between grade (necrosis) 0 and 1 (normal histology where grade cannot be assessed/well differentiated), the *ACE2* treated UBL5 KO mice had grade between 0 to 3 (well differentiated/ moderately

differentiated) and the UBL5 KO mice with vehicle were graded between 4 to 5 (undifferentiated) (Figure 6.17, D).

The representative pictures for control, vehicle treated UBL5 KO and ACE2 treated KO mice are illustrated in (Figure 6.18, A, B, C). The Oil RedO stain showed that the control mice treated with vehicle did not display fat deposition while there was significantly reduced (percentage) macro vesicular and micro vesicular steatosis in *ACE2* treated UBL5 KO mice compared to the UBL5 KO vehicle group (Figure 6.18, D, E). The micro vesicular fat was increased in UBL5 KO mice treated with ACE2 compared to control mice (Figure 6.18, E).

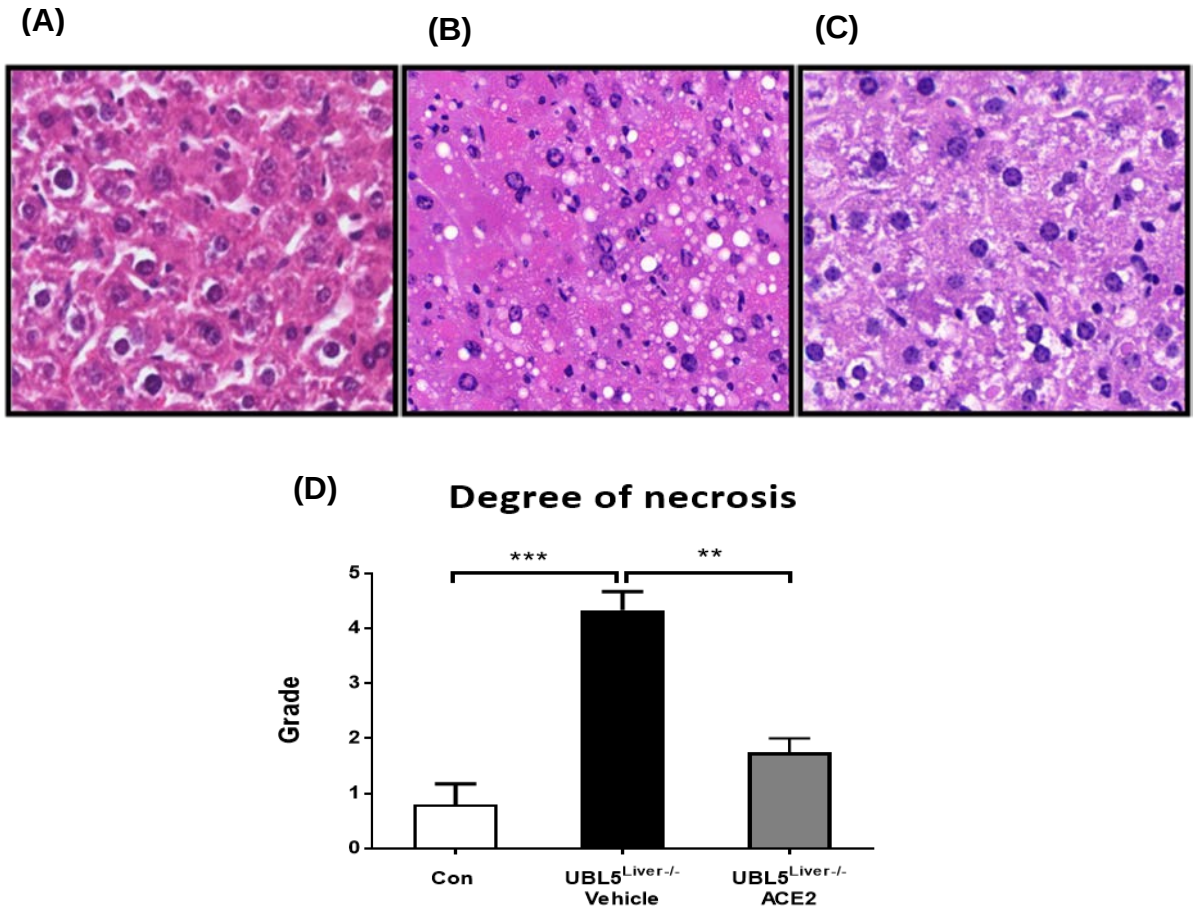

Figure 6.17: Hematoxylin and eosin (H&E) staining of livers samples from UBL5 KO and control mice treated with vector vehicle or vehicle with *ACE2*: Hematoxylin and eosin stain was done on fixed (in 10% formaldehyde) liver tissues from **(A)** Control mice treated with vehicle, **(B)** UBL5 KO ($UBL5^{Liver-/-}$) homozygous mice treated with vehicle, **(C) UBL5 KO (**$UBL5^{Liver-/-}$) homozygous mice treated with *ACE2*. **(D)** A graph that represents histological grade in between of groups compare to the control mice. N=4. ** P ≤ 0.01, ***P ≤0.001.

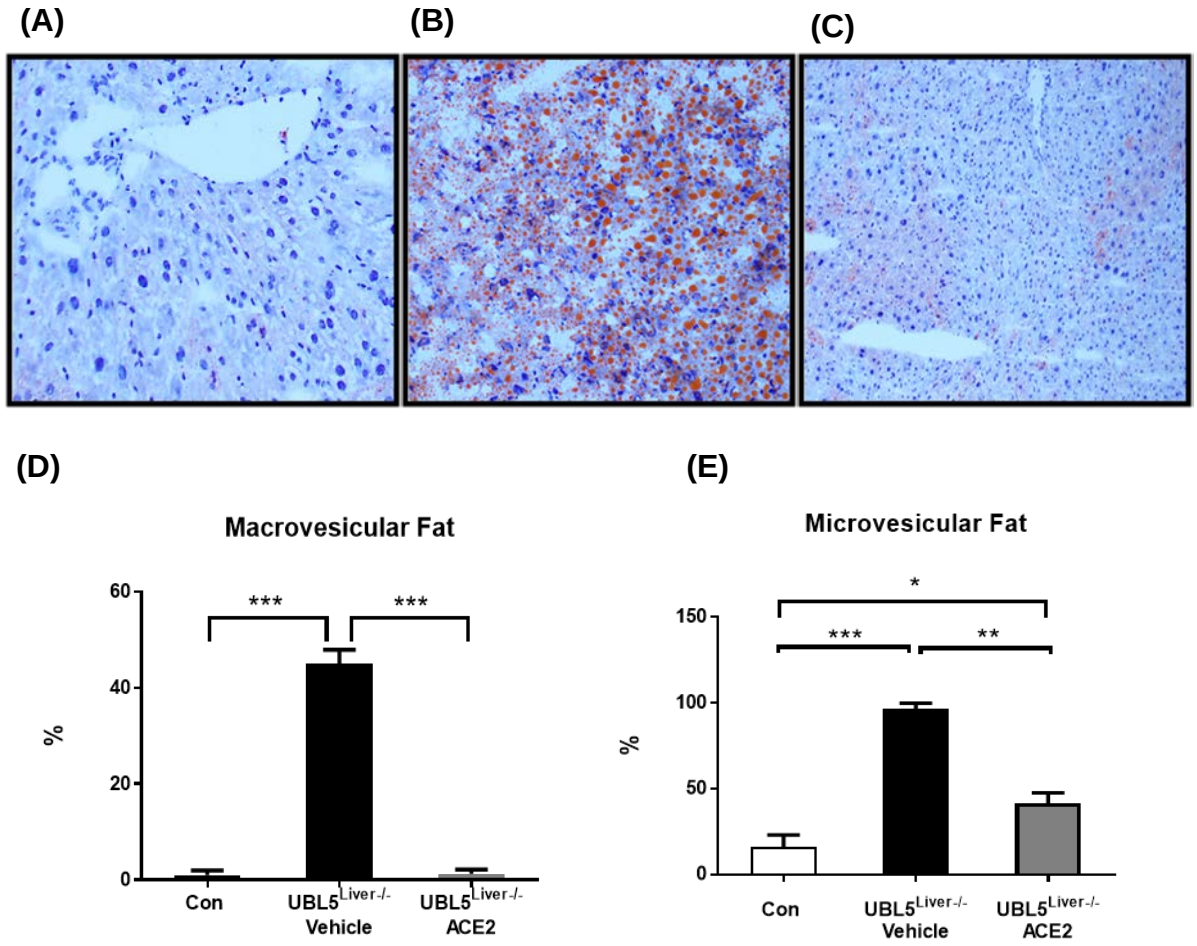

Figure 6.18: Oil RedO staining of livers samples from UBL5 KO and control mice treated with vector vehicle or vehicle with *ACE2*: Oil RedO stain was done on fresh liver tissues from **(A)** Control mice treated with vehicle, **(B) UBL5 KO** ($UBL5^{Liver-/-}$) homozygous mice treated with vehicle, **(C) UBL5 KO (**$UBL5^{Liver-/-}$) homozygous mice treated with *ACE2.* **(D)** A graph that shows percentage of macro vesicular steatosis in between of groups compare to the control mice, **(E)** a percentage of micro vesicular fat between of groups. N=4. *P ≤0.05, **P ≤0.01, ***P ≤0.001.

6.5.2.4 Liver enzyme levels (liver function test)

The UBL5 KO vehicle treated mice had significantly elevated levels of bilirubin compared to ACE2 treated KO and control mice (Figure 6.19, A). Similarly, ALT (Figure 6.19, B), AST (Figure 6.19, C) and AP (Figure 6.19, D) levels were elevated in vehicle treated UBL5 KO mice compared to control mice on vehicle and ACE2 treated UBL5 KO mice.

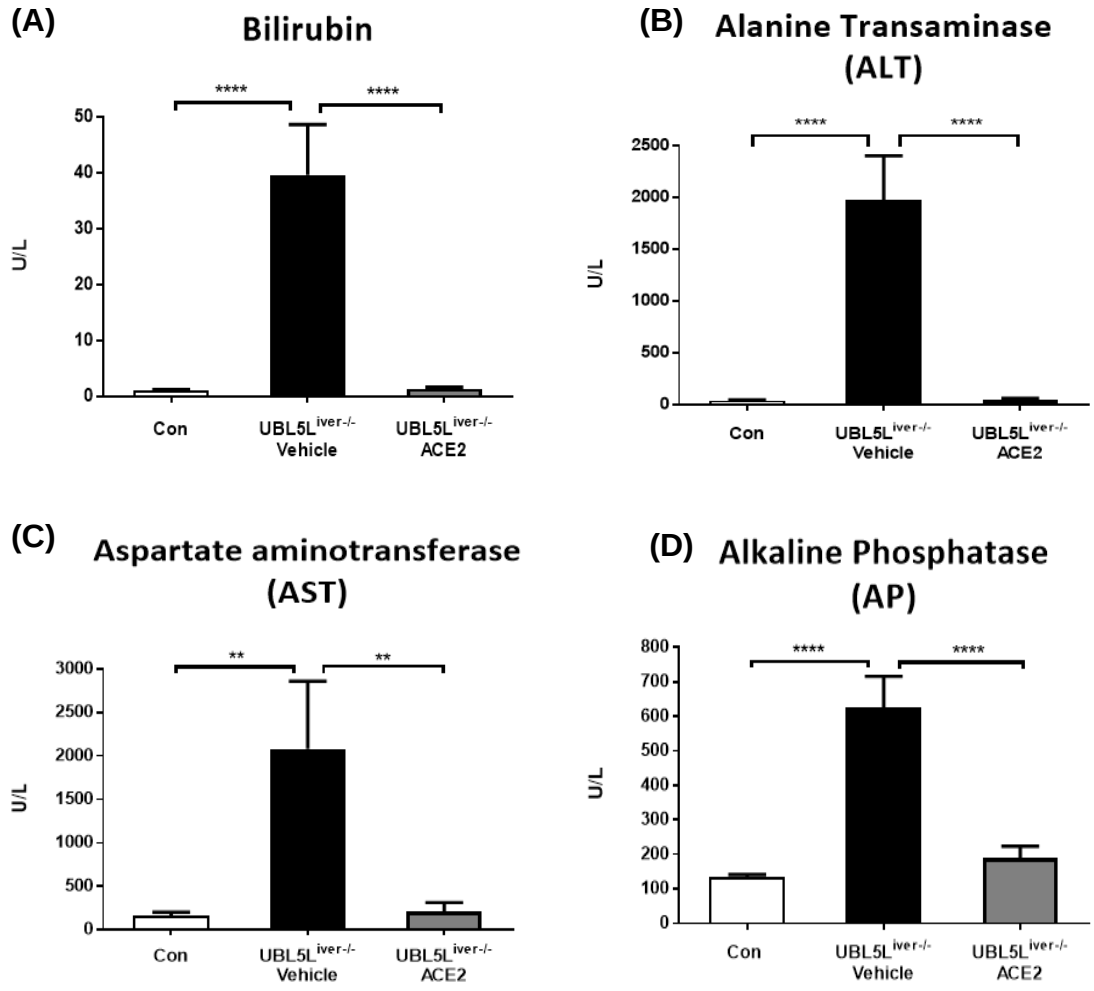

Figure 6.19: Liver plasma enzymes and bilirubin (Bili) levels from UBL5 KO and control mice: Liver function test, **(A)** Bilirubin, **(B)** alanine transaminase, **(C)** aspartate aminotransferase **(D)** alkaline phosphatase levels were assessed in ($UBL5^{Liver-/-}$) homozygous and control mice treated with either vehicle or ACE2. N=4-5. *P ≤0.05, **P ≤0.01, ***P ≤0.001, ****p< 0.0001.

6.5.2.5 Lipid profile

We assessed the lipid profile (cholesterol, triglycerides and beta-hydroxybutyrate / ketones) in the plasma from UBL5 KO that were either treated with vehicle or *ACE2* and control mice (Figure 6.20, A, B, C).

The cholesterol levels were elevated in the vehicle treated UBL5 KO mice compared to ACE2 treated KO and control mice (Figure 6.20, A).

Triglyceride levels were reduced in the vehicle treated UBL5 KO mice compared to control mice whilst the UBL5 KO mice treated with *ACE2* showed a trend towards reduced triglycerides compared to control mice but this was not statistically significant (Figure 6.20, B).

The beta-hydroxybutyrate/ketone levels were significantly elevated in UBL5 KO mice treated with vehicle compared to both control and the *ACE2* treated UBL5 KO mice (Figure 6.20, C).

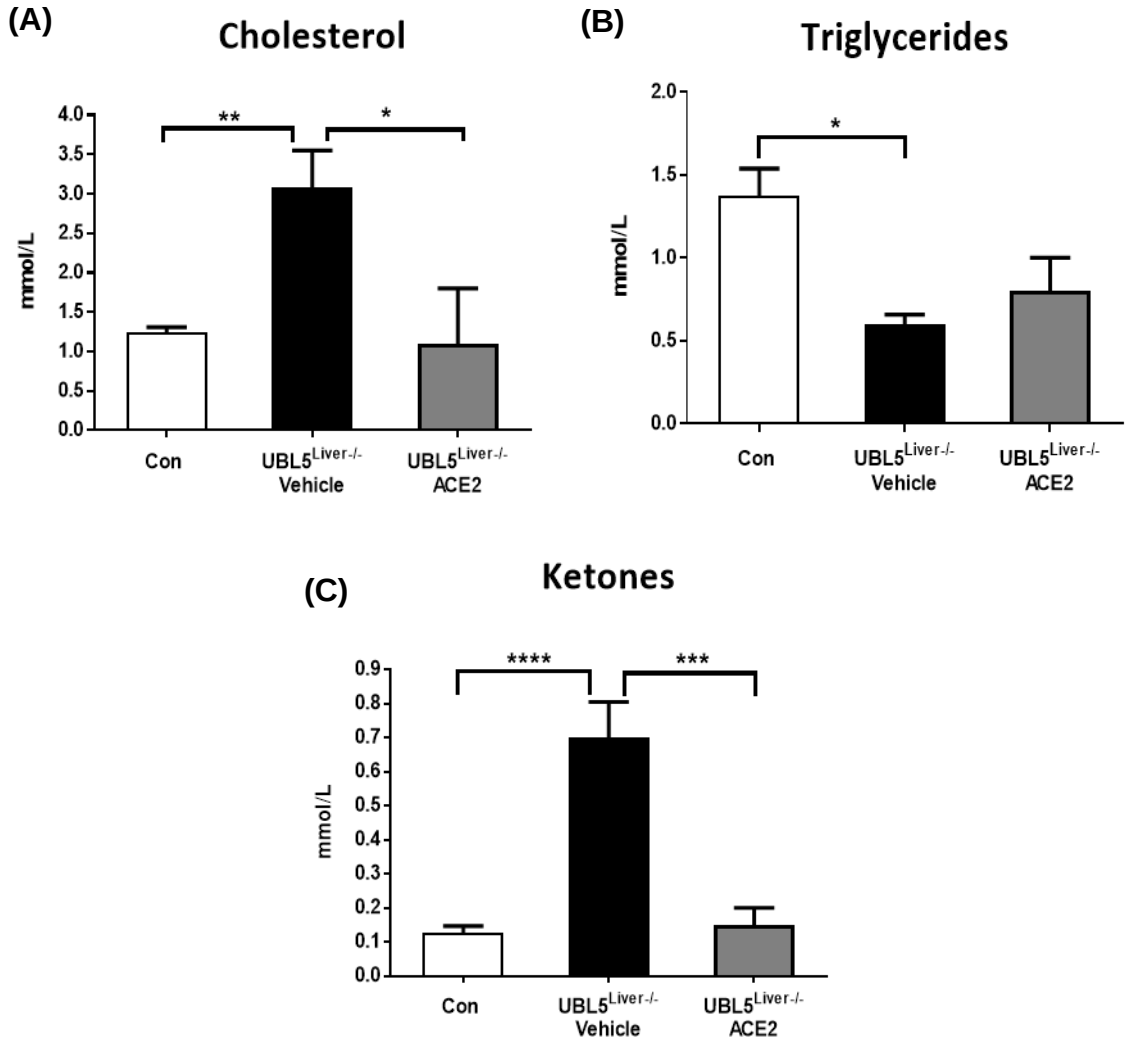

Figure 6.20: Cholesterol, triglyceride and ketone (BHB) levels from plasma of UBL5 KO and control mice treated with either vehicle or *ACE2*. (A) Cholesterol, **(B)** triglycerides and **(C)** ketone (BHB) levels were assessed in UBL5 KO (UBL5$^{Liver-/-}$) homozygous and control mice. N=4-5. *P ≤0.05, **P ≤0.01, ***P ≤0.001, ****p< 0.0001.

6.5.2.6 Expression of UPRmt genes

The expression levels of the transcription factors *CHOP* and *ATF-5* were normalised in *ACE2* treated UBL5 KO mice compared to the KO mice treated with vehicle, which when compared to the control mice, had significantly reduced levels of *ATF5* and *CHOP* (Figure 6.21, A, B).

The gene expression of heat shock protein *HSP70mt* was increased in the UBL5 KO mice treated with vehicle compared to both the control mice and the *ACE2* treated KO mice (Figure 6.21, C). *HSP60* was significantly reduced in both *ACE2* and vehicle treated KO mice compared to the controls (Figure 6.21, D).

The expression level of proteases *ClpX*, *ClpP and Lonp-1* were significantly reduced in UBL5 KO mice treated with vehicle compared to the controls. The *ACE2* treated KO mice had normalized levels of *lonp-1*, though the *ClpX* and *ClpP* remained reduced (Figure 6.21, E, F, G).

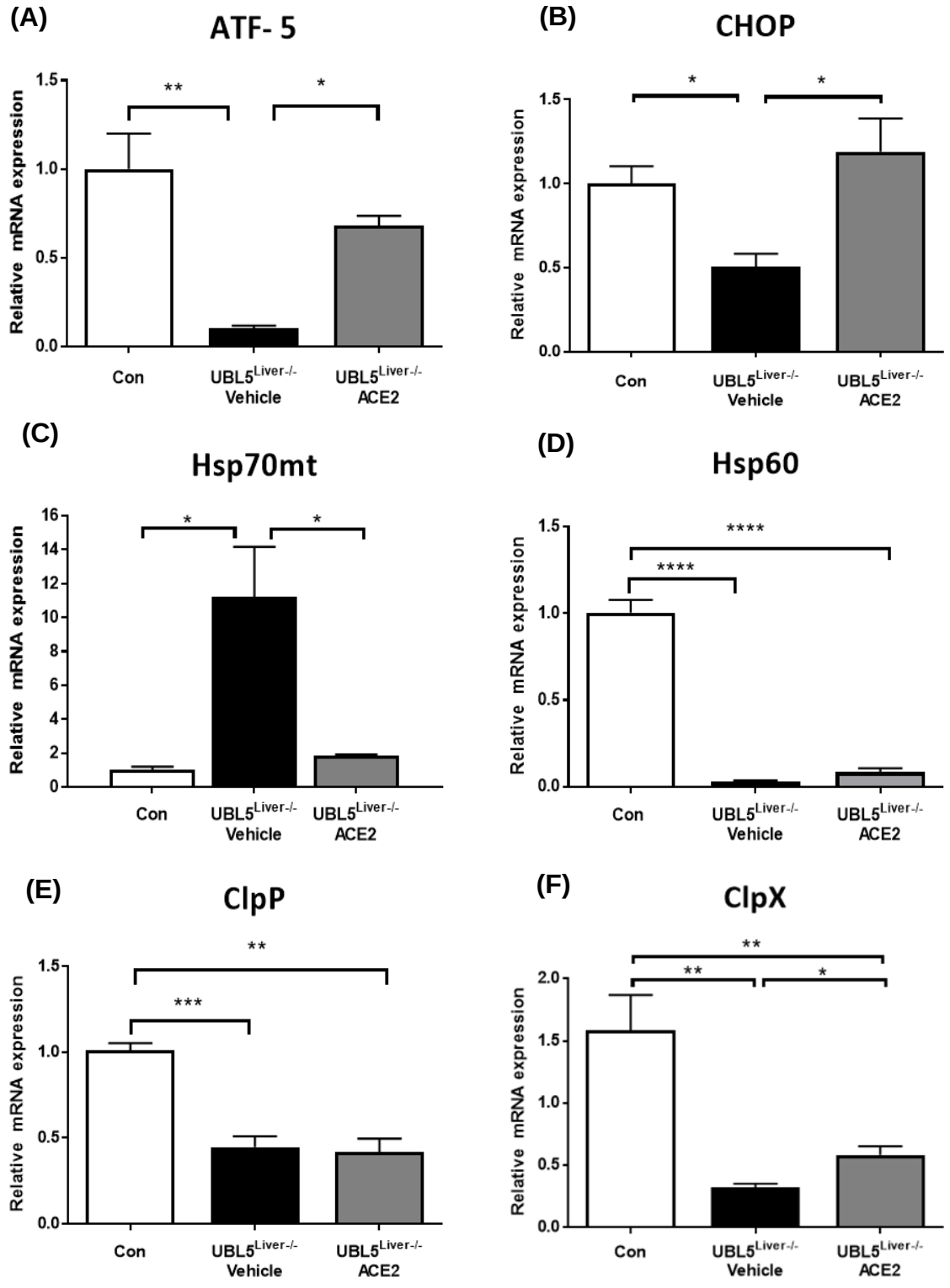
(A)
ATF- 5
Relative mRNA expression
1.5
1.0
0.5
0.0
**
*
Con
UBL5Liver-/- Vehicle
UBL5Liver-/- ACE2
(B)
CHOP
Relative mRNA expression
1.5
1.0
0.5
0.0
*
*
Con
UBL5Liver-/- Vehicle
UBL5Liver-/- ACE2
(C)
Hsp70mt
Relative mRNA expression
16
14
12
10
8
6
4
2
0
*
*
Con
UBL5Liver-/- Vehicle
UBL5Liver-/- ACE2
(D)
Hsp60
Relative mRNA expression
1.5
1.0
0.5
0.0
****
****
Con
UBL5Liver-/- Vehicle
UBL5Liver-/- ACE2
(E)
ClpP
Relative mRNA expression
1.5
1.0
0.5
0.0
**
***
Con
UBL5Liver-/- Vehicle
UBL5Liver-/- ACE2
(F)
ClpX
Relative mRNA expression
2.0
1.5
1.0
0.5
0.0
**
**
*
Con
UBL5Liver-/- Vehicle
UBL5Liver-/- ACE2

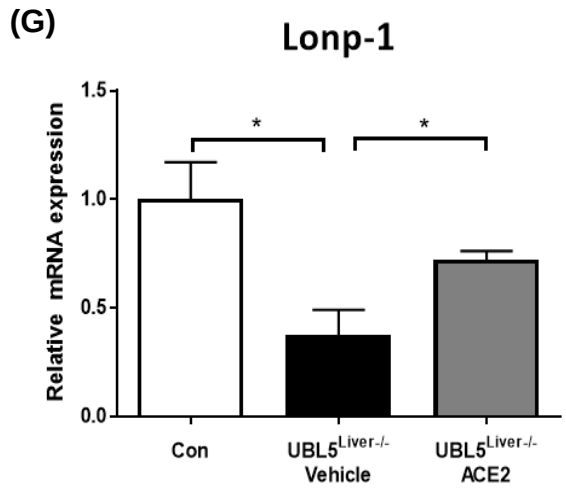

Figure 6.21: mRNA levels of UPRmt genes in the liver from UBL5 KO and control mice treated either with vehicle or *ACE2*: mRNA levels of (A) transcription factor *CHOP*, **(B)** *ATF-5,* **(C)** heat shock protein *Hsp70mt*, **(D)** HSP60 and **(E)** proteases *lonp-1*, (**F)** *ClpX* and **(G)** *ClpP* were expressed relative to the control and UBL5 KO (UBL5$^{Liver-/-}$) homozygous mice. The ΔΔCt method was used to calculate relative quantification of gene expression with GAPDH RNA as the housekeeper gene. Values represent mean ± SEM. n=4-5. *P ≤0.05, **P ≤0.01, ***P ≤0.001, ****p< 0.0001.

6.6 Discussion

In chapter 4 we demonstrated that 10 days following induction of liver complete UBL5 deletion, the homozygous mice had severe liver disease accompanied by increased steatosis and mitochondrial dysfunction. In this chapter, we attempted to test if this severe liver phenotype could be prevented through drug interventions. To achieve this, we chose pioglitazone, as it has been shown in several studies to reduce steatosis and inflammation in the liver (Boettcher, Csako, Pucino, Wesley, & Loomba, 2012). In addition to this pharmacotherapy intervention, we assessed whether gene therapy could also prevent the liver failure phenotype of our KO mice. Emerging evidence suggests that use of *ACE2* gene therapy could reverse fatty liver, oxidative stress and injury in the liver (Mak et al., 2015a). Therefore, as many of these hallmarks are a feature of our KO mice, we chose *ACE2* gene therapy as the other potential preventative arm.

6.6.1 Pioglitazone treatment

Several clinical and animal studies support the use of the drug pioglitazone in improving levels of steatosis and inflammation in the liver (Cusi et al., 2016; Fromenty, Berson, & Pessayre, 1997; Hsiao et al., 2017; Natarajan et al., 2006; Shadid & Jensen, 2003). In these studies patients with type 2 diabetes, NAFLD and NASH displayed significant improvement in hepatic fat content (Bajaj et al., 2003; Boettcher et al., 2012; Cusi et al., 2016; Shadid & Jensen, 2003). One of the main symptoms presented by the homozygous liver specific *UBL5* KO mice was an increase in hepatic fat accumulation. Following pre-treatment with pioglitazone, the UBL5 KO significantly reduced the level of steatosis, predominantly through a reduction in macro vesicular fat accumulation but not micro vesicular steatosis. Macro vesicular steatosis is primarily caused by an oversupply of lipids that accumulate within the hepatocytes usually because of increased triglyceride synthesis or decreased excretion (Tsutsumi, Nakamura, Ueno, Torimura, & Aguirre-García, 2017). Pioglitazone is a PPARγ agonist that acts to regulate fatty acid storage and inhibit lipogenesis and adipocyte differentiation (Rosen et al., 2002; Yu Zhang et al., 2014). Expression levels of *PPARγ* were significantly increased in the UBL5 KO mice treated with pioglitazone increased

to basal levels compared to control and placebo treated UBL5 KO mice. Thus, it is likely that the normalization of *PPARγ* gene expression led to the improvement of the hepatic steatosis in our mice. The lack of any beneficial effect on micro vesicular steatosis in the UBL5 KO mice is normally indicative of severe injury and complications with β-oxidation brought on by mitochondrial dysfunction and increased ROS production (Aita et al., 2001; Bioulac-Sage & Balabaud, 2009; Hautekeete, Degott, & Benhamou, 1990). Therefore, despite the improvement in fat deposition at the macro vesicular level, the data imply that treatment with pioglitazone and the subsequent normalization of *PPARγ* alone was not sufficient to improve mitochondrial function in our KO mice.

The general presentation in patients with diabetes and fatty liver are abnormal levels of liver enzymes and dyslipidemia (altered lipid profile including cholesterol and triglycerides) (Dixon et al., 2001; Matteoni et al., 1999). Pioglitazone is known to alleviate these abnormalities by reducing liver enzyme levels (Belfort et al., 2006a; Promrat et al., 2004; Sanyal et al., 2004) and improving the lipid profile (Aithal et al., 2008; Belfort et al., 2006a; Promrat et al., 2004; Razavizade et al., 2013). Our KO mice clearly showed that pre-treatment with pioglitazone prevented the rise in liver enzyme levels that were seen in the placebo treated KO mice, indicating an improvement in liver function. In terms of the lipid profile, pre-treatment lowered both cholesterol and ketone body levels but had little effect on triglyceride levels. Previous studies have reported the positive effect of pioglitazone on circulating cholesterol levels via PPARγ regulated systems that metabolise cholesterol through oxidized LDL receptor 1 (Aithal et al., 2008; Belfort et al., 2006a; Promrat et al., 2004; Razavizade et al., 2013). The improvement in ketone body levels could be an effect coming from the *PPARγ* normalization which led to improvement of fatty acid oxidation (Abdul-Ghani et al., 2019). Triglyceride levels have been shown to decrease with pioglitazone (Matthews, Charbonnel, Hanefeld, Brunetti, & Schernthaner, 2005) but our KO mice already displayed very low levels of triglycerides, thus explaining why we did not observe any differences between groups.

While there is, much evidence showing direct effects of pioglitazone on lowering lipids, little is known of whether pioglitazone could assert its beneficial effects via changes in the UPRmt. Increases in the expression profile of genes involved in the UPRmt could improve mitochondrial function and explain some of the reduced

symptoms seen in the treated group. Following the 4-weeks of pioglitazone pre-treatment, the KO mice did not exhibit any increases in *UBL5* expression. Since our inducible mouse model has both genomic copies deleted, it is unable to express any further *UBL5*. Even in the absence of *UBL5*, the pioglitazone pre-treatment achieved increases in UPRmt genes in UBL5 KO mice compared to placebo treated UBL5 KO mice. A study by Pan et al. indeed showed an increase in CHOP gene expression following pioglitazone treatment using an *in vitro* model of human adrenocortical carcinoma cells (HAC15) (Pan et al., 2014). While this published study was examining the UPR^{er}, it is known that CHOP acts in both the UPR^{er} and UPRmt (Aldridge et al., 2007a; T. Horibe & N. J. Hoogenraad, 2007; Quan Zhao, Jianghui Wang, Ilya V Levichkin, Stan Stasinopoulos, Michael T Ryan, & Nicholas J Hoogenraad, 2002). It is worth noting that in our mice the *HSP60* mRNA levels was undetectable in both the placebo and pioglitazone treated UBL5 KO mice. A study in human vascular endothelial cells showed that treatment with pioglitazone can inhibit *HSP60* expression (Artwohl et al., 2005) but in our KO mice *HSP60* was undetected and we could not detect any differences with pioglitazone treatment. We speculate that we see this outcome because UBL5 and HSP60 are possibly tightly connected and in the absence of one gene, expression could be prevented in the other gene. To our knowledge there is no literature demonstrating how pioglitazone affects the remaining genes involved in the UPRmt (*ATF5, ClpP, ClpX, lonp-1* and *HSP70*). We are unsure through which mechanism(s) these genes were upregulated in our UBL5 KO pioglitazone treated mice compared to placebo treated KO mice. We could speculate that relieving the liver of fat accumulation and normalizing some of the liver enzymes placed less burden on the liver and allowed the UPRmt to express more efficiently.

In conclusion, pioglitazone pre-treatment decreased some of the defects in our UBL5 KO mice such as fatty liver, liver injury and also improved the lipid profile. We saw an upregulation of the UPRmt in pioglitazone treated KO mice that possibly contributed to better health in our mice model. The placebo treated KO group that did not receive pioglitazone had downregulated levels of UPRmt and presented with severe liver dysfunction.

6.6.2 ACE2 overexpression in UBL5 KO mice and controls

An innovative gene therapy for fatty liver and oxidative stress treatment that has been proposed in animal studies is ACE2 overexpression (Mak et al., 2015b). Given our KO model displays the features of fatty liver, we explored whether the use of this novel intervention could reverse the defects and sustain the health of the animal. In this study the UBL5 KO mice treated with ACE2 overexpression displayed significant improvement in fat accumulation in the liver and in oxidative stress.

ACE2 was successfully overexpressed in our ACE2 virus treated mice, as confirmed by the increase in ACE2 mRNA levels. This had no effect on UBL5 levels in the KO mice as both vehicle treated and ACE2 treated mice maintained the complete deletion of *UBL5*. *ACE2* improved the appearance of the livers, which looked normal and similar to controls compared to the vehicle treated KO mice that had visible fat accumulation. ACE2 pre-treatment prevented the reduction in liver weight from liver damage seen in the KO mice. These findings are consistent with a previous study that showed a similar prevention of liver weight reduction following *ACE2* treatment (Cao et al., 2016).

Several studies have shown that short-term treatment with recombinant ACE2 protein amends experimental tissue injury in several organs including the liver (Österreicher et al., 2009). Likewise, our mice showed significant improvements in histology displaying better cellular structure and ameliorated patterns of cellular degradation and necrosis. *ACE2* overexpression significantly improved the steatosis in the liver of our KO mice, both at the macro vesicular and micro vesicular levels with fat droplets ameliorated with the therapy. This reduction may possibly have occurred because ACE2 mediated the Akt and ACE2/Ang-(1-7)/Mas mechanism in our ACE2 treated mice. It is known that ACE2 acts through this pathways (Cao et al., 2016), that can reduce lipid accumulation by regulation of lipid-metabolizing genes through ATP/P2 receptor/Calmodulin signaling pathway (Cao et al., 2016). Although we have not done further experiments to confirm this. There was a small percentage of micro vesicular fat still visible in our UBL5 KO mice pre-treated with *ACE2* compared to the controls which suggest that there was still a sign of impairment in mitochondrial β

oxidation of fatty acids (Hautekeete et al., 1990). Although compared to the placebo we saw a dramatic reduction of the small lipid droplets.

We observed that *ACE2* had a dramatic effect on overall levels of liver enzymes (Bili, ALT, AST, AP). Cao et al. showed in 2016 that *ACE2* improved liver enzymes in *db/db* mice, more specifically ALT levels (Cao et al., 2016). Similarly, different models of liver disease treated with rAAV2/8-*ACE2* had significantly lower levels of ALT enzymes (Mak et al., 2015a). In terms of the lipid profile *ACE2* has been shown to decrease triglyceride levels (Cao et al., 2016). In our study circulating triglycerides in the KO mice were reduced after deletion of *UBL5*, therefore we didn't see any significant change with *ACE2* treatment. Cholesterol levels were significantly improved in our mice on therapy which is contrast to the study by Cao et al who showed that *ACE2* did not affect the cholesterol levels. This could possibly be due to the different technique of *ACE2* overexpression and the mouse models used (Cao et al., 2016).

ACE2 clearly showed a strong ability to reverse the deleterious effects that deleting *UBL5* had in our mouse model. We did not investigate the ACE2/Ang-(1-7)/Mas pathway (Cao et al., 2016) because our study is mostly focused on the UPRmt. The treatment partially normalized the UPRmt response in our KO mice treated with ACE2. The transcription factors (*ATF5, CHOP*) were increased to normal levels as was *HSP70mt* was normalized. However, the levels of HSP60 were not increased. HSP60 is tightly connected to *UBL5* expression and for that reason it was unable to be increased. As it was shown in *C. elegans* a suppression of UBL5 prevented the UPRmt response including the *HSP60* gene from expressing (Benedetti et al., 2006). Which highlighted the importance of UBL5 in the ability of heat shock proteins (HSP60) to act. Similar results were found with our pioglitazone treatment where *HSP60* was undetectable in our UBL5 KO mice either with or without therapy. The proteases *ClpP* and *ClpX* were not affected by *ACE2. Lonp-1* protease was raised to normal levels with the therapy. There is no literature describing or proving that *ACE2* can affect the UPRmt, therefore, we are the first to show that *ACE2* can increase or normalize some of the protective UPRmt genes.

It is unclear from the current study whether the UPRmt was the major factor that kept the *ACE2* treated mice healthier than the mice treated with vehicle. Possibly at the time that we measured the levels of gene expression involved in UPRmt the

ACE2 treated KO mice were healthy so there was no biological reason for the UPRmt to be increased. The ACE2 possibly reduced oxidative stress in UBL5 KO mice through a decrease of Ang II and increase of Ang-(1-7)/Mas pathway. As mentioned before we have not studied this pathway in detail and we can only speculate based on the literature (Cao et al., 2016; Mak et al., 2015b; Rabelo, Alenina, & Bader, 2010). Recent evidence suggests that enhancement of Ang-(1-7)/Mas pathway improves ROS levels and oxidative stress (Mak et al., 2015b; Rabelo et al., 2010). We can speculate that the UBL5 KO mice treated with ACE2 had better mitochondrial function, therefore there was no need for the UPRmt to be activated. While with the pioglitazone treatment even if we had significant improvement in the overall metabolic health of the mice after treatment, they were still sick compared to controls. Thus, there was still increased stress in their cells and this could be reflecting through increased levels of UPRmt (Callegari et al., 2018). Although we are showing that increased levels of UPRmt are important for better functionality and health.

To conclude, ACE2 overexpression also showed dramatic improvement of liver function, fat accumulation and in UBL5 KO mice perhaps via Ang-(1-7)/Mas pathway. The UPRmt normalized in ACE2 treated UBL5 KO mice possibly due to the general heath improvement and lack of stress (that did not push the UPRmt higher than normal levels).

6.6.3 Overall conclusion

In this Chapter, we saw that the UPRmt increases in pioglitazone treated mice that have better liver function than the placebo treated UBL5 KO mice. Although compared to control mice they were more sick, which means that some of the stress was still present. On the other hand, the ACE2 treated KO mice were completely healthy when compared to control mice. The UPRmt in this case was normalized but not increased, possibly because these mice had normal livers and there was no mitochondrial stress. This highlights the importance of UPRmt in normal liver function.

CHAPTER 7: THESIS SUMMARY, CONCLUSION AND FUTURE DIRECTIONS

7.1 Summary

The main objective of this PhD thesis was focused on understanding the biological and physiological function of the mitochondrial unfolded protein response (UPRmt) and its relationship with ubiquitin like protein 5 (UBL5) in a mammalian system, specifically in the liver. UBL5 has been associated with several biological processes including body weight regulation (Collier et al., 2000; Walder et al., 2001; Walder et al., 2002) (Ziolkowska et al., 2004a; Ziolkowska et al., 2004c; Rucinski et al., 2005b) and mitochondrial homeostasis (Benedetti et al., 2006; Haynes et al., 2007; Haynes et al., 2010; Durieux et al., 2011). However, the exact physiological role of UBL5 has not been established. This thesis documented the generation of an inducible (tamoxifen induced after adulthood) liver specific UBL5 knockout model (UBL5 KO) (Chapter 3), phenotypic characterisation of the liver UBL5 knockout model (Chapter 4), high fat diet challenge of the heterozygous liver specific UBL5 knockout mice (Chapter 5) and finally the effects of therapeutic interventions using both drug (pioglitazone) and gene therapy (ACE2 overexpression) in the UBL5 KO mice (Chapter 6).

To generate the UBL5 KO mice, the Cre/lox system was used so that UBL5-floxed mice (UBL5lox$^{+/-}$) could be crossed with liver specific Cre-expressing mice (Cre$^{+/-}$, the inducible liver specific mer-cre-mer (MCM) receptor) to obtain complete and partial deletion of UBL5 in the liver. Ten days after tamoxifen induction (on a chow diet) the UBL5 KO mice (with 97% gene reduction) displayed a severe liver phenotype with increased liver enzymes (indication of liver damage), gross histology, severe hepatic steatosis, apoptosis, glucose intolerance, oxidative stress, mitochondrial damage,

reduced mitochondrial respiration, increased ROS levels and reduced expression of genes associated with the UPRmt. While the heterozygous mice with 60% gene reduction did not show any phenotype and appeared to have normal liver function despite having only 1 copy of the UBL5 allele.

Interestingly, the heterozygous mice that were challenged for two months with a high cholesterol, high fat diet (HFD) displayed better glucose tolerance, liver enzymes, cholesterol levels and less fat accumulation in the liver as assessed by histology, when compared to the HF-fed controls. The HF-fed heterozygous mice also had significantly increased expression of key UPRmt genes (*CHOP*, *ClpX*, *ClpP*, *HSP60*, *HSP10* and *HSP70mt*), that potentially contributed to their better health. The increase in UPRmt expression levels (as discussed extensively in Chapter 5) possibly facilitated the heterozygous mice to increase the number and quality of mitochondria leading to improved metabolism and liver function. When we extended the exposure time to this diet to a period of five months, we found the beneficial effects in liver function of heterozygous mice had started to diminish. The HF-fed heterozygous mice at this timepoint began to resemble the HF-fed control mice in terms of liver function with a worsening of liver enzyme levels, glucose tolerance (better glucose clearance in HF-fed heterozygous mice at the end of the experiment) and histological features (steatosis). The heterozygous mice had higher levels of UPRmt (*CHOP*, *ClpX*, *ClpP*, *HSP60*, *HSP10* and *HSP70mt*), than control mice on HFD and as with the 2 month exposure, likely contributed to the beneficial effects on liver function. However, our data does show that chronic consumption of the HFD will override any of the benefits seen earlier on in the mice. Importantly, our work was able to establish a link between fatty liver in humans and UBL5 with our data demonstrating increased liver expression of UBL5 in patients with fatty liver and cirrhosis compared to patients with normal livers. Together, our human and mouse data implicate the importance of UBL5 and possibly the UPRmt in severe fatty liver/liver dysfunction.

In order to investigate if the severe liver phenotype seen in UBL5 KO mice could be prevented, we took the approach of intervening therapeutically using two different arms: Drug pre-treatment with the T2D drug pioglitazone and gene therapy through overexpression of the ACE2 gene. Following pre-treatment with pioglitazone, we found

that the UPRmt (*CHOP*, *ATF5*, *ClpP*, *ClpX*, *Lonp-1*, *HSP70*, *HSP10*) was increased in UBL5 KO mice that led to an improvement in liver histology, hepatic fat accumulation, liver enzymes and lipid content. We believe that the increase of UPRmt in pioglitazone treated mice helped them to have better mitochondria (in number and quality) and this contributed towards better metabolism and liver function. Although further investigation is required. Similarly, pre-treating with the ACE2 vector resulting in ACE2 overexpression had a beneficial impact on the UBL5 KO mice. The vehicle treated mice had complete liver failure while we saw a striking improvement in liver function (steatosis, histology, liver enzymes and lipids) in ACE2 treated KO mice. The ACE2 treated UBL5 KO mice showed almost no change at all from controls, while the vehicle treated mice had severe liver failure. ACE2 overexpression prevented the global decrease UPRmt which indicates a lack of oxidative stress compared to the vehicle treated mice, though further investigation is required to answer with certainty, the mechanism by which this complete reversal of the liver failure phenotype occurs.

7.2 Conclusion

The overall findings from this thesis has provided us with a greater understanding of the physiological function of UBL5 in a mammalian system, particularly how it acts in the UPRmt. Together, UBL5 and the UPRmt proved to be vital for proper mitochondrial and liver function given that their absence leads to mitochondrial dysfunction and overall liver failure. As is illustrated in (Figure 7.1), we saw in our study that very low UBL5 levels prevented the UPRmt from being activated and this has an impacting liver health. Furthermore, in control mice that are under increased stress (severe liver failure) the expression of UBL5 increases. These very high levels of UBL5 also has a negative impact on the activation of the UPRmt in which the key genes do not express appropriately thereby negatively affecting liver health. Furthermore, when UBL5 was only partially deleted (as we saw in heterozygous mice), this triggers the UPRmt to the highest., leading to improved metabolism (via better mitochondrial function) and liver health. Further studies on UBL5 will reinforce our understanding of the UPRmt in mammals and its possible association with liver and mitochondrial dysfunction (and in other tissues). This study will undoubtedly add to our knowledge on the unknown cause-and-effect relationship between liver and mitochondrial dysfunction.

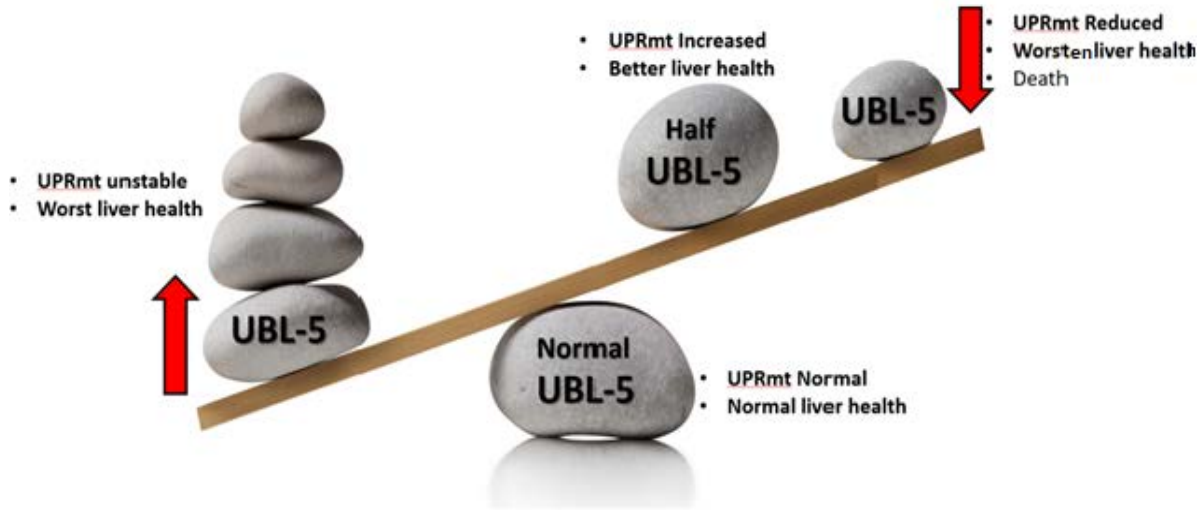

Figure 7.1: Schematic of the possible pathway of UBL5 in the UPRmt and liver function.

7.3 Future Directions

The findings from this thesis demonstrates the importance of UBL5 in the UPRmt in murine models, however, additional experiments are required to consolidate these observations. We have built a solid foundation of data that provides us with the necessary building blocks to advance the focus of this research in various directions. Below are several questions that have been raised from the work generated allowing for continuation in unravelling this important physiological system.

7.3.1 Can the overexpression of UBL5 contribute towards better or worsened health?

The UBL5 KO mice clearly showed a severe liver phenotype accompanied by reduced UPRmt and mitochondrial dysfunction implicating the importance of the two in a relationship that is essential for normal health. Our work also showed for the first time that patients with cirrhosis and fatty liver had increased expression levels of UBL5, which confirms that UBL5 increases in response to stress. It would be worth testing if the opposite is true and that overexpressing UBL5 in normal C57BL/6 would protect them from stress, such as the same high fat, high cholesterol diet (HFD) used in this study. Overexpression of UBL5 could increase the UPRmt levels leading to an

improvement in mitochondrial and cellular function that could potentially have a protective effect against the negative impact of a HFD. This study would validate the importance of UBL5 in a gain of function model and support the work from this loss of function model as seen in this thesis.

7.3.2 What is the mechanism(s) by which the UPRmt employs to improve mitochondrial/liver function?

We saw in our study that the heterozygous mice fed the HFD had increased UPRmt and their liver health was significantly better than that of the HF-fed control mice. However, we were unable to directly determine the actual mechanism involved. These results could be due to an increase in the number of mitochondria or better mitochondrial function. To test this, we could measure mitochondrial number in our mice by measuring the mitochondrial DNA number. Additionally, we could isolate mitochondria from the livers of our mice and perform respirometer tests such as oroboros. We could further investigate the master regulator of cellular oxidation and energy homeostasis the 5' adenosine monophosphate-activated protein kinase (AMPK) pathway by measuring levels of AMPK phosphorylation and the expression of key genes and proteins involved in this pathway (such as PGC1-α and CPT1α) to see how they react when the UPRmt is increased.

7.3.3 What were the mechanism(s) involved that led to the significant improvement of the ACE2 treated UBL5 KO mice?

The UBL5 KO mice treated with ACE2 showed significantly improved liver function when compared to vehicle treated UBL5 KO mice. The UPRmt was normalized in ACE2 treated UBL5 KO mice, but it did not increase any further unlike our other results from the heterozygous treated with HFD and UBL5 KO mice treated with pioglitazone. Perhaps the ACE2 treatment improved the mitochondrial action directly such that the UPRmt was not necessary to be increased. To clarify this we

could investigate further the ACE2/Ang(1-7)/Mas pathway that ACE2 acts within through analysis of key genes and proteins involved in this pathway such as Mas receptor specifically and the peptides Ang (1-7) to determine if they are increased. Finally, we can measure the peptide levels of Ang II (that is involved in the classic RAS) which we would expect to be decreased because alternative RAS is activated (Yim & Hwan Yoo, 2008). We could further investigate mitochondrial number, respiration and morphology to see how the mitochondria are specifically affected from treatment.

7.3.4 Will the therapeutic interventions be as beneficial after tamoxifen treatment when the UBL5 gene is completely deleted?

In our study, we pre-treated our UBL5 KO mice with either pioglitazone or ACE2. The liver failure was acute in these animals, therefore we speculated that treatment prior to tamoxifen induction would help them to minimize/prevent the symptoms (such as fatty liver and oxidative stress). Indeed, we saw a significant improvement in the health of the UBL5 KO mice under both pre-treatment arms. It would be interesting to see if the therapies would have similar effects if we applied them after tamoxifen induction; a treatment arm compared to the preventative arm. We also could attempt to leave the treated mice beyond 10 days and see if they can survive longer than the non-treated animals.

7.3.5 Determine how and why the heterozygous mice have better liver function and glucose tolerance?

We saw that the heterozygous mice had better glucose tolerance and general liver function after two months on a HFD. We also saw in the same mice an increase in the UPRmt pathway which indicates that these mice have better mitochondrial function. Although we have not conducted any further experiments to test this. We did not measure insulin levels in our mice during this study due to technical issues of

obtaining enough plasma from the tail tip (given that the OGTTs were performed in conscious mice). In order to fully understand the glucose tolerance data, we do need to determine whether the improvement is due to increased/better insulin secretion. As UBL5 was deleted specifically in the liver, we would assume that the pancreas would not be directly affected and thus insulin would not be different. However, this needs to be confirmed. Alternatively, the better liver and glucose function in these mice could be due to more mitochondria, and more healthier mitochondria. Therefore, it would be interesting to determine the number of mitochondria in these mice as an increased number in the heterozygous mice could contribute to better glucose metabolism.

BIBLIOGRAPHY

Abdul-Ghani, M. A., & DeFronzo, R. A. J. C. d. r. (2008). Mitochondrial dysfunction, insulin resistance, and type 2 diabetes mellitus. *8*(3), 173.

Abdul-Ghani, M., Migahid, O., Megahed, A., Singh, R., Fawaz, M., DeFronzo, R. A., . . . Metabolism. (2019). Pioglitazone prevents the increase in plasma ketone concentration associated with dapagliflozin in insulin-treated T2DM patients: Results from the Qatar Study. *21*(3), 705-709.

Aita, K., Jin, Y., Irie, H., Takahashi, I., Kobori, K., Nakasato, Y., . . . Shiga, J. J. H. p. (2001). Are there histopathologic characteristics particular to fulminant hepatic failure caused by human herpesvirus-6 infection? A case report and discussion. *32*(8), 887-889.

Aithal, G. P., Thomas, J. A., Kaye, P. V., Lawson, A., Ryder, S. D., Spendlove, I., . . . Webber, J. (2008). Randomized, placebo-controlled trial of pioglitazone in nondiabetic subjects with nonalcoholic steatohepatitis. *Gastroenterology, 135*(4), 1176-1184.

Al-Furoukh, N., Ianni, A., Nolte, H., Hölper, S., Krüger, M., Wanrooij, S., & Braun, T. (2015). ClpX stimulates the mitochondrial unfolded protein response (UPRmt) in mammalian cells. *Biochimica et Biophysica Acta (BBA) - Molecular Cell Research, 1853*(10, Part A), 2580-2591. doi:https://doi.org/10.1016/j.bbamcr.2015.06.016

Al Gharabally, A., & ACOSTA, R. (2007). A pilot study of pioglitazone for the treatment of non-alcoholic fatty liver disease.

Alberio, S., Mineri, R., Tiranti, V., & Zeviani, M. (2007). Depletion of mtDNA: syndromes and genes. *Mitochondrion, 7*(1), 6-12.

Alberts, B., Johnson, A., Lewis, J., Raff, M., Roberts, K., & Walter, P. (2002). Cell junctions, cell adhesion, and the extracellular matrix.

Alberts, P., Engblom, L., Edling, N., Forsgren, M., Klingstrom, G., Larsson, C., . . . Abrahmsen, L. (2002). Selective inhibition of 11beta-hydroxysteroid dehydrogenase type 1 decreases blood glucose concentrations in hyperglycaemic mice. *Diabetologia, 45*(11), 1528-1532.

Aldridge, J. E., Horibe, T., & Hoogenraad, N. J. (2007a). Discovery of genes activated by the mitochondrial unfolded protein response (mtUPR) and cognate promoter elements. *PLoS One, 2*(9), e874.

Aldridge, J. E., Horibe, T., & Hoogenraad, N. J. J. P. o. (2007b). Discovery of genes activated by the mitochondrial unfolded protein response (mtUPR) and cognate promoter elements. *2*(9), e874.

Altshuler, D., Hirschhorn, J. N., Klannemark, M., Lindgren, C. M., Vohl, M.-C., Nemesh, J., . . . Brewer, C. J. N. g. (2000). The common PPARγ Pro12Ala polymorphism is associated with decreased risk of type 2 diabetes. *26*(1), 76-80.

American Diabetes, A. (2009). Diagnosis and classification of diabetes mellitus. *Diabetes care, 32 Suppl 1*(Suppl 1), S62-S67. doi:10.2337/dc09-S062

Anderson, S., Bankier, A. T., Barrell, B. G., De Bruijn, M., Coulson, A. R., Drouin, J., . . . Sanger, F. (1981). Sequence and organization of the human mitochondrial genome.

Andersson, K. B., Winer, L. H., Mørk, H. K., Molkentin, J. D., & Jaisser, F. (2010). Tamoxifen administration routes and dosage for inducible Cre-mediated gene disruption in mouse hearts. *Transgenic research, 19*(4), 715-725.

Andrikopoulos, S., Blair, A. R., Deluca, N., Fam, B. C., & Proietto, J. (2008). Evaluating the glucose tolerance test in mice. *American Journal of Physiology-Endocrinology and Metabolism, 295*(6), E1323-E1332.

Andrikopoulos, S., Blair, A. R., Deluca, N., Fam, B. C., Proietto, J. J. A. J. o. P.-E., & Metabolism. (2008). Evaluating the glucose tolerance test in mice. *295*(6), E1323-E1332.

Anstee, Q. M., Day, C. P. J. N. r. G., & hepatology. (2013). The genetics of NAFLD. *10*(11), 645.

Armstrong, M. J., Gaunt, P., Aithal, G. P., Barton, D., Hull, D., Parker, R., . . . Aldersley, M. A. J. T. L. (2016). Liraglutide safety and efficacy in patients with non-alcoholic steatohepatitis (LEAN): a multicentre, double-blind, randomised, placebo-controlled phase 2 study. *387*(10019), 679-690.

Artwohl, M., Hölzenbein, T., Fürnsinn, C., Freudenthaler, A., Huttary, N., Waldhäusl, W. K., & Baumgartner-Parzer, S. M. (2005). Thiazolidinediones inhibit apoptosis and heat shock protein 60 expression in human vascular endothelial cells. *Thromb Haemost, 93*(05), 810-815. doi:10.1160/TH04-09-0615

Aynsley-Green, A., Biebuyck, J., & Alberti, K. (1973). Anaesthesia and insulin secretion: the effects of diethyl ether, halothane, pentobarbitone sodium and ketamine hydrochloride on intravenous glucose tolerance and insulin secretion in the rat. *Diabetologia, 9*(4), 274-281.

Bajaj, M., Suraamornkul, S., Pratipanawatr, T., Hardies, L. J., Pratipanawatr, W., Glass, L., . . . DeFronzo, R. A. (2003). Pioglitazone reduces hepatic fat content and augments splanchnic glucose uptake in patients with type 2 diabetes. *Diabetes, 52*(6), 1364-1370.

Baker, B. M., & Haynes, C. M. (2011). Mitochondrial protein quality control during biogenesis and aging. *Trends in biochemical sciences, 36*(5), 254-261.

Baker, T. A., & Sauer, R. T. (2012). ClpXP, an ATP-powered unfolding and protein-degradation machine. *Biochimica et Biophysica Acta (BBA) - Molecular Cell Research, 1823*(1), 15-28. doi:https://doi.org/10.1016/j.bbamcr.2011.06.007

Ballestri, S., Day, C. P., & Daly, A. K. J. G. (2011). Polymorphism in the farnesyl diphosphate farnesyl transferase 1 gene and nonalcoholic fatty liver disease severity. *140*(5), 1694-1695.

Barrett, P. V. D. (1971). The Effect of Diet and Fasting on the Serum Bilirubin Concentration in the Rat. *Gastroenterology, 60*(4), 572-576. doi:10.1016/S0016-5085(71)80062-8

Beal, M. F. J. J. o. b., & biomembranes. (2004). Mitochondrial dysfunction and oxidative damage in Alzheimer's and Parkinson's diseases and coenzyme Q 10 as a potential treatment. *36*(4), 381-386.

Begriche, K., Igoudjil, A., Pessayre, D., & Fromenty, B. J. M. (2006). Mitochondrial dysfunction in NASH: causes, consequences and possible means to prevent it. *6*(1), 1-28.

Belfort, R., Harrison, S. A., Brown, K., Darland, C., Finch, J., Hardies, J., . . . Pulcini, J. (2006a). A placebo-controlled trial of pioglitazone in subjects with nonalcoholic steatohepatitis. *New England Journal of Medicine, 355*(22), 2297-2307.

Belfort, R., Harrison, S. A., Brown, K., Darland, C., Finch, J., Hardies, J., . . . Pulcini, J. J. N. E. J. o. M. (2006b). A placebo-controlled trial of pioglitazone in subjects with nonalcoholic steatohepatitis. *355*(22), 2297-2307.

Benedetti, C., Haynes, C. M., Yang, Y., Harding, H. P., & Ron, D. (2006). Ubiquitin-like protein 5 positively regulates chaperone gene expression in the mitochondrial unfolded protein response. *Genetics, 174*(1), 229-239. doi:10.1534/genetics.106.061580

Berg, J. M., Tymoczko, J. L., & Stryer, L. (2008). *Biochemistry (Loose-Leaf)*: Macmillan.

Berger, J., & Moller, D. E. (2002). The mechanisms of action of PPARs. *Annual review of medicine, 53*(1), 409-435.

Berson, A., De Beco, V., Lettéron, P., Robin, M. A., Moreau, C., El Kahwaji, J., . . . Pessayre, D. J. G. (1998). Steatohepatitis-inducing drugs cause mitochondrial dysfunction and lipid peroxidation in rat hepatocytes. *114*(4), 764-774.

Billington, C., Briggs, J., Grace, M., & Levine, A. (1991). Effects of intracerebroventricular injection of neuropeptide Y on energy metabolism. *American Journal of Physiology-Regulatory, Integrative and Comparative Physiology, 260*(2), R321-R327.

Bioulac-Sage, P., & Balabaud, C. (2009). CHAPTER 40 - Toxic and Drug-Induced Disorders of the Liver. In R. D. Odze & J. R. Goldblum (Eds.), *Surgical Pathology of the GI Tract, Liver, Biliary Tract, and Pancreas (Second Edition)* (pp. 1059-1086). Philadelphia: W.B. Saunders.

Birbach, A., Casanova, E., & Schmid, J. A. (2009). A Probasin-MerCreMer BAC allows inducible recombination in the mouse prostate. *Genesis, 47*(11), 757-764. doi:doi:10.1002/dvg.20558

Boettcher, E., Csako, G., Pucino, F., Wesley, R., & Loomba, R. (2012). Meta-analysis: pioglitazone improves liver histology and fibrosis in patients with non-alcoholic steatohepatitis. *Alimentary pharmacology & therapeutics, 35*(1), 66-75.

Boright, A. P., Connelly, P. W., Brunt, J. H., Morgan, K., & Hegele, R. A. (1998). Association and linkage of LDLR gene variation with variation in plasma low density lipoprotein cholesterol. *Journal of human genetics, 43*(3), 153-159.

Borkman, M., Chisholm, D. J., Furler, S. M., Storlien, L. H., Kraegen, E. W., Simons, L. A., & Chesterman, C. N. J. D. (1989). Effects of fish oil supplementation on glucose and lipid metabolism in NIDDM. *38*(10), 1314-1319.

Bota, D. A., & Davies, K. J. J. N. c. b. (2002). Lon protease preferentially degrades oxidized mitochondrial aconitase by an ATP-stimulated mechanism. *4*(9), 674.

Boucher, J., Kleinridders, A., & Kahn, C. R. J. C. S. H. p. i. b. (2014). Insulin receptor signaling in normal and insulin-resistant states. *6*(1), a009191.

Bozaoglu, K., Curran, J. E., Elliott, K. S., Walder, K. R., Dyer, T. D., Rainwater, D. L., . . . Blangero, J. (2006a). Association of genetic variation within UBL5 with phenotypes of metabolic syndrome. *Human Biology, 78*(2), 147-159. doi:DOI 10.1353/hub.2006.0033

Bozaoglu, K., Curran, J. E., Elliott, K. S., Walder, K. R., Dyer, T. D., Rainwater, D. L., . . . Blangero, J. (2006b). Association of genetic variation within UBL5 with phenotypes of metabolic syndrome. *Hum Biol, 78*(2), 147-159.

Brailoiu, G. C., Dun, S. L., Chi, M., Ohsawa, M., Chang, J. K., Yang, J., & Dun, N. J. (2003). Beacon/ubiquitin-like 5-immunoreactivity in the hypothalamus and pituitary of the mouse. *Brain Res, 984*(1-2), 215-223.

Brailoiu, G. C., Dun, S. L., Yang, J., Chang, J. K., Castellino, S., & Dun, N. J. (2002). Beacon-like immunoreactivity in the hypothalamus of Sprague-Dawley rats. *Neurosci Lett, 317*(3), 166-168.

Braissant, O., Foufelle, F., Scotto, C., Dauça, M., & Wahli, W. (1996). Differential expression of peroxisome proliferator-activated receptors (PPARs): tissue distribution of PPAR-alpha,-beta, and-gamma in the adult rat. *Endocrinology, 137*(1), 354-366.

Bratic, I., & Trifunovic, A. (2010). Mitochondrial energy metabolism and ageing. *Biochimica et Biophysica Acta (BBA) - Bioenergetics, 1797*(6), 961-967. doi:https://doi.org/10.1016/j.bbabio.2010.01.004

Broadley, S. A., & Hartl, F. U. (2008). Mitochondrial stress signaling: a pathway unfolds. *Trends Cell Biol, 18*(1), 1-4. doi:10.1016/j.tcb.2007.11.003

Brown, E., Umino, Y., Loi, T., Solessio, E., & Barlow, R. (2005). Anesthesia can cause sustained hyperglycemia in C57/BL6J mice. *Visual neuroscience, 22*(05), 615-618.

Brown, E., Umino, Y., Solessio, E., Loi, T., Quinn, R., & Barlow, R. (2004). Anesthesia affects mouse ERG and blood glucose. *Investigative Ophthalmology & Visual Science, 45*(13), 742-742.

Bruning, J. C., Michael, M. D., Winnay, J. N., Hayashi, T., Horsch, D., Accili, D., . . . Kahn, C. R. (1998). A muscle-specific insulin receptor knockout exhibits features of the metabolic syndrome of NIDDM without altering glucose tolerance. *Mol Cell, 2*(5), 559-569.

Bukau, B., Weissman, J., & Horwich, A. (2006). Molecular chaperones and protein quality control. *Cell, 125*(3), 443-451.

Caldwell, S. H., Swerdlow, R. H., Khan, E. M., Iezzoni, J. C., Hespenheide, E. E., Parks, J. K., & Parker Jr, W. D. J. J. o. h. (1999). Mitochondrial abnormalities in non-alcoholic steatohepatitis. *31*(3), 430-434.

Callegari, S., Dennerlein, S. J. F. i. c., & biology, d. (2018). Sensing the Stress: a role for the UPRmt and UPRam in the quality control of mitochondria. *6*, 31.

Cao, X., Yang, F., Shi, T., Yuan, M., Xin, Z., Xie, R., . . . Yang, J.-K. (2016). Angiotensin-converting enzyme 2/angiotensin-(1–7)/Mas axis activates Akt signaling to ameliorate hepatic steatosis. *Scientific reports, 6*, 21592. doi:10.1038/srep21592

https://www.nature.com/articles/srep21592#supplementary-information

care, A. D. A. J. D. (2013). Diagnosis and classification of diabetes mellitus. *36*(Supplement 1), S67-S74.

Ceni, E., Mello, T., & Galli, A. (2014). Pathogenesis of alcoholic liver disease: role of oxidative metabolism. *World Journal of Gastroenterology: WJG, 20*(47), 17756.

Chacinska, A., Koehler, C. M., Milenkovic, D., Lithgow, T., & Pfanner, N. J. C. (2009). Importing mitochondrial proteins: machineries and mechanisms. *138*(4), 628-644.

Chakraborty, K., Chatila, M., Sinha, J., Shi, Q., Poschner, B. C., Sikor, M., . . . Hayer-Hartl, M. J. C. (2010). Chaperonin-catalyzed rescue of kinetically trapped states in protein folding. *142*(1), 112-122.

Chan, D. C. (2006). Mitochondria: Dynamic Organelles in Disease, Aging, and Development. *Cell, 125*(7), 1241-1252. doi:https://doi.org/10.1016/j.cell.2006.06.010

Chao, T., Ianuzzo, C., Armstrong, R., Albright, J., Anapolle, S. J. C., & research, t. (1976). Ultrastructural alterations in skeletal muscle fibers of streptozotocin-diabetic rats. *168*(2), 239-246.

Chappell, M. C. (2012). The Non-Classical Renin-Angiotensin System and Renal Function. *Comprehensive Physiology, 2*(4), 2733.

Chavez, P. N., Stanley, W. C., McElfresh, T. A., Huang, H., Sterk, J. P., Chandler, M. P. J. A. J. o. P.-H., & Physiology, C. (2003). Effect of hyperglycemia and fatty acid oxidation inhibition during aerobic conditions and demand-induced ischemia. *284*(5), H1521-H1527.

Cheng, M. Y., Hartl, F.-U., Martin, J., Pollock, R. A., Kalousek, F., Neuper, W., . . . Horwich, A. L. J. N. (1989). Mitochondrial heat-shock protein hsp60 is essential for assembly of proteins imported into yeast mitochondria. *337*(6208), 620.

Cohen, D. E., Anania, F. A., & Chalasani, N. J. T. A. j. o. c. (2006). An assessment of statin safety by hepatologists. *97*(8), S77-S81.

Collier, G. R., McMillan, J. S., Windmill, K., Walder, K., Tenne-Brown, J., de Silva, A., . . . Zimmet, P. Z. (2000). Beacon: a novel gene involved in the regulation of energy balance. *Diabetes, 49*(11), 1766-1771.

Collino, M., Aragno, M., Mastrocola, R., Gallicchio, M., Rosa, A. C., Dianzani, C., . . . Fantozzi, R. J. E. j. o. p. (2006). Modulation of the oxidative stress and inflammatory response by PPAR-γ agonists in the hippocampus of rats exposed to cerebral ischemia/reperfusion. *530*(1-2), 70-80.

Cunningham, S. C., Dane, A. P., Spinoulas, A., & Alexander, I. E. J. M. T. (2008). Gene delivery to the juvenile mouse liver using AAV2/8 vectors. *16*(6), 1081-1088.

Cusi, K., Orsak, B., Bril, F., Lomonaco, R., Hecht, J., Ortiz-Lopez, C., . . . Musi, N. (2016). Long-term pioglitazone treatment for patients with nonalcoholic steatohepatitis and prediabetes or type 2 diabetes mellitus: a randomized trial. *Annals of internal medicine, 165*(5), 305-315.

Dane, A., Wowro, S., Cunningham, S., & Alexander, I. J. G. t. (2013). Comparison of gene transfer to the murine liver following intraperitoneal and intraportal delivery of hepatotropic AAV pseudo-serotypes. *20*(4), 460.

Daneman, D. J. T. L. (2006). Type 1 diabetes. *367*(9513), 847-858.

Day, P. E. L., Chambers, K. F., Winterbone, M. S., García-Blanco, T., Vauzour, D., & Kroon, P. A. (2018). Validation of control genes and a standardised protocol for quantifying gene expression in the livers of C57BL/6 and ApoE-/- mice. *Scientific Reports, 8*(1), 8081-8081. doi:10.1038/s41598-018-26431-3

De, A. M. J. S. (1999). Heat shock proteins: facts, thoughts, and dreams. *11*(1), 1-12.

De Meyts, P. (2016). The insulin receptor and its signal transduction network. In *Endotext [Internet]*: MDText. com, Inc.

Dell'Agnello, C., Leo, S., Agostino, A., Szabadkai, G., Tiveron, C., Zulian, A., . . . Zeviani, M. J. H. m. g. (2007). Increased longevity and refractoriness to Ca2+-dependent neurodegeneration in Surf1 knockout mice. *16*(4), 431-444.

Demeilliers, C., Maisonneuve, C., Grodet, A., Mansouri, A., Nguyen, R., Tinel, M., . . . Pessayre, D. J. G. (2002). Impaired adaptive resynthesis and prolonged depletion of hepatic mitochondrial DNA after repeated alcohol binges in mice. *123*(4), 1278-1290.

Demol, S., Yackobovitch-Gavan, M., Shalitin, S., Nagelberg, N., Gillon-Keren, M., & Phillip, M. J. A. P. (2009). Low-carbohydrate (low & high-fat) versus high-carbohydrate low-fat diets in the treatment of obesity in adolescents. *98*(2), 346-351.

Dendup, T., Feng, X., Clingan, S., Astell-Burt, T. J. I. j. o. e. r., & health, p. (2018). Environmental risk factors for developing type 2 diabetes mellitus: a systematic review. *15*(1), 78.

Deocaris, C. C., Kaul, S. C., Wadhwa, R. J. C. s., & chaperones. (2006). On the brotherhood of the mitochondrial chaperones mortalin and heat shock protein 60. *11*(2), 116.

Diabetes, N. D. D. G. J. (1979). Classification and diagnosis of diabetes mellitus and other categories of glucose intolerance. *28*(12), 1039-1057.

Dikalova, A. E., Bikineyeva, A. T., Budzyn, K., Nazarewicz, R. R., McCann, L., Lewis, W., . . . Dikalov, S. I. J. C. r. (2010). Therapeutic targeting of mitochondrial superoxide in hypertension. *107*(1), 106.

Dixon, J. B., Bhathal, P. S., & O'Brien, P. E. (2001). Nonalcoholic fatty liver disease: predictors of nonalcoholic steatohepatitis and liver fibrosis in the severely obese. *Gastroenterology, 121*(1), 91-100.

Dobrian, A. D., Schriver, S. D., Khraibi, A. A., & Prewitt, R. L. J. H. (2004). Pioglitazone prevents hypertension and reduces oxidative stress in diet-induced obesity. *43*(1), 48-56.

Donati, G., Stagni, B., Piscaglia, F., Venturoli, N., Morselli-Labate, A., Rasciti, L., & Bolondi, L. J. G. (2004). Increased prevalence of fatty liver in arterial hypertensive patients with normal liver enzymes: role of insulin resistance. *53*(7), 1020-1023.

Dongiovanni, P., M Anstee, Q., & Valenti, L. J. C. p. d. (2013). Genetic predisposition in NAFLD and NASH: impact on severity of liver disease and response to treatment. *19*(29), 5219-5238.

Dongiovanni, P., Valenti, L., Rametta, R., Daly, A., Nobili, V., Mozzi, E., . . . Maggioni, M. J. G. (2010). Genetic variants regulating insulin receptor signalling are associated with the severity of liver damage in patients with non-alcoholic fatty liver disease. *59*(2), 267-273.

Donoghue, M., Hsieh, F., Baronas, E., Godbout, K., Gosselin, M., Stagliano, N., . . . Jeyaseelan, R. (2000). A novel angiotensin-converting enzyme–related carboxypeptidase (ACE2) converts angiotensin I to angiotensin 1-9. *Circulation Research, 87*(5), e1-e9.

dos Santos, A. R., Lopes-Costa, P. V., de Castro, J. C. D., Campos, I. C., Borges, R. S., Pires, C. G., . . . da Silva, B. B. (2008). Morphometric analysis of the urethra of castrated female rats treated with tamoxifen. *Maturitas, 59*(3), 275-280. doi:https://doi.org/10.1016/j.maturitas.2008.02.010

Dufour, J.-F., Clavien, P.-A., Graf, R., & Trautwein, C. (2010). *Signaling pathways in liver diseases*: Springer.

Duszka, K., Oresic, M., Le May, C., König, J., & Wahli, W. (2017). PPARγ Modulates Long Chain Fatty Acid Processing in the Intestinal Epithelium. *International journal of molecular sciences, 18*(12), 2559. doi:10.3390/ijms18122559

Eckel, R. H., Grundy, S. M., & Zimmet, P. Z. (2005). The metabolic syndrome. *The Lancet, 365*(9468), 1415-1428.

Eguchi, Y., Shimizu, S., & Tsujimoto, Y. (1997). Intracellular ATP Levels Determine Cell Death Fate by Apoptosis or Necrosis. *Cancer Research, 57*(10), 1835-1840.

Eilers, M., Hwang, S., & Schatz, G. J. T. E. j. (1988). Unfolding and refolding of a purified precursor protein during import into isolated mitochondria. *7*(4), 1139-1145.

Ekström, G., & Ingelman-Sundberg, M. (1989). Rat liver microsomal NADPH-supported oxidase activity and lipid peroxidation dependent on ethanol-inducible cytochrome P-450 (P-450IIE1). *Biochemical Pharmacology, 38*(8), 1313-1319. doi:https://doi.org/10.1016/0006-2952(89)90338-9

El-Hattab, A. W., Zarante, A. M., Almannai, M., Scaglia, F. J. M. g., & metabolism. (2017). Therapies for mitochondrial diseases and current clinical trials. *122*(3), 1-9.

Farrell, G. C., & Larter, C. Z. (2006). Nonalcoholic fatty liver disease: from steatosis to cirrhosis. *Hepatology, 43*(S1), S99-S112.

Felig, P. (1975). Amino Acid Metabolism in Man. *Annual Review of Biochemistry, 44*(1), 933-955. doi:10.1146/annurev.bi.44.070175.004441

Fellman, V., & Kotarsky, H. (2011). *Mitochondrial hepatopathies in the newborn period.* Paper presented at the Seminars in Fetal and Neonatal Medicine.

Fernández-Silva, P., Enriquez, J. A., & Montoya, J. (2003). Replication and transcription of mammalian mitochondrial DNA. *Experimental physiology, 88*(1), 41-56.

Fiorese, C. J., Schulz, A. M., Lin, Y.-F., Rosin, N., Pellegrino, M. W., & Haynes, C. M. J. C. B. (2016). The transcription factor ATF5 mediates a mammalian mitochondrial UPR. *26*(15), 2037-2043.

Friedman, J. S., Koop, B. F., Raymond, V., & Walter, M. A. (2001). Isolation of a ubiquitin-like (UBL5) gene from a screen identifying highly expressed and conserved iris genes. *Genomics, 71*(2), 252-255. doi:10.1006/geno.2000.6439

Frisard, M., & Ravussin, E. (2006). Energy metabolism and oxidative stress. *Endocrine, 29*(1), 27-32. doi:10.1385/ENDO:29:1:27

Fromenty, B., Berson, A., & Pessayre, D. (1997). Microvesicular steatosis and steatohepatitis: role of mitochondrial dysfunction and lipid peroxidation. *Journal of hepatology, 26*, 13-22. doi:https://doi.org/10.1016/S0168-8278(97)82328-8

Fromenty, B., & Pessayre, D. (1995). Inhibition of mitochondrial beta-oxidation as a mechanism of hepatotoxicity. *Pharmacology & Therapeutics, 67*(1), 101-154. doi:https://doi.org/10.1016/0163-7258(95)00012-6

Fromenty, B., Pessayre, D. J. P., & therapeutics. (1995). Inhibition of mitochondrial beta-oxidation as a mechanism of hepatotoxicity. *67*(1), 101-154.

Gale, E. A. (2006). Declassifying diabetes. In: Springer.

Gandhi, C. R., Chaillet, J. R., Nalesnik, M. A., Kumar, S., Dangi, A., Demetris, A. J., . . . Stankeiwicz, T. J. G. (2015). Liver-specific deletion of augmenter of liver regeneration accelerates development of steatohepatitis and hepatocellular carcinoma in mice. *148*(2), 379-391. e374.

García-Berumen, C. I., Ortiz-Avila, O., Vargas-Vargas, M. A., del Rosario-Tamayo, B. A., Guajardo-López, C., Saavedra-Molina, A., . . . Disease. (2019). The severity of rat liver injury by fructose and high fat depends on the degree of respiratory dysfunction and oxidative stress induced in mitochondria. *18*(1), 78.

García-Ruiz, I., Rodríguez-Juan, C., Díaz-Sanjuan, T., del Hoyo, P., Colina, F., Muñoz-Yagüe, T., & Solís-Herruzo, J. A. (2006). Uric acid and anti-TNF antibody improve mitochondrial dysfunction in ob/ob mice. *Hepatology, 44*(3), 581-591. doi:doi:10.1002/hep.21313

Ghezzi, D., & Zeviani, M. (2012). Assembly factors of human mitochondrial respiratory chain complexes: physiology and pathophysiology. In *Mitochondrial Oxidative Phosphorylation* (pp. 65-106): Springer.

Gispert, S., Parganlija, D., Klinkenberg, M., Dröse, S., Wittig, I., Mittelbronn, M., . . . Auburger, G. (2013). Loss of mitochondrial peptidase Clpp leads to infertility, hearing loss plus growth retardation via accumulation of CLPX, mtDNA and inflammatory factors. *Human Molecular Genetics, 22*(24), 4871-4887. doi:10.1093/hmg/ddt338 %J Human Molecular Genetics

Gloyn, A. L., Weedon, M. N., Owen, K. R., Turner, M. J., Knight, B. A., Hitman, G., . . . Halford, S. J. D. (2003). Large-scale association studies of variants in genes encoding the pancreatic β-cell KATP channel subunits Kir6. 2 (KCNJ11) and SUR1 (ABCC8) confirm that the KCNJ11 E23K variant is associated with type 2 diabetes. *52*(2), 568-572.

Gopaul, D. N., & Van Duyne, G. D. (1999). Structure and mechanism in site-specific recombination. *Current Opinion in Structural Biology, 9*(1), 14-20. doi:https://doi.org/10.1016/S0959-440X(99)80003-7

Grabacka, M., Pierzchalska, M., Dean, M., & Reiss, K. J. I. j. o. m. s. (2016). Regulation of ketone body metabolism and the role of PPARα. *17*(12), 2093.

Green, D. R. (2005). Apoptotic pathways: ten minutes to dead. *Cell, 121*(5), 671-674.

Gumieniczek, A. J. L. s. (2003). Effect of the new thiazolidinedione-pioglitazone on the development of oxidative stress in liver and kidney of diabetic rabbits. *74*(5), 553-562.

Guo, C., Yang, W., & Lobe, C. G. (2002). A cre recombinase transgene with mosaic, widespread tamoxifen-inducible action. *Genesis, 32*(1), 8-18. doi:doi:10.1002/gene.10021

Guo, Y., Darshi, M., Ma, Y., Perkins, G. A., Shen, Z., Haushalter, K. J., . . . Taylor, S. S. (2013). Quantitative Proteomic and Functional Analysis of Liver Mitochondria from High Fat Diet (HFD) Diabetic Mice. *12*(12), 3744-3758. doi:10.1074/mcp.M113.027441 %J Molecular & Cellular Proteomics

Ha, H. C., & Snyder, S. H. (1999). Poly(ADP-ribose) polymerase is a mediator of necrotic cell death by ATP depletion. *Proceedings of the National Academy of Sciences, 96*(24), 13978-13982. doi:10.1073/pnas.96.24.13978

Hagihara, B., Sato, N., Fukuhara, T., Tsutsumi, K., & Ōyanagui, Y. (1973). Spectrophotometric Analysis of Cytochromes in Morris Hepatomas. *Cancer Research, 33*(11), 2947-2953.

Haider, R., Robin, M.-A., Fang, J.-K., & Avadhani, N. G. J. B. J. (2002). Multiple isoforms of mitochondrial glutathione S-transferases and their differential induction under oxidative stress. *366*(1), 45-55.

Hajnóczky, G., Csordás, G., Das, S., Garcia-Perez, C., Saotome, M., Roy, S. S., & Yi, M. (2006). Mitochondrial calcium signalling and cell death: approaches for assessing the role of mitochondrial Ca 2+ uptake in apoptosis. *Cell calcium, 40*(5), 553-560.

Handschin, C., Lin, J., Rhee, J., Peyer, A.-K., Chin, S., Wu, P.-H., . . . Spiegelman, B. M. (2005). Nutritional Regulation of Hepatic Heme Biosynthesis and Porphyria through PGC-1α. *Cell, 122*(4), 505-515. doi:https://doi.org/10.1016/j.cell.2005.06.040

Hansen, P. A., Han, D. H., Marshall, B. A., Nolte, L. A., Chen, M. M., Mueckler, M., & Holloszy, J. O. J. J. o. B. C. (1998). A high fat diet impairs stimulation of glucose transport in muscle functional evaluation of potential mechanisms. *273*(40), 26157-26163.

Hanson, E. S., & Dallman, M. F. (1995). Neuropeptide Y (NPY) may integrate responses of hypothalamic feeding systems and the hypothalamo-pituitary-adrenal axis. *Journal of neuroendocrinology, 7*(4), 273-279.

Harper, M. E., Bevilacqua, L., Hagopian, K., Weindruch, R., & Ramsey, J. J. J. A. P. S. (2004). Ageing, oxidative stress, and mitochondrial uncoupling. *182*(4), 321-331.

Hartl, F.-U., Martin, J., Neupert, W. J. A. r. o. b., & structure, b. (1992). Protein folding in the cell: the role of molecular chaperones Hsp70 and Hsp60. *21*(1), 293-322.

Hartl, F. U., Bracher, A., & Hayer-Hartl, M. (2011). Molecular chaperones in protein folding and proteostasis. *Nature, 475*(7356), 324-332.

Häussinger, D., Sies, H., & Gerok, W. (1985). Functional hepatocyte heterogeneity in ammonia metabolism: the intercellular glutamine cycle. *Journal of hepatology, 1*(1), 3-14.

Hautekeete, M., Degott, C., & Benhamou, J.-P. J. A. C. B. (1990). Microvesicular steatosis of the liver. *45*(5), 311-326.

Haynes, C. M., Petrova, K., Benedetti, C., Yang, Y., & Ron, D. (2007). ClpP mediates activation of a mitochondrial unfolded protein response in C. elegans. *Dev Cell, 13*(4), 467-480.

Haynes, C. M., Petrova, K., Benedetti, C., Yang, Y., & Ron, D. J. D. c. (2007). ClpP mediates activation of a mitochondrial unfolded protein response in C. elegans. *13*(4), 467-480.

Haynes, C. M., & Ron, D. (2010). The mitochondrial UPR - protecting organelle protein homeostasis. *J Cell Sci, 123*(Pt 22), 3849-3855.

Haynes, C. M., Yang, Y., Blais, S. P., Neubert, T. A., & Ron, D. (2010). The Matrix Peptide Exporter HAF-1 Signals a Mitochondrial UPR by Activating the Transcription Factor ZC376.7 in C. elegans. *Molecular Cell, 37*(4), 529-540. doi:https://doi.org/10.1016/j.molcel.2010.01.015

Hellerstein, M. K. J. C. o. i. l. (2002). Carbohydrate-induced hypertriglyceridemia: modifying factors and implications for cardiovascular risk. *13*(1), 33-40.

Henze, K., & Martin, W. (2003). Essence of mitochondria. *Nature, 426*(6963), 127-128. doi:10.1038/426127a

Herlein, J. A., Fink, B. D., O'Malley, Y., & Sivitz, W. I. J. E. (2008). Superoxide and respiratory coupling in mitochondria of insulin-deficient diabetic rats. *150*(1), 46-55.

Holloszy, J. O., Oscai, L. B., Don, I. J., & Molé, P. A. (1970). Mitochondrial citric acid cycle and related enzymes: Adaptive response to exercise. *Biochemical and biophysical research communications, 40*(6), 1368-1373. doi:https://doi.org/10.1016/0006-291X(70)90017-3

Horibe, T., & Hoogenraad, N. J. (2007). The chop gene contains an element for the positive regulation of the mitochondrial unfolded protein response. *PLoS One, 2*(9), e835.

Horibe, T., & Hoogenraad, N. J. J. P. o. (2007). The chop gene contains an element for the positive regulation of the mitochondrial unfolded protein response. *2*(9), e835.

Hotamisligil, G. S. (2006). Inflammation and metabolic disorders. *Nature, 444*(7121), 860.

Hsiao, P.-J., Chiou, H.-Y. C., Jiang, H.-J., Lee, M.-Y., Hsieh, T.-J., & Kuo, K.-K. (2017). Pioglitazone Enhances Cytosolic Lipolysis, β-oxidation and Autophagy to Ameliorate Hepatic Steatosis. *Scientific Reports, 7*(1), 9030. doi:10.1038/s41598-017-09702-3

Hulin, B., McCarthy, P. A., & Gibbs, E. M. (1996). The glitazone family of antidiabetic agents. *Current Pharmaceutical Design, 2*(1), 85-102.

Huss Janice, M., & Kelly Daniel, P. (2004). Nuclear Receptor Signaling and Cardiac Energetics. *Circulation Research, 95*(6), 568-578. doi:10.1161/01.RES.0000141774.29937.e3

Ibdah, J. A., Perlegas, P., Zhao, Y., Angdisen, J., Borgerink, H., Shadoan, M. K., . . . Cline, J. M. J. G. (2005). Mice heterozygous for a defect in mitochondrial trifunctional protein develop hepatic steatosis and insulin resistance. *128*(5), 1381-1390.

Ikai, E., Noborizaka, Y., Tsuritani, I., Honda, R., Ishizaki, M., & Yamada, Y. J. O. r. (1993). Serum γ-Glutamyl Transpeptidase Levels and Hypertension in Non-drinkers: A Possible Role of Fatty Liver in the Pathogenesis of Obesity Related Hypertension. *1*(6), 469-474.

Imperatore, G., Knowler, W. C., Pettitt, D. J., Kobes, S., Fuller, J. H., Bennett, P. H., & Hanson, R. L. (2000). A Locus Influencing Total Serum Cholesterol on Chromosome 19p

Results From an Autosomal Genomic Scan of Serum Lipid Concentrations in Pima Indians. *Arteriosclerosis, thrombosis, and vascular biology, 20*(12), 2651-2656.

Isomaa, B. (2003). A major health hazard: the metabolic syndrome. *Life sciences, 73*(19), 2395-2411.

Jacobs, B., De Angelis-Schierbaum, G., Egert, S., Assmann, G., & Kratz, M. (2004). Individual Serum Triglyceride Responses to High-Fat and Low-Fat Diets Differ in Men with Modest and Severe Hypertriglyceridemia. *The Journal of Nutrition, 134*(6), 1400-1405. doi:10.1093/jn/134.6.1400 %J The Journal of Nutrition

Jaynes, J. B., Johnson, J. E., Buskin, J. N., Gartside, C. L., & Hauschka, S. D. (1988). The muscle creatine kinase gene is regulated by multiple upstream elements, including a muscle-specific enhancer. *Molecular and cellular biology, 8*(1), 62-70. doi:10.1128/mcb.8.1.62

Ji, C., & Kaplowitz, N. (2003). Betaine decreases hyperhomocysteinemia, endoplasmic reticulum stress, and liver injury in alcohol-fed mice. *Gastroenterology, 124*(5), 1488-1499.

Johannsen, D. L., & Ravussin, E. (2009). The role of mitochondria in health and disease. *Current opinion in pharmacology, 9*(6), 780-786. doi:10.1016/j.coph.2009.09.002

Johnson, J. E., Wold, B. J., & Hauschka, S. D. (1989). Muscle creatine kinase sequence elements regulating skeletal and cardiac muscle expression in transgenic mice. *Molecular and cellular biology, 9*(8), 3393-3399. doi:10.1128/mcb.9.8.3393

Johnston, D. E. (1999). Special considerations in interpreting liver function tests. *American family physician, 59*(8), 2223-2230.

Jowett, J. B., Elliott, K. S., Curran, J. E., Hunt, N., Walder, K. R., Collier, G. R., . . . Blangero, J. (2004). Genetic variation in BEACON influences quantitative variation in metabolic syndrome-related phenotypes. *Diabetes, 53*(9), 2467-2472.

Jurczak, M. J., Lee, A.-H., Jornayvaz, F. R., Lee, H.-Y., Birkenfeld, A. L., Guigni, B. A., . . . Shulman, G. I. (2012). Dissociation of inositol-requiring enzyme (IRE1α)-mediated c-Jun N-terminal kinase activation from hepatic insulin resistance in conditional X-box-binding protein-1 (XBP1) knock-out mice. *Journal of Biological Chemistry, 287*(4), 2558-2567.

Kaczmarczyk, S. J., & Green, J. E. J. N. a. r. (2003). Induction of cre recombinase activity using modified androgen receptor ligand binding domains: a sensitive assay for ligand-receptor interactions. *31*(15), e86-e86.

Kahn, S. E., Hull, R. L., & Utzschneider, K. M. J. N. (2006). Mechanisms linking obesity to insulin resistance and type 2 diabetes. *444*(7121), 840.

Kammoun, H. L., Chabanon, H., Hainault, I., Luquet, S., Magnan, C., Koike, T., . . . Foufelle, F. (2009). GRP78 expression inhibits insulin and ER stress–induced SREBP-1c activation and reduces hepatic steatosis in mice. *The Journal Of Clinical Investigation, 119*(5), 1201-1215.

Kang, P.-J., Ostermann, J., Shilling, J., Neupert, W., Craig, E. A., & Pfanner, N. J. N. (1990). Requirement for hsp70 in the mitochondrial matrix for translocation and folding of precursor proteins. *348*(6297), 137.

Kaprio, J., Tuomilehto, J., Koskenvuo, M., Romanov, K., Reunanen, A., Eriksson, J., . . . Kesäniemi, Y. J. D. (1992). Concordance for type 1 (insulin-dependent) and type 2 (non-insulin-dependent) diabetes mellitus in a population-based cohort of twins in Finland. *35*(11), 1060-1067.

Kebede, M., Favaloro, J., Gunton, J. E., Laybutt, D. R., Shaw, M., Wong, N., . . . Andrikopoulos, S. (2008). Fructose-1,6-bisphosphatase overexpression in pancreatic beta-cells results in reduced insulin secretion: a new mechanism for fat-induced impairment of beta-cell function. *Diabetes, 57*(7), 1887-1895. doi:10.2337/db07-1326

Kelley, D. E., He, J., Menshikova, E. V., & Ritov, V. B. (2002). Dysfunction of Mitochondria in Human Skeletal Muscle in Type 2 Diabetes. *Diabetes, 51*(10), 2944-2950. doi:10.2337/diabetes.51.10.2944

Kelley, D. E., He, J., Menshikova, E. V., & Ritov, V. B. J. D. (2002). Dysfunction of mitochondria in human skeletal muscle in type 2 diabetes. *51*(10), 2944-2950.

Kenny, T. C., Craig, A. J., Villanueva, A., & Germain, D. (2019). Mitohormesis Primes Tumor Invasion and Metastasis. *Cell Reports, 27*(8), 2292-2303.e2296. doi:https://doi.org/10.1016/j.celrep.2019.04.095

Kheong, C. W., Mustapha, N. R. N., Mahadeva, S. J. C. G., & Hepatology. (2017). A randomized trial of silymarin for the treatment of nonalcoholic steatohepatitis. *15*(12), 1940-1949. e1948.

Kiermayer, C., Conrad, M., Schneider, M., Schmidt, J., & Brielmeier, M. (2007). Optimization of spatiotemporal gene inactivation in mouse heart by oral application of tamoxifen citrate. *Genesis, 45*(1), 11-16.

Kikis, E. A., Gidalevitz, T., & Morimoto, R. I. (2010). Protein homeostasis in models of aging and age-related conformational disease. In *Protein Metabolism and Homeostasis in Aging* (pp. 138-159): Springer.

Kim, J.-a., Wei, Y., & Sowers James, R. (2008). Role of Mitochondrial Dysfunction in Insulin Resistance. *Circulation Research, 102*(4), 401-414. doi:10.1161/CIRCRESAHA.107.165472

Klinge, C. M. (2008). Estrogenic control of mitochondrial function and biogenesis. *Journal of cellular biochemistry, 105*(6), 1342-1351.

Knauf, C., Cani, P. D., Perrin, C., Iglesias, M. A., Maury, J. F., Bernard, E., . . . Burcelin, R. (2005). Brain glucagon-like peptide–1 increases insulin secretion and muscle insulin resistance to favor hepatic glycogen storage. *The Journal Of Clinical Investigation, 115*(12), 3554-3563. doi:10.1172/JCI25764

Kokoszka, J. E., Coskun, P., Esposito, L. A., & Wallace, D. C. J. P. o. t. N. A. o. S. (2001). Increased mitochondrial oxidative stress in the Sod2 (+/−) mouse results in the age-related decline of mitochondrial function culminating in increased apoptosis. *98*(5), 2278-2283.

Koopman, W. J., Willems, P. H., & Smeitink, J. A. (2012). Monogenic mitochondrial disorders. *New England Journal of Medicine, 366*(12), 1132-1141.

Kraegen, E., James, D., Storlien, L., Burleigh, K., & Chisholm, D. J. D. (1986). In vivo insulin resistance in individual peripheral tissues of the high fat fed rat: assessment by euglycaemic clamp plus deoxyglucose administration. *29*(3), 192-198.

Kulkarni, R. N., Bruning, J. C., Winnay, J. N., Postic, C., Magnuson, M. A., & Kahn, C. R. (1999). Tissue-specific knockout of the insulin receptor in pancreatic beta cells creates an insulin secretory defect similar to that in type 2 diabetes. *Cell, 96*(3), 329-339.

Lamont, B. J., Visinoni, S., Fam, B. C., Kebede, M., Weinrich, B., Papapostolou, S., . . . Andrikopoulos, S. (2006). Expression of human fructose-1, 6-bisphosphatase in the liver of transgenic mice results in increased glycerol gluconeogenesis. *Endocrinology, 147*(6), 2764-2772.

lancet, U. P. D. S. G. J. T. (1998). Intensive blood-glucose control with sulphonylureas or insulin compared with conventional treatment and risk of complications in patients with type 2 diabetes (UKPDS 33). *352*(9131), 837-853.

Lapointe, J., & Hekimi, S. J. J. o. B. C. (2008). Early mitochondrial dysfunction in long-lived Mclk1+/-mice. *283*(38), 26217-26227.

Lee, A.-H., Scapa, E. F., Cohen, D. E., & Glimcher, L. H. (2008). Regulation of hepatic lipogenesis by the transcription factor XBP1. *Science, 320*(5882), 1492-1496.

Lee, M. (2009). *Basic skills in interpreting laboratory data*: ASHP.

Lee, W. S., & Sokol, R. J. J. H. (2007). Mitochondrial hepatopathies: advances in genetics and pathogenesis. *45*(6), 1555-1565.

Leoni, S., Tovoli, F., Napoli, L., Serio, I., Ferri, S., & Bolondi, L. (2018). Current guidelines for the management of non-alcoholic fatty liver disease: A systematic review with comparative analysis. *World journal of gastroenterology, 24*(30), 3361-3373. doi:10.3748/wjg.v24.i30.3361

Lesnefsky, E. J., Moghaddas, S., Tandler, B., Kerner, J., & Hoppel, C. L. (2001). Mitochondrial Dysfunction in Cardiac Disease: Ischemia–Reperfusion, Aging, and Heart Failure. *Journal of Molecular and Cellular Cardiology, 33*(6), 1065-1089. doi:https://doi.org/10.1006/jmcc.2001.1378

Leung, C., Herath, C. B., Jia, Z., Andrikopoulos, S., Brown, B. E., Davies, M. J., . . . Angus, P. W. (2016). Dietary advanced glycation end-products aggravate non-alcoholic fatty liver disease. *World journal of gastroenterology, 22*(35), 8026-8040. doi:10.3748/wjg.v22.i35.8026

Lewandoski, M. (2001). Conditional control of gene expression in the mouse. *Nature Reviews Genetics, 2*, 743. doi:10.1038/35093537

https://www.nature.com/articles/35093537#supplementary-information

Li, X., Fang, P., Mai, J., Choi, E. T., Wang, H., & Yang, X.-f. (2013). Targeting mitochondrial reactive oxygen species as novel therapy for inflammatory diseases and cancers. *J Hematol Oncol, 6*(1), 19.

Li, Z., & Srivastava, P. (2004). Heat-shock proteins Current protocols in immunology/edited by John E Coligan [et al.]. In: Appendix.

Liberman, E., Fong, Y.-L., Selby, M. J., Choo, Q.-L., Cousens, L., Houghton, M., & Yen, T. B. (1999). Activation of the grp78 andgrp94 Promoters by Hepatitis C Virus E2 Envelope Protein. *Journal of virology, 73*(5), 3718-3722.

Lies, M., & Maurizi, M. R. J. J. o. B. C. (2008). Turnover of endogenous SsrA-tagged proteins mediated by ATP-dependent proteases in Escherichia coli. *283*(34), 22918-22929.

Lin, Y.-F., & Haynes, C. M. J. M. c. (2016). Metabolism and the UPRmt. *61*(5), 677-682.

Lindquist, S., & Craig, E. (1988). The heat-shock proteins. *Annu Rev Genet, 22*(1), 631-677.

Lindquist, S., & Craig, E. A. (1988). The heat-shock proteins. *Annu Rev Genet, 22*, 631-677.

Lithgow, T. J. F. l. (2000). Targeting of proteins to mitochondria. *476*(1-2), 22-26.

Liu, G., Coulston, A., Hollenbeck, C., Reaven, G. J. T. J. o. C. E., & Metabolism. (1984). The effect of sucrose content in high and low carbohydrate diets on plasma glucose, insulin, and lipid responses in hypertriglyceridemic humans. *59*(4), 636-642.

Liu, G. C., Coulston, A. M., & Reaven, G. M. J. M. (1983). Effect of high-carbohydrate-low-fat diets on plasma glucose, insulin and lipid responses in hypertriglyceridemic humans. *32*(8), 750-753.

Liu, Q., Krzewska, J., Liberek, K., & Craig, E. A. J. J. o. B. C. (2001). Mitochondrial Hsp70 Ssc1: role in protein folding. *276*(9), 6112-6118.

Lonardo, A., Bellini, M., Tartoni, P., Tondelli, E. J. I. j. o. g., & hepatology. (1997). The bright liver syndrome. Prevalence and determinants of a" bright" liver echopattern. *29*(4), 351-356.

Lonardo, A., & Trande, P. (2000). Are there any sex differences in fatty liver? A study of glucose metabolism and body fat distribution. *15*(7), 775-782. doi:10.1046/j.1440-1746.2000.02226.x

Lowell, B. B., & Shulman, G. I. (2005). Mitochondrial Dysfunction and Type 2 Diabetes. *Science, 307*(5708), 384. doi:10.1126/science.1104343

Lu, M., Wan, M., Leavens, K. F., Chu, Q., Monks, B. R., Fernandez, S., . . . Birnbaum, M. J. J. N. m. (2012). Insulin regulates liver metabolism in vivo in the absence of hepatic Akt and Foxo1. *18*(3), 388.

Lu, Y., & Song, S. J. P. o. t. N. A. o. S. (2009). Distinct immune responses to transgene products from rAAV1 and rAAV8 vectors. *106*(40), 17158-17162.

Lubel, J. S., Herath, C. B., Burrell, L. M., & Angus, P. W. (2008). Liver disease and the renin–angiotensin system: recent discoveries and clinical implications. *Journal of gastroenterology and hepatology, 23*(9), 1327-1338.

Lutchman, G., Modi, A., Kleiner, D. E., Promrat, K., Heller, T., Ghany, M., . . . Premkumar, A. (2007). The effects of discontinuing pioglitazone in patients with nonalcoholic steatohepatitis. *Hepatology, 46*(2), 424-429.

Mak, K. Y., Chin, R., Cunningham, S. C., Habib, M. R., Torresi, J., Sharland, A. F., . . . Herath, C. B. (2015a). ACE2 Therapy Using Adeno-associated Viral Vector Inhibits Liver Fibrosis in Mice. *Molecular therapy : the journal of the American Society of Gene Therapy, 23*(9), 1434-1443. doi:10.1038/mt.2015.92

Mak, K. Y., Chin, R., Cunningham, S. C., Habib, M. R., Torresi, J., Sharland, A. F., . . . Herath, C. B. (2015b). ACE2 Therapy Using Adeno-associated Viral Vector Inhibits Liver Fibrosis in Mice. *Molecular Therapy, 23*(9), 1434-1443. doi:https://doi.org/10.1038/mt.2015.92

Mangelsdorf, D. J., Thummel, C., Beato, M., Herrlich, P., Schütz, G., Umesono, K., . . . Chambon, P. J. C. (1995). The nuclear receptor superfamily: the second decade. *83*(6), 835.

Manning-Krieg, U., Scherer, P., & Schatz, G. J. T. E. j. (1991). Sequential action of mitochondrial chaperones in protein import into the matrix. *10*(11), 3273-3280.

Manoli, I., Alesci, S., Blackman, M. R., Su, Y. A., Rennert, O. M., & Chrousos, G. P. (2007). Mitochondria as key components of the stress response. *Trends in Endocrinology & Metabolism, 18*(5), 190-198.

Mansouri, A., Fromenty, B., Berson, A., Robin, M.-A., Grimbert, S., Beaugrand, M., . . . Pessayre, D. J. J. o. h. (1997). Multiple hepatic mitochondrial DNA deletions suggest premature oxidative aging in alcoholic patients. *27*(1), 96-102.

Mansouri, A., Gattolliat, C.-H., & Asselah, T. J. G. (2018). Mitochondrial dysfunction and signaling in chronic liver diseases.

Mantena, S. K., Vaughn, D. P., Andringa, K. K., Eccleston, H. B., King, A. L., Abrams, G. A., . . . Bailey, S. M. J. B. J. (2009). High fat diet induces dysregulation of hepatic oxygen gradients and mitochondrial function in vivo. *417*(1), 183-193.

Marchesini, G., Brizi, M., Bianchi, G., Tomassetti, S., Bugianesi, E., Lenzi, M., . . . Melchionda, N. (2001). Nonalcoholic Fatty Liver Disease. *Diabetes, 50*(8), 1844. doi:10.2337/diabetes.50.8.1844

Marchesini, G., Brizi, M., Bianchi, G., Tomassetti, S., Bugianesi, E., Lenzi, M., . . . Melchionda, N. (2001). Nonalcoholic fatty liver disease: a feature of the metabolic syndrome. *Diabetes, 50*(8), 1844-1850.

Marchesini, G., Brizi, M., Morselli-Labate, A. M., Bianchi, G., Bugianesi, E., McCullough, A. J., . . . Melchionda, N. (1999). Association of nonalcoholic fatty liver disease with insulin resistance. *Am J Med, 107*(5), 450-455.

Marchesini, G., Bugianesi, E., Forlani, G., Cerrelli, F., Lenzi, M., Manini, R., . . . Rizzetto, M. (2003). Nonalcoholic fatty liver, steatohepatitis, and the metabolic syndrome. *Hepatology, 37*(4), 917-923. doi:doi:10.1053/jhep.2003.50161

Marchesini, G., Bugianesi, E., Forlani, G., Cerrelli, F., Lenzi, M., Manini, R., . . . Rizzetto, M. (2003). Nonalcoholic fatty liver, steatohepatitis, and the metabolic syndrome. *Hepatology, 37*(4), 917-923.

Marinari, U. M., Monacelli, R., Cottalasso, D., & Novelli, A. J. A. d. l. (1974). Effects of alloxan diabetes and insulin on morphology and certain functional activities of mitochondria of the rat liver and heart. *11*(4), 296-314.

Markan, K. R., & Potthoff, M. J. (2016). Metabolic fibroblast growth factors (FGFs): Mediators of energy homeostasis. *Seminars in Cell & Developmental Biology, 53*, 85-93. doi:https://doi.org/10.1016/j.semcdb.2015.09.021

Marker, T., Sell, H., Zillessen, P., Glode, A., Kriebel, J., Ouwens, D. M., . . . Habich, C. (2012). Heat shock protein 60 as a mediator of adipose tissue inflammation and insulin resistance. *Diabetes, 61*(3), 615-625. doi:10.2337/db10-1574

Matteoni, C. A., Younossi, Z. M., Gramlich, T., Boparai, N., Liu, Y. C., & McCullough, A. J. (1999). Nonalcoholic fatty liver disease: A spectrum of clinical and pathological severity. *Gastroenterology, 116*(6), 1413-1419. doi:https://doi.org/10.1016/S0016-5085(99)70506-8

Matthews, D. R., Charbonnel, B. H., Hanefeld, M., Brunetti, P., & Schernthaner, G. (2005). Long-term therapy with addition of pioglitazone to metformin compared with the addition of gliclazide to metformin in patients with type 2 diabetes: a randomized, comparative study. *21*(2), 167-174. doi:10.1002/dmrr.478

Mayer, M., Bukau, B. J. C., & sciences, m. l. (2005). Hsp70 chaperones: cellular functions and molecular mechanism. *62*(6), 670.

McBride, H. M., Neuspiel, M., & Wasiak, S. (2006). Mitochondria: More Than Just a Powerhouse. *Current Biology, 16*(14), R551-R560. doi:https://doi.org/10.1016/j.cub.2006.06.054

McCullough, A. J. J. C. i. l. d. (2004). The clinical features, diagnosis and natural history of nonalcoholic fatty liver disease. *8*(3), 521-533.

McNally, T., Huang, Q., Janis, R. S., Liu, Z., Olejniczak, E. T., & Reilly, R. M. (2003). Structural analysis of UBL5, a novel ubiquitin-like modifier. *Protein Sci, 12*(7), 1562-1566. doi:10.1110/ps.0382803

Meigs, J. B., Cupples, L. A., & Wilson, P. J. D. (2000). Parental transmission of type 2 diabetes: the Framingham Offspring Study. *49*(12), 2201-2207.

Melber, A., & Haynes, C. M. J. C. r. (2018). UPR mt regulation and output: a stress response mediated by mitochondrial-nuclear communication. *28*(3), 281.

Metzger, D., Clifford, J., Chiba, H., & Chambon, P. (1995). Conditional site-specific recombination in mammalian cells using a ligand-dependent chimeric Cre recombinase. *Proceedings of the National Academy of Sciences, 92*(15), 6991-6995. doi:10.1073/pnas.92.15.6991

Miele, L., Beale, G., Patman, G., Nobili, V., Leathart, J., Grieco, A., . . . Bugianesi, E. J. G. (2008). The Kruppel-like factor 6 genotype is associated with fibrosis in nonalcoholic fatty liver disease. *135*(1), 282-291. e281.

Milenkovic, D., Müller, J., Stojanovski, D., Pfanner, N., & Chacinska, A. J. B. c. (2007). Diverse mechanisms and machineries for import of mitochondrial proteins. *388*(9), 891-897.

Miller, G., Suzuki, N., Ciftci-Yilmaz, S., & Mittler, R. (2010). Reactive oxygen species homeostasis and signalling during drought and salinity stresses. *Plant, cell & environment, 33*(4), 453-467.

Mirmiranpour, H., Mousavizadeh, M., Noshad, S., Ghavami, M., Ebadi, M., Ghasemiesfe, M., . . . Complications, i. (2013). Comparative effects of pioglitazone and metformin on oxidative stress markers in newly diagnosed type 2 diabetes patients: a randomized clinical trial. *27*(5), 501-507.

Mishra, S. K., Ammon, T., Popowicz, G. M., Krajewski, M., Nagel, R. J., Ares, M., . . . Jentsch, S. (2011). Role of the ubiquitin-like protein Hub1 in splice-site usage and alternative splicing. *Nature, 474*(7350), 173-178.

Mizzen, L., Kabiling, A., & Welch, W. (1991). The two mammalian mitochondrial stress proteins, grp 75 and hsp 58, transiently interact with newly synthesized mitochondrial proteins. *Cell regulation, 2*(2), 165-179.

Mizzen, L. A., Chang, C., Garrels, J., & Welch, W. (1989). Identification, characterization, and purification of two mammalian stress proteins present in mitochondria, grp 75, a member of the hsp 70 family and hsp 58, a homolog of the bacterial groEL protein. *Journal of biological chemistry, 264*(34), 20664-20675.

Morino, K., Petersen, K. F., Dufour, S., Befroy, D., Frattini, J., Shatzkes, N., . . . Sono, S. J. T. J. o. c. i. (2005). Reduced mitochondrial density and increased IRS-1 serine phosphorylation in muscle of insulin-resistant offspring of type 2 diabetic parents. *115*(12), 3587-3593.

Moriya, K., Nakagawa, K., Santa, T., Shintani, Y., Fujie, H., Miyoshi, H., . . . Koike, K. (2001). Oxidative Stress in the Absence of Inflammation in a Mouse Model for Hepatitis C Virus-associated Hepatocarcinogenesis. *Cancer Research, 61*(11), 4365-4370.

Mottis, A., Jovaisaite, V., & Auwerx, J. (2014). The mitochondrial unfolded protein response in mammalian physiology. *Mammalian Genome, 25*(9-10), 424-433.

Murea, M., Ma, L., & Freedman, B. I. J. T. r. o. d. s. R. (2012). Genetic and environmental factors associated with type 2 diabetes and diabetic vascular complications. *9*(1), 6.

Naidoo, N., & Brown, M. (2012). The endoplasmic reticulum stress response in aging and age-related diseases. *Frontiers in Physiology, 3*(263). doi:10.3389/fphys.2012.00263

Nargund, Amrita M., Fiorese, Christopher J., Pellegrino, Mark W., Deng, P., & Haynes, Cole M. (2015). Mitochondrial and Nuclear Accumulation of the Transcription Factor ATFS-1 Promotes OXPHOS Recovery during the UPRmt. *Molecular Cell, 58*(1), 123-133. doi:https://doi.org/10.1016/j.molcel.2015.02.008

Nargund, A. M., Fiorese, C. J., Pellegrino, M. W., Deng, P., & Haynes, C. M. J. M. c. (2015). Mitochondrial and nuclear accumulation of the transcription factor ATFS-1 promotes OXPHOS recovery during the UPRmt. *58*(1), 123-133.

Nargund, A. M., Pellegrino, M. W., Fiorese, C. J., Baker, B. M., & Haynes, C. M. (2012). Mitochondrial import efficiency of ATFS-1 regulates mitochondrial UPR activation. *Science, 337*(6094), 587-590.

Natarajan, S. K., Eapen, C. E., Pullimood, A. B., & Balasubramanian, K. A. (2006). Oxidative stress in experimental liver microvesicular steatosis: Role of mitochondria and peroxisomes. *21*(8), 1240-1249. doi:10.1111/j.1440-1746.2006.04313.x

Neupert, W. (1997). Protein import into mitochondria. *Annu Rev Biochem, 66*, 863-917.

Neuschwander-Tetri, B. A., & Caldwell, S. H. (2003). Nonalcoholic steatohepatitis: summary of an AASLD Single Topic Conference. *Hepatology, 37*(5), 1202-1219.

Ng, Y. K., Brailoiu, G. C., Dun, S. L., Ling, E. A., Yang, J., Chang, J. K., & Dun, N. J. (2006). Beacon immunoreactivity in the rat hypothalamus. *J Neurosci Res, 83*(6), 1106-1117. doi:10.1002/jnr.20808

Nieminen, A.-L. J. I. r. o. c. (2003). Apoptosis and necrosis in health and disease: role of mitochondria. *224*, 29-55.

Nishikawa, T., Edelstein, D., Du, X. L., Yamagishi, S.-i., Matsumura, T., Kaneda, Y., . . . Hammes, H.-P. (2000). Normalizing mitochondrial superoxide production blocks three pathways of hyperglycaemic damage. *Nature, 404*(6779), 787-790.

Nishina, P. M., Johnson, J. P., Naggert, J. K., & Krauss, R. M. (1992). Linkage of atherogenic lipoprotein phenotype to the low density lipoprotein receptor locus on the short arm of chromosome 19. *Proceedings of the National Academy of Sciences, 89*(2), 708-712.

Nobuhir, S., Takenobu, K., Hiroshi, A., Toshihiko, S., Sunao, K., Noroi, H., . . . Bunji, H. (1977). Simultaneous measurement of mitochondrial and microsomal cytochrome levels in human liver biopsy. *Clinica Chimica Acta, 80*(2), 243-251. doi:https://doi.org/10.1016/0009-8981(77)90031-6

Oka, Y., Varmark, H., Vitting-Seerup, K., Beli, P., Waage, J., Hakobyan, A., . . . Bekker-Jensen, S. (2014). UBL5 is essential for pre-mRNA splicing and sister chromatid cohesion in human cells. *EMBO reports, 15*(9), 956-964.

Ortiz, G. G., Pacheco-Moises, F., Torres-Sánchez, E., E. Sorto-Gómez, T., Mireles-Ramírez, M., León-Gil, A., . . . Velázquez-Brizuela, I. (2016). Multiple Sclerosis and Its Relationship with Oxidative Stress, Glutathione Redox System, ATPase System, and Membrane Fluidity. In.

Ostermann, J., Voos, W., Kang, P. J., Craig, E. A., Neupert, W., & Pfanner, N. J. F. l. (1990). Precursor proteins in transit through mitochondrial contact sites interact with hsp70 in the matrix. *277*(1-2), 281-284.

Österreicher, C. H., Taura, K., De Minicis, S., Seki, E., Penz-Österreicher, M., Kodama, Y., . . . Penninger, J. M. J. H. (2009). Angiotensin-converting-enzyme 2 inhibits liver fibrosis in mice. *50*(3), 929-938.

Ouvrard-Pascaud, A., Puttini, S., Sainte-Marie, Y., Athman, R., Fontaine, V., Cluzeaud, F., . . . Jaisser, F. (2004). Conditional gene expression in renal collecting duct epithelial cells: use of the inducible Cre-lox system. *American Journal of Physiology-Renal Physiology, 286*(1), F180-F187. doi:10.1152/ajprenal.00301.2002

Özcan, U., Yilmaz, E., Özcan, L., Furuhashi, M., Vaillancourt, E., Smith, R. O., . . . Hotamisligil, G. S. (2006). Chemical chaperones reduce ER stress and restore glucose homeostasis in a mouse model of type 2 diabetes. *Science, 313*(5790), 1137-1140.

Pan, Z.-q., Xie, D., Choudhary, V., Seremwe, M., Tsai, Y.-Y., Olala, L., . . . Bollag, W. B. (2014). The effect of pioglitazone on aldosterone and cortisol production in HAC15 human

adrenocortical carcinoma cells. *Molecular and Cellular Endocrinology, 394*(1), 119-128. doi:https://doi.org/10.1016/j.mce.2014.07.007

Parks, E. J., Krauss, R. M., Christiansen, M. P., Neese, R. A., & Hellerstein, M. K. J. T. J. o. c. i. (1999). Effects of a low-fat, high-carbohydrate diet on VLDL-triglyceride assembly, production, and clearance. *104*(8), 1087-1096.

Patil, C., & Walter, P. (2001). Intracellular signaling from the endoplasmic reticulum to the nucleus: the unfolded protein response in yeast and mammals. *Curr Opin Cell Biol, 13*(3), 349-355.

Pellegrino, M. W., Nargund, A. M., & Haynes, C. M. (2013). Signaling the mitochondrial unfolded protein response. *Biochim Biophys Acta, 1833*(2), 410-416. doi:10.1016/j.bbamcr.2012.02.019

Penn, D. J., Damjanovich, K., & Potts, W. K. J. P. o. t. N. A. o. S. (2002). MHC heterozygosity confers a selective advantage against multiple-strain infections. *99*(17), 11260-11264.

Pérez-Carreras, M., Del Hoyo, P., Martın, M. A., Rubio, J. C., Martın, A., Castellano, G., . . . Solis-Herruzo, J. A. J. H. (2003). Defective hepatic mitochondrial respiratory chain in patients with nonalcoholic steatohepatitis. *38*(4), 999-1007.

Pérez-Carreras, M., Del Hoyo, P., Martín, M. A., Rubio, J. C., Martín, A., Castellano, G., . . . Solis-Herruzo, J. A. (2003). Defective hepatic mitochondrial respiratory chain in patients with nonalcoholic steatohepatitis. *Hepatology, 38*(4), 999-1007.

Pessayre, D., Berson, A., Fromenty, B., & Mansouri, A. (2001). Mitochondria in steatohepatitis. *Semin Liver Dis, 21*(1), 57-69.

Pessayre, D., & Fromenty, B. (2005). NASH: a mitochondrial disease. *Journal of Hepatology, 42*(6), 928-940. doi:10.1016/j.jhep.2005.03.004

Pessayre, D., & Fromenty, B. J. J. o. h. (2005). NASH: a mitochondrial disease. *42*(6), 928-940.

Pessayre, D., Mansouri, A., & Fromenty, B. (2002). V. Mitochondrial dysfunction in steatohepatitis. *American Journal of Physiology-Gastrointestinal and Liver Physiology, 282*(2), G193-G199.

Pessayre, D., Mansouri, A., Haouzi, D., Fromenty, B. J. C. b., & toxicology. (1999). Hepatotoxicity due to mitochondrial dysfunction. *15*(6), 367-373.

Pessayre, D. J. J. o. g., & hepatology. (2007). Role of mitochondria in non-alcoholic fatty liver disease. *22*, S20-S27.

Peterson, R. E. J. T. J. o. c. i. (1960). Adrenocortical steroid metabolism and adrenal cortical function in liver disease. *39*(2), 320-331.

Petrof, E. O., Ciancio, M. J., & Chang, E. B. (2004). Role and regulation of intestinal epithelial heat shock proteins in health and disease. *5*(2), 45-50. doi:10.1111/j.1443-9573.2004.00154.x

Pizzorno, J. (2014). Mitochondria-Fundamental to Life and Health. *Integrative medicine (Encinitas, Calif.), 13*(2), 8-15.

Pomplun, D., Möhlig, M., Spranger, J., Pfeiffer, A. F., & Ristow, M. (2004). Elevation of blood glucose following anaesthetic treatment in C57Bl/6 mice. *Hormone and metabolic research, 36*(1), 67-69.

Promrat, K., Lutchman, G., Uwaifo, G. I., Freedman, R. J., Soza, A., Heller, T., . . . Hoofnagle, J. H. (2004). A pilot study of pioglitazone treatment for nonalcoholic steatohepatitis. *Hepatology, 39*(1), 188-196.

Rabelo, L. A., Alenina, N., & Bader, M. (2010). ACE2–angiotensin-(1–7)–Mas axis and oxidative stress in cardiovascular disease. *Hypertension Research, 34*, 154. doi:10.1038/hr.2010.235

Ramelot, T. A., Cort, J. R., Yee, A. A., Semesi, A., Edwards, A. M., Arrowsmith, C. H., & Kennedy, M. A. (2003). Solution structure of the yeast ubiquitin-like modifier protein Hub1. *Journal of structural and functional genomics, 4*(1), 25-30.

Rath, E., Berger, E., Messlik, A., Nunes, T., Liu, B., Kim, S. C., . . . Haller, D. J. G. (2012). Induction of dsRNA-activated protein kinase links mitochondrial unfolded protein response to the pathogenesis of intestinal inflammation. *61*(9), 1269-1278.

Ratziu, V., Bonyhay, L., Di Martino, V., Charlotte, F., Cavallaro, L., Sayegh-Tainturier, M. H., . . . Poynard, T. (2002). Survival, liver failure, and hepatocellular carcinoma in obesity-related cryptogenic cirrhosis. *Hepatology, 35*(6), 1485-1493.

Rausa, F. M., Tan, Y., Zhou, H., Yoo, K. W., Stolz, D. B., Watkins, S. C., . . . Costa, R. H. (2000). Elevated levels of hepatocyte nuclear factor 3β in mouse hepatocytes influence expression of genes involved in bile acid and glucose homeostasis. *Molecular and cellular biology, 20*(21), 8264-8282.

Razavizade, M., Jamali, R., Arj, A., Matini, S. M., Moraveji, A., & Taherkhani, E. (2013). The effect of pioglitazone and metformin on liver function tests, insulin resistance, and liver fat content in nonalcoholic Fatty liver disease: a randomized double blinded clinical trial. *Hepatitis monthly, 13*(5).

Rector, R. S., Thyfault, J. P., Uptergrove, G. M., Morris, E. M., Naples, S. P., Borengasser, S. J., . . . Ibdah, J. A. (2010). Mitochondrial dysfunction precedes insulin resistance and hepatic steatosis and contributes to the natural history of non-alcoholic fatty liver disease in an obese rodent model. *Journal of Hepatology, 52*(5), 727-736. doi:https://doi.org/10.1016/j.jhep.2009.11.030

Reece, J. B., Urry, L. A., Cain, M. L., Wasserman, S. A., Minorsky, P. V., & Jackson, R. B. J. C. B. (2011). Cellular respiration and fermentation. 162-184.

Rhee, J., Inoue, Y., Yoon, J. C., Puigserver, P., Fan, M., Gonzalez, F. J., & Spiegelman, B. M. (2003). Regulation of hepatic fasting response by PPARγ coactivator-1α (PGC-1): Requirement for hepatocyte nuclear factor 4α in gluconeogenesis. *Proceedings of the National Academy of Sciences, 100*(7), 4012-4017. doi:10.1073/pnas.0730870100

Richter, K., Haslbeck, M., & Buchner, J. (2010). The heat shock response: life on the verge of death. *Mol Cell, 40*(2), 253-266.

Ritov, V. B., Menshikova, E. V., He, J., Ferrell, R. E., Goodpaster, B. H., & Kelley, D. E. J. D. (2005). Deficiency of subsarcolemmal mitochondria in obesity and type 2 diabetes. *54*(1), 8-14.

Rivera, L., Leung, C., Pustovit, R., Hunne, B., Andrikopoulos, S., Herath, C., . . . Motility. (2014). Damage to enteric neurons occurs in mice that develop fatty liver disease but not diabetes in response to a high-fat diet. *26*(8), 1188-1199.

Roep, B. O. J. D. (2003). The role of T-cells in the pathogenesis of Type 1 diabetes: from cause to cure. *46*(3), 305-321.

Rolfe, D. F., & Brown, G. C. (1997). Cellular energy utilization and molecular origin of standard metabolic rate in mammals. *Physiological Reviews, 77*(3), 731-758. doi:10.1152/physrev.1997.77.3.731

Rolo, A. P., Teodoro, J. S., Palmeira, C. M. J. F. r. b., & medicine. (2012). Role of oxidative stress in the pathogenesis of nonalcoholic steatohepatitis. *52*(1), 59-69.

Rosca, M. G., Vazquez, E. J., Chen, Q., Kerner, J., Kern, T. S., & Hoppel, C. L. J. D. (2012). Oxidation of fatty acids is the source of increased mitochondrial reactive oxygen species production in kidney cortical tubules in early diabetes. *61*(8), 2074-2083.

Rosen, E. D., Hsu, C.-H., Wang, X., Sakai, S., Freeman, M. W., Gonzalez, F. J., & Spiegelman, B. M. (2002). C/EBPα induces adipogenesis through PPARγ: a unified pathway. *Genes & development, 16*(1), 22-26.

Rossier, M. F. (2006). T channels and steroid biosynthesis: in search of a link with mitochondria. *Cell calcium, 40*(2), 155-164.

Rotter, J. I., Bu, X., Cantor, R. M., Warden, C. H., Brown, J., Gray, R. J., . . . Lusis, A. J. (1996). Multilocus genetic determinants of LDL particle size in coronary artery disease families. *American journal of human genetics, 58*(3), 585.

Rucinski, M., Andreis, P. G., Ziolkowska, A., Nussdorfer, G. G., & Malendowicz, L. K. (2005). Differential expression and function of beacon in the rat adrenal cortex and medulla. *Int J Mol Med, 16*(1), 35-40.

Rui, L. (2014). Energy metabolism in the liver. Compr Physiol 4 (1): 177–197. In.

Rui, L. J. C. p. (2011). Energy metabolism in the liver. *4*(1), 177-197.

Rutkowski, D. T., Wu, J., Back, S.-H., Callaghan, M. U., Ferris, S. P., Iqbal, J., . . . Fornek, J. (2008). UPR pathways combine to prevent hepatic steatosis caused by ER stress-mediated suppression of transcriptional master regulators. *Developmental cell, 15*(6), 829-840.

Sambasiva Rao, M., & Reddy, J. K. J. H. (2004). PPARα in the pathogenesis of fatty liver disease. *40*(4), 783-786.

Samuel, V. T., Liu, Z.-X., Qu, X., Elder, B. D., Bilz, S., Befroy, D., . . . Shulman, G. I. J. J. o. B. C. (2004). Mechanism of hepatic insulin resistance in non-alcoholic fatty liver disease. *279*(31), 32345-32353.

Sangle, G. V., Chowdhury, S. K. R., Xie, X., Stelmack, G. L., Halayko, A. J., & Shen, G. X. (2010). Impairment of mitochondrial respiratory chain activity in aortic endothelial cells induced by glycated low-density lipoprotein. *Free Radical Biology and Medicine, 48*(6), 781-790. doi:https://doi.org/10.1016/j.freeradbiomed.2009.12.017

Santamaría, E., Avila, M. A., Latasa, M. U., Rubio, A., Martín-Duce, A., Lu, S. C., . . . Corrales, F. J. J. P. o. t. N. A. o. S. (2003). Functional proteomics of nonalcoholic steatohepatitis: mitochondrial proteins as targets of S-adenosylmethionine. *100*(6), 3065-3070.

Santoro, S. W., & Schultz, P. G. (2002). Directed Evolution of the Site Specificity of Cre Recombinase. *Proceedings of the National Academy of Sciences of the United States of America, 99*(7), 4185-4190.

Sanyal, A. J., Campbell–Sargent, C., Mirshahi, F., Rizzo, W. B., Contos, M. J., Sterling, R. K., . . . Clore, J. N. (2001a). Nonalcoholic steatohepatitis: association of insulin resistance and mitochondrial abnormalities. *Gastroenterology, 120*(5), 1183-1192.

Sanyal, A. J., Campbell–Sargent, C., Mirshahi, F., Rizzo, W. B., Contos, M. J., Sterling, R. K., . . . Clore, J. N. J. G. (2001b). Nonalcoholic steatohepatitis: association of insulin resistance and mitochondrial abnormalities. *120*(5), 1183-1192.

Sanyal, A. J., Chalasani, N., Kowdley, K. V., McCullough, A., Diehl, A. M., Bass, N. M., . . . Unalp, A. (2010a). Pioglitazone, vitamin E, or placebo for nonalcoholic steatohepatitis. *New England Journal of Medicine, 362*(18), 1675-1685.

Sanyal, A. J., Chalasani, N., Kowdley, K. V., McCullough, A., Diehl, A. M., Bass, N. M., . . . Unalp, A. J. N. E. J. o. M. (2010b). Pioglitazone, vitamin E, or placebo for nonalcoholic steatohepatitis. *362*(18), 1675-1685.

Sanyal, A. J., Mofrad, P. S., Contos, M. J., Sargeant, C., Luketic, V. A., Sterling, R. K., . . . Mills, A. S. (2004). A pilot study of vitamin E versus vitamin E and pioglitazone for the treatment of nonalcoholic steatohepatitis. *Clinical Gastroenterology and Hepatology, 2*(12), 1107-1115.

Sauer, B. (1994). Site-specific recombination: developments and applications. *Current Opinion in Biotechnology, 5*(5), 521-527. doi:https://doi.org/10.1016/0958-1669(94)90068-X

Sauer, B., & Henderson, N. (1988). Site-specific DNA recombination in mammalian cells by the Cre recombinase of bacteriophage P1. *Proceedings of the National Academy of Sciences, 85*(14), 5166-5170. doi:10.1073/pnas.85.14.5166

Sauer, R., & Baker, T. J., 587–612. (2011). AAA+ proteases: ATP-fueled machines of protein destruction. Ann. Review Biochem.

Scherer, P. E., Krieg, U. C., Hwang, S. T., Vestweber, D., & Schatz, G. J. T. E. J. (1990). A precursor protein partly translocated into yeast mitochondria is bound to a 70 kd mitochondrial stress protein. *9*(13), 4315-4322.

Schieber, M., & Chandel, Navdeep S. (2014). ROS Function in Redox Signaling and Oxidative Stress. *Current Biology, 24*(10), R453-R462. doi:https://doi.org/10.1016/j.cub.2014.03.034

Schröder, M. (2006). The unfolded protein response. *Molecular biotechnology, 34*(2), 279-290.

Schröder, M., & Kaufman, R. J. J. A. R. B. (2005). The mammalian unfolded protein response. *74*, 739-789.

Schulz, A. M., & Haynes, C. M. J. B. e. B. A.-B. (2015). UPRmt-mediated cytoprotection and organismal aging. *1847*(11), 1448-1456.

Schwimmer, J. B., Celedon, M. A., Lavine, J. E., Salem, R., Campbell, N., Schork, N. J., . . . Middleton, M. S. J. G. (2009). Heritability of nonalcoholic fatty liver disease. *136*(5), 1585-1592.

Sentinelli, F., Romeo, S., Cambuli, V. M., Cossu, E., Cavallo, M. G., Zavarella, S., . . . Baroni, M. G. (2008). Identification of sequence variants in the UBL5 (ubiquitin-like 5 or BEACON) gene in obese children by PCR-SSCP: no evidence for association with obesity. *J Pediatr Endocrinol Metab, 21*(12), 1139-1145.

Shadid, S., & Jensen, M. D. (2003). Effect of pioglitazone on biochemical indices of non-alcoholic fatty liver disease in upper body obesity. *Clinical Gastroenterology and Hepatology, 1*(5), 384-387.

Shen, X., Zhang, K., & Kaufman, R. J. (2004). The unfolded protein response—a stress signaling pathway of the endoplasmic reticulum. *Journal of Chemical Neuroanatomy, 28*(1), 79-92. doi:https://doi.org/10.1016/j.jchemneu.2004.02.006

Sherlock, S. J. G. (1983). Acute fatty liver of pregnancy and the microvesicular fat diseases. *24*(4), 265.

Shoffner, J. (1995). Oxidative phosphorylation diseases. *The metabolic and molecular bases of inherited disease*, 1566-1569.

Shutt, T. E., & Shadel, G. S. (2010). A compendium of human mitochondrial gene expression machinery with links to disease. *Environmental and molecular mutagenesis, 51*(5), 360-379.

Siegel, G. J., Agranoff, B. W., Albers, R. W., Fisher, S. K., & Uhler, M. D. (1999). Basic neurochemistry.

Sivitz, W. I., & Yorek, M. A. (2010). Mitochondrial dysfunction in diabetes: from molecular mechanisms to functional significance and therapeutic opportunities. *Antioxidants & redox signaling, 12*(4), 537-577. doi:10.1089/ars.2009.2531

Sobaniec-Lotowska, M. E., & Lebensztejn, D. M. J. T. A. j. o. g. (2003). Ultrastructure of hepatocyte mitochondria in nonalcoholic steatohepatitis in pediatric patients: usefulness of electron microscopy in the diagnosis of the disease. *98*(7), 1664.

Sohal, D. S., Nghiem, M., Crackower, M. A., Witt, S. A., Kimball, T. R., Tymitz, K. M., . . . Molkentin, J. D. (2001). Temporally regulated and tissue-specific gene manipulations in the adult and embryonic heart using a tamoxifen-inducible Cre protein. *Circulation Research, 89*(1), 20-25.

Sookoian, S., & Pirola, C. J. J. H. (2011). Meta-analysis of the influence of I148M variant of patatin-like phospholipase domain containing 3 gene (PNPLA3) on the susceptibility and histological severity of nonalcoholic fatty liver disease. *53*(6), 1883-1894.

Sparks, L. M., Xie, H., Koza, R. A., Mynatt, R., Hulver, M. W., Bray, G. A., & Smith, S. R. J. D. (2005). A high-fat diet coordinately downregulates genes required for mitochondrial oxidative phosphorylation in skeletal muscle. *54*(7), 1926-1933.

Speakman, J. R., Talbot, D. A., Selman, C., Snart, S., McLaren, J. S., Redman, P., . . . Brand, M. D. J. A. c. (2004). Uncoupled and surviving: individual mice with high metabolism have greater mitochondrial uncoupling and live longer. *3*(3), 87-95.

Sreekumar, R., Unnikrishnan, J., Fu, A., Nygren, J., Short, K., Schimke, J., . . . Metabolism. (2002). Impact of high-fat diet and antioxidant supplement on mitochondrial functions and gene transcripts in rat muscle. *282*(5), E1055-E1061.

Srinivasan, K., Viswanad, B., Asrat, L., Kaul, C. L., & Ramarao, P. (2005). Combination of high-fat diet-fed and low-dose streptozotocin-treated rat: A model for type 2 diabetes and pharmacological screening. *Pharmacological Research, 52*(4), 313-320. doi:https://doi.org/10.1016/j.phrs.2005.05.004

Stallons, L. J., Funk, J. A., & Schnellmann, R. G. J. C. p. r. (2013). Mitochondrial homeostasis in acute organ failure. *1*(3), 169-177.

Starkenburg, S. R., Chain, P. S. G., Sayavedra-Soto, L. A., Hauser, L., Land, M. L., Larimer, F. W., . . . Hickey, W. J. (2006). Genome Sequence of the Chemolithoautotrophic Nitrite-Oxidizing Bacterium Nitrobacter winogradskyi Nb-255. *Applied and Environmental Microbiology, 72*(3), 2050-2063. doi:10.1128/aem.72.3.2050-2063.2006

Sumida, Y., Yoneda, M., Tokushige, K., Kawanaka, M., Fujii, H., Yoneda, M., . . . Ono, M. (2020). Antidiabetic Therapy in the Treatment of NASH.

Suomalainen, A., & Isohanni, P. (2010). Mitochondrial DNA depletion syndromes–many genes, common mechanisms. *Neuromuscular Disorders, 20*(7), 429-437.

Švéda, M., Častorálová, M., Lipov, J., Ruml, T., & Knejzlík, Z. (2013). Human UBL5 protein interacts with coilin and meets the Cajal bodies. *Biochemical and biophysical research communications, 436*(2), 240-245.

Tang, L.-Q., Wei, W., Chen, L.-M., & Liu, S. J. J. o. E. (2006). Effects of berberine on diabetes induced by alloxan and a high-fat/high-cholesterol diet in rats. *108*(1), 109-115.

Taniguchi, C. M., Emanuelli, B., & Kahn, C. R. J. N. r. M. c. b. (2006). Critical nodes in signalling pathways: insights into insulin action. *7*(2), 85-96.

Tannour-Louet, M., Porteu, A., Vaulont, S., Kahn, A., & Vasseur-Cognet, M. (2002). A tamoxifen-inducible chimeric Cre recombinase specifically effective in the fetal and adult mouse liver. *Hepatology, 35*(5), 1072-1081.

Tardif, K. D., Mori, K., & Siddiqui, A. (2002). Hepatitis C virus subgenomic replicons induce endoplasmic reticulum stress activating an intracellular signaling pathway. *Journal of virology, 76*(15), 7453-7459.

Tarnopolsky, M. J. A. d. d. r. (2008). The mitochondrial cocktail: rationale for combined nutraceutical therapy in mitochondrial cytopathies. *60*(13-14), 1561-1567.

Tatemoto, K., Carlquist, M., & Mutt, V. (1982). Neuropeptide Y—a novel brain peptide with structural similarities to peptide YY and pancreatic polypeptide.

Tatsuta, T., & Langer, T. (2008). Quality control of mitochondria: protection against neurodegeneration and ageing. *The EMBO journal, 27*(2), 306-314.

Tatsuta, T., & Langer, T. (2009). AAA proteases in mitochondria: diverse functions of membrane-bound proteolytic machines. *Research in microbiology, 160*(9), 711-717.

Tatsuta, T., & Langer, T. J. R. i. m. (2009). AAA proteases in mitochondria: diverse functions of membrane-bound proteolytic machines. *160*(9), 711-717.

Tatsuta, T., & Langer, T. J. T. E. j. (2008). Quality control of mitochondria: protection against neurodegeneration and ageing. *27*(2), 306-314.

Tian, Y., Garcia, G., Bian, Q., Steffen, K. K., Joe, L., Wolff, S., . . . Dillin, A. J. C. (2016). Mitochondrial stress induces chromatin reorganization to promote longevity and UPRmt. *165*(5), 1197-1208.

Tipnis, S. R., Hooper, N. M., Hyde, R., Karran, E., Christie, G., & Turner, A. J. (2000). A Human Homolog of Angiotensin Converting Enzyme-Cloning and Functional Expression As A Captopril Insensitive Carboxypeptidase. *Journal of Biological Chemistry*.

Tissiéres, A., Mitchell, H. K., & Tracy, U. M. (1974). Protein synthesis in salivary glands of Drosophila melanogaster: Relation to chromosome puffs. *Journal of Molecular Biology, 84*(3), 389-398. doi:https://doi.org/10.1016/0022-2836(74)90447-1

Tiwari, B. S., Belenghi, B., & Levine, A. (2002). Oxidative Stress Increased Respiration and Generation of Reactive Oxygen Species, Resulting in ATP Depletion, Opening of Mitochondrial Permeability Transition, and Programmed Cell Death. *Plant Physiology, 128*(4), 1271-1281. doi:10.1104/pp.010999

Tsutsumi, V., Nakamura, T., Ueno, T., Torimura, T., & Aguirre-García, J. (2017). Chapter 2 - Structure and Ultrastructure of the Normal and Diseased Liver. In P. Muriel (Ed.), *Liver Pathophysiology* (pp. 23-44). Boston: Academic Press.

Valerio, A., Cardile, A., Cozzi, V., Bracale, R., Tedesco, L., Pisconti, A., . . . Moncada, S. J. T. J. o. c. i. (2006). TNF-α downregulates eNOS expression and mitochondrial biogenesis in fat and muscle of obese rodents. *116*(10), 2791-2798.

Vial, G., Chauvin, M.-A., Bendridi, N., Durand, A., Meugnier, E., Madec, A.-M., . . . Acquaviva, C. J. D. (2015). Imeglimin normalizes glucose tolerance and insulin sensitivity and improves mitochondrial function in liver of a high-fat, high-sucrose diet mice model. *64*(6), 2254-2264.

Vickers, C., Hales, P., Kaushik, V., Dick, L., Gavin, J., Tang, J., . . . Hsieh, F. (2002). Hydrolysis of biological peptides by human angiotensin-converting enzyme-related carboxypeptidase (ACE2). *Journal of Biological Chemistry*.

Vidal-Puig, A. J., Considine, R. V., Jimenez-Liñan, M., Werman, A., Pories, W. J., Caro, J. F., & Flier, J. S. (1997). Peroxisome proliferator-activated receptor gene expression in

human tissues. Effects of obesity, weight loss, and regulation by insulin and glucocorticoids. *The Journal Of Clinical Investigation, 99*(10), 2416-2422.

Voet, D., Judith, V., & Pratt, C. W. (2006). Fundamentals of Biochemistry: Life at the molecular Level 2nd Edition. Publisher: Asia. In: John Wiley & Sons.

Voet, D., Voet, J. G., & Pratt, C. W. (1999). *Fundamentals of biochemistry*: Wiley New York.

Wadhwa, R., Taira, K., & Kaul, S. C. (2002). An Hsp70 family chaperone, mortalin/mthsp70/PBP74/Grp75: what, when, and where? *Cell Stress Chaperones, 7*(3), 309-316.

Walder, K., Segal, D., Jowett, J., Blangero, J., & Collier, G. R. (2003). Obesity and diabetes gene discovery approaches. *Curr Pharm Des, 9*(17), 1357-1372.

Walder, K., Ziv, E., Kalman, R., Whitecross, K., Shafrir, E., Zimmet, P., & Collier, G. R. (2002). Elevated hypothalamic beacon gene expression in Psammomys obesus prone to develop obesity and type 2 diabetes. *Int J Obes Relat Metab Disord, 26*(5), 605-609.

Wallace, D. C. (1992). Mitochondrial genetics: a paradigm for aging and degenerative diseases? *Science, 256*(5057), 628-632.

Wallace, D. C. (2005). A Mitochondrial Paradigm of Metabolic and Degenerative Diseases, Aging, and Cancer: A Dawn for Evolutionary Medicine. *39*(1), 359-407. doi:10.1146/annurev.genet.39.110304.095751

Wang, F., Tian, D. R., Tian, N., Chen, H., Shi, Y. S., Chang, J. K., . . . Han, J. S. (2006). Distribution of beacon immunoreactivity in the rat brain. *Peptides, 27*(1), 165-171. doi:10.1016/j.peptides.2005.07.011

Wang, X., & Michaelis, E. (2010). Selective neuronal vulnerability to oxidative stress in the brain. *Frontiers in Aging Neuroscience, 2*(12). doi:10.3389/fnagi.2010.00012

Wang, Y., DeMayo, F. J., Tsai, S. Y., & O'Malley, B. W. (1997). Ligand-inducible and liver-specific target gene expression in transgenic mice. *Nat Biotechnol, 15*(3), 239-243.

Wang, Y., Xu, J., Pierson, T., O'Malley, B. W., & Tsai, S. Y. (1997). Positive and negative regulation of gene expression in eukaryotic cells with an inducible transcriptional regulator. *Gene Ther, 4*(5), 432-441.

Waris, G., & Ahsan, H. (2006). Reactive oxygen species: role in the development of cancer and various chronic conditions. *Journal of carcinogenesis, 5*, 14.

Wei, Y., Rector, R. S., Thyfault, J. P., & Ibdah, J. A. (2008). Nonalcoholic fatty liver disease and mitochondrial dysfunction. *World journal of gastroenterology, 14*(2), 193-199. doi:10.3748/wjg.14.193

Weiss, C., Schneider, S., Wagner, E. F., Zhang, X., Seto, E., & Bohmann, D. J. T. E. j. (2003). JNK phosphorylation relieves HDAC3-dependent suppression of the transcriptional activity of c-Jun. *22*(14), 3686-3695.

Whitfield, J., Littlewood, T., & Soucek, L. J. C. S. H. p. (2015). Tamoxifen administration to mice. *2015*(3), pdb. prot077966.

Wicksteed, B., Brissova, M., Yan, W., Opland, D. M., Plank, J. L., Reinert, R. B., . . . Dempsey, P. J. (2010). Conditional gene targeting in mouse pancreatic b-Cells: analysis of ectopic Cre transgene expression in the brain. *Diabetes, 59*(12), 3090-3098. doi:10.2337/db10-0624

Wilkinson, C. R., Dittmar, G. A., Ohi, M. D., Uetz, P., Jones, N., & Finley, D. (2004). Ubiquitin-like protein Hub1 is required for pre-mRNA splicing and localization of an essential splicing factor in fission yeast. *Current Biology, 14*(24), 2283-2288.

Williamson, J. R., & Corkey, B. E. (1969). [65] Assays of intermediates of the citric acid cycle and related compounds by fluorometric enzyme methods. *Methods in enzymology, 13*, 434-513.

Willson, T. M., Brown, P. J., Sternbach, D. D., & Henke, B. R. (2000). The PPARs: from orphan receptors to drug discovery. *Journal of medicinal chemistry, 43*(4), 527-550.

Wilson, B. A., Nautiyal, M., Gwathmey, T. M., Rose, J. C., & Chappell, M. C. (2016). Evidence for a mitochondrial angiotensin-(1–7) system in the kidney. *310*(7), F637-F645. doi:10.1152/ajprenal.00479.2015

Wilson, D., Merz, R. D. J. A. o. b., & biophysics. (1967). Inhibition of mitochondrial respiration by uncouplers of oxidative phosphorylation. *119*, 470-476.

Wu, G. (1998). Intestinal Mucosal Amino Acid Catabolism. *The Journal of Nutrition, 128*(8), 1249-1252. doi:10.1093/jn/128.8.1249

Wu, H., Wade, M., Krall, L., Grisham, J., Xiong, Y., & Van Dyke, T. (1996). Targeted in vivo expression of the cyclin-dependent kinase inhibitor p21 halts hepatocyte cell-cycle progression, postnatal liver development and regeneration. *Genes & Development, 10*(3), 245-260.

Xiong, D., Yajima, T., Lim, B.-K., Stenbit, A., Dublin, A., Dalton, N. D., . . . Wessely, R. (2007). Inducible cardiac-restricted expression of enteroviral protease 2A is sufficient to induce dilated cardiomyopathy. *Circulation, 115*(1), 94-102.

Xirouchaki, C. E., Mangiafico, S. P., Bate, K., Ruan, Z., Huang, A. M., Tedjosiswoyo, B. W., . . . Blair, A. R. J. M. m. (2016). Impaired glucose metabolism and exercise capacity with muscle-specific glycogen synthase 1 (gys1) deletion in adult mice. *5*(3), 221-232.

Xu, Z., Jensen, G., & Yen, T. (1997). Activation of hepatitis B virus S promoter by the viral large surface protein via induction of stress in the endoplasmic reticulum. *Journal of virology, 71*(10), 7387-7392.

Yamano, K., Kuroyanagi-Hasegawa, M., Esaki, M., Yokota, M., & Endo, T. J. J. o. B. C. (2008). Step-size analyses of the mitochondrial Hsp70 import motor reveal the Brownian ratchet in operation. *283*(40), 27325-27332.

Yamashina, S., Sato, N., Kon, K., Ikejima, K., & Watanabe, S. (2009). Role of mitochondria in liver pathophysiology. *Drug Discovery Today: Disease Mechanisms, 6*(1), e25-e30. doi:https://doi.org/10.1016/j.ddmec.2010.05.003

Yashiroda, H., & Tanaka, K. (2004). Hub1 is an essential ubiquitin-like protein without functioning as a typical modifier in fission yeast. *Genes to Cells, 9*(12), 1189-1197.

Yee, C., Yang, W., & Hekimi, S. (2014). The Intrinsic Apoptosis Pathway Mediates the Pro-Longevity Response to Mitochondrial ROS in C. elegans. *Cell, 157*(4), 897-909. doi:https://doi.org/10.1016/j.cell.2014.02.055

Yim, H., & Hwan Yoo, K. (2008). Renin-Angiotensin System - Considerations for Hypertension and Kidney. *Electrolyte & blood pressure : E & BP, 6*, 42-50. doi:10.5049/EBP.2008.6.1.42

Yoneda, T., Benedetti, C., Urano, F., Clark, S. G., Harding, H. P., & Ron, D. (2004). Compartment-specific perturbation of protein handling activates genes encoding mitochondrial chaperones. *Journal of cell science, 117*(18), 4055-4066.

Yoneda, T., Benedetti, C., Urano, F., Clark, S. G., Harding, H. P., & Ron, D. (2004). Compartment-specific perturbation of protein handling activates genes encoding mitochondrial chaperones. *J Cell Sci, 117*(Pt 18), 4055-4066. doi:10.1242/jcs.01275

Young, J. C., Agashe, V. R., Siegers, K., & Hartl, F. U. (2004). Pathways of chaperone-mediated protein folding in the cytosol. *Nature reviews Molecular cell biology, 5*(10), 781-791.

Younossi, Z. M., Stepanova, M., Afendy, M., Fang, Y., Younossi, Y., Mir, H., & Srishord, M. (2011). Changes in the Prevalence of the Most Common Causes of Chronic Liver Diseases in the United States From 1988 to 2008. *Clinical Gastroenterology and Hepatology, 9*(6), 524-530.e521. doi:https://doi.org/10.1016/j.cgh.2011.03.020

Zhang, K., & Kaufman, R. J. (2006). The unfolded protein response. *A stress signaling pathway critical for health and disease, 66*(1 suppl 1), S102-S109. doi:10.1212/01.wnl.0000192306.98198.ec

Zhang, Y., Wat, N., Stratton, I. M., Warren-Perry, M. G., Orho, M., Groop, L., & Turner, R. C. (1996). UKPDS 19: heterogeneity in NIDDM: separate contributions of IRS-1 and beta 3-adrenergic-receptor mutations to insulin resistance and obesity respectively with no evidence for glycogen synthase gene mutations. UK Prospective Diabetes Study. *Diabetologia, 39*(12), 1505-1511.

Zhang, Y., Yu, L., Cai, W., Fan, S., Feng, L., Ji, G., & Huang, C. (2014). Protopanaxatriol, a novel PPARγ antagonist from Panax ginseng, alleviates steatosis in mice. *Scientific reports, 4*, 7375-7375. doi:10.1038/srep07375

Zhao, Q., Wang, J., Levichkin, I. V., Stasinopoulos, S., Ryan, M. T., & Hoogenraad, N. J. (2002). A mitochondrial specific stress response in mammalian cells. *Embo J, 21*(17), 4411-4419.

Zhao, Q., Wang, J., Levichkin, I. V., Stasinopoulos, S., Ryan, M. T., & Hoogenraad, N. J. (2002). A mitochondrial specific stress response in mammalian cells. *EMBO J, 21*(17), 4411-4419.

Zhao, Q., Wang, J., Levichkin, I. V., Stasinopoulos, S., Ryan, M. T., & Hoogenraad, N. J. J. T. E. j. (2002). A mitochondrial specific stress response in mammalian cells. *21*(17), 4411-4419.

Zhao, Y., Abreu, E., Kim, J., Stadler, G., Eskiocak, U., Terns, M. P., . . . Wright, W. E. (2011). Processive and distributive extension of human telomeres by telomerase under homeostatic and nonequilibrium conditions. *Mol Cell, 42*(3), 297-307.

Ziolkowska, A., Rucinski, M., Di Liddo, R., Nussdorfer, G. G., & Malendowicz, L. K. (2004). Expression of the beacon gene in endocrine glands of the rat. *Peptides, 25*(1), 133-137. doi:10.1016/j.peptides.2003.11.015

Zordan, M. A., Cisotto, P., Benna, C., Agostino, A., Rizzo, G., Piccin, A., . . . Tognon, G. J. G. (2006). Post-transcriptional silencing and functional characterization of the Drosophila melanogaster homolog of human Surf1. *172*(1), 229-241.

BARASTOC

GR2 RAT & MOUSE CUBES

FEATURES:

- A complete and balanced diet to support growth and health of mice and rats in a laboratory environment.
- Product is Gamma Irradiated at a rate of 25 kilo gray.
- Pelleted product 12mm in diameter and an average of 20mm in length.

TYPICAL ANALYSIS (AS-FED):

Crude Protein	20%
Crude Fat	3%
Crude Fibre	3.2%
Starch	35%
DE_HORSE	13.5 MJ/kg
Calcium	0.9%
Available Phosphorous	0.3 %
Sodium	0.25%
Potassium	0.76%
Chloride	0.47%
Magnesium	0.17%
Lysine	1.15%
Methionine	0.4%
Linoleic Acid	0.98%
Added Vitamins and Trace Minerals	
Vitamin A	15 IU/g
Vitamin D3	2 IU/g
Vitamin E	260mg/kg

Vitamin K3	55mg/kg
Vitamin B1	64mg/kg
Vitamin B2	48mg/kg
Vitamin B6	30mg/kg
Vitamin B12	0.08mg/kg
Niacin	400mg/kg
Panto	220mg/kg
Biotin	1.48mg/kg
Folic	11mg/kg
Iron	51 mg/kg
Zinc	60mg/kg
Manganese	120mg/kg

INGREDIENTS:

- Wheat, Wheat Byproducts, Fish Meal, Tallow/vegetable Oil blend, Soybean Meal, Skim Milk Powder, Yeast, Molasses, Limestone, Salt, Vitamins, Trace Minerals.

IMPORTANT NOTES:

Product code 102099

- For more information about this feed or its use please contact our customer service center on 1300 666 657.

PRESENTATION:

- 10kg net weight
- Packaged in a double walled paper bag, then placed in a 200 micron plastic bag, which is vacuum packed and heat-sealed. This sealed package is then sewn in a single walled paper bag and then packed in a cardboard outer carton for shipping.
- Product is packed 48 per pallet.

Specialty Feeds
3150 Great Eastern Hwy
Glen Forrest
Western Australia 6071
p: +61 8 9298 8111
F: +61 8 9298 8700
Email: info@specialtyfeeds.com

Diet SF11-109

21% Fat, 2% Cholesterol Semi-Pure Rodent Diet

A semi-pure high fat diet formulation for laboratory rats and mice based on SF05-031.

- This Diet was developed to generate arteriosclerotic lesions in a range of susceptible mice strains.
- Cholesterol has been increased from 0.15% to 2.0%
- Fructose has been added at 10%
- Vitamin and mineral inclusion rate has been increased to compensate for a suspected reduction in voluntary feed intake due to increased cholesterol.
- We have evidence that irradiation at 25KGy can cause vitamin losses and possibly other changes in the diet. Please contact us if the diet is to be irradiated.

Calculated Nutritional Parameters	
Protein	19.0%
Total Fat	21.0%
Total Carbohydrate	42.2%
Crude Fibre	4.7%
AD Fibre	4.7%
Digestible Energy	19.4 MJ / Kg
% Total calculated digestible energy from lipids	40.0%
% Total calculated digestible energy from protein	17.0%

Diet Form and Features

- Semi pure high fat diet. 12 mm diameter pellets.
- Pack size 1.5 Kg trays, vacuum packed in oxygen impermeable plastic bags, under nitrogen. Bags are packed into cardboard cartons to protect them during transit. Smaller pack quantity on request.
- Diet suitable for irradiation but not suitable for autoclave.
- Lead time 2 weeks for non-irradiation or 4 weeks for irradiation.

Ingredients	
Casein (Acid)	195 g/Kg
Sucrose	211 g/Kg
Fructose	100 g/Kg
Clarified Butter (Ghee)	210 g/Kg
Cellulose	50 g/Kg
Wheat Starch	112 g/Kg
Dextrinised Starch	22 g/Kg
L Methionine	5.0 g/Kg
Calcium Carbonate	28.5 g/Kg
Sodium Chloride	4.1 g/Kg
AIN93 Trace Minerals	2.3 g/Kg
Potassium Citrate	4.1 g/Kg
Potassium Dihydrogen Phosphate	11.4 g/Kg
Potassium Sulphate	2.7 g/Kg
Choline Chloride (75%)	4.2 g/Kg
AIN93 Vitamins	17 g/Kg
USP Cholesterol	20 g/Kg
Oxicap E2	0.04 g/Kg

Calculated Amino Acids	
Valine	1.23%
Leucine	1.80%
Isoleucine	0.85%
Threonine	0.80%
Methionine	1.02%
Cysteine	0.06%
Lysine	1.50%
Phenylalanine	1.00%
Tyrosine	1.00%
Histidine	0.59%
Tryptophan	0.30%

Calculated Total Minerals	
Calcium	0.98%
Phosphorous	0.42%
Magnesium	0.15%
Sodium	0.19%
Chloride	0.25%
Potassium	0.64%
Sulphur	0.29%
Iron	120 mg/Kg
Copper	11 mg/Kg
Iodine	0.3 mg/Kg
Manganese	29 mg/Kg
Cobalt	No data
Zinc	72 mg/Kg
Molybdenum	0.3 mg/Kg
Selenium	0.4 mg/Kg
Cadmium	No data
Chromium	1.6 mg/Kg
Fluoride	1.6 mg/Kg
Lithium	0.2 mg/Kg
Boron	1.9 mg/Kg
Nickel	0.8 mg/Kg
Vanadium	0.2 mg/Kg

Calculated Total Vitamins	
Vitamin A (Retinol)	8 330 IU/Kg
Vitamin D (Cholecalciferol)	1 670 IU/Kg
Vitamin E (a Tocopherol acetate)	130 mg/Kg
Vitamin K (Menadione)	2 mg/Kg
Vitamin C (Ascorbic acid)	None added
Vitamin B1 (Thiamine)	10 mg/Kg
Vitamin B2 (Riboflavin)	10 mg/Kg
Niacin (Nicotinic acid)	50 mg/Kg
Vitamin B6 (Pryridoxine)	12 mg/Kg
Pantothenic Acid	27 mg/Kg
Biotin	330 ug/Kg
Folic Acid	3 mg/Kg
Inositol	None added
Vitamin B12 (Cyancobalamin)	170 ug/Kg
Choline	2 400 mg/Kg

Calculated Fatty Acid Composition	
Saturated Fats C12:0 or less	1.80%
Myristic Acid 14:0	2.60%
Palmitic Acid 16:0	7.00%
Stearic Acid 18:0	2.40%
Palmitoleic Acid 16:1	0.40%
Oleic Acid 18:1	5.50%
Gadoleic Acid 20:1	No data
Linoleic Acid 18:2 n6	0.40%
a Linolenic Acid 18:3 n3	0.20%
EPA 20:5 n3	No data
DHA 22:6 n3	No data
Total n3	0.35%
Total n6	0.41%
Cholesterol	0.15%
Total Mono Unsaturated Fats	6.23%
Total Polyunsaturated Fats	0.77%
Total Saturated Fats	13.99%

Calculated data uses information from typical raw material composition. It could be expected that individual batches of diet will vary from this figure. **Diet post treatment by irradiation or auto clave could change these parameters**. We are happy to provide full calculated nutritional information for all of our products, however we would like to emphasise that these diets have been specifically designed for manufacture by Specialty Feeds.

UBL5 Expression in liver disease (Human)

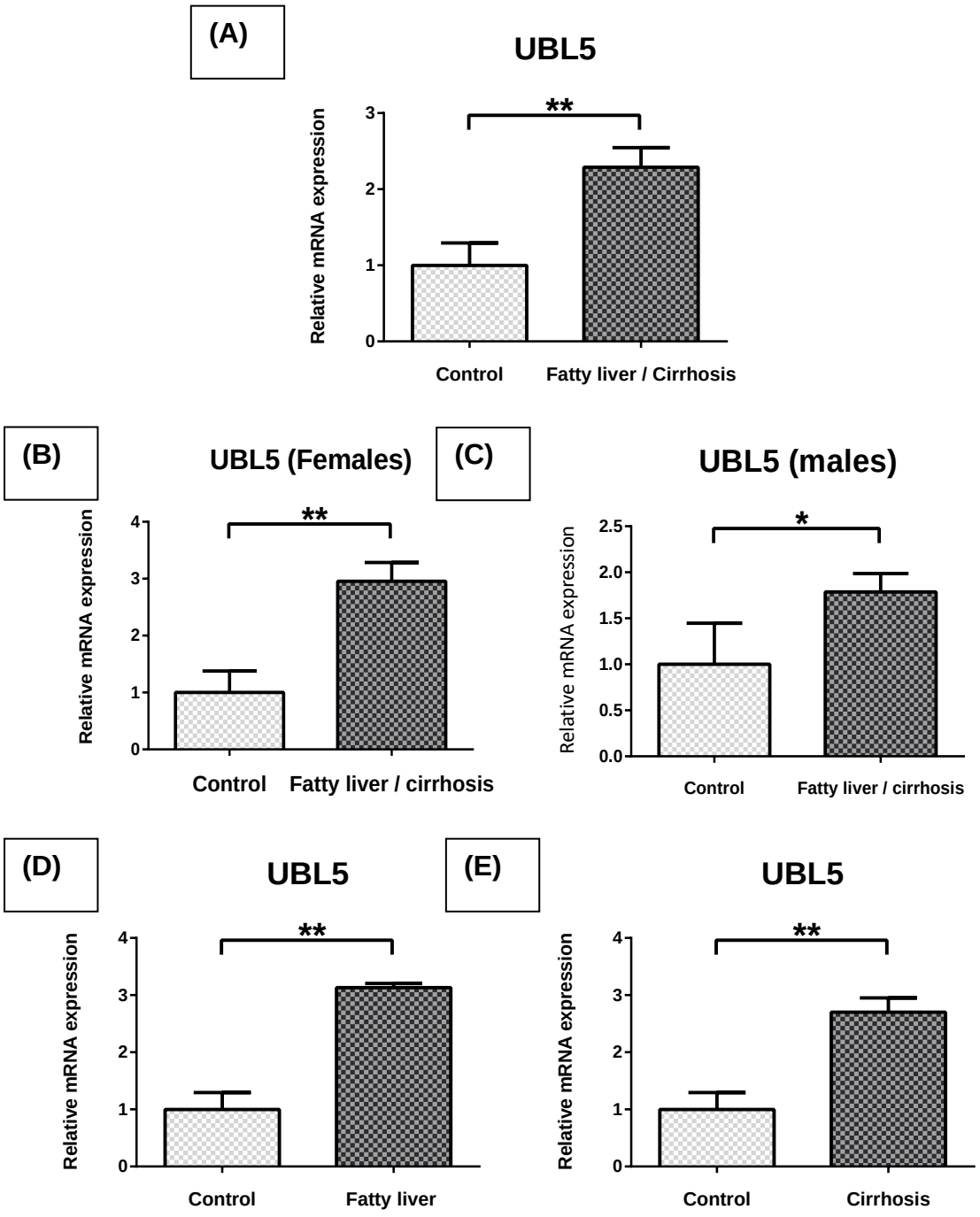

***UBL5* mRNA levels in human livers from patients with fatty liver and cirrhosis and controls:** mRNA levels were expressed relative to the control sample. The ΔΔCt method was used to calculate relative quantification of gene expression with 18s rRNA as the housekeeper gene. Values presented as mean ± SEM. **(A)** All female, male patients with fatty liver and cirrhosis. n=9-10. **(B)** Female patients with fatty liver and cirrhosis. N 9-6. **(C)** Male patients with fatty liver and cirrhosis. N 9-6. **(D)** All female, male patients with fatty liver. n=2-9. **(E)** All female, male patients with cirrhosis. n=3-9. * P ≤ 0.05, ** P ≤ 0.01.